RAMON MARIA ALLER ASTRONOMICAL OBSERVATORY

DEPARTMENT OF APPLIED MATHEMATICS

The Modeling of the Physical and Dynamical Properties of Spectroscopic Binaries with an Orbit

---

AHMAD ALI ABUSHATTAL

Santiago de Compostela, 2017

USC
UNIVERSIDADE
DE SANTIAGO
DE COMPOSTELA

The Modeling of the Physical and Dynamical Properties of Spectroscopic Binaries with an Orbit

by

AHMAD ALI ABUSHATTAL

DOCTORAL DISSERTATION

Submitted for the degree of

DOCTOR EN MATEMATICAS

UNIVERSIDADE DE SANTIAGO DE COMPOSTELA

Santiago de Compostela, 2017

USC
UNIVERSIDADE
DE SANTIAGO
DE COMPOSTELA

The Modeling of the Physical and Dynamical Properties of Spectroscopic Binaries with an Orbit

Fdo. Ahmad Ali Abushattal

Memoria para optar al grado de Doctor realizada en el Observatorio Astronómico Ramón María Aller en el Programa de Doctorado de Matemáticas de la Universidade de Santiago de Compostela, bajo la dirección del Profesor José Ángel Docobo Durántez.

Santiago de Compostela, a 27 de Abril de 2017

Fdo. Prof. José Ángel Docobo Durántez

USC
UNIVERSIDADE
DE SANTIAGO
DE COMPOSTELA

The Modeling of the Physical and Dynamical Properties of Spectroscopic Binaries with an Orbit

AUTURIZACION DEL DIRECTOR/TUTOR DE LA TESIS

Prof. José Ángel Docobo Durántez, Catedrático de Astronomía del Departamento de Matemática Aplicada de la Universidade de Santiago de Compostela, como Director de la Tesis Doctoral titulada "The Modeling of the Physical and Dynamical Properties of Spectroscopic Binaries with an Orbit", presentada por D. Ahmad Ali Abushattal, alumno del programa de Doctorado en Matemáticas,

AUTORIZO la presentación de la Tesis Doctoral indicada para optar al grado de Doctor por la Universidade de Santiago de Compostela, considerando que reúne los requisitos exigidos en artículo 34 del reglamento de Estudos de Doutoramento, y que como Director de la misma no incurren causas de abstención establecidas en la ley 40/50.

Santiago de Compostela, a 27 de Abril de 2017

Fdo. Prof. José Ángel Docobo Durántez

USC
UNIVERSIDADE
DE SANTIAGO
DE COMPOSTELA

Acknowledgements

Thank Allah, the most gracious, the most merciful.

This Doctoral dissertation was elaborated at the Ramon Maria Aller Astronomical Observatory (OARMA) of the University of Santiago de Compostela (Galicia, Spain), being proposed and directed by Professor Jose Angel Docobo, an outstanding international specialist in binaries. I remember when I arrived in Santiago de Compostela in 2013, Dr. Docobo told me "I have reserved an interesting doctoral subject for you, I hope that you will be able to do it".

Sincere gratitude to the source of endless knowledge whom does not stop giving, the OARMA Director and my supervisor Professor Docobo who has not held back any effort to finish this Ph.D. he has given support from all scientific angles. During the past three and half years, he has been my guide and the adviser. He has simplified the most complicated issues faced and has explained the modern scientific methods to cope with the latest developments in the field. He not only suggested all of the contents of this work but he also help me to structure the different Chapters. I worked very close to him all of the time and he always responded to my requests. His role was more than upholding scientific responsibilities but has exceeded to care for my social life, for he was a second father to me. He has shared with me moments of happiness, sadness, tiredness, and sickness. Everyday, I learn something new from him at both the scientific and social level. Many thanks to Dr. Docobo for his trust in me.

Prof. Docobo considered that, in the development of this work, it was essential to spend some stays at the Institute of Astronomy of Cambridge working with Professor Roger F. Griffin, one of the most famous experts on spectroscopic binaries in the world. My two visits to Cambridge took place thanks to the good friendship and mutual scientific collaboration between these two professors. I wish to express my sincere gratitude to Prof. Griffin for not only receiving to me at the Cambridge Observatory but, fundamentally, for all of the things that he taught me and for the observational experience achieved.

All thanks goes to my inspiration and Professor in Astrophysics in Jordan, Professor Mashhoor Ahmad Al-Wardat. He has stood by me ever since I started my Bachelor at Al Hussein Bin Talal University and has supervised my Master thesis at Mu'tah University.

To whom supported me through of all my encounters, well-educated in all scientific and technical aspects, the OARMA researcher, Mr. Pedro Pablo Campo. I had the honor to work with him and I am thankful for all of the time he spent to educate me in very different questions to accomplish my work.

To Lorel Scott, Ph.D., the English language proof reader. She has helped to raise the language quality of the thesis. I thank her for all the time spent to revise the smallest details and for her advice that enhanced my intellectual and language abilities.

This work would not have been completed without the presence of effective people during the past years. My father, whom has made my dream his own and who has sacrificed everything he owns and endured more than he could take, my dearest father, Ali Marzouq Abushattal. He has taught me patience, life, and responsibility. To whom raised me and taught me humanity, to whom I learned from her sacrifice and caring for others, to whom taught me that the mind rests by having a kind heart, my precious mother, Azeza Dahi Al-Nimat. Thanks to whom provided me with comfort, stability, and security, to whom has a pure heart, to my second half, my beloved wife, Sanaa Al-Naimat. She has endured distance and being apart and has suffered a lot with me being away. My eldest brother, Mohammad, who gave me advice and brought me to the beginning of the road and who taught me to be realistic in thought and logical in decision-making.

I thank many others who supported me to accomplish this work via the Erasmus Mundus project represented by Enrique Lopez Veloso, Sonia Cordido Méndez, Dr. Sami Ashour, Dr. Bassam Abu Karaki, and Al-Hussein Bin Talal University represented by the Deanship of scientific research and postgraduate studies.

I thank my uncle, Ismihan Abushattal, who taught me not give up and to reach my goals. I thank Mosa Ali Al-Naimat who supported me at the beginning of my journey even though he was facing hardship and has left a great mark on my life. To all others who have touched my life profoundly including Dr. Ahmad Al-Jamal, Dr. Khaled Abu-Ameereh, Dr. Saleem Aladaileh, Hossam Abushattal, Mohammad Abdullah Dwerij, Jaser Suliman Al-Naimat, and Ala' Salim Al-Naimat, Hatem Al-Ameryeen, Tareq Mahmod Al-Zu'bi, Mohammad Al-Zu'bi, Sattam Mattarneh, Anas Suliman Al-Naimat, Zeyad Al-Zarkle.

Many thanks to all of them.

I Dedicate this work to my mother, father, my beloved wife, my brothers and uncles.

To the soul of my uncle Salih Dahi Al-Naimat, my grandparents Marzouq, Dahi, and A'shiqa, and my uncle Ali Khalaf Abushattal

To my home University, Al-Hussein Bin Talal University.

Abstract

This Memory, devoted on Spectroscopic Binaries (SBs), was realized by Ahmad Ali Marzouq Abushattal at the Ramon Maria Aller Astronomical Observatory (OARMA) of the University of Santiago de Compostela (Galicia, Spain), and was proposed and directed by Professor José-Ángel Docobo.
The motivation for this project is the attempt to establish a methodology that will permit the prediction of which spectroscopic binaries are able to be optically resolved by means of a specific telescope. The resolution of the double-lined SBs is of great astronomical interest because, if it is possible to have both the spectroscopic and visual orbits, then the individual masses, the orbital parallax, and the three-dimensial orbit can be obtained with great precision (see, e.g. Docobo et al., 2014b, 2017).

After the Introduction, where apart of justify the interest of researching in binaries, their position into the IAU, showing a brief history of their study, and presenting the main goals of the OARMA in this Astronomy field, Chapter 1 describes the fundamentals of spectroscopic binaries, the reference system, the orbital elements, the radial velocity, the singled-lined (SB1) and double-lined (SB2) types, the principal methods of orbital determination, and a comparison test among them. My personal experience observing spectroscopic binaries, acquired at the Cambridge Observatory working with Professor Roger F. Griffin, is described in Chapter 2 . First, I commented on the brilliant professional trajectory of R. F. Griffin, particularly regarding his investigation of spectroscopic binaries and then described all of the operations realized along a night of observation from the dome opening to the binary registers using the Photoelectric Radial Velocity Spectrometer attached to the 36-inch telescope. Finally, an explanation of the radial velocities observed is given.

The main body of the dissertation corresponds to Chapter 3 where all of the different steps necessary to obtain the most probable 3-dimensional model of the spectroscopic binaries are explained, especially their apparent orbits, which permit to us to have an idea about their separations in order to try to resolve them optically with the adequate telescope. The methodology (programmed in MATLAB) is applied to 25 real cases as well as the testing with 5 SBs resolved by means of speckle interferometry. New spectral type-mass calibrations are presented and used in this process.

Once the model of the SBs is created and the most probable values between the components established, it is possible to study the possibility of the existence of exoplanets in the system. In the case of SBs, the great majority of the stable orbits correspond to circumbinary planets due to the short distances between the star components. In Chapter 4, we include also research regarding the possible habitability of these exoplanets taking into account the different characteristics of the host stars. The results obtained were put in practice with the 30 SBs mentioned in Chapter 3. This Memory has incorporated a long list of references and the bibliography used in its development, and three Appendices.

Resumen

MODELIZACIÓN DE LAS PROPIEDADES FÍSICAS Y DINÁMICAS DE LAS BINARIAS ESPECTROSCÓPICAS CON ÓRBITA

Resumen abreviado:

Después de la Introducción, en la que se justifica el interés de la investigación en estrellas dobles o binarias, su ubicación dentro de la IAU, una breve historia de su estudio y finalmente una muestra de los principales logros del OARMA en este campo de la Astronomía, en el Capítulo 1 de esta tesis se describen los fundamentos de las binarias espectrocópicas (SBs), el sistema de referencia usado, los elementos orbitales, las velocidades radiales, los tipos de SBs: de línea simple (SB1) y de doble línea (SB2), los princiales métodos de cáculo de órbitas, y una comparación entre ellos aplicándolos a un caso concreto.

La experiencia del autor adquirida en el Observatorio de Cambridge trabajando con el Profesor Roger F. Griffin, es comentada en el Capítulo 2. Primero describiendo la brillante trayectoria profesional de R.F. Griffin, particularmente en relación con sus investigaciones en SBs, y posteriormente desarrollando todas las operaciones llevadas a cabo en una sesión nocturna de observación desde la apertura de la cúpula hasta la obtención de velocidades radiales usando el espectrómetro Coravel instalado en el telescopio de 36 pulgadas de dicho Observatorio. Finalmente, se da una explicación sobre los registros de velocidades radiales observadas.

El cuerpo principal de esta Tesis Doctoral podemos decir que corresponde al Capítulo 3, donde se exponen todos los pasos necesarios para construir un algoritmo que permite establecer el modelo en tres dimensiones más probable de las SBs y especialmente su órbita aparente, la cual permite evaluar la separación angular entre las componentes con objeto de intentar separarlas opticamente mediante técnicas de alta resolución sugiriendo el telescopio adecuado. La metodología diseñada se aplica a 25 SBs y es testada con otras 5 SBs, las cuales han sido resueltas previamete mediante interferometría speckle.

Como consecuencia de este estudio, se presentan las nuevas calibraciones tipo espectral-masa que fueron utilizadas. Una vez que el modelo de las SBs ha sido creado, es factible estudiar asi mismo la posibilidad de exoplanetas en tales sistemas que, debido a las pequeñas distancias entre sus componentes, mayoritariamente resultan ser planetas circumbinarios, es decir, en movimiento en torno a las dos estrellas. En este Capítulo 4 se estudia la estabilidad de tales órbitas asi como las condiciones de habitabilidad de los posibles planetas teniendo en cuenta su distancia a las estrellas anfitrionas y las características de estas últimas. Todo ello es aplicado a las 30 SBs comentadas en el Capítulo 3. La presente Memoria tiene incorporada una larga lista de referencias y tres Apéndices.

Resumen

Esta Memoria, que versa sobre Binarias Espectroscópicas (SBs), fue realizada por Ahmad Ali Abushattal en el Observatorio Astronómico Ramón María Aller (OARMA) de la Universidade de Santiago de Compostela (USC), habiéndo sido propuesta y dirigida por el Catedrático de Astronomía de la USC, José Ángel Docobo Durántez.

La motivación de la misma surge al tratar de establecer una metodología que permita preever que binarias espectroscópicas son susceptibles de ser resueltas opticamente por un telescopio dado. La resolución especialmente de binarias espectroscópicas de doble línea tiene un enorme interés astronómico ya que si se dispone de ambas órbitas, espectroscópica y visual, entonces se pueden obtener con gran precisión las masas individualizadas, la paralaje orbital y la propia órbita en tres dimensiones, ver por ejemplo (Docobo et al., 2014b, 2017).

Una estrella doble o binaria es un par de estrellas cuyas componentes estan ligadas por su mutua atracción gravitatoria y, como consecuencia de ello, ambas describen órbitas en torno al centro de masas del sistema. En Mecánica Celeste se estudia que tales movimientos son equivalentes a considerar una de ellas, la estrella principal, como fija y , en este supuesto, la otra, la secundaria, describe en torno a aquella una órbita kepleriana, salvo que la presencia de otras fuerzas externas produzan perturbaciones que afecten a su dinámica. Hoy en dia se considera que la mayoría de las estrellas que podemos obsevar son binarias pero también un buen número de ellas están formando parte de sistemas estelares múltiples.

El estudio de las binarias es importante en Astrodinámica y Astrofísica por numerosas razones, pero especialmente por que a partir de sus órbitas y paralajes es posible determinar las masas estelares, que son parámetros esenciales en el camino evolutivo de las mismas. Por otra parte, los sistemas binarios y múltiples son magnificos escaparates donde quedan reflejados distintos fenómenos físicos y dinámicos: pérdida de masa, componentes variables, efectos relativistas, el fenómeno Nova, estrellas Flare, binarias de Rayos X, componentes Wolf-Rayet, estudio de perturbaciones, descubrimiento de subcomponentes incluso de enanas marrones y exoplanetas, cálculo de órbitas, etc.

La teoría y las técnicas de observación han ido progresando conjuntamente a lo largo de la historia, por ello creemos que es importante, antes de comenzar un trabajo como este, explorar en los siglos precedentes cuales han sido los principales logros conseguidos en este campo de la Astronomía. En este sentido, libros como The Binary Stars (Aitken, 1935), Close Binary Stars (Kopal, 1959), Properties of Double Stars (Binnendijk, 1960), Binary and Multiple Stars (Batten, 1989), L'Observation des Etoiles Doubles Visuelles (Couteau, 1978), o Double Stars (Heintz, 1978), entre otros, son referencias fundamentales.

Teniendo en cuenta la técnica utilizada para su descubrimiento y posterior estudio, las estrellas dobles se suelen clasificar en tres clases: visuales, espectroscópicas y eclipsantes. En las primeras, la naturaleza binaria es establecida por medios ópticos, usando el micrómetro, cámaras CCD , o modernas técnicas de alta resolución como la interferometría speckle. En otros casos, utilizando incluso grandes telescopios no es posible resolver la binaria, sin embargo otras técnicas si lo pueden hacer posible, por ejemplo midiendo el desplazamiento periódico de las rayas espectrales y obteniendo las velocidades radiales correspondientes por medio del efecto Doppler-Fizeau. Estas serían las binarias espectroscópicas. Finalmente, en numerosas ocasiones, las variaciones periódicas de la magnitud de una estrella nos informan de la existencia de una compañera que produce eclipses (Kopal, 1990).

Hoy en dia, la precisión de los receptores acoplados a grandes telescopios ha hecho posible poder estudiar un alto número de binarias por medio de dos o tres técnicas a la vez, lo cual, como se verá a lo largo de la Memoria, permite obtener una información casi completa

de estos sistemas. Más aun, las técnicas tradicionales usadas en la investigación de las estrellas dobles, han sido las que han permitido descubrir la mayoría de los planetas extrasolares, tanto por el método de las velocidades radiales como con el de tránsitos.

La Astronomía de las estrellas dobles ha estado siempre representada en el organismo que a nivel mundial coordina las actividades astronómicas al más alto nivel, la Unión Astronómica Internacional (IAU). Tradicionalmente, en la IAU hubo dos Comisiones dedicadas al estudio de las binarias, la No.26, Double and Multiple Stars, y la 42, Close Binaries. La Figura 1.2 muestra la lista de Presidentes/as, Vice-Presidentes/as y Secretarios/as de la Comisión 26. El Profesor Docobo, Director del presente trabajo, fue Vice-Presidente en el periodo 2006-2009, y Presidente de la Comisión 26 entre 2009 y 2012. Otros miembros del OARMA como los doctores Josefina Ling y Vakhtang Tamazian fueron asi mismo miembros del Comité Organizador de dicha Comisión. El propio Dr. D. Ramón María Aller Ulloa, fundador del OARMA fue el primer español miembro de la Comisión 26 y, al mismo tiempo, el introductor del estudio de las estrellas dobles en España (Aller, 1930, 1932, 1934, 1936, 1941, 1947). En la Asamblea General de la IAU celebrada en Hawaii en 2015, las Comisiones 26 y 42 se unieron en una nueva Comisión, la G1, denominada Binaries and Multiple Stars.

Discípulos del Padre Aller, como los Profesores Vidal Abascal y Cid Palacios, tuvieron también aportaciones destacadas sobre todo en lo que se refiere al diseño de métodos de cálculo de órbitas. Enrique Vidal (Vidal, 1948) fue el primero en publicar que con tres observaciones, o lugares normales, (θ, ρ, t) es posible calcular la órbita parabólica de una estrella doble, y diez años después, Rafael Cid, (Cid Palacios, 1958, 1960) resolvió también por vez primera el caso elíptico que consiste en determinar los siete elementos orbitales usando solamente datos de observación (tres lugares normales y el angulo de posición en un cuarto instante), es decir, sin tener que calcular la constante de las áreas como se hace en el cásico método de Thiele-Innes-Van den Bos.

J.A.Docobo comenzó sus estudios sobre estrellas dobles y múltiples en la Universidad de Zaragoza, siendo R. Cid el Director de su tesis doctoral, Aplicación de la Teoría de Perturbaciones al Estudio de Sistemas Estelares Triples. Más tarde, ya en Santiago de Compostela, desarrolló un algoritmo muy práctico y versátil que permite la determinación de la órbita de una estrella dobles visual a partir de tres lugares normales. El método de Docobo (Docobo, 1985, 2012) está basado en una aplicación del intervalo (0, 2π) o (0, ∞) en el conjunto de órbitas keplerianas elípticas cuyas órbitas aparentes pasan por los tres lugares normales (puntos base) elegidos, seleccionando en cada caso la solución chequeando los residuos obtenidos con el resto de las observaciones disponibles, o utilizando otros criterios como la coincidencia de la paralaje dinámica de cada órbita con la paralaje medida por el satélite Hipparcos (en breve también Gaia), la masa total obtenida y su concordancia con aquellas esperadas para los tipos espectrales de las componentes, la armonía entre los valores de la constante de las áreas deducidas de cada órbita, del conjunto de las generadas, con aquel valor obtenido previamente a partir de todas las observaciones, cotejando el angulo de posición en una cuarta época, etc. Desde una prespectiva matemática, este algorítmo analítico pude considerarse el camino natural para obtener los elementos orbitales y puede probarse que, por ejemplo, tanto el método de Thiele-Innes-Van den Bos (Dommanget, 1981) como el de Cid, pueden ser considerados casos particulares de él. Más de 300 órbitas han sido calculadas con tal método en las últimas décadas en varios paises. Independientemente de esto,

el equipo de investigación del OARMA, dirigido por el Profesor Docobo, ha llevado a cabo un amplio número de proyectos de investigación en binarias y organizado varios congresos nacionales e internacionales en este campo de la Astronomía. También fueron establecidos acuerdos de colaboración con instituciones extranjeras como el Special Astrophysical Observatory de Rusia, el Buyrakan Astrophysical Observatory de Armenia o la Universidad de Chile, con objeto de realizar medidas speckle de binarias con grandes telescopios y, al mismo tiempo, preparar artículos científicos conjuntamente. En este sentido, hay que recordar que el OARMA dispone de dos cámaras para realizar interferometría speckle, la ICCD y la EMCCD. La larga lista de publicaciones del OARMA puede ser consultada en su web (`http://www.usc.es/astro/publicaciones/publicacionesing.htm`), pero además debe de resaltarse la elaboración del catálogo de órbitas y efemérides OARMAC (Docobo et al., 2001) y la edición de la Circular de información de la Comisión G1 (antes comisión 26) de la IAU. En efecto, en 1992 el Profesor Docobo recibió del Dr. Paul Couteu y con el visto bueno de la IAU, el encargo de editar dicha Circular. Docobo nombró a J.F.Ling como co-editora y desde entonces la Circular es publicada en inglés desde el OARMA.

El Capítulo 1 de la tesis está dedicado a exponer los fundamentos del estudio de las binarias espectroscópicas (SBs), en las que se focalizará el trabajo. Después de exponer un concepto básico en este campo, cual es la velocidad radial y la forma de obtener su medida, se establece de forma precisa el sistema de referencia con el que es necesario trabajar con las órbitas de las binarias. Tal es (Figura 1) un sistema cartesiano ortogonal levógiro que haga compatible el criterio de que la velocidad radial sea positiva cuando la correspondiente componente del sistema doble se aleje del observador, con el hecho de contar los angulos de posición en sentido N-E-S-W.

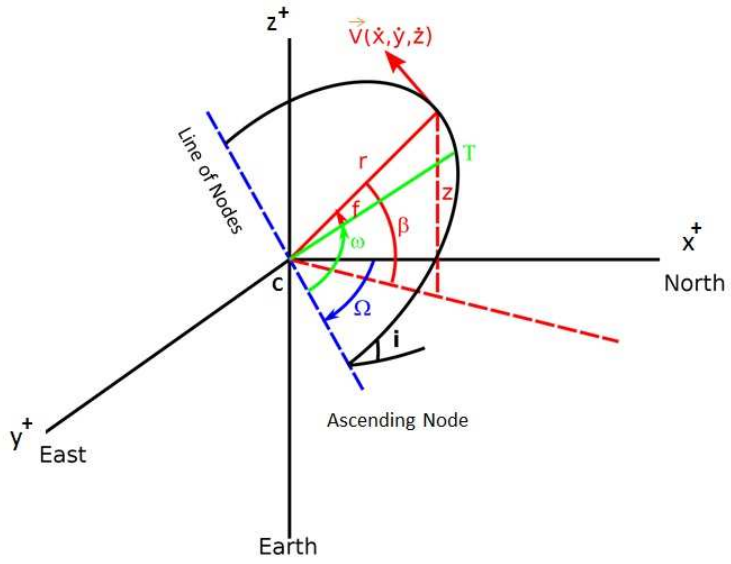

FIGURE 1: Sistema de referencia y elementos orbitales.

Definidos los elementos orbitales de una SB, V_o (velocidad del centro de masas), P (periodo orbital), T (época de paso por el periastro), e (excentricidad de la órbita), a.sen(i) (producto del semieje mayor de la elipse por el seno de la inclinación) y ω (argumento del

periastro), seguidamente se deduce paso a paso la expresión que relaciona la velocidad radial con dichos elementos, y que es fundamental para el cálculo de órbitas. En este sentido, y después de desarrollar los métodos clásicos de Lehmann-Filhés (Lehmann-Filhés, 1894) y Wilsing-Russell (Russell, 1902; Wilsing, 1893), se realiza un estudio comparativo entre ellos que consiste en la recuperación de una órbita teórica previamente establecida y a partir de la cual se han obtenido efemérides en 25 instantes, las cuales una vez modificadas adecuadamente (de tres formas distintas), se convieten en las teóricas observaciones disponibles para prodecer al cálculo de la órbita. Se trata de ver como los distintos métodos recuperan la órbita inicial. En este sentido, hemos tenido en cuenta también el uso de funciones de aproximación con objeto de obtener curvas de velocidad radial que se ajusten bien a las observaciones y, en concreto, los polinomios de interpolación cúbicos Spline (Elipe and Lanchares, 1988).

Finalmente se han obtenido y se han estudiado los resultados de un total de 21 órbitas: 3 calculadas directamente por el método de Lehmann-FiIhés, 9 usando las funciones Spline, y otras 9 obtenidas con el método de Wilsing-Russell, para las cuales se han calculado las RMS de los residuos con las correspondientes observaciones para que sirvieran de control en la comparación propuesta.

El Director de la tesis quiso que el doctorando tuviese la máxima información posible sobre el tema a tratar y de esta forma sugirió el desplazamiento al Observatorio de la Universidad de Cambridge por dos veces para trabajar con el Professor Roger F. Griffin, una de las autoridades mundiales en binarias espectroscópicas. Fundamentalmente se trataba de aprender todo el proceso de obtención de velocidades radiales, dato fundamental para el posterior cálculo de órbitas. El Capítulo 2 está dedicado precisamente a esto. Primero se hace una semblanza del enorme trabajo desarrollado por el Prof. Griffin desde 1975 en todo lo relativo a la observación y cálculo de órbitas (ver por ejemplo, (Griffin, 1980, 1985, 1990, 1995, 2005, 2010, 2015b; Griffin and Eitter, 2000; Griffin and Emerson, 1975)). Posteriormente, el Profesor Docobo nos indicó que era fundamental desarrollar por lo menudo una noche de trabajo en Cambridge, comentando todos los pasos hasta obtener el dato de una velocidad radial (RV), incluyéndo la descripción de todo el instrumental usado . En nuestra segunda visita, realizada en julio de 2015, hemos podido obtener un total de 47 observaciones. Los resultados de las mismas están incluidas en las Figuras tituladas “Radial velocity observations of SB1”, y “ Radial velocity observations of SB2”. Aparte de ello se hace un extenso comentario acerca de toda la información a mayores que se puede obtener de un sistema binario a partir de un registro RV: tipo espectral y clase de luminosidad, velocidad de rotación, metalicidades, etc.

Como ya se comentó anteriormente, en las últimas décadas ha sido posible desdoblar un buen número de SBs. El interés astrofísico de ello yace en el hecho de que con ello es posible tener conocimiento de los valores individuales de las masas de las componentes. En efecto, las órbitas de las SB2 nos proporcionan el cociente de la masas, en tanto que las órbitas visuales dan cuenta de la suma de ellas. Sin embargo, a la hora de preparar una lista de binarias espectroscópicas para tratar de resolverlas con un telescopio determinado, deberíamos de contestar previamente a preguntas como: ¿Es posible tener una idea del telescopio necesario en cada caso?, o ¿ Que lista debemos de preparar para el telescopio en el que tenemos tiempo de observación?. En este Capítulo 3, trataremos de contestar a estas

preguntas trabajando tanto con binarias espectroscópicas de línea simple (SB1) como con las de doble línea (SB2) con órbita y paralaje conocidas. Nuestro objetivo es construir un modelo tridimensional de cada una de esas SBs y finalmente proponer sus órbitas aparentes y, consecuentemente, los valores máximo y mínimo de sus separaciones angulares. En este estudio, daremos cuenta también de los parámetros físicos más probables de estos sistemas.

En el caso de las SB1, los elementos orbitales disponibles son : P, T, e, a_1.sen(i), and ω_1, asi como la llamada función de masa:

$$f(\mathcal{M}) = \frac{(\mathcal{M}_2.sin(i))^3}{(\mathcal{M}_1 + \mathcal{M}_2)^2} \tag{1}$$

Suponemos asi mismo conocidos el espectro compuesto, la magnitud global aparente, y la paralaje (en general la paralaje de Hipparcos, aunque en algunos casos ya está disponible la paralaje medida por la sonda Gaia). El primer paso es obtener información acerca de los espectros individuales de cada componente. Para ello haremos uso del proceso de Edwards (Edwards, 1976). Una vez que ya tenemos los dos espectros en función de la diferencia de magnitud, es necesario asignar las masas a cada uno de tales tipos espectrales. Por esta razón, hemos hecho un análisis previo de las distintas calibraciones y, a partir de todas ellas, obtuvimos otras tanto para estrellas de la secuencia principal como para subgigantes y gigantes, siendo estas nuevas calibraciones las que empleamos a lo largo del trabajo.

El conocimiento de las masas (con sus correspondientes incertidumbres), nos permite primero obtener la inclinación orbital en (1) y seguidamente los valores de los tres semiejes, a, a_1 y a_2 expresados en unidades astronómicas de distancia mediante

$$\frac{a}{\mathcal{M}_1 + \mathcal{M}_2} = \frac{a_1}{\mathcal{M}_2} = \frac{a_2}{\mathcal{M}_1}, \tag{2}$$

o bien determinar primero el valor de a en la conocida expresión

$$\mathcal{M}_1 + \mathcal{M}_2 = \frac{a^3}{P^2}. \tag{3}$$

y luego los de los otros semiejes. El siguiente paso es calcular a'', es decir, el semieje mayor de la órbita relativa en segundos de arco. En estas condiciones, excepto el nodo ascendente, ya tendríamos todos los elementos de la órbita visual, no obstante es preciso hacer dos comentarios:

- Primero. Como la inclinación es determinada a partir de sen(i), dos valores son válidos en principio, i y i' = 180° - i . Si la binaria no es resuelta opticamente, resulta imposible saber si el movimiento es directo o retrógrado.

- Segundo. El angulo del nodo permanece desconocido, pero eso no es un problema para nuestros propósitos y, en principio, lo podemos tomar como 0°.

Por último, podremos calcular efemérides con cada órbita y dibujar asi mismo sus órbitas aparentes. A partir de estas últimas, deduciremos los valores extremos de la separación angular, ρ, y, por tanto, podremos ya establecer el tamaño necesario del telescopio que resolvería el sistema espectroscopico. Todos estos pasos son convenientemente desarrollados

en sucesivas subsecciones de la tesis. Obviamente en esta secuencia de cálculos es imprescindible tener en cuenta la transmisión de errores.

Cuando se trata de una SB2, es decir cuando las dos familias de líneas espectrales están presentes en el espectro de la binaria y tenemos también su órbita y paralaje, todo lo comentado previamente sigue siendo válido pero ahora tenemos una información adicional que es el valor del cociente de las masas,

$$q = \frac{\mathcal{M}_1}{\mathcal{M}_2} = \frac{a_2.sin(i)}{a_1.sin(i)}, \tag{4}$$

Admitiremos que si la binaria es SB2, entonces Δm es menor que 1.5 o 2.0. Es incluso posible que en algunos casos con Δm =2.5 pueda ser una SB2, pero esto tampoco representa un problema ya que haremos la selección de la solución por medio del valor de q.

Toda la metodologia elaborada ha sido programada en MATLAB, y antes de ser aplicada a 25 binarias spectrocópicas (SB1: HD 471, HD 4703, HD 10171, HD 22521, HD 26083, HD 79888, HD 110583, HD 111224, HD 119915, HD 134169, HD 143107, HD 159220, HD 174103, HD 176526, HD 183629, HD 196758 y SB2: HD 74089, HD 74855, HD 85843, HD 112475, HD 129560, HD 171802, HD 194765, HD 197952, HD 198048), ha sido convenientemente testada en 5 binarias espectroscópicas (1 SB1 y 4 SB2) que ya han sido resueltas por medio de interferometría speckle y que, por tanto, ya sabemos el tamaño del telescopio que las ha resuelto. En todos estos casos el test ha sido satisfactorio, resultando que las órbitas aparentes propuestas mediante el uso de nuestra metodología son muy parecidas a las órbitas aparentes reales, lo que demuestra la bondad de nuestra propuesta (ver por ejemplo Figura 2)

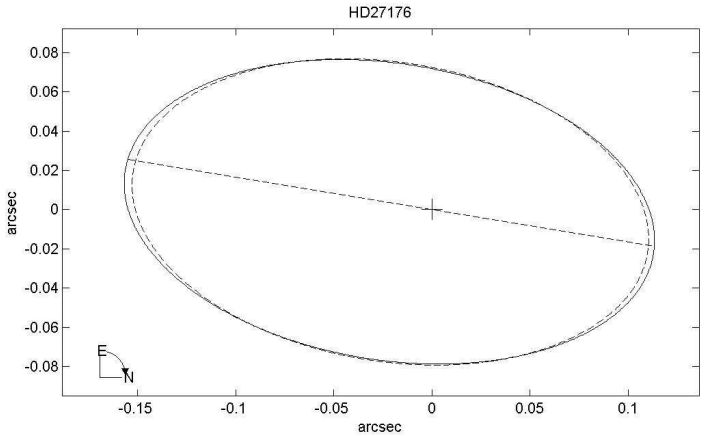

FIGURE 2: HD 71176. Gran concordancia entre ambas órbitas. En verde (línea continua, la órbita speckle, y, a puntos, la obtenida con nuestra metodología) .

Una vez que el modelo de las SBs ha sido creado, es factible estudiar asi mismo la posibilidad de la existencia de exoplanetas en tales sistemas que, debido a las pequeñas distancias entre sus componentes, mayoritariamente resultan ser planetas circumbinarios, es decir, en movimiento en torno a las dos estrellas. En este Capítulo 4 se estudia la estabilidad de tales órbitas asi como las condiciones de habitabilidad de los posibles planetas teniendo en cuenta su distancia a las estrellas anfitrionas y las características de estas últimas.

En cuanto a la estabilidad, nos basamos en las fórmulas empíricas de (Holman and Wiegert, 1999; Wiegert and Holman, 1997) en las que se tienen en cuenta tanto la relación de masas de las estrellas como la excentricidad orbital, siendo aplicadas a los tipos de órbitas propuestos por R. Dvorak in 1984: las órbitas tipo satélite (S-type) y las tipo planeta (P-type). Para el estudio de la posible habitabilidad de tales planetas, trabajamos con la definición propuesta por (Cockell et al., 2016) y asi mismo hicimos uso de la web interactiva (`http://astro.twam.info/hz/`) desarrollada por T. Muller y N. Haghighipour en 2014. Todo ello es aplicado a las 30 SBs comentadas en el Capítulo 3, para las que se proporciona en sus correspondientes gráficas las zonas de estabilidad orbital de posibles exoplanetas(liñeas de puntos), asi como las zonas de habitabilidad (zonas en verde) de los mismos (ver por ejemplo Figura 3).

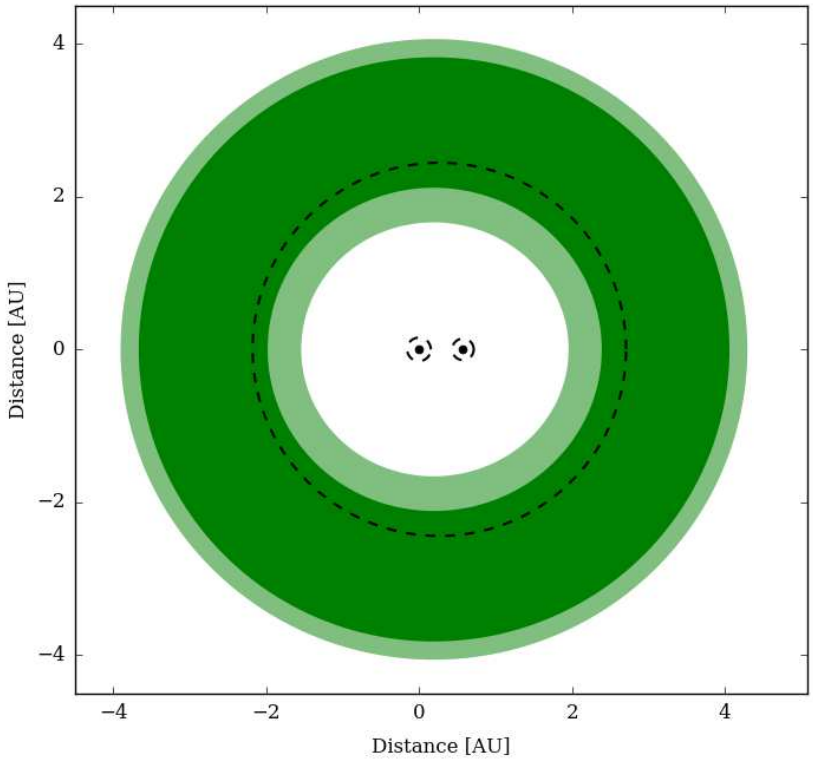

FIGURE 3: Zonas de estabilidad y habitabilidad para la SB2, HD 194765.

La presente Memoria tiene incorporada una larga lista de referencias y tres Apéndices.

Contents

USC
UNIVERSIDADE
DE SANTIAGO
DE COMPOSTELA

Introduction

A binary star is a pair of stars the components of which components are bound by gravity to each other and, for this reason, they orbit the common center of mass. One of these movements around the center of mass can be considered to be fixed (the primary) and the other (the secondary) can be considered to be relative with respect with respect to the first. Several estimations (e.g., (Abt and Levy, 1976; Duquennoy and Mayor, 1991)) claim that more than half of the observed stars are binary or belong to multiple systems with three, four, or more components. However, depending on the distance between the two stars, the orbital periods of the binaries can vary from hours to centuries. The study of binaries and multiple stars is important in Astrophysics and Astrodynamics for different and interesting reasons but, especially because from their orbits and parallaxes, it is possible to obtain the values of the stellar masses. It is well-known that the mass is a fundamental parameter for the study the evolutionary tracks of the stars but it is possible also to obtain information about other physical parameters of great interest such as the sizes of the components, their parallax (dynamical and orbital parallax), luminosities, and their precises orbital elements among other data.

On the other hand, binary systems are like "shop windows" in which many physical process can be reflected: mass loss, exchange of mass, variability of the components, relativistic process, the Nova phenomenon, Flare, Ray-X and Wolf-Rayet components, etc., and from the dynamical point of view: the study of perturbations, the discovery of dark components such as brown stars and exoplanets, the orbit calculation methods, etc.

Theory and observation techniques have progressed jointly throughout history and it is important at the beginning of this study to explore the previous centuries in order to list the main goals and highlights that took place and the achievements of all of the astronomers who have made an impact on the development of this important branch of Astronomy. Emblematic books such as Binary Stars by Robert. G. Aitken (Aitken, 1935), Close Binary Stars (Kopal, 1959), Properties of Double Stars (Binnendijk, 1960), Binary and Multiple Systems of Stars (Batten, 1973), L' Observation des Etoiles Doubles Visuelles (Couteau, 1978), or Double Stars (Heintz, 1978), and others are essential references that provide a wide perspective in this subject. It seems that the first double star, Mizar (Xi Ursae Majoris), was discovered in 1650 by the Italian astronomer, Jean Baptiste Riccioli, although perhaps Galileo Galiei resolved this star earlier. The term "double star" was used for the first time by John Michell in 1767. In any case, using the telescope, they had only observed two stars where, with the naked-eye, it is possible to see nothing more than one. The real beginning of double star astronomy occurred at the end of the 18th century when Sir William Herschel detected the orbital motions in a few pairs. Indeed, between 1782 and 1785, while trying to discover the parallax motion, Herschel was able to recognize the first orbital motions outside of the Solar System and, consequently, to prove the universality of the Gravitational Law of Isaac

Newton.

It is necessary to highlight the following events that followed: 1783, John Goodricke suggested that the variability of Algol is due to the eclipses produced by a second star moving around the primary; 1842, Chistian Doppler proposed the variation of the light wave-length when a radial desplacement exits between the focus and the receptor, later known as the famous Doppler Shift that is a fundamental tool in double star research; 1844, Friedrich W. Bessel found oscillations in the proper motion of some stars such as Procyon and Sirius and suggested that it is produced by an invisible companion; 1848, Armand H.L. Fizeau gave the correct interpretation of the Doppler principle in terms of a shift of the spectral lines; 1857, George P. Bond and John A. Whipple made the first photograph of a binary (Mizar, again) at Harvard; 1862, Alvan G. Clarck was able to observe the companion of Sirius; 1868, William Huggins measured the radial velocity of a star for the first time and S.W. Burnham conducted micrometric observations of double stars using the 36-inch Lick refractor; and in 1889, Annie J. Cannon and Edward C. Pickering determined the periodic motion of the spectral lines in the main component of Mizar. In the same year, Hermann K. Vogel and Julius Scheiner established the orbital motion of Algol by means of radial velocities thereby confirming the suggestion of Groodricke; 1906. Sherburne W. Burnham edited the double stars catalog known as BDS; and in 1932, Robert G. Aitken published the New General Catalogue of Double Stars within 120º of the North Pole (ADS).

At the beginning of the past century, numerous observatories equipped with large refractors and telescopes were erected along the world, especially in Europe and North America and, in many cases, the observation of binaries was a priority objective. Therefore, many relevant astronomers pointed to double stars as an interesting astronomical field involving very different lines of research.

Traditionally and taking into account the technique used to discover and later study of them, binaries are classified into three categories: visual, spectroscopic, and eclipsing. In the first, the binary nature is established by optical means: direct vision through an eyepiece, by photographic cameras (traditional cameras or CCDs), or by utilizing modern high resolution techniques such as speckle interferometry. In other cases, even when using very large telescopes, it is not possible to optically resolve the binary. However, other techniques may possibly serve, for example, observing the periodic variation of the spectral lines as a practice of the Doppler-Fizeau effect (spectroscopic binaries). Periodic variations of the stellar magnitude frequently inform us of the existence of a companion that produces eclipses (Kopal, 1990).

Nowadays, thanks to the improvement of precision devices attached to very large telescopes, it has been possible to study a number of binaries by means of two or three different techniques and, as we will see along this Memory, the information obtained is almost complete in these cases. Moreover, traditional observation techniques used during decades in binary research have permitted the discovery of the majority of the exoplanets by means of the Doppler-Fizeau effect and the transit method. For example, using the orbits of the visual binaries and knowing the parallax (Hipparcos or Gaia parallax), we can deduce the total mass of the system. If we can observe the two families of spectral lines of the same binary, it is possible to determine the mass ratio and, as a combination of these results, the individual masses of the components can be calculated. In the most favorable cases, it is even possible

to obtain the thee-dimensional orbit of the system. For this reason, when speckle interferometry began (Labeyrie, 1970), astronomers such as Harold A. McAlister, Yuri Y. Balega, Daniel Bonneau, Andrei Tokovinin, and William F. Van Altena, among others, took advantage of the fact that this procedure permits resolutions close to the separator power of the telescope. They tried, with success in many cases, to resolve spectroscopic binaries (see e.g. (Balega and Ryadchenko, 1984; Balega and Tikhonov, 1977; Labeyrie et al., 1974; McAlister, 1976a,b)).

Nevertheless, many authors consider that a better classification of binaries takes into account the distance between the components. In this sense, we have the Wide Binaries. This type can be described as "long distance stellar relationships" and the separation is more than 50 astronomical units (AU) within them. This distance is sufficient to consider that the components do not influence each other relative to the evolution of the system. By the way, in the very wide binaries, it is not clear that the forming process follows Fragmentation Theory as occurs when the separation is much smaller. The majority of the visual binaries belongs to this category as well as an important number of spectroscopic binaries and a few eclipsing binaries.

On the other hand, Close Binaries are those interacting binaries (Sahade and Wood, 1978) in which the evolution of the system is affected by the physical process between the components, especially the exchange of mass. In this scenario, it is usual that the size of the components is comparable to the mutual distance. Close binaries are sub-classified in Detached, Semidetached, and Contact binaries (Kopal, 1959), attending the filling mass the Roche lobes (see Figure 4). Examples of these three subcategories are successively, beta Aurigae, Algol, and W Ursae Majoris.

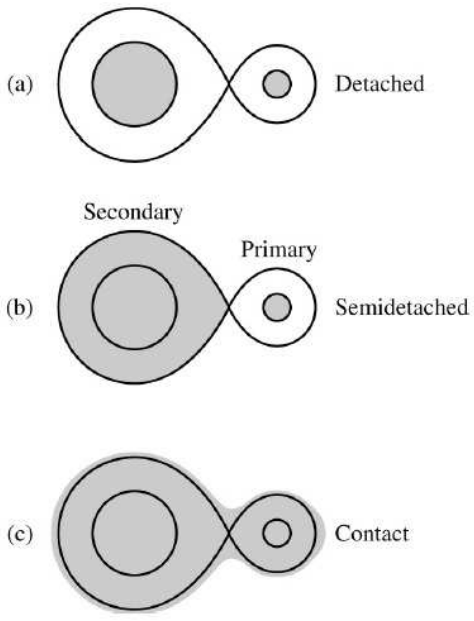

FIGURE 4: Classification of binaries by Roche lobes

.

Traditionally, two IAU Commissions are dedicated to binaries, No. 26: Double and Multiple Stars and No. 42: Close Binaries. Figure 5 shows the list of Officers of Commission 26 and Figure 6 , the members of the Organizing Committee (OC) of said Commission. Professor Jose Angel Docobo, the Director of this Doctoral dissertation, was Vice-president in the period of 2006-2009 and President of Commission 26 from 2009-2012. Other members of the Ramon Maria Aller Observatory (OARMA) of the University of Santiago de Compostela, specifically Josefina Ling and Vakhtang Tamazian, were members of the OC. During the IAU General Assembly of 2015, Commissions 26 and 42 merged in a new Commission, G1, with the name, Binaries and Multiple Stars.

Term	President	Vice President	Secretary
1919-1922	Robert Aitken		
1922-1925	Robert Aitken		
1925-1928	Robert Aitken		
1928-1932	Ejnar Hertzsprung		George van Biesbroeck
1932-1935	Ejnar Hertzsprung		
1935-1938	Ejnar Hertzsprung		
1938-1948			
1948-1952	Willem van den Bos (R. Aitken, honorary)		
1952-1955	Paul Muller		
1955-1958	Paul Muller		Peter van de Kamp
1958-1961	Peter van de Kamp		Sarah Lippincott
1961-1964	Peter van de Kamp	Richard Woolley	Sarah Lippincott
1964-1967	Kai Strand	Paul Couteau	Jean Dommanget
1967-1970	Paul Couteau	Jean Dommanget	Sarah Lippincott
1970-1973	Jean Dommanget	Sarah Lippincott	Otto Franz
1973-1976	Sarah Lippincott	Paul Muller	Otto Franz
1976-1979	Paul Muller	Otto Franz	
1979-1982	Otto Franz	Mario Fracastoro	Jean Dommanget
1982-1985	Mario Fracastoro	Karl Rakos	
1985-1988	Karl Rakos	Harold McAlister	
1988-1991	Harold McAlister	Helmut Abt	
1991-1994	Helmut Abt	Charles Worley	
1994-1997	Charles Worley	Hans Zinnecker	
1997-2000	Hans Zinnecker	Colin Scarfe	
2000-2003	Colin Scarfe	William Hartkopf	
2003-2006	William Hartkopf	Christine Allen	
2006-2009	Christine Allen	Jose Docobo	
2009-2012	Jose Docobo	Brian Mason	
2012-2015	Brian Mason	Yuri Y. Balega	

FIGURE 5: Officers of IAU Commission 26

.

Commission G1 called “Binary and Multiple Star Systems" is now part of the IAU Division G (Stars and Stellar Physics). Its primary purpose is to foster worldwide communication and collaboration among astronomers working in the field of binary and multiple stars. Commission G1 consists of 273 IAU individual members, being governed by the Officers of its Organizing Committee who are Andrej Prsa (President), Virginia Trimble (Vice-President), and Cristopher Adam Tout (Secretary) as well as Brian Mason, Robert

Term	Organizing Committee (note: the OC in each term also includes the immediate past president)
1961-1964	O. Eggen, P. Muller, K. Strand, W. van den Bos
1964-1967	O. Eggen, P. Muller, J. Dommanget, P. Kulikovsky, R. Petrie
1967-1970	O. Eggen, P. Muller, K. Strand, P. Kulikovsky, P. van de Kamp
1970-1973	P. Couteau, P. Muller, K. Strand, A. Deutsch, P. van de Kamp
1973-1976	P. Couteau, A. Batten, K. Strand, A. Deutsch, J. Dommanget, O. Franz
1976-1979	R. Harrington, A. Batten, M. Fracastoro, C. Worley, S. Lippincott
1979-1982	R. Harrington, P. Kulikovsky, P. Muller, C. Worley, A. Poveda, C. Scarfe
1982-1985	J. Dommanget, O. Franz, W. Heintz, H. McAlister, A. Poveda, C. Scarfe
1985-1988	J. Dommanget, H. Abt, P. Couteau, M. Fracastoro, R.S. Harrington, A. Kiselyov
1988-1991	P. Bernacca, E. van Dessel, P. Couteau, R. Harrington, A. Kiselyev, K. Rakos
1991-1994	P. Bernacca, E. van Dessel, H. Zinnecker, Y. Balega, F. Fekel, C. Scarfe
1994-1997	C. Allen, W. Hartkopf, A. Tokovinin, Y. Balega, F. Fekel, C. Scarfe
1997-2000	C. Allen, W. Hartkopf, A. Tokovinin, J. Armstrong, R. Mathieu, M. Valtonen
2000-2003	F. Fekel, P. Lampens, J. Ling, J. Armstrong, R. Mathieu, M. Valtonen
2003-2006	F. Fekel, P. Lampens, J. Ling, J. Davis, E. Oblak, T. Oswalt
2006-2009*	Y. Balega, B. Mason, D. Pourbaix, C. Scarfe, J. Davis, E. Oblak, T. Oswalt
2009-2012	Y. Balega, D. Pourbaix, C. Scarfe, F. Arenou, M. Scardia, V. Tamazian
2012-2015*	F. Arenou, M. Scardia, V. Tamazian, T. ten Brummelaar, P. Lampens, B. Reipurth, A. Tokovinin

* additional member due to tie in vote

FIGURE 6: Organizing Committee of IAU commission 26

.

D. Mathieu, Terry D. Oswallt, Johon Southworth, and Tomas Zwitter as current OC members. Within the Commission, Working Groups (WGs) are created to undertake certain well-defined tasks for limited time periods. These are: Active B stars, Maintenance of the Visual Double Star Database, the Catalog of Orbital Elements of Spectroscopic Binary Systems, and Nominal Units for Stellar and Planetary Astronomy. More information about the new G1 Commission, publications, meetings, conferences, databases, catalogs, surveys, computer codes, etc. can be found at the following websites: `http://www.astro.gsu.edu`, `https://www.iau.org/science/scientific_bodies/commissions/G1/`

As commented earlier, the present work was elaborated at OARMA, a Universitary Observatory belonging to the University of Santiago de Compostela (Galicia, Spain) that, besides many other activities, has binary and multiple stars as its main research line. For this reason, it is convenient to describe the important work of this center.

Ramon Maria Aller (1878-1966), the founder of the Observatory, was the person that introduced the study of double stars in Spain. He not only performed several lists of micrometric measurements Aller, 1930, 1932, 1934, 1936, 1941, 1947 , the first in his personal Observatory of Lalin and, since 1944, in the new installations of Santiago de Compostela. He was also the person that calculated the first double star orbits (Aller, 1935, 1939) in Spain (systems STT 77 and STF 1932). His doctoral students, Enrique Vidal and Rafael Cid (who later served as Professors at the Universities of Santiago de Compostela and Zaragoza) were also devoted to the theoretical study of double stars and particularly to orbit calculation methods.

E. Vidal was the first that publish that, with three observations (θ, ρ, t) or three normal points, is possible to calculate the parabolic orbit of a binary (Vidal, 1948). R. Cid resolved the so-called Main Problem for the first time that consisted of obtaining the seven orbital elements of a visual binary using only seven observation data (three normal points and the position angle, a fourth time), that is to say, without using the areal constant (Cid Palacios,

1958, 1960).

J. A. Docobo began to study binaries and multiple stars in university of Zaragoza and R. Cid was the Director of his Doctoral dissertation, Application of the Perturbation Theory to the Study of Triple Stellar Systems. Later, in Santiago de Compostela, heh developed a very practical and versatile algorithm that permits the determination of the visual orbit from three normal points. Docobo's method (Docobo, 1985, 2012) is based on an application from the interval $(0, 2\pi)$ or $(0, \infty)$ into the set of elliptic Keplerian orbits whose corresponding apparent orbits pass through the three base points, selecting the solution in each case by checking the residuals obtained with all of the observations available or by using other criteria (agreement of the dynamical parallax with those measured by Hipparcos or Gaia, the total mass obtained with a concrete parallax and its agreement with mass weighted from the spectral types, the agreement of the areal constant calculated for each orbit with that previously determined from observations, the position angle in a fourth epoch, etc). From a mathematical perspective, this algorithm can be considered to be the natural way to obtain the orbital elements. It can be proven that the Thiele-innes-Van den Bos (Dommanget, 1981) and Cid methods are particular cases of it. More than 300 orbits of visual binaries have been calculated during the last decades in several countries using the analytic method of Docobo.

Independent of this, the OARMA research team directed by Prof. Docobo has developed a number of research projects on binaries supported by official bodies and has organized several international and national scientific meetings. Some collaboration agreements were established with foreign institutions such as the Special Astrophysical Observatory, the Buyrakan Astrophysical Observatory, and the University of Chile in order to perform speckle measurements of binaries and prepare papers jointly. In this sense, it is important to remember that OARMA has two speckle interferometry cameras, the ICCD and the EMCCD.

Prof. Docobo also was and is the Director of a great number of Master Theses and Doctoral Dissertations specifically related to binary and multiple star systems and exoplanets.

J.A. Docobo also suggested the creation of the OARMAC, a catalog of double star orbits and ephemerides (Docobo et al., 2001), which is currently maintained on-line by Docobo himself, J.F. Ling, and P.P Campo (`http://www.usc.es/astro/catalog.htm`).

In 1993 (I.C. No 120), Prof Docobo received, from Dr. Paul Couetau, the responsibility to edit the Information Circular of IAU Commission 26. Docobo named J.F.Ling as a co-editor and, since then, the Circular is published in English from OARMA by Docobo and Ling. The Memory that is presented here is devoted to Spectroscopic Binaries (SBs). The results obtained from SBs are complementary with Visual Binaries. Therefore, as we commented in other part of this Introduction, it would be ideal to observe binaries using the two techniques, speckle interferometry and spectroscopy in order to obtain information about practically all of the physical parameters. When speckle interferometry began to be used in the seventies of the past century, one of the main goals was to try to resolve spectroscopic binaries, (see, e.g.;(Balega and Tikhonov, 1977; Bonneau et al., 2010; Hartkopf et al., 1996; Horch et al., 2012; Labeyrie et al., 1974; Mason et al., 2001; McAlister, 1976b; Tokovinin et al., 2013)) and, at that time, the logical question arose: What SBs can we try to resolve with our telescopes?. Forty years later, we recovered the same subject but with much more precise information about the parallaxes, spectroscopic orbits, and mass-luminosity calibrations.

Under these more favorable conditions, we decided to model the physical and dynamical properties of SBs with an orbit, trying to determine three-dimensional models of them and, consequently, to establish their most probable apparent orbits, that is to say, the most probable maximum and minimum separations between the components. The last is fundamental information to be elaborated on in an observation program for a concrete telescope.

A robust algorithm, checked using several interferometric-spectroscopic systems, has been built based on several steps, always making use of the fundamental concepts used in binary and astrodynamic research. Moreover, once we have achieved the model for each binary, we can speculate about the possible existence of exoplanets in them and, sequentially, study the stability of their orbits. Finally, we can investigate the the hypothetical habitability of them.

During the three years and one-half years spent in the preparation of this work at OARMA, the author has participated in the following two publications:

- "Physical and Geometrical Parameters of CVBS. XII. Fin 350 (HIP 64838)" Authors: M.A. Al-Wardat, J.A. Docobo, A.A. Abushattal, and P.P. Campo. Journal: Astrophysical Bulletin, 2017, Vol 72. No 1, pp.24-34 (Quality control: JCR position 41 /62)

In this paper, a complete astrophysical and dynamical study of the close visual binary sysem, Finsen 350, is presented. Al-Wardat's complex method for analyzing close binaries was applied as a reverse method of building the individual and entirely synthetic SEds of the system.

- "Precise orbital elements, masses and parallax of the spectroscopic-interferometric binary HD 26441" Authors: J.A.Docobo, R.G. Griffin, P.P. Campo, and A.A. Abushattal. Journal: Monthly Notices of the Royal Astronomical Society. Accepted, 2017 (Quality control: JCR position 13/62).

A new speckle orbit is presented for this system. The orbital elements demonstrate very good agreement with those of the spectroscopic orbit calculated previously. The combination of both sets of results lead to very precise values of the masses and orbital parallax. A robust three-dimensional model of this binary is also obtained.

Moreover, the author of this work attended the international meeting: Second International Conference on Arabs' & Muslims' History of Science (University of Sharjah, Sharjah, UAE. December, 2014), presenting the communication entitled: Physical Properties and Dynamical Elements of Spectroscopic Binary Stars (authors: A. Abushattal, J.A.Docobo, and M. Al-wardat).

Finally, the author of this work realized two scientific stays at Cambridge Observatory in order to learn the observation techniques and orbital calculation of spectroscopic binaries. The motivation for this project is the attempt to establish a methodology that will permit the prediction of which spectroscopic binaries are able to be optically resolved by means of a specific telescope. The resolution of the double-lined SBs is of great astronomical interest because, if it is possible to have both the spectroscopic and visual orbits, then the individual masses, the orbital parallax, and the three-dimensial orbit can be obtained with great precision (see, e.g. Docobo et al., 2014b, 2017). This Doctoral dissertation is structured

as follows. After the Introduction, Chapter 1 describes the fundamentals of spectroscopic binaries, the reference system, the orbital elements, the radial velocity, the singled-lined (SB1) and double-lined (SB2) types, the principal methods of orbital determination, and a comparison test among them. My personal experience observing spectroscopic binaries, acquired at the Cambridge Observatory working with Professor Roger F. Griffin, is included in Chapter 2 . First, I commented on the brilliant professional trajectory of Griffin, particularly regarding his investigation of spectroscopic binaries and then described all of the operations realized along a night of observation from the dome opening to the binary registers using the Photoelectric Radial Velocity Spectrometer attached to the 36-inch telescope. Finally, an explanation of the radial velocities observed is given. The main body of the dissertation corresponds to Chapter 3 where all of the different steps necessary to obtain the most probable 3-dimensional model of the spectroscopic binaries are explained, especially their apparent orbits, which permit to us to have an idea about their separations in order to try to resolve them optically with the adequate telescope. The methodology is applied to 25 real cases as well as the testing with 5 SBs resolved by means of speckle interferometry. New spectral type-mass calibrations are presented and used in this process. Once the model of the SBs is created and the most probable values between the components established, it is possible to study the possibility of the existence of exoplanets in the system. In the case of SBs, the great majority of the stable orbits correspond to circumbinary planets due to the short distances between the star components. In Chapter 4, we include also research regarding the possible habitability of these exoplanets taking into account the different characteristics of the host stars. The results obtained were put in practice with the 30 SBs mentioned in Chapter 3. This Memory has incorporated a long list of references and the bibliography used in its development, and three Appendices.

Chapter 1

Spectroscopic Binaries

It is well known that when the light of a star is analyzed by means of a spectrograph, an image appears that is composed of a continuous background with a number of dark lines (absorption lines). Such is the case with the solar spectrum (the spectrum of Fraunhofer). The presence of these lines is intimately related to the temperature or the spectral type and the information that they provide goes further than the chemical elements that exist in the stellar atmospheres. They also transmit a high quantity of information that is of extraordinary value in Astronomy.

In 1842, the physicist and professor at the University of Vienna, Christian Andreas Doppler, suggested that the wavelength of the light must vary proportionally with the velocity of movement of the source of light with respect to the observer. The theory of Doppler was proven in 1844 with sound waves and, four years later, the French physicist and astronomer, Armand Hippolyte Louis Fizeau, applied this theory to electromagnetic waves. Because of the important results obtained, this effect was named the Doppler-Fizeau effect, although it is frequently referred to only as the Doppler Effect.

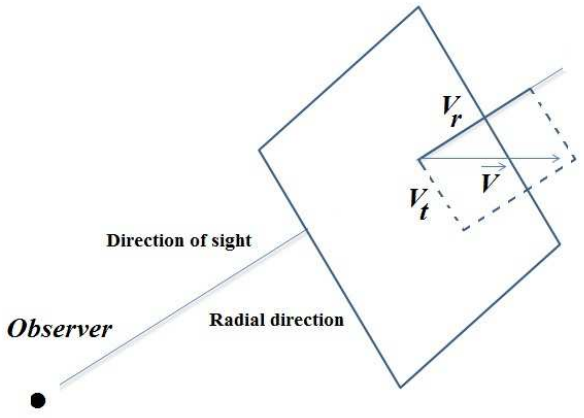

FIGURE 1.1: Orbital elements

The vector velocity, $\vec{V}$, of a certain star with respect to the observer can be resolved into two orthogonal components: the transverse, V_t, perpendicular to our view, and the radial

velocity, V_r, along the line of sight (Figure 1.1).

By convention, the radial velocity of the receiver relative to the source is considered to be positive if the source is moving away from the receiver. In the opposite case, V_r is negative. It is clear that if the movement occurs on the plane that is perpendicular to the visual, then the vector velocity only has a transverse component because, in this case, $V_r = 0$.

The Doppler-Fizeau principle informs us that if a source emits energy with a λ wavelength and if displacement exists with respect to the receiver of such radiation, it is received as a wavelength, λ', given by:

$$\lambda' = \lambda \left(1 + \frac{V_r}{c}\right) \tag{1.1}$$

where "c" is the velocity of light.

According to the previous comments, if $\lambda' > \lambda$ (redshift), then it must necessarily be that $V_r > 0$, that is, the star is receding from us. Inversely, if $\lambda' < \lambda$ (blue-shift,) then it turns out that $V_r < 0$ and, in this case, the two bodies (star and receiver) are approaching each other.

Measuring the difference, λ' - λ, between the wavelength observed and the standard (measured in the laboratory), the following expression gives us the value of V_r by means of

$$V_r = c \left(\frac{\lambda' - \lambda}{\lambda}\right) \tag{1.2}$$

Application of the Doppler-Fizeau effect is the basis for the detection and later study of a large number of binaries that, the most part of which, have not been resolved optically. The orbital movement (that produces successive mutual approaching and receding) is reflected in the values of λ' that also change periodically from being greater than λ to being less. In other words, the spectral lines periodically move from red to blue (see Figure 1.2).

It was in this way that, in 1889, on examining the spectrum of the Mizar A star, the astronomers at the University of Harvard, Annie Jump Cannon and Edward Charles Pickering, realized that there were double lines whose positions varied in a period of a bit more than 20 days. It was the first spectroscopic binary discovered.

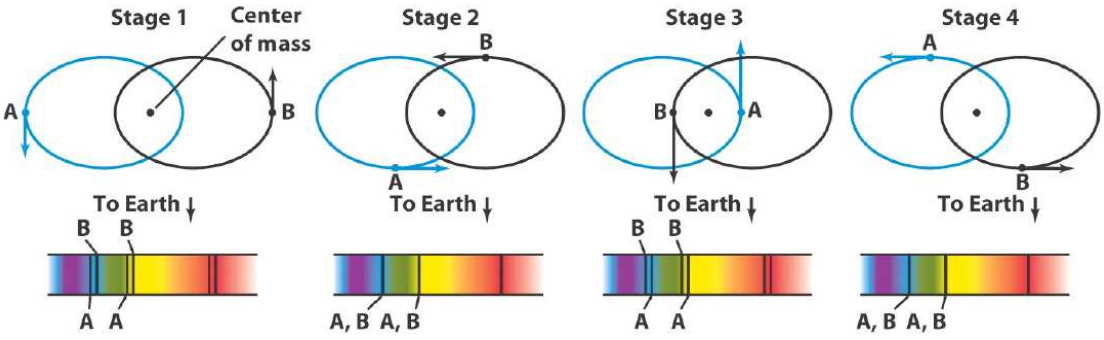

FIGURE 1.2: Doppler-Fizeau effect in a double star

The number of spectroscopic binaries very large. Of these, the orbits of more than 3.500 have been calculated. The majority of these orbits have very short periods on the order of

days or weeks. However, there are also numerous cases in which the orbital revolution is less than days or more than weeks or even months. In fact, as we will see later, it is possible to obtain the radial velocities of a good number of visual binaries which yield relevant information when both orbits (the visual and the spectroscopic) are known.

We should keep in mind that only the lines of the brighter component can be observed in the majority of spectroscopic binaries. That is due to the difference of magnitude between the two components. In general terms, we can consider that this occurs when $\Delta m > 1.5$, although this depends on the instrumentation utilized. In fact, there are cases where even with $\Delta m = 2.5$, the lines of both components can be seen in the spectrum.

In any case, when we can detect only the spectral lines of one component, we will say that this concerns a single-lined spectroscopic binary (SB1) and, in them, only the orbit of the brighter component can be calculated with respect to the center of mass of the system, C.

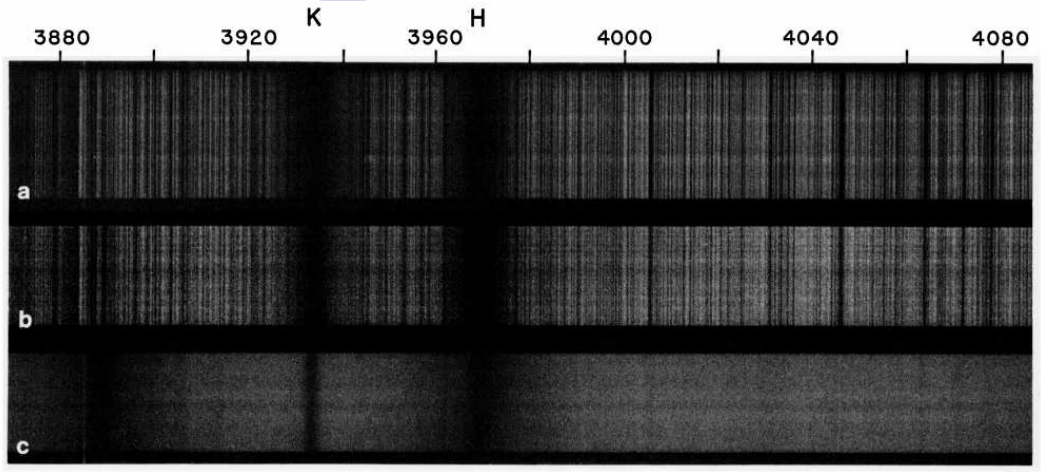

FIGURE 1.3: Spectrum of τ Per as a SB1 (Griffin et al., 1992)

On the other hand, when the spectral lines of both components are visible in the spectrum, those are called double-lined spectroscopic binaries (SB2). In these cases, it is possible to determine the orbit of each component with respect to the center of mass (and, as consequence, the relative orbit) as well as the ratio between the masses of the binary components.

1.1 Reference System and Orbital Elements

The following two rules that have been established in the study of binaries:

- In visual binaries, the angle of position is counted from the North to the East, and
- In spectroscopic binaries, the radial velocity is positive when "moving away".

In order to make them compatible, it is necessary to use an orthogonal clockwise Cartesian reference system whose axis x+ is precisely directed toward the North and the axis y+,

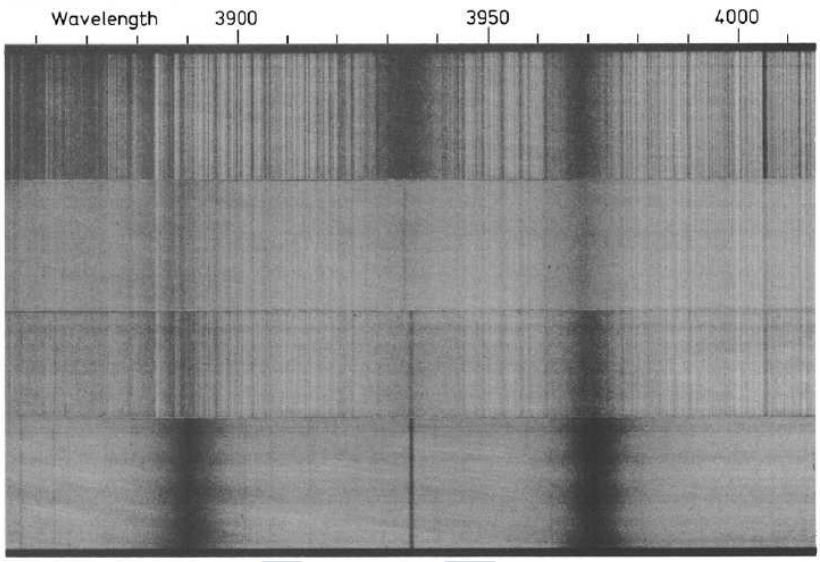

FIGURE 1.4: Spectrum of HR 6902 as a SB2 (Griffin and Griffin, 1986)

toward the East. Both axes are located on the plane that is perpendicular to the direction of observation, while the direction of axis z+ is from the observer to the star (see Figure 1.3).

In the case of visual binaries, the principal star (the brighter) is located at the origin of the coordinates but, when we study spectroscopic binaries, said point is the location of the center of mass of both components.

The orbital elements that are usually considered are those of Campbell, listed as follows: P, is the orbital period, T, is the epoch of the periastron passage. e, is the eccentricity of the ellipse, a, is the semi-axis major of the ellipse, i, is the inclination or angle that forms the angular moment vector ($\vec{c} = \frac{1}{2}\,\vec{r} \wedge \dot{\vec{r}}$) with the z+ axis. If the motion is direct the inclination has values between 0° and 90°. In the case of retrograde motion, it will be between 90° and 180°. Ω is the angle of the node or that which forms the northern direction with the ascendant node (this is counted clockwise.), and Ω is the argument of the periastron or the angle counted in the direction of motion on the orbital plane from the ascendant node to the periastron.

As is usual in the two-body problem, we use *f*, E, and M to denote the true anomaly, the eccentric anomaly, and the mean anomaly, respectively, with n= $\frac{2\pi}{P}$ being the mean motion. Observer (Earth)

If we are dealing with a visual binary, the semi-axis major is given in arc seconds as it is an angle and it is usually expressed as a'', and regarding the angle of the node, Ω, it is not possible to determine the ascendant node by only using astrometric measurements. For that reason, Ω <180° is used by convention.

On the other hand, if the observation data are only radial velocities (spectroscopic binaries), it is not possible to determine the angle of the node (Ω), the semi-axis major (a), nor the inclination (i) as separate values. Nevertheless and as we will can see with SB2s, it is possible to obtain, in units of distance (i.e., in astronomical units or in Gm), the product of a.sin(i) = (a_1 + a_2). sin(i) (where a_1 and a_2 are the semi-axes major of the orbits of each component

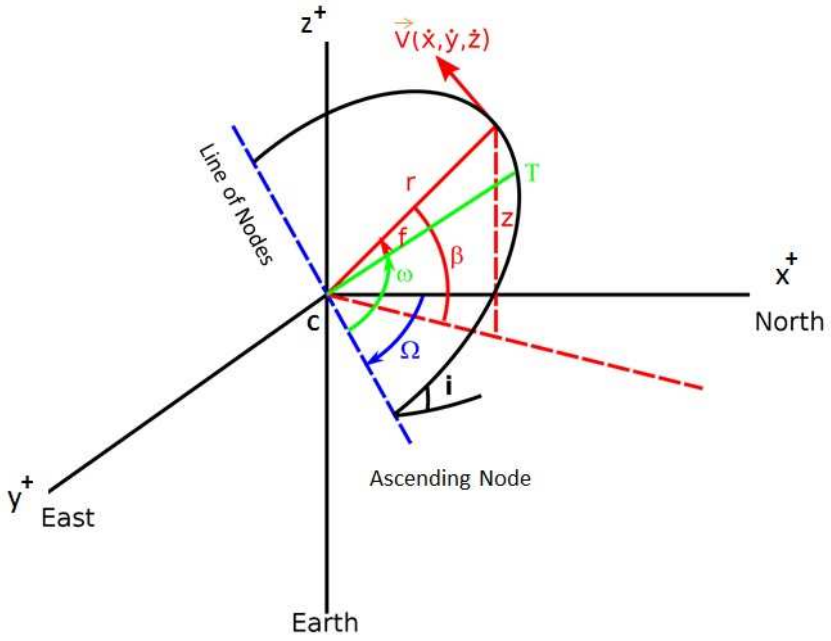

FIGURE 1.5: Orbital elements

with respect to the center of mass).
From that, it follows that for a double-lined spectroscopic binary, the orbital information is: P, T e, a.sen(i) (in Gm) and ω (in a SB1, we obtain $\omega_1 = \omega + 180°$ from the orbit calculation). In the case that it is possible to also calculate its the visual orbit: P, T, e, a$''$, i, Ω, we can deduce not only the orbital parallax, $\pi'' = \frac{a''}{a_{(in\ a.u)}}$, but the masses of each separate component as well. In effect, in visual binaries, the sum of the masses is calculated, as follows:

$$\mathcal{M}_1 + \mathcal{M}_2 = \left(\frac{a''}{\pi''}\right)^3 \cdot \frac{1}{P^2} \tag{1.3}$$

(π'', the orbital parallax) while, as we just mentioned and will explain in the next section, we can obtain the ratio, $\mathcal{M}_1$ / $\mathcal{M}_2$ for SB2 systems.

We can see the undoubtable interest in trying to resolve spectroscopic binaries by high resolution techniques such as speckle interferometry. In the last decades, several astronomers have been involved in such research: (Balega et al., 2002; Bonneau et al., 2010; Hartkopf et al., 1996; Horch et al., 2012; Mason et al., 2001; McAlister, 1976b; Tokovinin et al., 2013)

Three years ago, Docobo et al.(2014) proved that with only one precise speckle measurement and the parallax, it is possible to obtain the three dimensional orbit of a spectroscopic binary with an orbit (Docobo et al., 2014a). However, it is advisable to have at one's disposal a collection of speckle measurements in order to proceed to the calculation of a more consistent visual orbit.

1.1.1 Radial Velocity in the Terms of the Orbital Elements

In accordance with Figure 1.6, it is clear that the radial velocity of a component of a binary with respect to the observer, Vr, can be resolved in the following manner:

$$V_r = V_r + \dot{z} \tag{1.4}$$

with $V_\circ$ being the radial component of the velocity vector of the center of mass, C, with respect to the observer, and z being the radial component of the star with respect to C.

If β is the angle that forms the vector, $\vec{r}$ (x,y,z), with its projection on the xy plane, it is clear that

$$z = r \,.\, sin(\beta) \tag{1.5}$$

On the other hand, we extend the straight lines that contain the position vector, $\vec{r}$, its orthogonal projection over the xy plane, and to the line of the nodes respectively, and we cut them with a sphere of unit radius. The result is that a right angled spherical triangle is formed; two of the sides are β and $\omega + f$ and the inclination, i, is one angle of said triangle (see Figure 1.6).

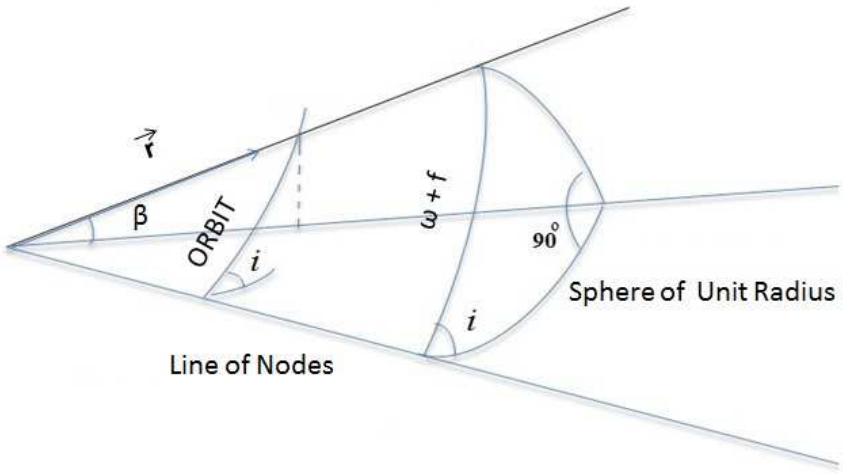

FIGURE 1.6: 3D orbital elements

If we now apply the mnemonic rule of the pentagon of Neper, we obtain:

$$cos\,(90^\circ - \beta) = sin\,(i).sin\,(\omega + f) \tag{1.6}$$

or

$$sin\,(\beta) = sin\,(i).sin\,(\omega + f) \tag{1.7}$$

Carrying over the last formula to (2), we obtain

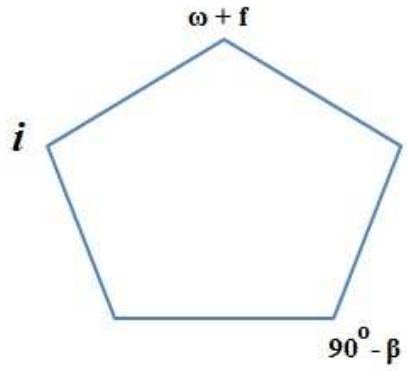

FIGURE 1.7: Pentagon of Neper.

$$z = r \,.\, sin\,(i).sin\,(\omega + f\,) \tag{1.8}$$

Deriving this function with respect to time and keeping in mind the known expressions of the two-body problem:

$$r = \frac{p}{1+e.cos(f)},$$

$$\dot{r} = \frac{2ce}{p} \,.\, \sin(f)\ ,$$

$$2c = r^2 . \dot{f}$$

the result is that

$$\dot{z} = \frac{2c.sin(i)}{p}.[cos(\omega + f\,) + e.cos(\omega)] \tag{1.9}$$

Here, "c" is the areal velocity, and "p" is the parameter, p = a. (1 - e^2), of the ellipse. Finally, if we use

$$\frac{2c}{p} = \frac{n\,.\,a}{\sqrt{1\,-\,e^2}} \tag{1.10}$$

we arrive at

$$\dot{z} = \frac{n\,.\,a.\,sin\,(i)}{\sqrt{1\,-\,e^2}}\,[cos\,(\omega\,+f\,) + e\,.\,cos\,(\omega)] \tag{1.11}$$

or

$$\dot{z} = K\,[cos\,(\omega\,+f\,) + e\,.\,cos\,(\omega)] \tag{1.12}$$

where

$$K = \frac{n \,.\, a. \, sin\,(i)}{\sqrt{1 - e^2}} \tag{1.13}$$

In this way, the radial velocity, V_r, according to the expression (1), can be written as

$$V_r = V_\circ + K.\,[cos\,(\omega + f) + e \,.\, cos\,(\omega)] \tag{1.14}$$

1.2 Orbital determination

One of the classical methods to determine the orbit of a spectroscopic binary is the Lehmann-Filhes method (Binnendijk, 1960; Lehmann-Filhés, 1894) and is based on the computation of some relevant parameters of the radial velocity curve. Another useful method is that designed by J. Wilsing and H.N. Russell (Russell, 1902; Wilsing, 1893). Both methods start from the known value of the orbital period. In this first case, the main inconvenience is to draw the curve that fits the (V_r, t) observations. For this reason and trying to resolve this problem, some authors have utilized interpolation polynomials in order to arrange an analytic expression of the function V_r(t). In concert, A.Elipe and V. Lanchares suggested the use of the Spline cubic interpolation polynomials, achieving very good results (Elipe and Lanchares, 1988).

In the following subsections, first we will explain both methods mentioned as well as the use of the Spline polynomials and, later, we will put these methods into practice by checking them via a multiple test.

Starting from prefixed orbits ($V_\circ$, P, T, e, a sin(i), and ω_1) that corresponding to a theoretical SB1, we used as observations the ephemerides of that orbit calculated in 25 epochs along one period, but slightly modified. These small changes in the radial observations must be considered as distributed aleatory observational errors. The goal of this practice is to check as the different methods recover the initial orbit.

1.2.1 Method of Lehmann-Filhés

Taking "time" as the abscissas axis and "radial velocity" as the ordinates axis, the observations (V_r, t) of a spectroscopic binary fit by means of a curve similar to that showed in the Figure (1.8), which will be denominated the Radial Velocity Curve. The radial velocity of the center of masses, C, of the system with respect to the Earth, $V_\circ$, can be consider a constant, and along an orbital revolution, the star observed returns to the same position with respect to C. According to this, the total variation of V_r with respect to $V_\circ$ must be zero in each period, that is to say,

$$\int_t^{t+P} (V_r).dt = \int_t^{t+P} (\dot{z}).dt = \int_t^{t+P} dz = z_{t-P} - z_t = 0 \tag{1.15}$$

In this manner, if we draw a line, DD$'$ (see Figure 1.8) parallel to the x-axis (the ordinate of which is $V_\circ$), the surfaces limited by the curve and that parallel (in the same orbital period), have to be equal according to the integral (1.15).

In the practice, we have to proceed in the inverse sense looking for the DD′ parallel that makes the two surfaces, S1 and S2, equal in the example of the Figure (1.8), $V_\circ$ = +10.2 Km/sec.

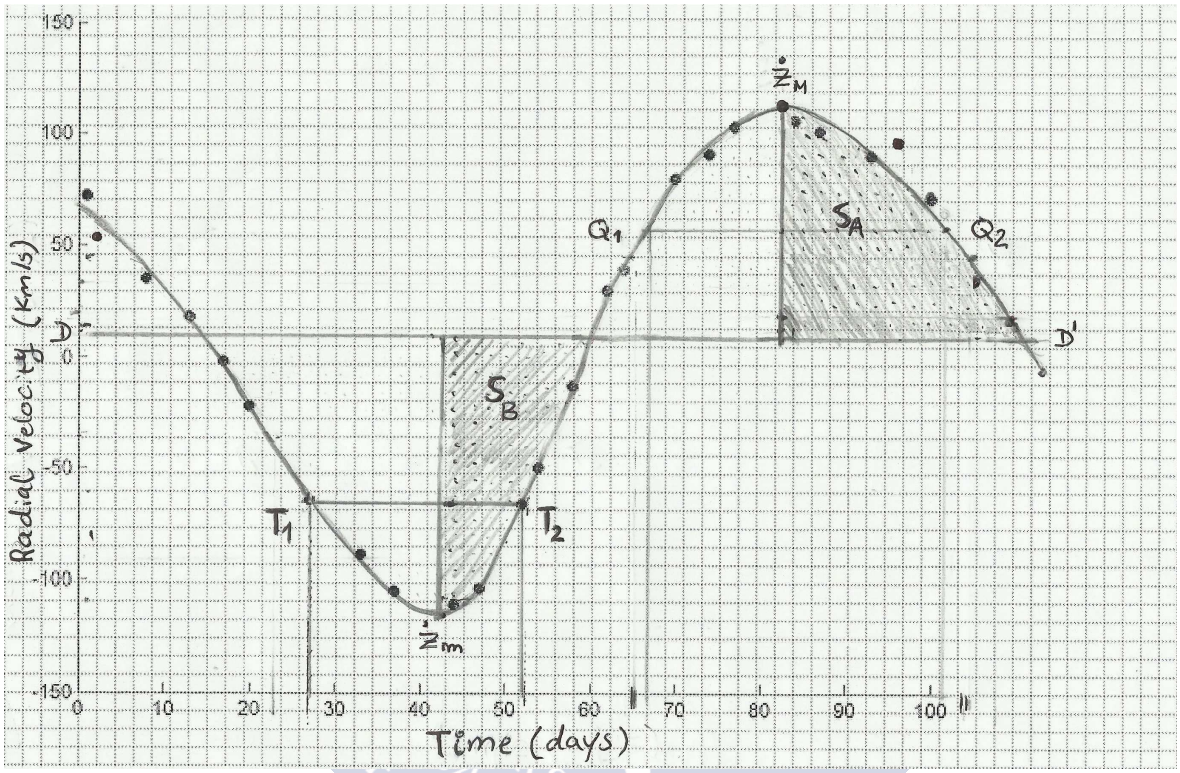

FIGURE 1.8: Radial velocity curve for the data set No. 1.

Fixing our attention in the curve

$$\dot{z}(t) = K.\,[e.\,cos\,(\omega\, +\, f\,) + e\,.\,cos\,(\omega)] \tag{1.16}$$

, where $\dot{z}_M$, $\dot{z}_m$ are its maximum and minimum values. We have

$$z_M \;=\; K.\,(e.\,cos(\omega) + 1),$$

$$z_m \;=\; K.\,(e.\,cos(\omega) - 1)$$

So, measuring $\dot{z}_M$ and $\dot{z}_m$ in the graph, we obtain the values of K and e. cos(ω):

$$K = \frac{\dot{z}_M + \dot{z}_M}{2} \tag{1.17}$$

$$e.cos(\omega) = \frac{\dot{z}_M - \dot{z}_M}{2K} \tag{1.18}$$

In order to deduce the value of e. sin (ω), we will proceed as follows.

At the points A and B of the curve $\dot{z}$(t), we have $\dot{z}_A = \dot{z}_B = 0$, because $V_r = V_\circ$, then

$$\cos(\omega + f_A) = \cos(\omega + f_B) \Rightarrow \omega + f_A - (\omega + f_B).$$

According to (1.8), we will have:

$$z_A = r_A.\ \sin(i).\ \sin(\omega + f_A)$$

$$z_B = r_B.\ \sin(i).\ \sin(\omega + f_B),$$

and from here:

$$\frac{z_A}{z_B} = - \frac{1+e.cos(f_B)}{1+e.cos(f_A)}$$

$$\frac{z_A+z_B}{z_A-z_B} = - \frac{e.(cos(f_A)-cos(f_B))}{2+e.(cos(f_A)-cos(f_B))}$$

On the other hand,

$$\cos(f_A) = \cos(f_A + \omega).\ \cos(\omega) + \sin(f_A + \omega).\ \sin(\omega)$$

but as:

$$\cos(\omega + f_A) = \cos.\ (\omega + f_B) = - e.\ \cos(\omega)$$

the result is

$$\cos(f_A) = - e.\ \cos^2(\omega) \pm \sin(\omega).\ \sqrt{1 - e^2.cos^2(\omega)}$$

and, similarly

$$\cos(f_B) = - e.\ \cos^2(\omega) \mp \sin(\omega).\ \sqrt{1 - e^2.cos^2(\omega)}$$

Substituting these expressions of cos (f_A) and cos (f_B) in (2.19), we can write:

$$\frac{z_A+z_B}{z_A-z_B} = \mp \frac{e.sin(\omega)}{\sqrt{1-e^2.cos^2(\omega)}},$$

and from here we deduce

$$e.\ \sin(\omega) = \mp \frac{z_A+z_B}{z_A-z_B}\ .\ \sqrt{1 - e^2.cos^2\omega}$$

Now we will explain our calculation of the values of z_A and z_B. From the Figure (1.8), we have

$$S_A = \int_{t_M}^{t_A} (\dot{z}).dt = \int_{z_M}^{z_A} (dz) = z_A - z_M = Z_A$$

because in the ascending node is

$$\omega + f_M = 0,$$

then,

$$z_M = r_M . \sin(i). \sin(\omega + f_M) = 0.$$

In the same form, we arrive to

$$S_B = \int_{t_m}^{t_B} (\dot{z}).dt = \int_{z_m}^{z_B} (dz) = z_B - z_m = z_B$$

being that, in this second case,

$$\omega + f_m = 180°, z_m \Rightarrow 0°$$

Therefore, it will necessary to measure the surfaces S_A and S_B in the graph to determine the value of e. sin (ω), and as e. cos (ω) was known in (1.18), we will have the two values of "e" and "ω".

Regarding the periastron passage, T, in said instant the value of $\dot{z}$ will be

$$\dot{z} (T) = K. (1 + e). \cos(\omega),$$

because in it, f = 0°. On the other hand, in the apoastron, Q, is f = 180°, and then

$$\dot{z} (Q) = K(e - 1). \cos (\omega)$$

In the Figure (1.8) there are two points at which the function, $\dot{z}$, takes the value

$$\dot{z}(T) = K. (1 + e). \cos (\omega),$$

and another two when

$$\dot{z}(Q) = K. (e - 1). \cos(\omega).$$

Among these four points, it is necessary to select those two in which the difference T - Q is a semi-period (P/2).

Finally, from (2.13) we can deduce the value of

$$a.\sin (i) = \frac{K.\sqrt{1-e^2}}{n} = \frac{K.\sqrt{1-e^2}.P}{2\pi}$$

This value is given in distance units, usually in Km. or multiples of it as Gm (10^9m).

1.2.2 Method of J. Wilsing and H.N Russell

This method is useful when the eccentricity is small and the orbital period is supposed to be known. In the case, e = 0, the graph of the function

$$V_r = V_\circ + K.\left[cos\,(\omega + f) + e\,.\,cos\,(\omega)\right], \tag{1.19}$$

corresponds to the cosine function. The curve distorns when the orbit is elliptic. In these conditions, we can consider Vr developed in Fourier series to be in the form:

$$V_r = A_0 + A_1.\,cos\,(nt + \alpha_1) + A_2.\,e.cos\,(2n\,t + \alpha_2), \tag{1.20}$$

where $\alpha_1 = \omega$ - n.T, $\alpha_2 = \omega$ - 2 n.T, A_0= V_0, A_1= n. a sin(i), n = $\frac{2\pi}{P}$.
It is possible to rewrite this expression as

$$V_r = B_0 + B_1.\,cos\,(nt) + B_2.\,sin\,(n\,t) + B_3.\,cos\,(2n\,t) + B_2.\,sin\,(2n\,t) \tag{1.21}$$

Indeed, starting from

$$z = r.\,sin(i)\left[sin\,(f).\,cos\,(\omega) + cos\,(f).\,sin(\omega)\right], \tag{1.22}$$

and deriving with respect to the time, we obtain

$$\dot{z} = sin(i)\left[cos\,(\omega)\frac{d}{dt}(r.\,sin\,(f) + sin(\omega)) + (\frac{d}{dt}(r.\,cos\,(f))\right]. \tag{1.23}$$

Now, if we take into account the well-known developments:

$$r.\,sin\,(f) = a\,sin\,(M) + \frac{1}{2}a.\;e.\,sin(2M) + ... \tag{1.24}$$

$$r.\,cos\,(f) = \frac{1}{2}\,a\,.e + a\,cos(M) + \frac{1}{2}a.\,e\,cos(2M) + ... \tag{1.25}$$

where M = nt - nT is the mean anomaly. Substituting (1.24) and (1.25) in (1.23), results:

$$\dot{z} = n.\,a.\,sin\,(i)\left[cos\,(\alpha_1 + nt) + e.\,cos\,(\alpha_2 + 2nt)\right] \tag{1.26}$$

Comparing now the expressions (1.20), (1.21), and (1.26), We have:

B_0 = A_0 = V_0,
B_1 = A_1 cos (α_1),
B_2 = A_1 sin (α_1),
B_3 = A_1 e. cos (α_2),
B_4 = A_1 e. sin (α_2).

If the equation (1.21) is resolved by means of the least square technique using a large number of observations (V_r, t), the coefficients B_i can be calculated. From them we deduce:

$$V_0 = B_0$$

$$A_1 = \sqrt{(B_1)^2 + (B_2)^2}$$

$$\sin(\alpha_1) = \frac{B_2}{A_1}$$

$$\cos(\alpha_2) = \frac{B_1}{A_1}$$

$$e = \sqrt{\frac{B_3^2 + B_4^2}{A_1^2}}$$

$$\sin(\alpha_2) = \frac{B_4}{A_1.e}$$

$$\cos(\alpha_2) = \frac{B_3}{A_1.e}$$

$$T = \frac{\alpha_2 - \alpha_1}{n}$$

$$\omega = \alpha_1 + n.T = \alpha_2 + 2.n.T$$

$$a.\sin(i) = \frac{A_1}{n}$$

This method is used fundamentally for e < 0.1 but (Russell, 1902) extended it to second order terms, increasing its utility. An important advantage of this method is that observations near the maximum and minimum of the curve are not necessary.

1.3 Application of the orbit calculation methods

We start from the following SB1:

$$\begin{aligned} P &= 100\ days \\ T &= 50\ days \\ e &= 0.2 \\ a \cdot sin(i) &= 150\ Gm \\ \omega_1 &= 225^\circ \\ V_0 &= 10\ km/s \end{aligned}$$

As we commented in (1.2), from the orbits, ephemerides in 25 times were calculated. These ephemerides were modified in three different ways giving place to three sets of data: 1, 2, and 3.

For the first set of data, the observations are almost even distributed along one period (see Table 1.1, left columns). For the set no. 2, the observations are clustered around the maximum and minimum values of the radial velocity (see Table 1.1, central columns). Finally, the last set of data is taken for observations that poorly cover the maximum and the minimum of the radial velocity (see Table 1.1, right columns).

t	V_r
1	76.2
3	52.0
8	35.5
13	18.0
17	-7.1
20	-22.0
27	-68.0
33	-88.3
37	-105.0
44	-110.6
47	-108.3
52	-62.0
54	-49.5
58	-18.0
62	33.0
64	39.5
70	80.1
74	86.0
77	103.4
83	112.5
84	106.0
87	97.3
93	83.7
97	89.5
100	71.0

No. 1

t	V_r
1	76.2
13	18.0
22	-27.0
33	-88.3
37	-105.0
40	-122.0
41	-110.3
43	-119.0
44	-110.6
47	-108.3
49	-93.9
52	-62.0
58	-18.0
74	86.0
77	103.4
79	100.6
81	99.0
83	112.5
84	106.0
86	100.8
87	97.3
90	99.8
91	91.2
93	83.7
97	89.5

No. 2

t	V_r
1	76.2
3	52.0
5	51.0
8	35.5
11	26.8
13	18.0
16	10.8
20	-22.0
22	-27.0
37	-105.0
43	-119.0
47	-108.83
53	-56.4
54	-49.5
58	-18.0
59	7.0
62	33.0
64	39.5
67	69.3
70	80.1
79	100.6
83	112.5
91	91.2
93	83.7
97	89.5

No. 3

TABLE 1.1: Three sets of synthetic observations covering different situations with different random errors. Left table shows almost even distributed observations. Central table stands for observations covering the vicinity of the maximum and minimum velocity epochs. Right table scarcely covers the maximum and the minimum.

1.3.1 Application of the Lehman–Filhés method

First, we applied this method in the traditional way, working by hand. For each set of data, we drew the corresponding curve that fits the observations and then, using it, we obtained successively the values of the V_0, e, ω, T, Q, K, and $a.\sin(i)$, according with that described in (1.2.1). Although we start from an approximate value of the period, P_0, the final value of this orbital element is deduced from P = 2 (Q − T). Figure 1.8 shows the graph of the radial velocity curve for case 1. For the other two cases, the modus operandi is similar. We named these sub-cases LF_1, LF_2, and LF_3.

1.3.2 Using approximation functions

Let us assume that the period of the orbit, P, is known and we have all the observations reduced to one period. Our goal is to obtain a smooth curve fitting the observations. The use of Spline cubic interpolation polynomials under appropriate boundary conditions have been used to this end (Elipe and Lanchares, 1988). However, in many cases the corresponding linear system to determine the coefficients is ill conditioned and numerical errors appear. To overcome ill conditioned linear systems, we use a piecewise cubic polynomial under periodicity conditions, in a similar way as it is done for a method that combine visual and spectroscopic data (Lanchares, 1992). In this way, we divide the interval $[0, P]$ into four sub-intervals

$$I_1 \equiv [0, t_1], \quad I_2 \equiv [t_1, t_2], \quad I_3 \equiv [t_2, t_3], \quad I_4 \equiv [t_4, P]$$

and consider in each one a cubic polynomial

$$p_j(t) = a_0^j + a_1^j t + a_2^j t^2 + a_3^j t^3, \quad j = 1, \ldots, 4. \tag{1.27}$$

These polynomials satisfy the following equations

$$\begin{aligned} &p_j(t_j) = p_{j+1}(t_j), \quad p_j'(t_j) = p_{j+1}'(t_j), \quad p_j''(t_j) = p_{j+1}''(t_j), \quad j = 1, 2, 3, \\ &p_1(0) = p_4(P), \quad p_1'(0) = p_4'(P), \quad p_1''(0) = p_4''(P). \end{aligned} \tag{1.28}$$

To complete determine the polynomials (1.27) 16 equations are needed, and equations (1.28) sum up only 12. Thus, there are four free coefficients we can choose in order to get the best fit to the observations by means of the least square procedure. Let us assume that the undetermined coefficients are a_0^j, $j = 1, \ldots, 4$ and a_1^1. Then, these coefficients are chosen to minimize

$$R = \sum_{i=1}^{N} (F(t_i) - v_i)^2,$$

where $F(t)$ is the piecewise polynomial function, and they satisfy the linear system

$$\frac{\partial R}{\partial a_0^j} = 0, \quad j = 1, \ldots, 4, \qquad \frac{\partial R}{\partial a_1^1} = 0.$$

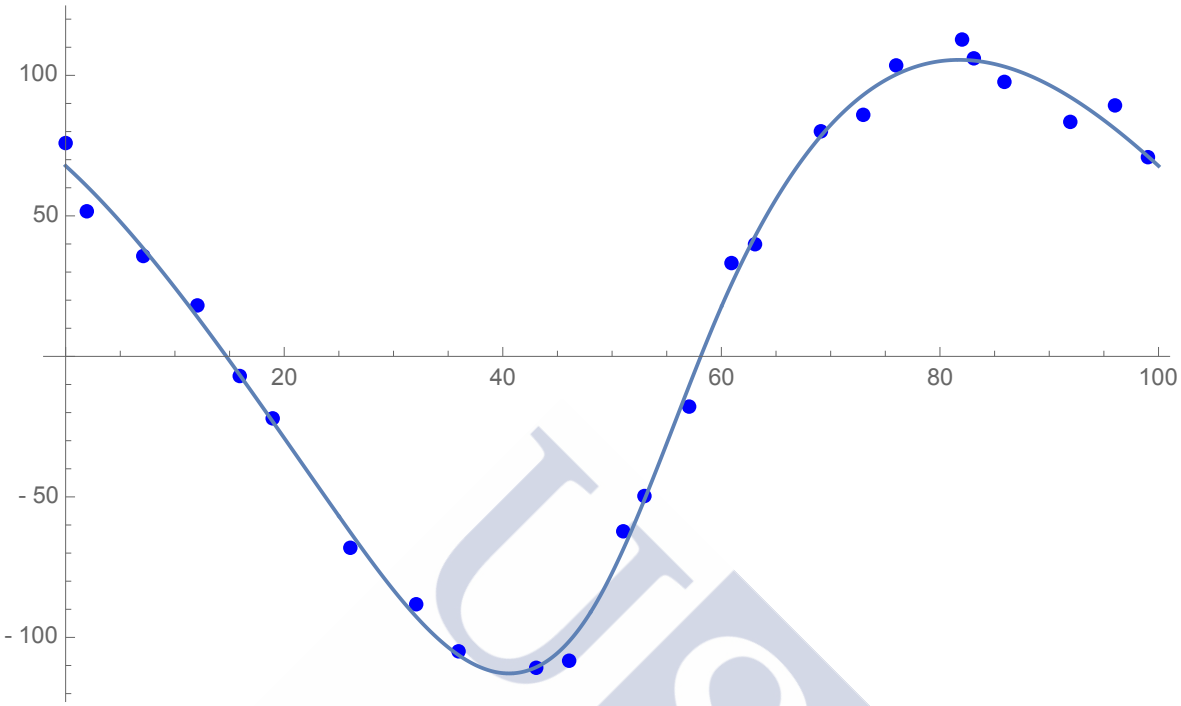

FIGURE 1.9: Piecewise approximation of the function for the data set No. 1.

Once the approximation function is obtained, we mimic the Lehmann-Filhés method.

For the first set of data and P = 100 days, the piecewise approximation function is the following one:

$$W_{1\ 100} = \begin{cases} 0.00147091t^3 - 0.094817t^2 - 3.53327t + 67.7819 & 0 \leq t \leq 25 \\ 0.00692427t^3 - 0.503820t^2 + 6.69179t - 17.4270 & 25 \leq t \leq 48 \\ -0.02104430t^3 + 3.523650t^2 - 186.627t + 3075.67 & 48 \leq t \leq 60 \\ 0.00180812t^3 - 0.589779t^2 + 60.1790t - 1860.44 & 60 \leq t \leq 100 \end{cases}$$

which is represented in Figure 1.9. The selection of intervals is done in an iterative way trying to get the best fit. The starting point is an equal spaced division of the interval [0,100].

We will apply this process to periods of 100, 95, and 105 days. We will have 9 subcases that we named: S_{ij}, with i = 1,2,3, and j = 100,95,105.

As an example, other approximation functions are:

$$W_{2\ 100} = \begin{cases} 0.00212138t^3 - 0.143872t^2 - 2.73983t + 72.4331 & 0 \leq t \leq 25 \\ 0.00719480t^3 - 0.524378t^2 + 6.77283t - 6.83907 & 25 \leq t \leq 48 \\ -0.02185530t^3 + 3.658830t^2 - 194.021t + 3205.87 & 48 \leq t \leq 60 \\ 0.00213912t^3 - 0.660159t^2 + 65.1182t - 1976.92 & 60 \leq t \leq 100 \end{cases}$$

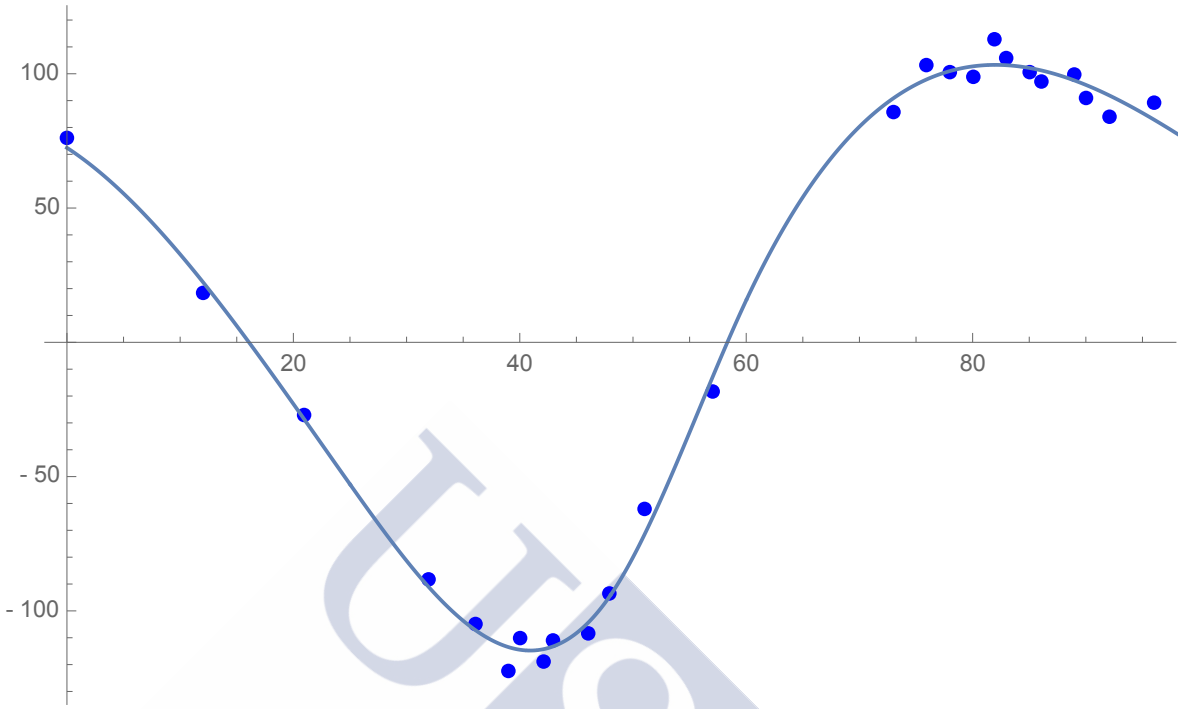

FIGURE 1.10: Piecewise approximation of the function for the data set No. 2.

$$W_{3\ 100} = \begin{cases} 0.000374312t^3 - 0.0642974t^2 - 3.31673t + 66.5067 & 0 \leq t \leq 25 \\ 0.009059050t^3 - 0.7156530t^2 + 12.9672t - 69.1923 & 25 \leq t \leq 47 \\ -0.021918500t^3 + 3.6521800t^2 - 192.321t + 3146.99 & 47 \leq t \leq 60 \\ 0.002273800t^3 - 0.7024320t^2 + 68.9557t - 2078.55 & 60 \leq t \leq 100 \end{cases}$$

See Figures 1.10 and 1.11, respectively.

1.3.3 Application of the Wilsing–Russell method

In this case, we have applied the method to the same nine cases studied in the last section, that is to say, using the fixed periods: 100, 95, 105, and the data sets no. 1, 2, and 3.

We will use the following notation for these sub-cases: WR_{ij}; i = 1,2,3; j = 100,95,105, using only the first order procedure, not the extension of Russell to second order.

We have considered 21 sub-cases in total, 3 LF_i, 9 S_{ij}, and 9 WR_{ij}. The orbital elements corresponding to these sub-cases are shown in Table 1.2, in which column 1 shows the different studied cases, columns 2 to 7 the orbital elements expressed in the usual units, and in column 8 we have calculated the Root Mean Squares (RMS) of the residuals, obtained with the 25 observations, as a quality control.

Solution	V_0 (km/s)	P (d)	T (d)	e	$a \cdot \sin(i)$ (Gm)	ω_1 (°)	RMS
LF_1	10.2	99.5	55	0.150	156	219	18.117
LF_2	10.0	100.0	53	0.160	140	221	13.979
LF_3	11.2	103.8	49.1	0.198	160	216	11.094
$S_{1\ 100}$	9.2	100.0	51.89	0.194	147.3	232.6	5.426
$S_{2\ 100}$	10.1	100.0	50.53	0.203	146.8	224.4	4.981
$S_{3\ 100}$	10.7	100.0	51.02	0.210	149.8	228.8	5.388
$S_{1\ 95}$	6.0	95.0	54.29	0.228	139.4	246.7	11.256
$S_{2\ 95}$	6.6	95.0	51.61	0.197	141.5	233.5	7.065
$S_{3\ 95}$	7.8	95.0	51.56	0.216	145.9	235.3	8.906
$S_{1\ 105}$	9.2	105.0	52.95	0.208	147.3	234.0	8.373
$S_{2\ 105}$	13.7	105.0	50.62	0.255	154.0	227.4	6.318
$S_{3\ 105}$	13.6	105.0	50.51	0.261	155.0	226.5	5.856
$WR_{1\ 100}$	9.1	100.0	50.33	0.181	146.3	227.2	5.925
$WR_{2\ 100}$	8.8	100.0	49.05	0.189	146.0	218.4	5.625
$WR_{3\ 100}$	9.8	100.0	50.18	0.214	148.6	227.1	7.477
$WR_{1\ 95}$	6.1	95.0	51.47	0.137	141.1	232.4	7.165
$WR_{2\ 95}$	5.6	95.0	49.88	0.139	140.8	222.3	5.568
$WR_{3\ 95}$	6.7	95.0	51.98	0.172	143.0	235.1	7.038
$WR_{1\ 105}$	11.9	105.0	49.07	0.233	150.5	221.8	9.149
$WR_{2\ 105}$	12.1	105.0	47.94	0.239	150.8	213.6	8.643
$WR_{3\ 105}$	12.6	105.0	48.77	0.262	153.2	221.2	11.226

TABLE 1.2: Orbital elements and RMS for the 21 subcases studied.

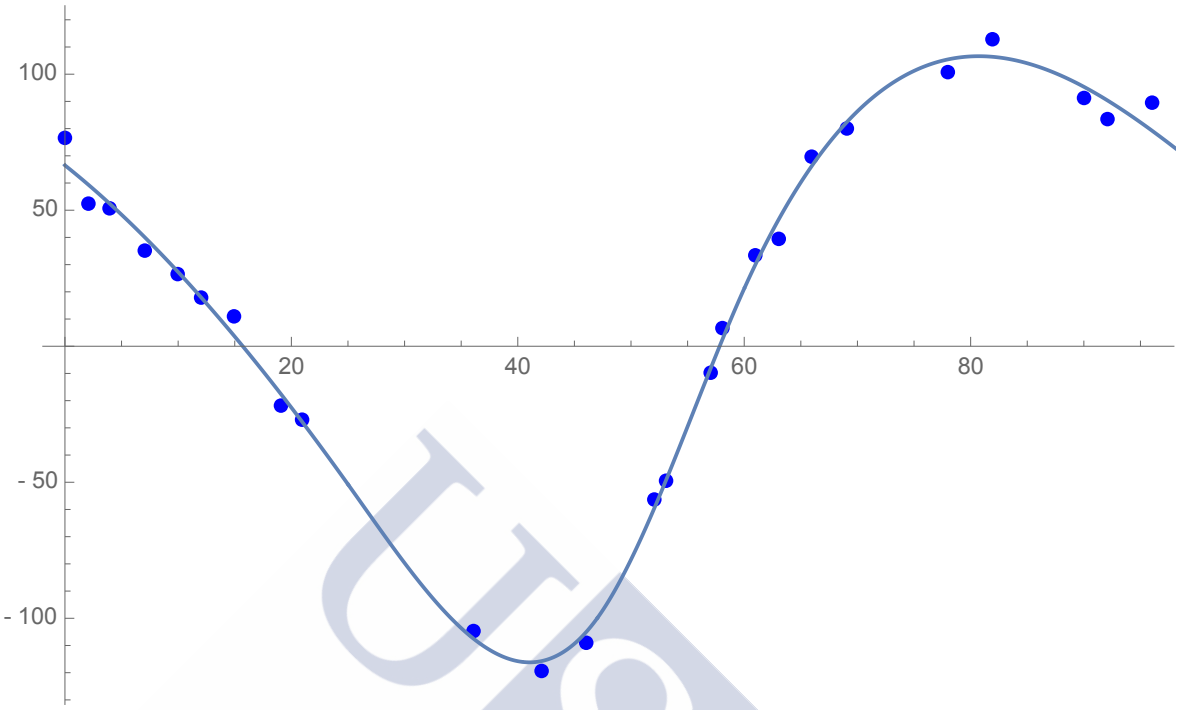

FIGURE 1.11: Piecewise approximation of the function for the data set No. 3.

1.3.4 Comments about the results

As we could expect, the best results are obtained by using the approximation functions (in this case the Spline functions) in order to use a correct curve V(t) to calculate the orbital elements. Drawing by hand these curves, we deduced only approximate results.

Regarding the application of the Wilsing-Russell method, in spite of working only with first order, a few cases give acceptable results.

From Table 1.2, we can find that the best cases follow this order: $S_{2\ 100}$, $S_{3\ 100}$, $S_{1\ 100}$, $WR_{2\ 95}$, $WR_{2\ 100}$, $S_{3\ 105}$, and $WR_{1\ 100}$.

In any case, all of these solutions can be improved using ad-hoc algorithms, for example the classical least-squares minimization or equivalents.

USC
UNIVERSIDADE
DE SANTIAGO
DE COMPOSTELA

Chapter 2

CORAVEL Radial Velocity Observations at Cambridge Observatory

This study has represented a wonderful and unique opportunity to work as a link between two of the oldest and highest level universities in Europe, the University of Santiago de Compostela (Spain) and the University of Cambridge (United Kingdom). This relationship was the result of ongoing scientific communication and the good collaboration between Prof. Roger Griffin from the Cambridge University (36-inch Observatory) and Prof. Jose Angel Docobo from the Ramon Maria Aller Observatory at the University of Santiago de Compostela. In this study, we have worked on the construction of a model of spectroscopic binaries. The major part of our observational work at Cambridge was monitored by Professor Griffin using the 36-inch telescope. In this text, we will also talk about Professor Griffin, achievements, and his efforts in this field as well as use of a spectrometer to monitor these binaries.

2.1 Roger Griffin

Roger Francis Griffin is one of the most important astronomers in the world in the study of double stars, especially spectroscopic binaries. He was born in Banstead, Surrey, England on August 23, 1935. He finished Secondary School in 1954 at Caterham School, Surrey and he graduated with a Bachelor degree in 1957. He obtained the Ph.D. in 1960 from St. John's College, Cambridge University. Next, we present his principal academic merits.

2.1.1 Memberships

Prof. Griffin is an active member of many Astronomical organizations

- 1949 British Astronomical Association (BAA).
- 1957 Royal Astronomical Society (RAS).
- 1961 International Astronomical Union (IAU).

FIGURE 2.1: Prof. Roger Francis Griffin (Institute of astronomy University of Cambridge)

.

- 1965 Astronomical Society of The Pacific (ASP).
- 1983 Astronomical Society of India (ASI).

2.1.2 Awards

- 1953 Major Open Scholarship, St. John College, Cambridge.
- 1955,1956 Prizes for Tripos performance.
- 1958 Sir Henry Strakosch Award to visit South Africa observatories.
- 1980 Jackson - Gwilt Medal & Gift, Royal Astronomical Society, England.
- 1991 International conference held in his Honour at a venue in the Swiss Alps.

2.1.3 Academic Positions

- 1960 - 1961 Carnegie Fellow, Mount Wilson Observatory, California.
- 1962-1965 Junior Assistant Observer, Cambridge observatories.
- 1962-1965 Research Fellow, St. John's College, Cambridge.
- 1965-1970 Mr. & Mrs. John Jaffe Research Fellow of the Royal Society.

- 1970-1972 Consultant Astrophysicist to St. John's College, Cambridge.
- 1972 Fellow, St. John's College, Cambridge.
- 1973-1992 Assistant Director of Research, institute of astronomy, Cambridge University.
- 1992-2001 Reader in Observational Astronomy, Cambridge.
- 2001-2002 Professor of Observational Astronomy, Cambridge.
- 2002 Nominally retired but still at work as always.

2.1.4 Astronomical Visits

Professor Griffin carried out numerous scientific visits as a Guest Investigator, Visiting Associate, or Visiting Observer in order to observe binaries, share experience, and develop new observational methods in various countries, e.g., about 45 visits Mount Wilson & Palmer (California), 41 visits to Haut-Provence (France), 11 to Dominion Astrophysical Observatory (Victoria, B.C), 7 visits to Calar Alto (Spain), and 5 to the European Southern Observatory (Chile).

2.1.5 Publications

Roger Griffin expended tremendous effort in scientific writing; he has published about 500 research papers. The first paper was entitled "Coronal lines in the post-maximum spectra of RS OPH" and was published in The Observatory journal (Griffin and Thackeray, 1958). The second one was in 1960, "Photoelectric Measurements of the λ 4200 A CN Band and the G Band in G8-K5 Spectra" in the journal, Monthly Notices of the Royal Astronomical Society (Griffin and Redman, 1960). These were the beginning of a series of research papers that serve as a guide to the study and analysis of spectroscopic binaries and the development and invention of new methods to analyze the spectra of stars. One of these wonderful efforts is the series of individual research papers entitled, "Spectroscopic Binary Orbits from Photoelectric Radial Velocity", with the first paper in this series being: "Photoelectric radial velocities of four K stars" (Griffin, 1969). As of march 2016 the total has reached 246 papers. **See Appendix B**, Griffin Binary Orbits from Photoelectric Radial Velocity series. Speaking about such a large number of research papers, we asked what, in his opinion, the most interesting paper among all of them. He said that he enjoyed working with all of them but there are two special ones. The first one is "A photoelectric radial-velocity spectrometer" (Griffin, 1967) in which the principle of directly measuring radial velocity directly by using the photoelectric spectrometer was discussed, as well as his modifications and his inventions of instrumentation that had the effect of improving and facilitating the study of spectroscopic binaries until today. The second one is "Spectroscopic binary orbits from photoelectric radial velocities. Paper 150: Zeta Cancri C"(Griffin, 2000b). Zeta Cancri is well-known a triple system and the paper contains 47 pages which required a long time to prepare and analyze in order to resolve this interesting system.

Spectroscopic binary orbits from photoelectric radial velocities series, a total of orbits 291 for 289 stars were published in this series through paper number 200, two star, have two orbit, (HD 158609 and HD 100518). Griffin has a habit of publishing a summary of works for every 50 published research articles. These summaries provide assistance and facilitate research in this area concerning making comparisons between different results and offering the greatest possible benefit scientific (Griffin, 1983, 1991, 2000a, 2008) .

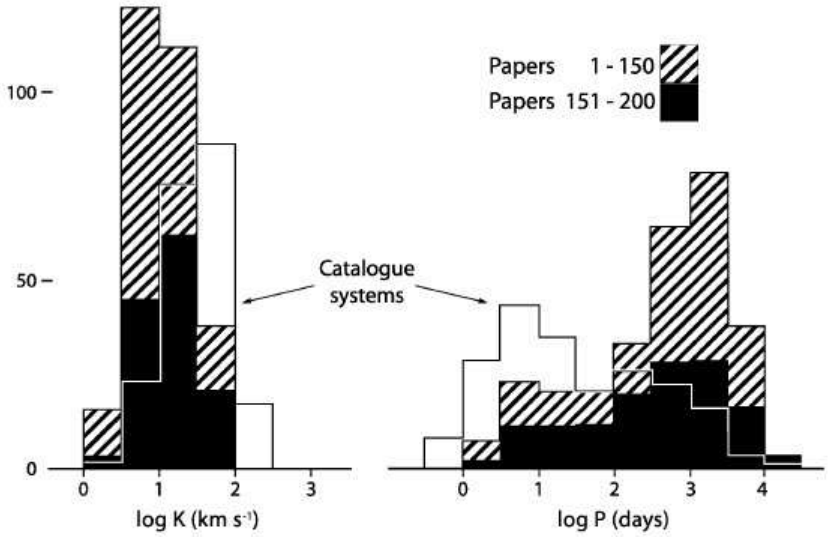

FIGURE 2.2: Distribution of the radial velocity amplitudes and period of 291 SB orbits.

Figure 2.2 shows the relationship between the distribution of the radial velocity amplitudes and period of the orbit (Griffin, 2008). This Figure also shows the monitoring operations during the first 200 papers and those found in The Seventh Catalogue of the Orbital Elements of Spectroscopic Binary System (Batten, Fletcher, and Mann, 1978). From the histogram, the difference can be seen between the two figures because of the relation between the radial velocity amplitude as the inverse cube roots of the period. We can see that the range of the radial velocity amplitude is smaller than the period and also note that all efforts were concentrated on short period and high amplitude. In the same Figure, we can also notice a large difference in values between the 1-150 research papers and the 151-200. We note that the first 150 papers deal with 157 star whereas the last 50 papers explain 134 stars. The explanation for that is that the second set of papers concerned a large number of double-lined systems which have high eccentricity, amplitude, and period of only a few years.

Figure 2.3 is the plot (e - log P) that shows the relation between the eccentricity of the binaries in all of the 200 papers with different kinds of double-lined and single-lined systems. This graph was introduced as a new plot at the conference held to celebrate the publication of Paper 100 in 1991 at the Swiss Alps venue. We can note the expected rise of mean eccentricity with long periods to the right of the plot. In a paper given at a conference, H. A. Abt noted that, from the study of the relation between the eccentricity and the period for the

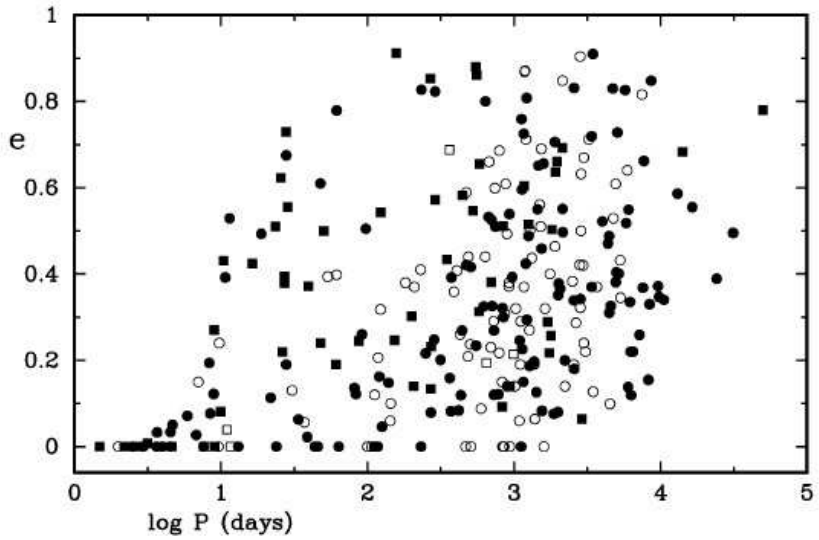

FIGURE 2.3: Distribution of the eccentricities of 291 SB orbits

.

spectroscopic binary stars, the double-lined have larger mean eccentricities than the single-lined , which are at least for the short period (Hartkopf, Harmanec, and Guinan, 2007).

2.2 36-Inch Telescope Observatory

There are four astronomical telescopes at the University of Cambridge: the Northumberland refractor of 11.6 inches installed in 1833, the Thornwood Telescope refractor of 8 inches, the 36-inch reflector, and the Three-Mirror Telescope erected in 1987. The 36-Inch Observatory at Cambridge University is one of the most important resources for analysis of spectroscopic binaries around the world. It was built by the firm of Sir Howard Grubb, Parsons & Co. at Newcastle-upon Tyne (1951). It replaced a much older telescope of the same aperture which was brought to Cambridge from South Kensington when the Solar Physics Observatory moved in 1913.

The average of the clear nights in Cambridge is about 140/year and the telescope is active practically all of these days. The 36-inch telescope has a primary mirror of 37-inches diameter, 36 inches (0.9144 m) clear aperture, six inches (0.1524 m) thick, weighting about 200 kg with a piece of Pyrex glass. The primary mirror produces an image on the top of the telescope tube after light beams cross the secondary small convex mirror which returns the beams coming closer together to the third mirror. The third mirror (Coude flat), which is located in the center of the axis of the rotation of the telescope, sends the beam to the polar axis. There is a short black horizontal cylinder that contains the two totally reflecting quartz prisms which redirect the light vertically downward through a pipe to a small lens that re-images the initial one to calculate the radial velocity of the star, using the Doppler Shift in the spectra of the star (see graph). That method described above is called “cross-correlation”

FIGURE 2.4: 36-Inch Telescope observatory

.

and it was developed by Griffin, in 1967. It caused a revolution in the field of radial velocity due to increased accuracy that it affords.

FIGURE 2.5: The 36-Inch Telescope (the spectrometer is located on the right "the black box")

.

FIGURE 2.6: The primary Mirror

.

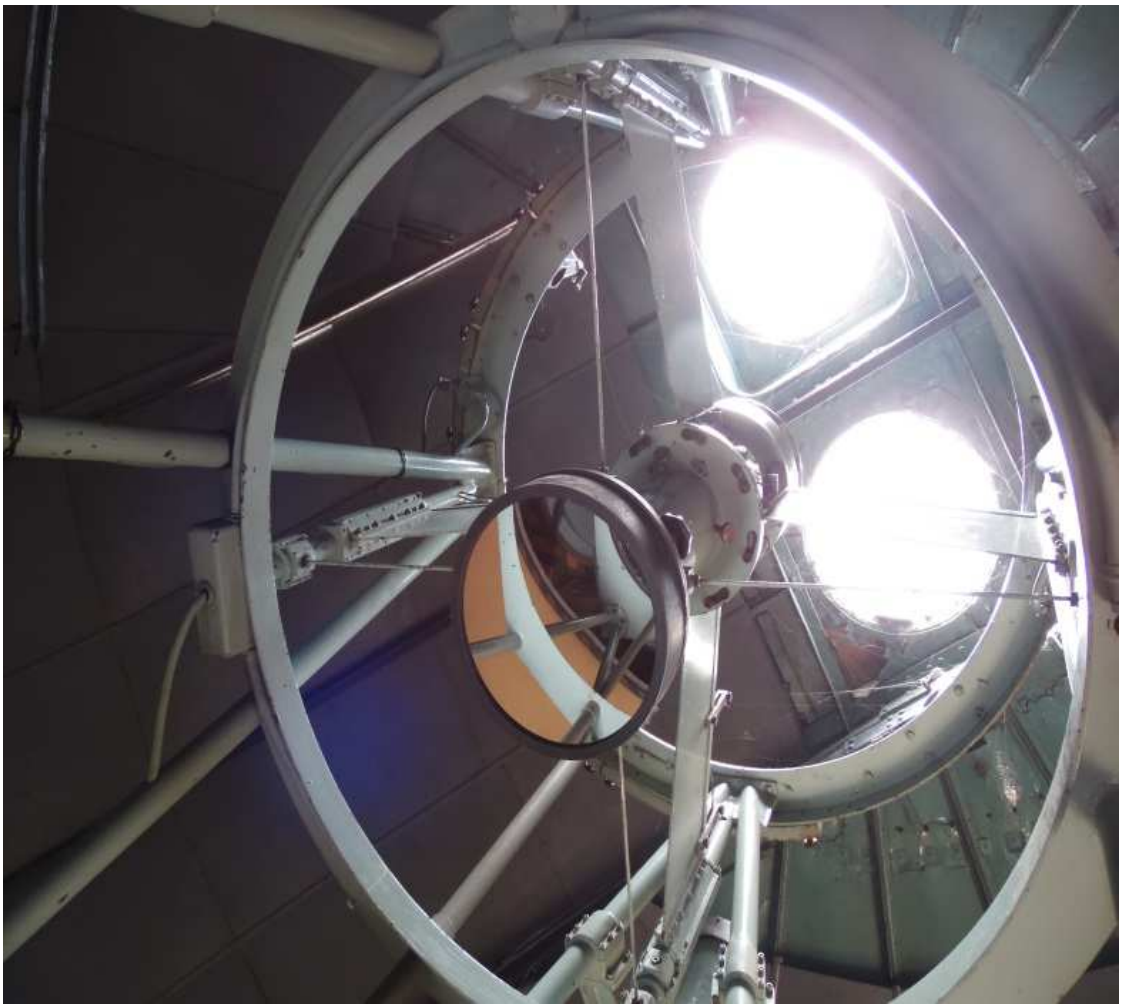

FIGURE 2.7: The secondary Mirror

.

FIGURE 2.8: Third mirror (Coude flat)

.

FIGURE 2.9: Black horizontal cylinder

.

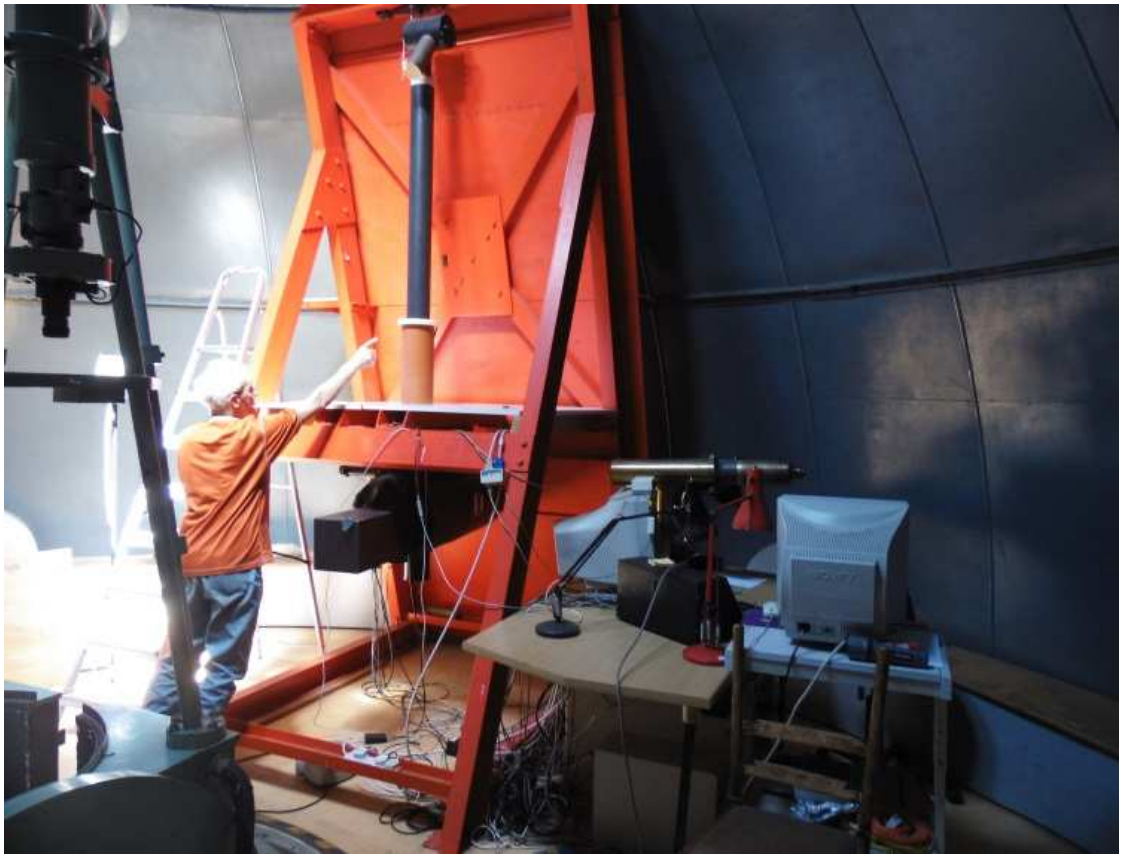

FIGURE 2.10: Vertical pipe

.

FIGURE 2.11: RV Instrument (Black Box)

.

2.3 Photoelectric Radial-Velocity Spectrometer

The beginning of measuring stellar radial velocity taken place in 1868, when sir William Huggins analyzed the emission line of the hydrogen discharge tube to describe the displacement of Ballmer lines visually. Radial velocity was applied photographically for the first time by Vogel (1892). He used a prism with a reciprocal dispersion 13 Å/mm in order to study the spectrogram of the sunlight which is the standard one, as well as the (Hγ) line from the hydrogen Lampe as a stellar spectrogram. He determined the velocity of the star by calculating the displacement between the (Hγ) lines when the solar and stellar spectra register next to each other (Griffin, 1961, 1967; Griffin and Redman, 1960; van Citters, 1974) The Spectrometer analyzes the liner shift (Doppler shift) in the spectrum to determine the stellar radial velocity, using matching technique. The spectrum of the star is registered with a diaphragm which scanning it along the direction of dispersion with a micrometer screw and the match photo-electrically monitored. The transmitted light after the diaphragm of limiting wavelengths λ 4369 Å- λ 4827 Åpass through the Fabry lens to the photomultiplier to measure it as image with absorption lines using this principle of this instrument that called it radial velocity spectrometer (RVS). In Cambridge 36-inch Observatory, the spectrometer has 6-inch collimator and doublet camera lens of 103-inch focal length with dispersion 3.17 Å/mm.

The RVS work began in 1966 and the observations produced by this tool using the 36-inch telescope have the same accuracy as the quality of the velocity in the General Catalogue of Stellar Radial Velocity (Wilson, 1953).

Griffin focused on the comparison between the spectrum of the mask with the star spectrum in the focal plane of the spectrograph. The mask moves at 80 km sec.min^{-1} along the dispersion to the violet region until a match occurs and re-scans back. The distance between the match and that for a comparison star yields to calculate the radial velocity. CORAVEL recorded the transmitted light to determine the dips, which is look like Gaussian distribution (Griffin, 1961; Griffin and Redman, 1960; van Citters, 1974).

2.4 One night work session at Cambridge Observatory

In this work, we try to present a three-dimensional model of the orbits of spectroscopic binaries, both single-lined (SB1) and double-lined (SB2), but the Director of this research, Prof. J.A. Docobo, considered that it was necessary to combine and connect the theoretical processes with the practical side in order to achieve a comprehensive overview of the matter and try to cover all aspects. In this sense, he recommended that it was fundamental that who subscribes goes to Cambridge to perform radial velocities under the supervision of Prof. Griffin. We measured the velocities directly using the photoelectric method in the CORAVEL spectrometer (CORrelation - RAdial -VELocities). In these sections, we will describe in detail the processes to measure the radial velocity by using the 36-inch telescope at Cambridge University. Professor Roger Griffin, who is the responsible of the Observatory, explained the instruments used for the measurements as we described in previous sections (36-Inch Telescope, CORAVEL Spectrometer). A few minutes are required in order to observe spectroscopic binaries with a radial velocity spectrometer.

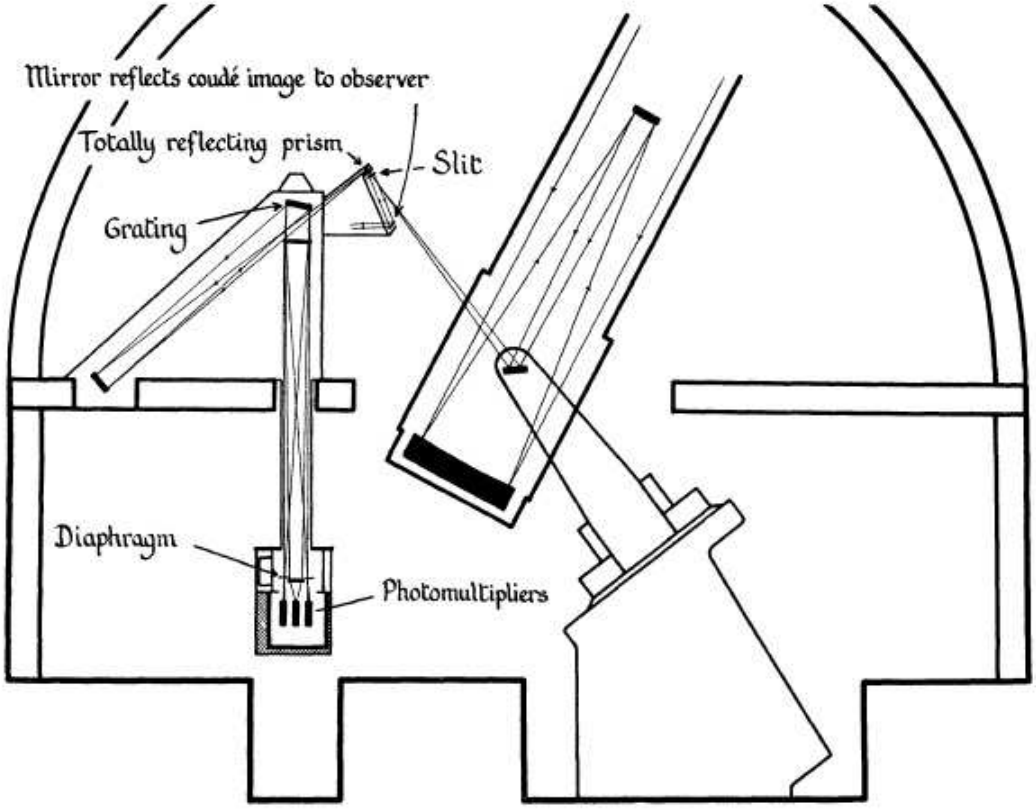

FIGURE 2.12: Diagram of the Cambridge 36-inch telescope and its complimentary instrumentation.

There are a few things that we have to take into account, the sky conditions, and the spectral type less than F0 (this is a technical limitation of the spectrometer) if it is known. We prepared our lists of binaries which contained spectroscopic binaries from the Simbad database, visual binaries from the Washington Catalog and the OARMAC (Catalog of Orbits and Ephemerides of Visual Double Stars), and stars from Professor Griffin's own list. Then we started to measure the radial velocity according to the steps listed below.

- Select the binary star to observe and retrieve its coordinates: the right ascension (α) and the declination (δ).
- Use the control board (see Figure 2.13) to move the telescope to the corresponding coordinates.
- Use the eyepiece on the upper right (see Figure 2.14) to fit the star within the slit. So that its light enters the spectrometer.

FIGURE 2.13: Control-board.

.

- Measure the counts of the number of photons that pass through the mask to the photometer after the slit diffracts the light. (In the Figure 2.15, we can see the change in the photon count).

- The CORAVEL control software (Figure 2.16) uses those values of photon counts to try to plot a graph that describes it as a dip in the intensity of the received light which tells us if the star is single-lined (if there is one dip), or double-lined (if there are two). We can deduce which one is the brightest star and calculate the rotational velocity, as well as the mass ratio of the stars from the ratio between the dips in the case of a double-lined binary.

Each of these tables has 12 columns. Their description is as follows. Column 1, the order number; column 2, the identification of the binary; column 3 and 4, the coordinates of the star; column 5, observing Universal Time; column 6, heliocentric modified Julian day; columns 7, 8, 9, and 10, the profile parameters, column 11, the radial velocity; column 12, the standard deviation in the radial velocity.

We will present now high precise radial velocity observations, performed by the author of this work, during his visits to 36-inch telescope at Cambridge university, under supervision of Prof. R.F. Griffin. Form these radial velocity (RV) registers, we can derive different relevant information. First, about the type of the binary as SB1 (in case one dip, Figure 2.19) or SB2 (in case 2 dips, Figure 2.20), in addition, the stellar rotation, v.sin(I);

FIGURE 2.14: The Observation system.

.

FIGURE 2.15: The photon counter.

large widths means high rotation (see Figure 2.21). Regarding, the sub class of the star, long dep means bigger star, also means more bright (see Figure 2.22), and it is possible also to achieve information about the metallicities of the binaries (see Figure 2.23), taken from

http://mao.tfai.vu.lt, where, V_r, is the radial velocity, and CCF, is cross-correlation function (Baranne, Mayor, and Poncet, 1979). After this, using an specific software, the heliocentric radial velocity is obtained. Observations covering an orbital period are necessary to obtain a good result. Next tables (Figure 2.17 and 2.18) show the results of Radial velocity observations for spectroscopic binaries using Coravel attached to 36-inch telescope at university of Cambridge. These observations were performed for us in the nights from July 7 to 8 and 8 to 9, 2015.

The CORAVEL spectrometer uses a mask of a KIII type star, in which the zones corresponding to the spectral lines are transparent and the rest opaque. The mask moves horizontally over the detector so that when the spectral lines of the star match the ones of the mask, the detector receives less light and we get a dip in the photon count. The displacement of the mask from the central position gives us the radial velocity. In the next graphs, Figures from 2.24 to 2.35 show precise RV measurements performed with the 36 inch reflector by the author of this work during his visits to Cambridge under the supervision of Prof. R. F. Griffin. The points represent the photon count in each position of the mask, and only the part in which the dips appear is shown. When we are observing a single-lined binary see Figure 2.26 (Griffin, 2015c) there is only a dip in the graph, while for double-lined see Figure 2.27 two of them can be seen (Griffin, 2013).

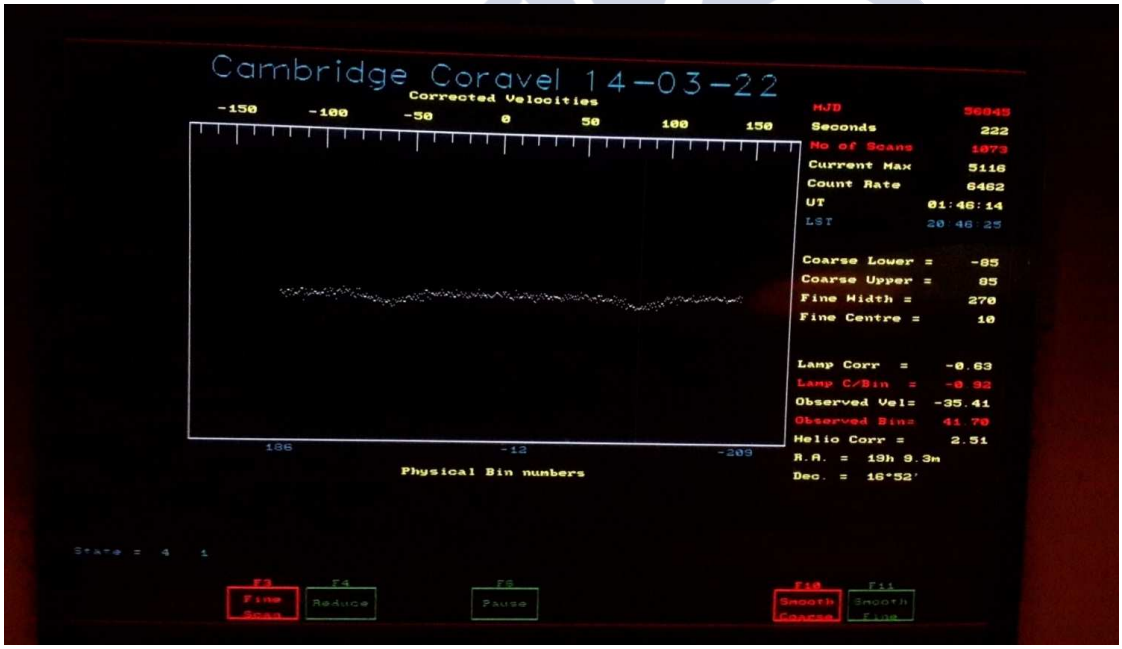

FIGURE 2.16: The CORAVEL control software

.

2015 July 8

Record	Star	RA	Dec	U.T.	HMJD	Profile Parameters depth	E.W.	vsini	merit	Vel.	S.D.
1	Beta CVn	12 34 35.7	41 15 45	21 31	57211.895	18.75	3.09	2.5	1.23	5.13	0.05
2	Eps CrB	15 58 14.1	26 49 59	21 38	57211.904	40.16	6.47	0.5	1.27	-33.98	0.03
3	HR 5534	14 50 56.1	23 50 16	21 43	57211.906	18.75	3.42	7.5	0.98	-3.78	0.10
4	HD 116499	13 24 31.2	18 7 46	21 48	57211.908	28.50	5.27	8.0	0.99	6.62	0.30
5	HD 116636	13 25 20.0	23 6 50	21 53	57211.911	30.07	5.18	5.5	0.78	-27.97	0.42
6	HD 116636	13 25 20.0	23 6 50	21 57	57211.915	32.61	5.53	5.0	0.98	-28.26	0.22
7	HR 6364	17 6 57.8	22 3 37	22 6	57211.925	40.75	6.54	0.5	1.26	-98.54	0.07
8	BD +29 2933	17 5 23.9	29 39 9	22 10	57211.927	39.49	6.50	2.5	0.85	-5.73	0.15
9	HD 117348	13 29 56.6	30 59 7	22 22	57211.932	11.03	1.92	6.0	1.33	-1.16	0.56
10	HD 147254	16 21 52.3	-6 38 38	22 39	57211.948	19.41	3.11	0.5	1.12	68.17	0.50
11	HR 6538	17 32 36.1	34 14 56	22 47	57211.953	23.24	3.74	0.5	0.83	-52.83	0.10
12	HD 162338	17 49 28.3	37 2 46	23 1	57211.962	6.75	1.28	8.0*	0.86	-10.90	
						6.87*	1.59	13.0*		-1.65	
13	HD 159220	17 31 42.5	45 37 52	23 44	57211.991	6.17	2.51	27.5	0.98	-55.36	0.54
14	HD 141690	15 50 11.2	25 24 50	0 18	57212.015	9.36	2.71	18.0*	1.17	-62.22	
						2.37*	0.38	0.0*		-37.98	
15	HR 6985	18 37 12.5	9 7 38	0 43	57212.035	7.16	1.41	9.0	1.49	-40.84	
						5.40	0.86	0.0		-4.00	
16	113 Her	18 55 23.9	22 39 42	0 55	57212.043	24.15	4.21	6.0	1.27	-12.04	0.04
17	HD 179484 N	19 11 39.4	38 48 26	1 4	57212.047	23.13	3.92	5.0	0.79	16.63	0.17
18	HD 179484 S	19 11 39.4	38 48 26	1 9	57212.051	23.48	3.76	0.0	0.89	24.77	0.16
19	HR 7368	19 24 7.8	33 14 24	1 19	57212.059	28.50	4.58	0.5	1.35	-23.02	0.05
20	HD 193215	20 15 31.7	64 14 22	1 31	57212.063	20.44	4.44	12.0	0.94	-2.77	0.19
21	BD +45 3310	20 53 17.0	46 10 16	1 44	57212.075	18.64	2.99	0.0*	1.33	-19.18	
						5.97*	0.96	0.0*		-22.02	
22	HR 8062	21 2 57.5	44 50 18	1 54	57212.082	29.41	5.87	10.0	1.28	-2.31	0.10
23	Delta Equ	21 15 14.2	10 4 37	2 2	57212.090	7.68	1.48	8.5	3.94	-33.23	
						7.59	1.22	0.0		-0.60	

FIGURE 2.17: Radial velocities observations for 23 spectroscopic binaries performed at 2015 July 8.

2015 July 9

Record	Star	RA	Dec	U.T.	HMJD	Profile Parameters depth	E.W.	vsini	merit	Vel.	S.D.
1	HR 5534	14 50 56.1	23 50 16	21 52	57212.912	18.95	3.34	6.5	1.22	-3.46	0.08
2	14 Ser	15 37 21.8	0 36 2	21 57	57212.918	16.64	2.66	0.0	0.84	-4.21	0.11
3	HR 5534	14 50 56.1	23 50 16	22 3	57212.920	18.91	3.45	7.5	0.95	-3.69	0.06
4	HR 5472	14 41 4.6	21 54 11	22 15	57212.928	5.36	1.79	21.0	1.07	-26.95	0.34
5	HD 151168	16 46 32.4	0 48 47	22 34	57212.945	13.56	2.25	4.0	1.06	-25.61	0.23
6	HR 6377	17 8 35.5	35 53 58	22 44	57212.950	2.44	2.22	63.0	1.13	-30.23	0.96
7	HR 6469	17 22 14.0	39 57 15	22 49	57212.954	16.00	2.56	0.0	1.08	3.33	0.08
8	HD 159304	17 33 3.1	34 44 0	22 56	57212.959	9.00	2.29	15.5	1.06	5.67	0.38
9	Mu Her	17 47 6.4	27 43 19	23 4	57212.965	28.81	4.62	0.0	1.41	-19.37	0.04
10	HR 6538	17 32 36.2	34 14 56	0 17	57213.015	23.67	3.89	3.5	1.26	-52.66	0.12
11	HR 6697	17 57 52.4	23 59 7	0 23	57213.020	22.36	3.58	0.0	1.39	-26.00	0.06
12	HD 183629	19 29 54.6	30 34 17	0 35	57213.028	38.99	6.29	0.5	0.92	-33.94	0.09
13	HD 174123	18 43 8.0	69 21 18	0 47	57213.033	7.48	1.20	0.0*	1.44	-26.40	
						6.65*	1.07	0.0*		-34.41	
14	HR 6985	18 37 12.5	9 7 38	1 3	57213.049	6.48	1.18	7.0*	1.27	-28.83	
						6.47*	1.18	7.0*		-15.69	
15	HD 187299	19 49 3.1	25 2 11	1 14	57213.056	36.37	7.59	11.0	1.19	-5.28	0.09
16	31 Cyg	20 14 6.8	46 46 58	1 22	57213.059	32.64	6.28	9.0	3.72	-0.51	0.04
17	32 Cyg	20 15 57.5	47 45 14	1 27	57213.063	35.26	6.78	9.0	1.48	-28.45	0.03
18	Eps Cyg	20 46 47.2	34 0 17	1 32	57213.067	35.12	5.65	0.5	3.22	-16.25	0.03
19	HR 7955	20 45 45.1	57 38 17	1 37	57213.069	12.89	2.09	2.0*	1.08	-37.17	
						8.88*	1.46	3.0*		-29.59	
20	HR 8035	20 58 52.1	44 30 50	1 43	57213.074	34.43	5.53	0.5	1.12	-23.14	0.05
21	HR 7914	20 41 26.2	19 58 33	1 48	57213.079	21.77	3.58	3.5	0.79	-36.58	0.07
22	HR 8062	21 2 57.5	44 50 19	1 55	57213.082	28.93	6.03	10.0	1.24	-2.42	0.09
23	HR 8364	21 55 1.0	19 46 41	2 2	57213.088	32.42	5.21	0.0	1.10	0.38	0.08
24	23 Vul	20 16 25.1	27 51 12	2 8	57213.093	37.56	6.18	2.5	0.75	-3.90	0.04

FIGURE 2.18: Radial velocities observations for 24 spectroscopic binaries performed at 2015 July 9.

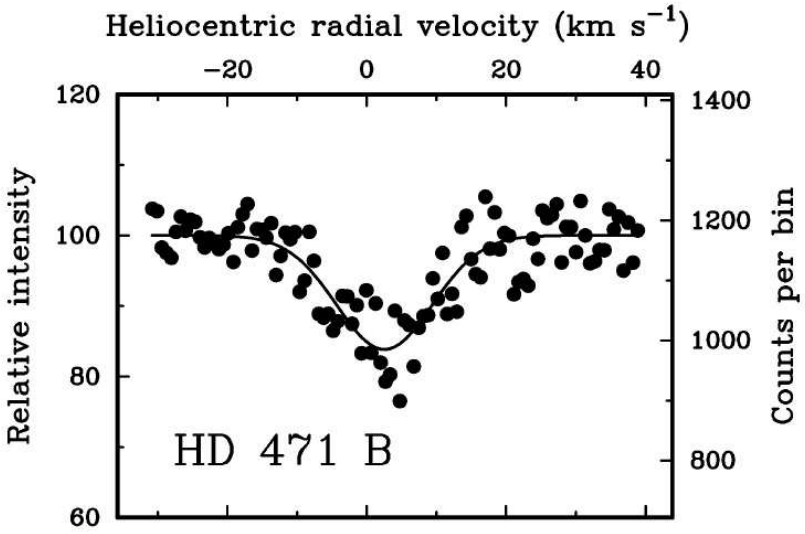

FIGURE 2.19: The dip for HD 471 B single-lined spectroscopic binary.

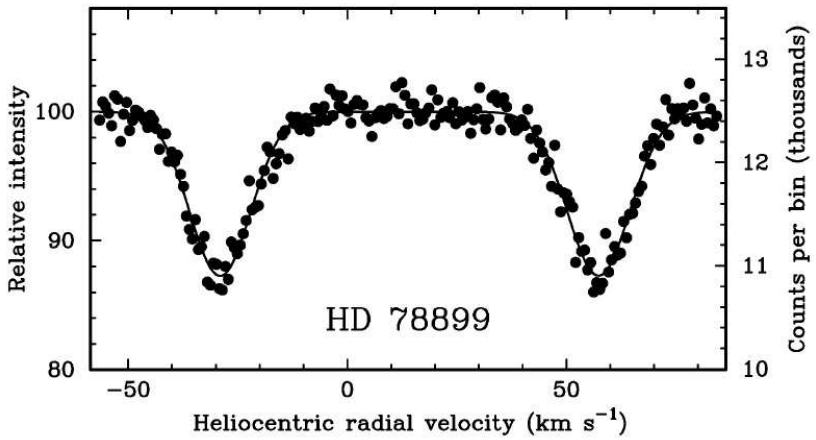

FIGURE 2.20: The dips for HD 78899 double-lined spectroscopic binary.

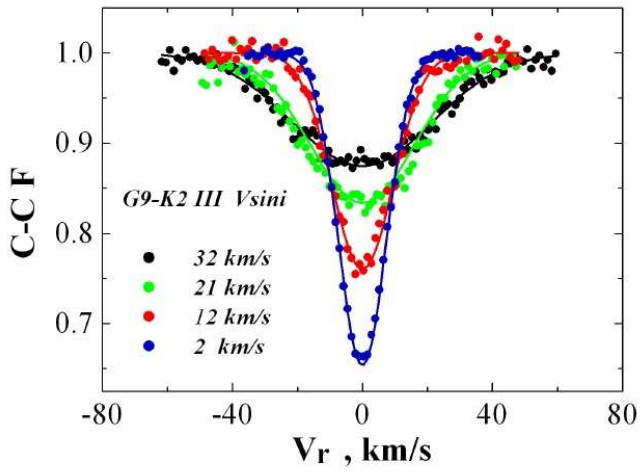

FIGURE 2.21: The rotational velocities.

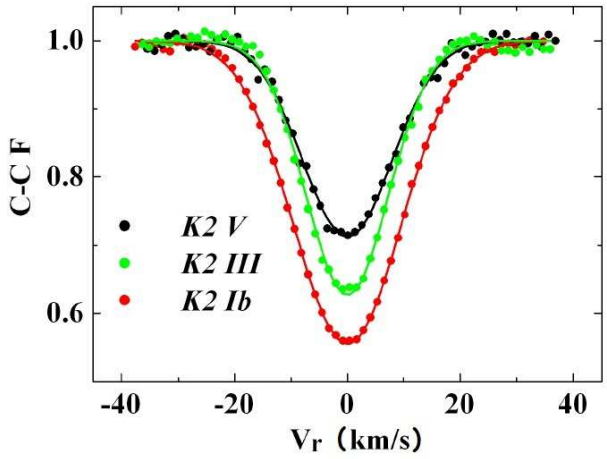

FIGURE 2.22: Spectral type.

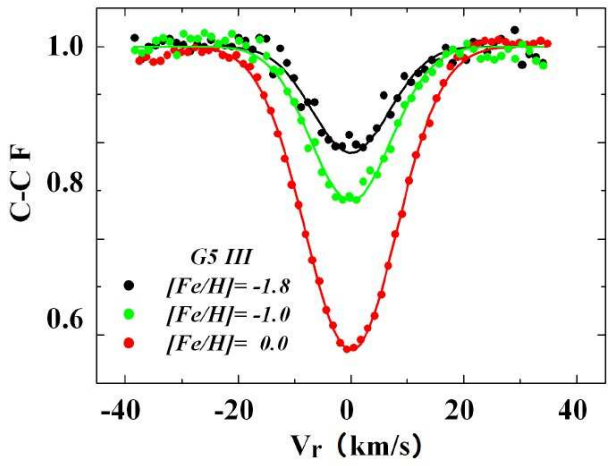

FIGURE 2.23: The metallicities.

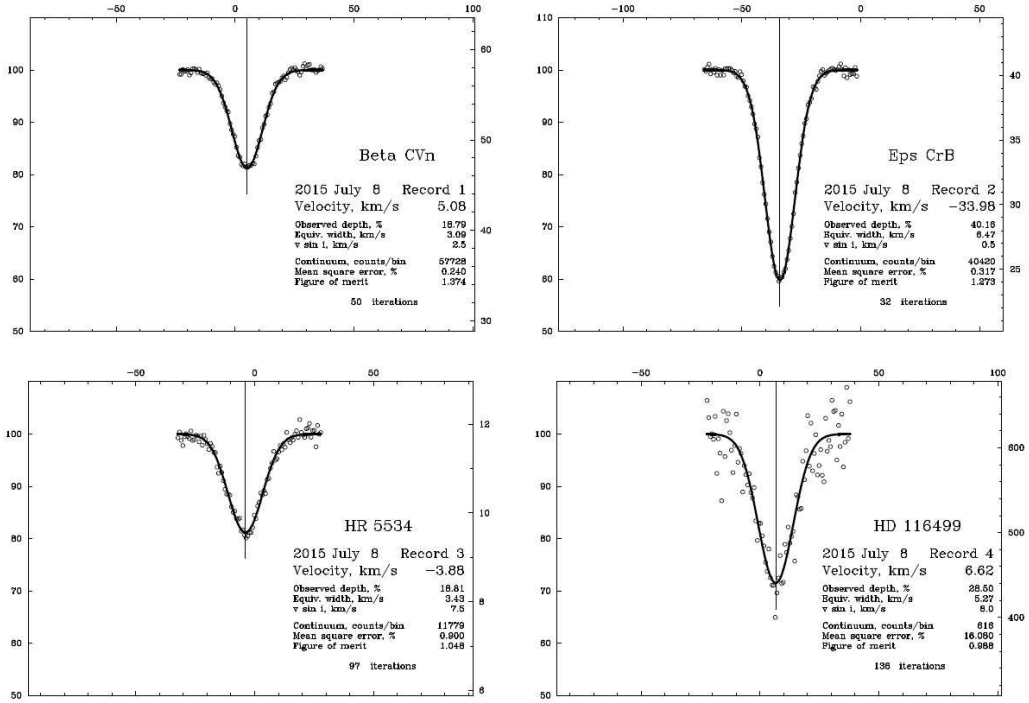

FIGURE 2.24: Radial velocity observations of SB1

.

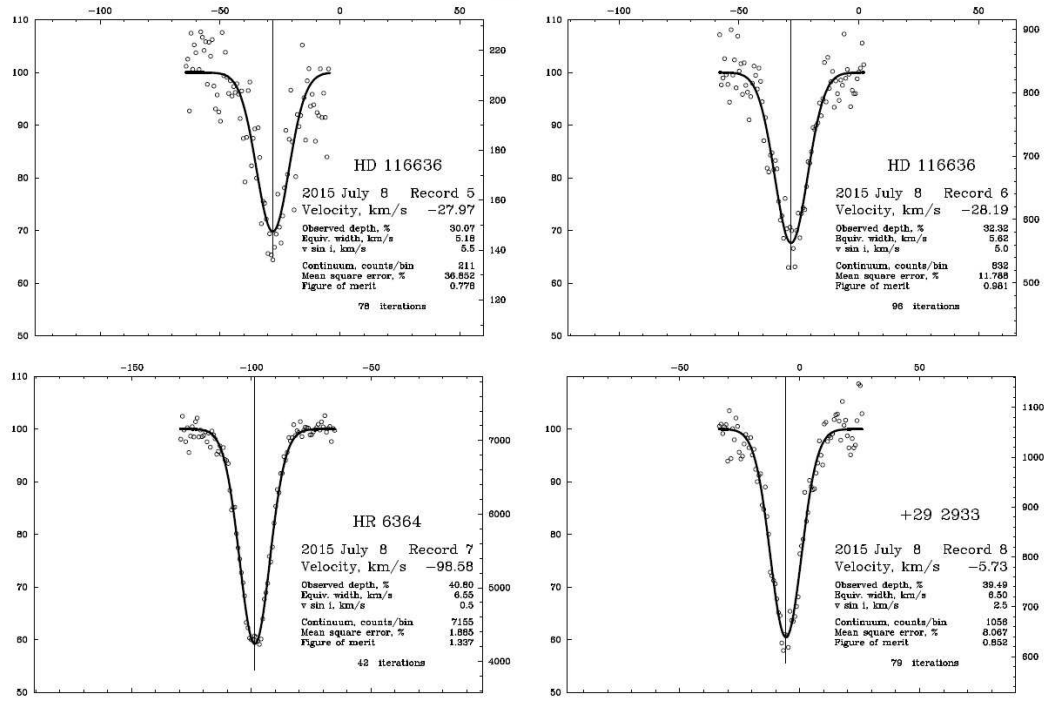

FIGURE 2.25: Radial velocity observations of SB1. Continuation.

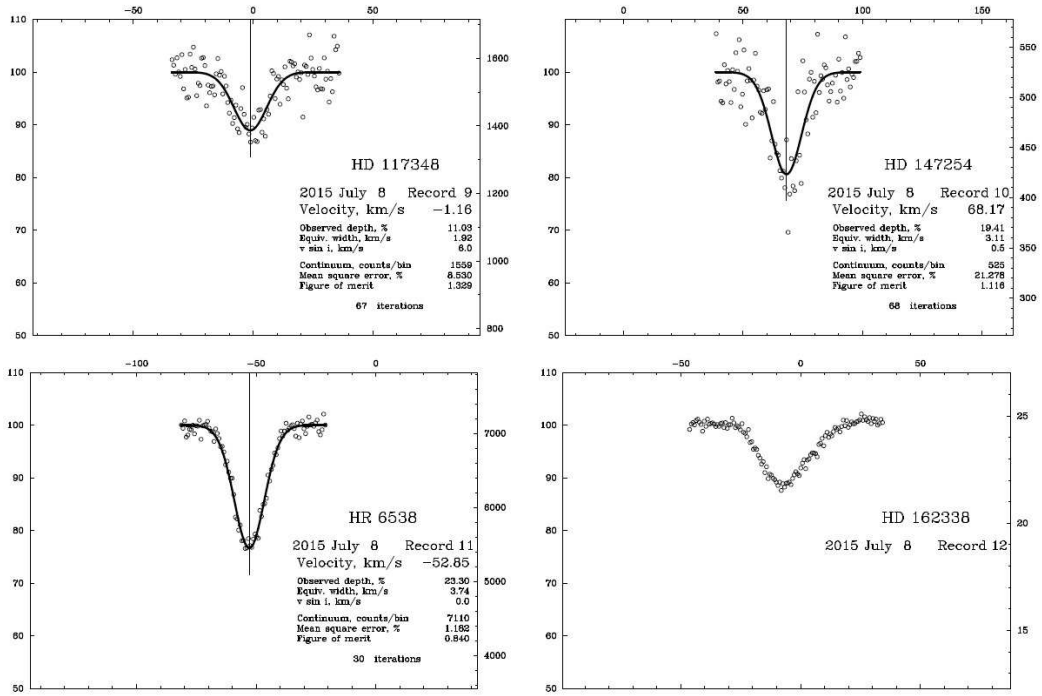

FIGURE 2.26: Radial velocity observations of SB1. Continuation.

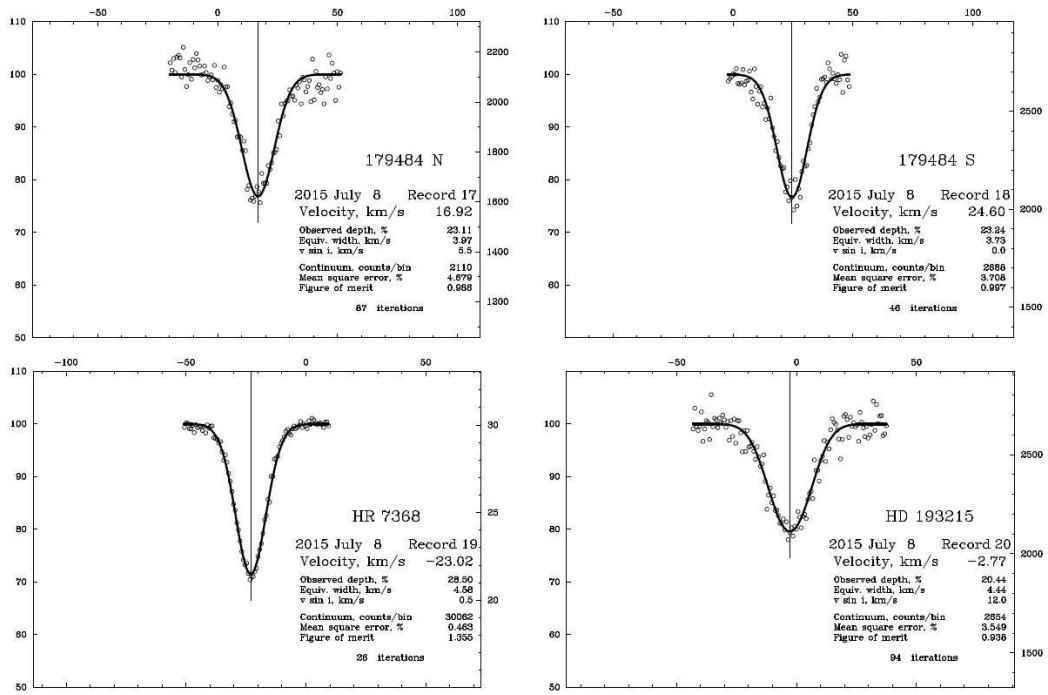

FIGURE 2.27: Radial velocity observations of SB1. Continuation.

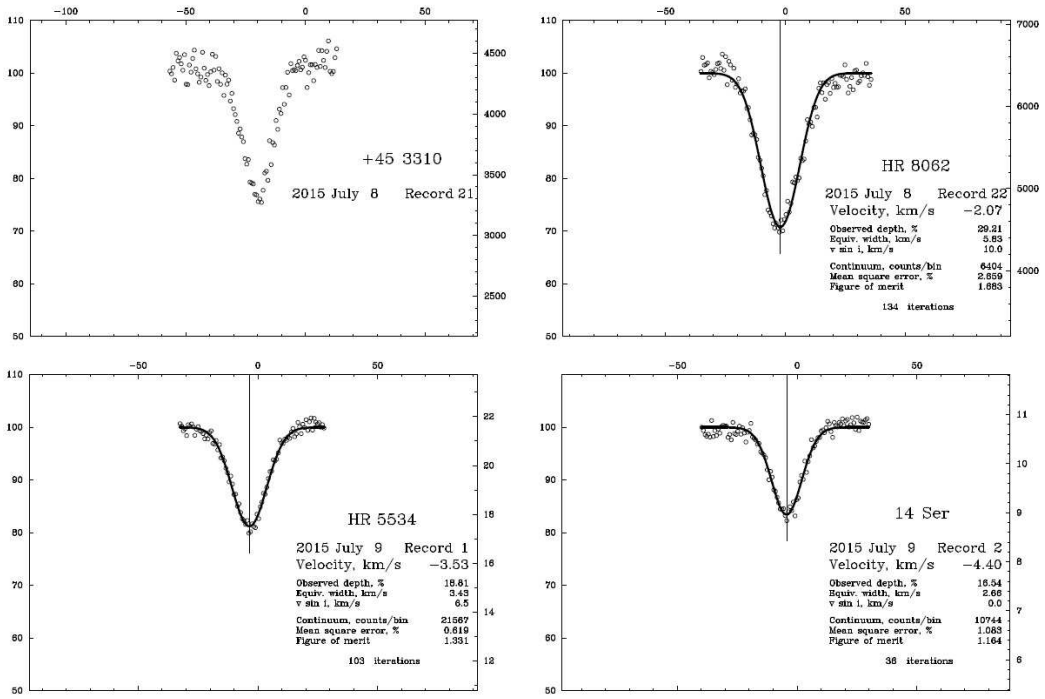

FIGURE 2.28: Radial velocity observations of SB1. Continuation.

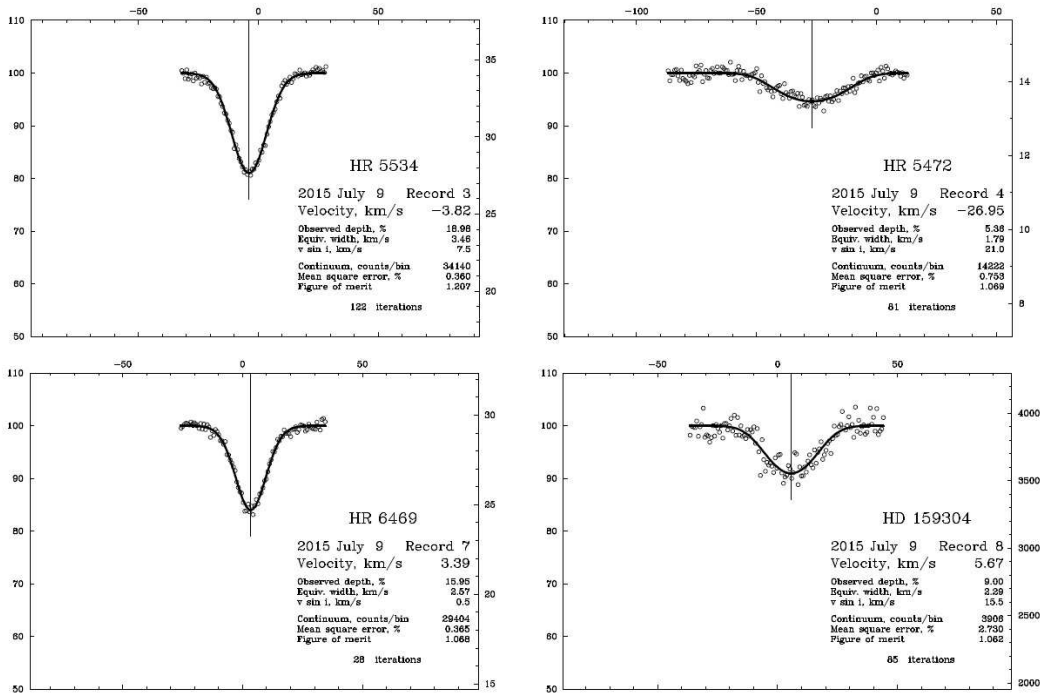

FIGURE 2.29: Radial velocity observations of SB1. Continuation.

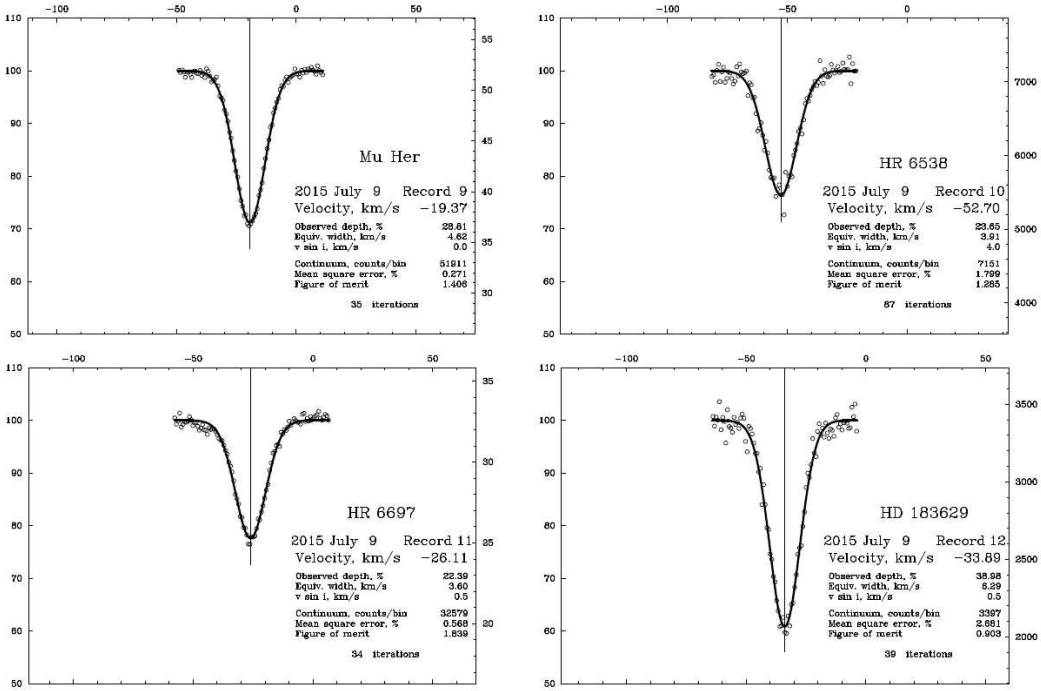

FIGURE 2.30: Radial velocity observations of SB1. Continuation.

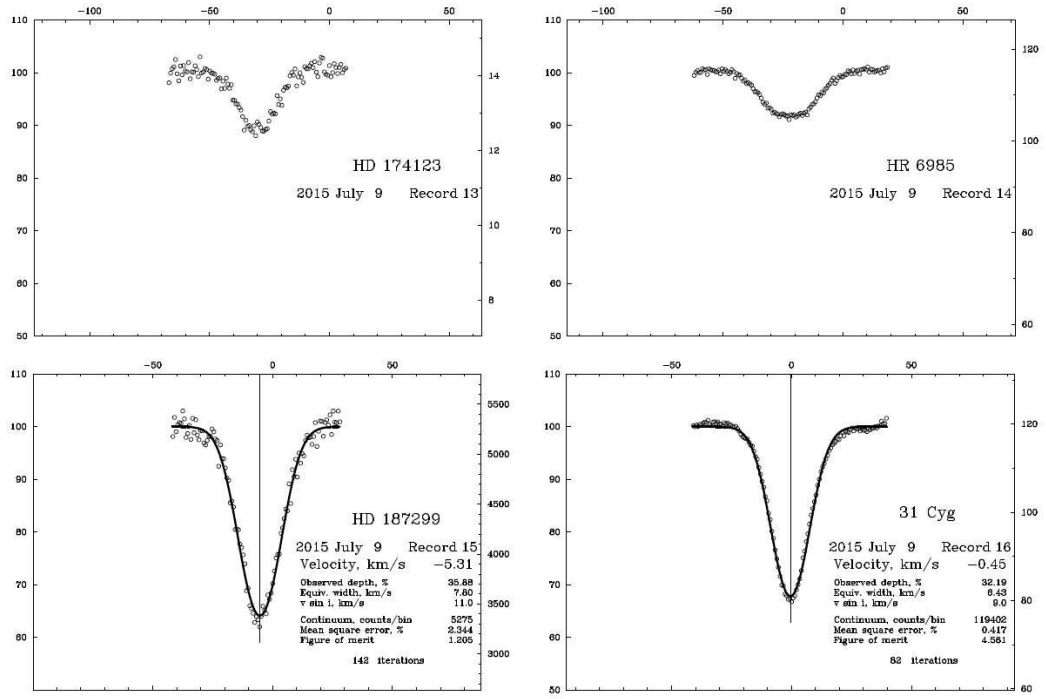

FIGURE 2.31: Radial velocity observations of SB1. Continuation.

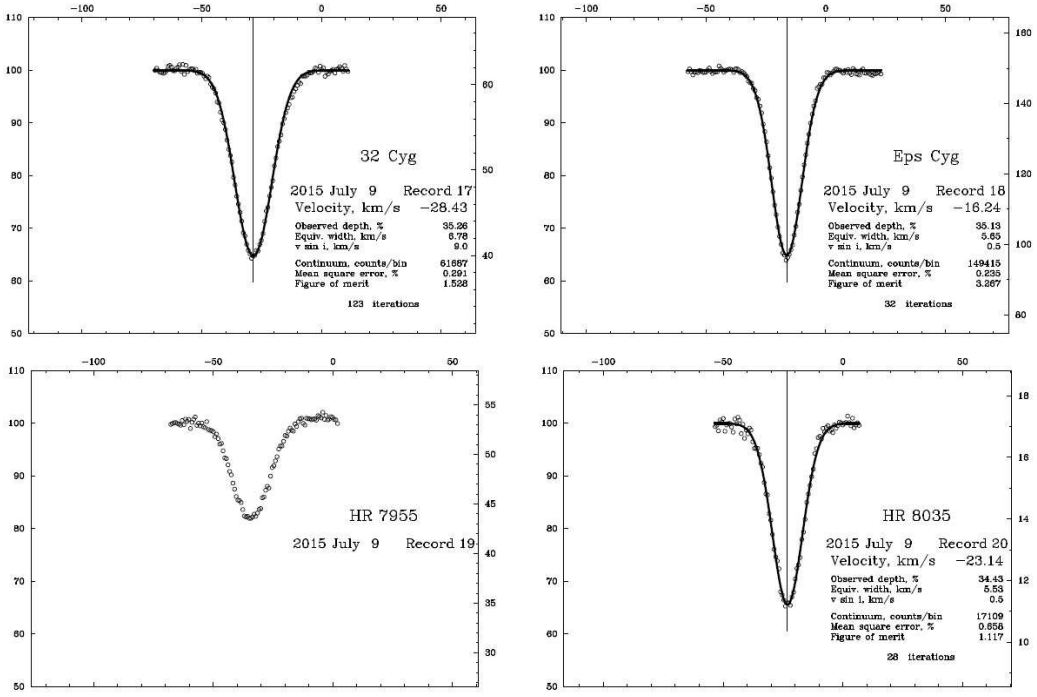

FIGURE 2.32: Radial velocity observations of SB1. Continuation.

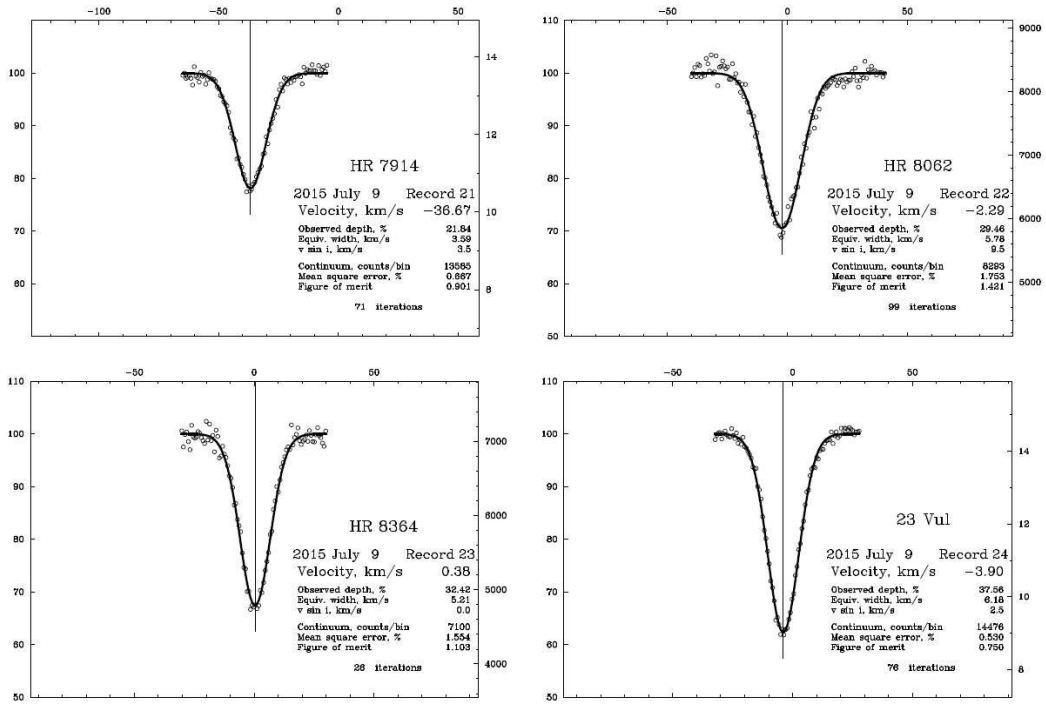

FIGURE 2.33: Radial velocity observations of SB1.

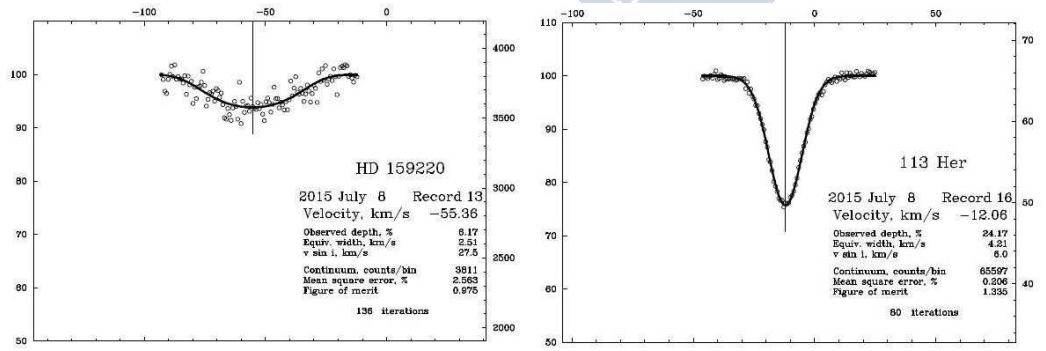

FIGURE 2.34: Radial velocity observations of SB1. Continuation.

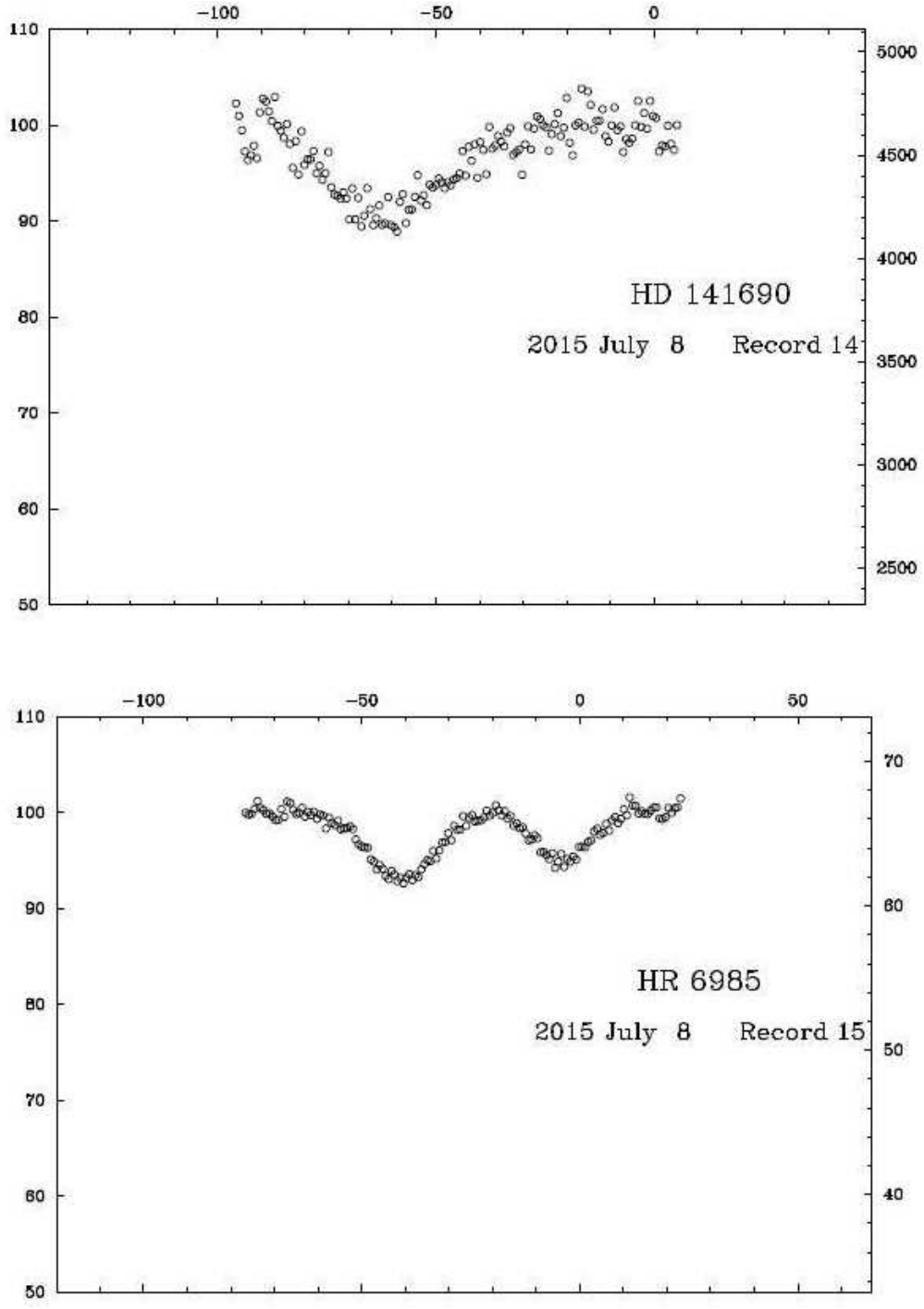

FIGURE 2.35: Radial velocity observations of SB2.

2.5 Radial velocities in visual binaries

We have explained in the Introduction the great interest to observer binaries performing both radial velocities and relative positions. In these cases the information obtained for these systems can be complete, especially when the periods are short and the orbits can be calculate with precision. Nevertheless, in other cases the radial velocities also play an important roll. For example:

2.5.1 Determining the ascending node

Usually in visual binaries, the nodes keep undetermined and only radial velocities are able to give us the correct information. For this reason, it is recommendable to try to perform RV in the neighborhood of the nodes. The ascending node will be that in which the RV is positive.

2.5.2 When two different orbits are possible

Another application appears when the magnitudes of the components are similar and in this case it is not easy to discriminate between a long period with a small eccentricity orbit from a short period with high eccentricity orbit. In these situations, the RV can help us to select the true orbit.

Regarding these scenarios, we have prepared a list of candidates in order to be observe with the 36-inch telescope.

Chapter 3

The Most Probable 3-D Orbit for Spectroscopic Binaries

3.1 Introduction

As commented in this Memory, in the last decades, using high resolution techniques, it has been possible to resolve a number of SB. The astrophysical interest of this subject lies in the fact that we can obtain the individual masses of the components (the ratio, by means of the SB2 orbits and the sum from the visual orbits). Nevertheless, before preparing the list of SB in order to try to resolve them with a concrete telescope, we should try to answer the following questions: Is it possible to have an idea of the telescope size that we would need in each case ? or, What list must we prepare for our telescope? We will try to answer these questions in the present chapter. We will pay attention in the SB (single-lined and double lined) with an orbit and known parallax. Our target is to build a three-dimensional model for each one of these SB and finally to propose their apparent orbit and, in consequence, the maximum and minimum angular separation. In this study we will also provide the most probable values of the physical parameters (spectral type, magnitudes, and masses) of these systems.

3.2 Single-lined spectroscopic binaries

First we consider a single-lined spectroscopic binary with an orbit, that is to say, we know the following orbital parameters: P (the period), T (the epoch of the periastron), e (the eccentricity), $A_1 = a_1.\sin(i)$ (a_1 is the semimajor axis of the orbit of the main component, and i, the inclination), ω (the argument of the periastron corresponding to the orbit of the main component), and the mass function,

$$f(\mathcal{M}) = \frac{(\mathcal{M}_2.sin(i))^3}{(\mathcal{M}_1 + \mathcal{M}_2)^2} \tag{3.1}$$

We assume that are also known the composite spectrum, the global apparent magnitude, and the parallax (in general the Hipparcos parallax, and next the Gaia parallax) are also known. The first step will be to obtain information about the individual spectrum of each star. For that, we will use the Edwards process (Edwards, 1976). Once we have the two

spectra depending on the difference of the magnitude, Δm, it is necessary to assign the corresponding mass to each of them. For this reason, the current calibrations must be analyzed.The knowledge of the masses permits us to obtain the three semimajor axes: a (relative orbit), a_1, and a_2 (these last being those of the orbits of each component around the center of mass), all of them are expressed in astronomical units. The following step is to calculate a$''$ (the semimajor axis of the relative orbit expressed in arc seconds) and the orbital inclination, i.
In these conditions, except for the node, we already have the elements of the "visual binary". Nevertheless, two comments are necessary.

- First, because we will determine the inclination by means of sin(i), two values of this element are possible: i and $i^{'}$=180° - i. If the binary is not resolved optically, it is impossible to know if the motion is direct or retrograde.

- Second, the angle of the node (Ω), remains unknown but this is not a problem for us. For our purposes, we can take it as zero.

Finally, the ephemerides can be calculated and it is possible also to drawn the apparent orbit. From that, the maximum and minimum values of the separation in arc seconds, consequently, the size of telescope necessary to try to resolve the system is deduced. In the next subsections, we will develop all of these steps.

3.2.1 The initial information

When any research work is starting, several subjects should be taken into account. They include: the sources, availability, and credibility of information, and to get to what we see today of organizing and arranging for astronomical data. All of this information comes after a hard work for may years by astronomers, astrophysicists, software developers around the world. In our case, research the information coordinates, parallax, magnitudes, spectral type, radial velocities, proper motion, and the previous studies, each of them was obtained from various sources as:

- The Astronomical Database **SIMBAD** (**S**et of **I**ndications **M**easurements and **B**ibliography for **A**stronomical **D**ata) is a database for millions of astronomical objects:

  - 1.500.000 stars; 450.000 galaxies; 100.000 planetary nebulae,

  - 650.000 objects observed with different methods (X, IR, Radio).

It also contains a bibliography and identification for them. This resource is the results of a collaboration among the Observatoire de Paris, the Institut d'Astrophysique de Paris, and the Observatoire de Bordeaux (Wenger et al., 2000). The Simbad website (`http://simbad.u-strasbg.fr/simbad/`), provides easy access to the database, and permits searching with identifier, coordinates, and the physical criteria of each object.

- The VizieR Database, an astronomical catalogue published by the Centre de Données of Strasbourg, is another Big Data resource.
  The website is http://vizier.u-strasbg.fr/index.gml and it contains links to different catalogues, and has been available since 1996 (Ochsenbein, Bauer, and Marcout, 2000). It is one of the data sources of the Astrophysical Virtual Observatory which is the European Virtual Observatory (EURO-VO), a huge Database which contains data centres, scientists, developers of astro-software, and astronomical data archives.

- The Aladin Sky Atlas was developed by the Centre de Données of Strasbourg in 1999. It provides a compilation of the valuable data from The VizieR and SIMBAD. The objective is to obtain the best visualization of large numbers of stars and galaxies as well as and the celestial sphere components. The website is,
  http://aladin.u-strasbg.fr/aladin.gml.

- The SAO/NASA Astrophysics Data System (ADS) is a Digital Library for Physics and Astronomy, considered to be the most important source for our research. It is possible to find, latest scientific papers, information about astronomical objects, and external links to various topics in astronomical fields. This library portal is a global astronomical connection point. And it contains about 11 million records of Physics, and Astronomy. The Smithsonian Astrophysical Observatory (SAO) supervises it, supported by NASA grant, see (http://adsabs.harvard.edu/).

- The 9th Catalogue of Spectroscopic Binary Orbits contains 2694 orbits of 2386 systems (SB1 and SB2) and 55 spectroscopic triple systems in the website
  http://sb9.astro.ulb.ac.be/. It provides easy access in order to search for the object using catalogues identifiers (HD, HIP, BD), coordinates, publication's bibcod, etc. It lists the parameters of components, magnitudes, the spectral type, the orbital elements with their standard errors, and radial velocity curve. It also contains 1500 orbits reported in more than 500 articles concerning nearly 1200 new systems (Pourbaix et al., 2004).

- Roger Griffin Scientific articles series entitled " Spectroscopic binary orbits from photoelectric radial velocities". This project required decades of work and is still ongoing, having published more than 245 papers in The Observatory journal since 1975. The first one was "Spectroscopic binary orbits from photoelectric radial velocities. I - HD 45088 ", Griffin and Emerson, 1975. In this series, Griffin used the radial velocity observations that were performed with the 36- inch telescope at the Cambridge Observatory and another that observed while visiting different observatories at Mount Wilson & Palmer (California), Dominion Astrophysical Observatory (Canada), Haut-Provence (France), and visits to Calar Alto (Spain), as well as European Southern Observatory (Chile). (This paper series have been an essential task to carry out this research.) The author of this investigation, thanks again to the advice and the contacts of Professor Docobo, realized two academic visits to the Astronomy Department at Cambridge University in the last years in order to work with Prof. Roger Griffin and obtain the radial velocities for about 60 spectroscopic binary stars using the 36- inch telescope.

3.2.2 The Edwards process

In 1976, Terry Edwards described a procedure that permits us to separately obtain the spectrum of each component of a binary from the composite spectrum as a function of the difference of magnitude , Δm = m_2 - $m_1 \geq 0$.
In his paper (Edwards, 1976), commented that "The MK spectral class decompositions have previously been considered by Christy and Walker (1969) who gave individual MK classification for both components of 142 visual binary system. Their procedure, adopted here with only slight modification, is to employ a stranded luminosity calibration for the MK system (Blaauw, 1963; Schmidt-Kaler, 1965) and to assume that the MK spectral type of the individual binary components, weighted by their luminosities, could be linearly interpolated to form the composite type. Quantitatively, the individual MK types S(1) and S(2) are assumed to be related to the composite MK type S(1+2) and the visual magnitude difference by :

$$M(S_1) + x.M(S_2) = (1+x)M\,[S(1+2)] \tag{3.2}$$

$$M(S_2) - M(S_1) = \triangle m = -2.5\,log\,(\frac{I_2}{I_1}) = -2.5\,log\,(x) \tag{3.3}$$

where is M(S) is the standard MK luminosity calibration (absolute magnitude).

We can express the two equations of Edwards in the form:

$$M_1 + xM_2 = (1+x)M \tag{3.4}$$

$$\Delta m = M_2 - M_1, \tag{3.5}$$

and from them, we deduce

$$M_1 = M - \frac{x.\triangle m}{1+x}. \tag{3.6}$$

This last expression yields the relation between the absolute magnitude of the main components(M_1) and the total absolute magnitude (M) by means of a step, S:

$$S = \frac{x.\triangle m}{1+x}. \tag{3.7}$$

Therefore, we can consider S as a function of Δm. The graph of the function S (Δm) is represented in Figure 3.1

S has a maximum value, 0.3023, for $\Delta m = 1.4$.
Table 3.1 gives the values of S for different values of Δm.

In practice, the composite spectrum and the global absolute magnitude (M) are valuable so, for each value of Δm, we must obtain the corresponding value of S in Table 3.1 or in Figure

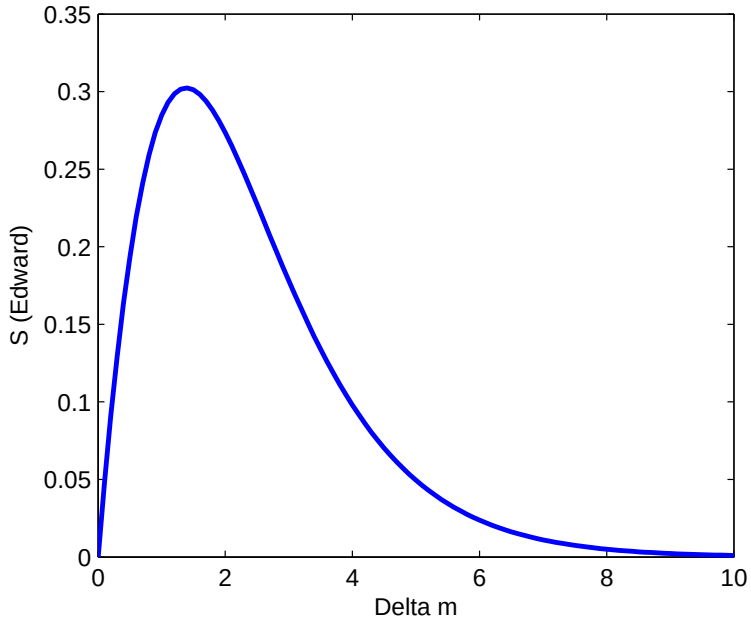

FIGURE 3.1: Representation of the S = S (Δm) function

Δ m	0.0	0.5	1.0	1.5	2.0	2.5	3.0	3.5	4.0	4.5	5.0	5.5	6.0	6.5	7.0	7.5
S	0.0	0.19	0.29	0.30	0.27	0.23	0.18	0.14	0.10	0.07	0.05	0.03	0.02	0.02	0.01	0.00

TABLE 3.1: Values of the Edwards step corresponding to Δm.

3.1 and then , the relation (1.6)

$$M_1 = M - S, \tag{3.8}$$

gives us the absolute magnitude of the main component and, from it, the calibration used provides the corresponding spectral type. Finally, the spectral type of the secondary component can be determined in the same manner once we have M_2=M_1+Δm.

Example of application We are going to apply the Edwards process to a concrete case.
The single-lined spectroscopic binary, HD 11540
Data :
(1) Composite spectrum, K2V
(2) Global absolute magnitude, M = 6.4
(a) Supposing that Δm = 3.0, Table 3.1 gives S= 0.18. So, M_1= 6.4 - 0.18 = 6.22 which corresponds to the spectral type, K1V. Finally, M_2 = M_1+Δm = 9.22 and, checking the calibration, we obtain the spectral type, M0V, for the secondary component.
(b) For example, in the case of Δm = 5.0, the results are: M_1 = 6.35 $\rightarrow$ Sp$_1$ = K1V M_2 = 11.35 $\rightarrow$ Sp$_2$ = M4V

3.2.3 Spectral type-mass calibrations of stars

There are two fundamental parameters involved in the study of the evolution of stars: the mass and the temperature. Due to the improvement in the research tools and observational methods in the last decades, the accuracy of the measurement of these parameters has significantly increased. Also, the knowledge of the parallax allows us to determine the luminosity values and, consequently, the Mass-Luminosity Relation (MLR) can be established.

Wullff Heintz in his book wrote " The name of Hertzsprung and Russell are immortalized by well-known spectrum-luminosity diagram of stars. Some years later, in 1923, the same authors discovered empirically the relation connecting stellar masses and luminosities. Eddington's work then was so far advanced that he showed shortly thereafter the theoretical basis for the existence of a relationship of this kind.

The empirical finding became a weighty support of the theory, as is demonstrated in his 1926 classic ' The Internal Constitution of The Stars, and it also provided the first grave objection against the then widely held hypothesis of stellar evolution from giants to dwarfs. As pressure and, hence, the energy generation increase with mass, the MLR is consequence of the pressure and temperature gradient inside the star, and its validity extends beyond Eddington's special star models to all stars with a chemically homogeneous interior composition." (Heintz, 1978).

In this deduction of the MLR diagram, the well-known orbits of the binary stars and the parallaxes play a fundamental roll. Since then, there have been many attempts to establish this relationship empirically, using increasing samples of stars. Adding the study of eclipsing binaries, it was also possible to obtain also a Mass-Radius Relation (MRR). Then, using the Stefan-Boltzmann law applied to the stars:

$$L = 4\pi\sigma R^2 T^4 \tag{3.9}$$

where L is the luminosity, σ is the Stefan-Boltzmann constant, and R is the radius of the star, we can derive its effective temperature, T. Using relevant relations, it is possible to build calibrations in which each star (with its spectral type and the luminosity class) is assigned a standard value for different parameters (mass, absolute magnitude, radius, effective temperature, etc.). There are several calibrations that can be used. For this reason, we thought that it would be convenient to take all of them into account in order to prepare a new weighted calibration and use it in the present research.

The calibration of absolute magnitudes (Straizys and Kuriliene, 1981) is based on observational data, while the masses and other parameters are derived by means of zero-age main sequence (ZAMS) models and theoretical evolutionary tracks.

In 2005 D.F Gray used the earlier work of D.M Popper to construct his mass calibration for main-sequence stars (Gray, 2005; Popper, 1980). In that work, Popper calculated the masses of a large sample of binaries of all types (eclipsing, spectroscopic, and visual) with well-known orbits, which supported the importance of this research.

J.A Docobo and M. Andrade published powerful formulas to calculate the mass and determine the spectral type of each component of multiple stellar systems, (Docobo and Andrade, 2006) basically rely on the fit of data that was collected from the Stellar Mass Catalog (Belikov, 1995) and at the Website: `http://cdsarc.u-strasbg.fr`). This Website contains different luminosity classes (main-sequence, sub-giant, and giants) and Schmidt-Kaler (Aller et al., 1982) to obtain the spectral type with a mean error of two or three subclasses . They derive the equation for each class,

$$\begin{aligned} \mathcal{M}_{III} &= (a + b \cdot e^{-s})^2 \\ \mathcal{M}_{IV} &= a \cdot s^b \\ \mathcal{M}_{V} &= a + \frac{b}{s^2} \end{aligned} \tag{3.10}$$

the permanent three equations relate the mass with the spectral type for each component. Two coefficients (”a” and ”b”) have different values for the luminosity classes and s is a variable that depends on the spectral type defined analytically by de Jager and Nieuwenhuijzen, 1987. The values of the coefficients are given in Table **??** and the variable, s, in Table **??**.

Luminosity class	2*a	2*b	Spectral range
III	1.34 ± 0.17	20.8 ± 2.5	B4-K4
IV	19.29 ± 0.86	-1.660 ± 0.065	B0.5-K3.5
V	-0.117 ± 0.090	27.47 ± 0.61	B0.5-M6

TABLE 3.2: Values of the coefficients in (Docobo and Andrade, 2006) mass calibration

Spectral Range	2*s	2*s-step
O1-O9	0.1-0.9	0.1
O9-B2	0.9-1.8	0.3
B2-A0	1.8-3.0	0.15
A0-F0	3.0-4.0	0.1
F0-G0	4.0-5.0	0.1
G0-K0	5.0-5.5	0.05
K0-M0	5.5-6.5	0.1
M0-M10	6.5-8.5	0.2

TABLE 3.3: Values of the variable in (Docobo and Andrade, 2006) mass calibration

O.Y Malkov used an extensive compilation of binaries of all types to calculate several relationships among the parameters of the different spectral classes (main-sequence). He gave several formulas that relate the mass, the luminosity, the temperature, and the radius of main-sequence stars (Malkov, 2007). Comparing the values obtained for the masses with Malkov's formulas, several discrepancies arise with other calibrations. We contacted the

author for clarification and he sent a new correction, after he recalculated the approximation with the observational data ($log(\mathcal{M}) - log(T)$) and obtained the equation:

$$log(\mathcal{M}) = -6.1 + 1.8\, log\,(T) + 0.043\, log^2\,(T) \tag{3.11}$$

We used this equation in order to achieve stellar masses for different temperatures. Malkov based his equations on the work of Strizys and Kuriliene (1981). Malkov also introduced two equations to calculate the masses and using it, we prepared a table for each to obtain the masses.

In order to obtain the final calibration of masses and absolute magnitudes, we prepared a weighted mean of the available calibrations for each luminosity class. Table **??** summarizes the data used. The first column shows the calibrations used, Columns 2-4 contain the weights used to calculate the mass, and columns 5-7, the weights for the absolute magnitude (with blank spaces when the calibration does not have data for that luminosity class).

	Weights (Mass)			Weights (absolute magnitude)		
Calibration	Class III	Class IV	Class V	Class III	Class IV	Class V
Str-Kur	3	3	3	3	3	3
Sch-Kal	3	–	3	3	3	3
Gray	–	–	4	4	–	4
Doc-And	4	4.5	4.5	–	–	–
Malkov	–	–	4	–	–	–

TABLE 3.4: Calibrations and weights

Where Str-Kur refers to Strayzis and Kuriliene, Sch-Kal to Schmidt-Kaler, and Doc-And to Docobo and Andrade. The tables with the calibrations are included in the Appendix C.

3.2.4 The determination of the semimajor axis and the orbital inclination

From the Two-Body Problem, we know that

$$G(\mathcal{M}_1 + \mathcal{M}_2) = \frac{4\pi^2.a^3}{P^2} \tag{3.12}$$

where G is the gravitational constant, $\mathcal{M}_1$ and $\mathcal{M}_2$ are the masses, a is the semimajor axis in length units, and P is the orbital period. We can suppose that the expression (1.10) corresponds to a binary star. If we write the same expression for the Sun-Earth (and Moon) system, we have

$$G(\mathcal{M}_\odot + \mathcal{M}) = \frac{4\pi^2.a^3}{P_0^2} \tag{3.13}$$

$\mathcal{M}_\odot$ indicate the solar mass, $\mathcal{M}$ is the mass of the Earth + Moon subsystem (that we can ignore in this case), a_0 is the astronomical unit, and P_0 represents one year.
So, dividing (1.12) by (1.13), the result is

$$\mathcal{M}_1 + \mathcal{M}_2 = \frac{a^3}{P^2}. \tag{3.14}$$

In this expression, $\mathcal{M}_1$ and $\mathcal{M}_2$ are given in solar masses, a in astronomical units, and P in years. Once we have determined the masses in the preceding subsection and, putting the period of the spectroscopic binary in years, the expression (1.14) provides the value of the semimajor axis of the relative orbit in astronomical units. On other hand, the well-known relations :

$$\frac{a}{\mathcal{M}_1 + \mathcal{M}_2} = \frac{a_1}{\mathcal{M}_2} = \frac{a_2}{\mathcal{M}_1} \tag{3.15}$$

permits us to obtain the values of a_1 and a_2, that is to say, the semimajor axes of the orbits that each component describes around the center of mass.
Now, if we multiply the values of a, a_1, and a_2 (in a.u), by the parallax, π'', we obtain their values in arcseconds: a'', a''_1, and a''_2. The orbital inclination is determined by:

$$sin(i) = \frac{A_1}{a_1} \tag{3.16}$$

or using the mass function:

$$sin(i) = \frac{\sqrt[3]{f(\mathcal{M}).(\mathcal{M}_1 + \mathcal{M}_2)^2}}{\mathcal{M}_2} \tag{3.17}$$

giving two complementary values that correspond to the direct and the retrograde motions.

3.2.5 The drawing of the apparent orbit. Maximum and minimum separation

We have everything necessary to calculate the ephemerides by means of the typical algorithm used in visual binaries. We need to obtain the position of the secondary with respect to the main component in the apparent plane, that being the plane perpendicular to the line of sight or the plane where the polar coordinates θ, and ρ are defined.
In this case it is important to remember that, because the angle of the node is unknown, the position angle , θ, is measured from the line of the nodes. For an epoch, t, we calculate the coordinates, r.f, in the relative orbit according to the procedure described in the Two-Body Problem.
First, we obtain the mean anomaly, M. Then we resolve the Kepler Equation and determine the eccentric anomaly, E. Finally, we calculate the distance

$$r'' = a''.\,(1 - e.cos\,(E)\,) \tag{3.18}$$

and the true anomaly,

$$tan\,(\frac{f}{2}) = \sqrt{\frac{1+e}{1-e}}\,.\,tan\,(\frac{E}{2}). \tag{3.19}$$

Next , the formulas:

$$\rho''.\,sin\,(\theta-\Omega) = r''.\,sin\,(\omega+f).\,cos(i) \tag{3.20}$$

$$\rho''.\,cos\,(\theta-\Omega) = r''.\,cos\,(\omega+f) \tag{3.21}$$

written in the form:

$$tan\,(\theta-\Omega) = \,tan\,(\omega+f).\,cos(i) \tag{3.22}$$

$$\rho'' = r''.\,\frac{cos\,(\omega+f)}{cos\,(\theta-\Omega)} \tag{3.23}$$

yield us θ and ρ''.
In these expressions, is ω = 180° + ω_1, and Ω = 0°.
In order to draw the apparent orbit, it is sufficient giving values from 0° to 360° to the angle θ in (3.20), calculating *f*, and finally obtaining ρ in (3.21), and calculating the corresponding ρ in arc seconds.
Once all of this is done, the maximum and minimum values of the separation, ρ, can be obtained.

3.2.6 The power separation of the telescope

The resolution of the telescope describes its ability to view the details of an observed object. In the case of a double star, the clarity of separation of two stars, depends on many factors including the seeing conditions, the amount of scattered or background light, the relative brightnesses of the two stars and there apparent colors, light pollution, sky conditions, mirror and lens coatings, obstructed or unobstructed optical system, and even the experience of the observer (Mullaney, 2005).

Using a high telescope, the star seen look like a bright disk surrounded by rings of light. Figure 3.2 shows the diffraction pattern of said star and the maximum and minimum intensity moving outward from the center.

There are a star in the constellation Lyra with name Epsilon Lyrae known as "The Double Double", that when we use the field glasses to see it will be as double star, but when we observe it with a large enough telescope, the two stars can see them as double stars also (components AB, and CD), and this giving a simple idea about the relation between the angular separation with the size of telescope.
Three Criteria concern the resolution of the observations: Dawes, Rayleigh, and Markowitz Criterion, based on behavior of optical properties by the light diffracting .

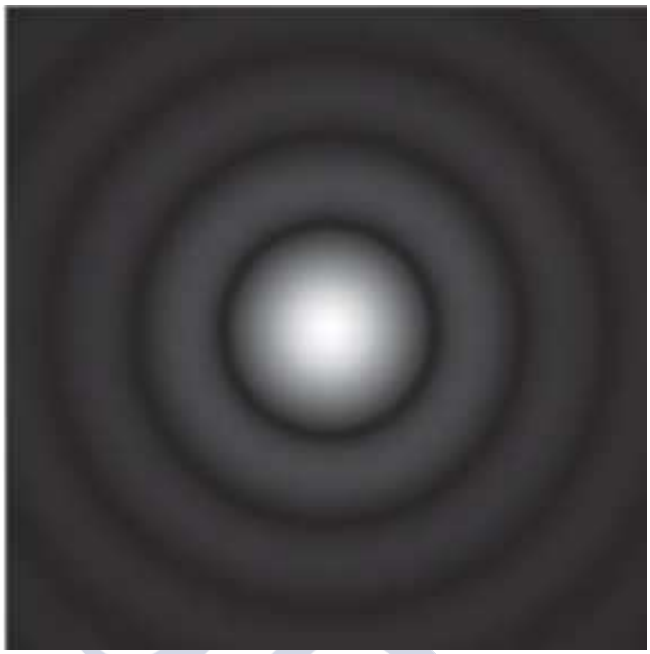

FIGURE 3.2: Diffraction Pattern

William Dawes (1799-1868) English astronomer, proposed a formula for the power seperation of a telescope depending on its the diameter, called "Dawes limit".

$$\rho'' = \frac{11.7}{D} \tag{3.24}$$

Where ρ is the angular separation in arc second, and D is the diameter in centimeter. This equation is true for stars have equal brightness about sixth magnitude. Expression (1.24) transforms in (1.25) if the diameter is given in inches.

$$\rho'' = \frac{4.56}{D} \tag{3.25}$$

In the The table below we can see the limiting magnitudes for various size telescopes with different objective diameter (size) in (inch) and the different resolution for each criterion in arc-second(ibid.).

The resolving power using Dawes criterion is better than Rayleigh's theoretical criterion about 20% (Roy and Clarke, 2003).

FIGURE 3.3: Epsilon Lyrae "The Double Double" http://aladin.u-strasbg.fr

3.3 The Photometry

Electromagnetic radiation (EMR) is an amount of energy and it is the key to study the celestial objects around us. We receive this amount as a quantity called flux. Photometry is the technique that permits us to study and measure the flux over broad wavelength bands of radiation, and the color is the difference between the wavelength regions (Romanishin, 2002). The relation between the flux (I) and the term magnitude (m) is given by the well-known expression called the Pogson formula :

$$m_1 - m_2 = -2.5 \ log_{10} \left(\frac{I_1}{I_2} \right). \tag{3.26}$$

The star, Vega, is the standard Star for Photometry, with a magnitude of 0.00. Any other star magnitude or apparent magnitude is proportional with the flux ratio of that star with Vega:

$$m_1 = -2.5 \ log_{10} \left(\frac{I_1}{I_{Vega}} \right) \tag{3.27}$$

Size	Mag	Dawes	Rayleigh	Markowitz
2.0	10.30	2.28	2.75	3.00
2.4		1.90	2.29	2.50
3.0	11.2	1.52	1.83	2.00
3.5		1.30	1.57	1.71
4.0	11.8	1.14	1.38	1.50
4.5		1.01	1.22	1.33
5.0		0.91	1.10	1.20
6.0	12.7	0.76	0.92	1.00
7.0		0.65	0.79	0.86
8.0	13.3	0.57	0.69	0.75
10.0	13.8	0.46	0.55	0.60
11.0		0.42	0.50	0.55
12.0		0.38	0.46	0.50
12.5	14.3	0.36	0.44	0.48
13.0		0.35	0.42	0.46
14.0	14.5	0.33	0.39	0.43

FIGURE 3.4: Limiting magnitude and power resolution for different telescopes size in inches (Mullaney, 2005).

3.3.1 Filter Systems

Filters are optical components that permits only certain wavelengths of electromagnetic radiation (EMR) to pass through it, Filters can eliminate the effects of light pollution on the observation. There are three types of filters: Neutral density filters **(NDF)** change intensity but not wavelength, Color Glass Filters **(CGF)** block some wave lengths but not others, and Interference Filters **(IF)** are very narrow band filters for specific wavelengths.

We call the system which used a system filter in an optical region with the **U**ltraviolet, **B**lue, **V**isual system (**UBV**). The Hertzsprung-Russell diagram is based on B and V filters. There is another system called "the ugriz system" used by the Sloan Digital Survey.

3.3.2 Photometric Systems

Introduced in 1953, the Johnson-Morgan, UBV photometric system was the first standard system. There are four categories for the photometric systems having schematic passbands with wavelengths and widths in angstroms (see Figures 3.5-8):

- **Broad Band** where ($\Delta\lambda < 1000$ Å). Such systems include: the Johnson-Cousins UBVRI system, the Washington CMT_1T_2 system, the Sloan Digital Sky Survey ugriz system, the Hipparcos-Tycho HpB_TV_T system, and the Hubble Space Telescope WFPC2 system (see Figure 3.5, 3.6).

- **Intermediate Band** where (70 < $\Delta\lambda$ < 400 Å). these system in corporate: the Stromgren 4-color uvby system, the DDO system, the Geneva system, the Vilnius system, and the Walraven WULBV system (see Figure 3.7, 3.8).

- **Narrow Band** where ($\Delta\lambda$ < 70 Å). there are two of these: the Oke AB magnitude system, and the Wing 8-color system.

- **Ultra-broad band** with band-widths wider than BVRI broad-band, Hipparcos and Sloan are the two systems available.

The color index is the difference between the magnitudes in two different passbands (a range of wavelengths). For example, we can determine it for the B and V bands:

$$B - V = m_B - m_A = -2.5 \ log_{10} \left(\frac{I_B}{I_A} \right). \tag{3.28}$$

In this work, we refereed to, for each of the spectroscopic binaries (SB), the values for various color indices which were taken form the previous publications of the Griffin series, and from the valuable astronomical database such as the Simbad website. Our methodology is fundamentally based on the determination of the spectral type for the components of each SB. We found that there are various possibilities for the spectral type and luminosity class for some of these binaries, (e.g., HD 74089, HD 129560, and HD 198048).

The value of color indices plays an important role in the determination of the spectral type for each system, using Gray's table in his book titled "The Observation and Analysis of Stellar Photospheres, 2005 " for main sequence stars and class III giants (see Figure 3.9, 3.10), and the publication by V. Straizys and R. Lazauskaite entitled "Intrinsic color indices and luminosity sequences of stars in the 2MASS two-color diagram", in which the intrinsic color indices for all spectral classes of main-sequence stars and the late-type giant (see Figure 3.11, 3.12).

3.3.3 The errors transmission

We measure parameters in order to describe there behavior. I is will-known that errors occur in measurements, errors increase uncertainty and decrease the quality. We used error analysis to decrease mistakes in the measurements to a minimum (Taylor and Cohen, 1998). The two most important basic statical calculation are arithmetic mean or the average ($\bar{\mathbf{x}}$), and the standard deviation (σ). If we have many measurements, the average is nearest to

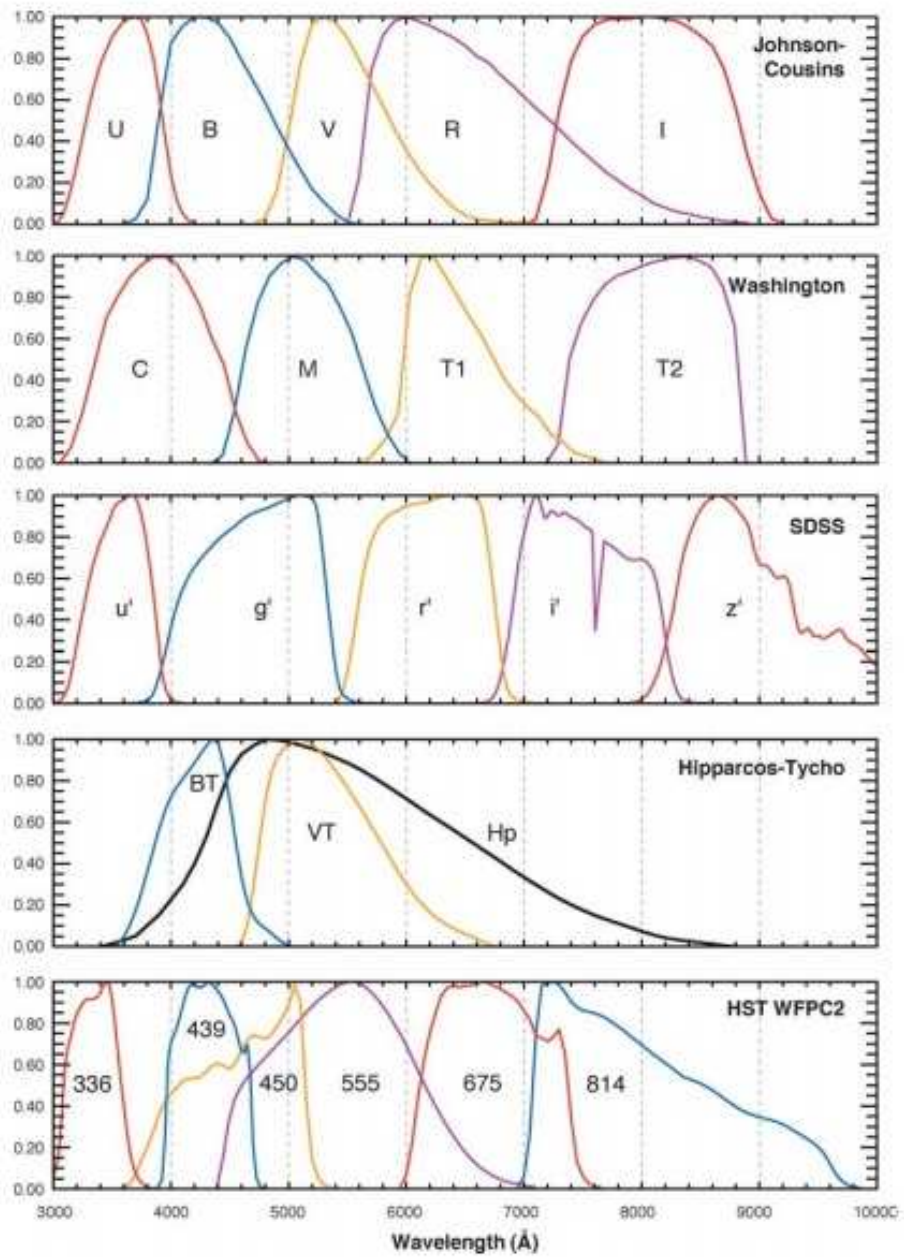

FIGURE 3.5: Schematic passbands of broad-band systems (Bessell, 2005).

the true value. The standard deviation (σ) indicates the deference between the individual measurement and the average ($\bar{\mathbf{x}}$) (Bell, 2001).

$$\bar{\mathbf{x}} = \frac{\sum_{i=1}^{N}(x_i)}{N} = \frac{x_1 + x_2 + ... + x_N}{N} \tag{3.29}$$

UBVRI			Washington			SDSS			Hipparcos			WFPC2		
	λeff	Δλ		λeff	Δλ		λeff	Δλ		λeff	Δλ		λeff	Δλ
U	3663	650	C	3982	1070	u'	3596	570	H_P	5170	2300	F336	3448	340
B	4361	890	M	5075	970	g'	4639	1280	B_T	4217	670	F439	4300	720
V	5448	840	T_1	6389	770	r'	6122	1150	V_T	5272	1000	F555	5323	1550
R	6407	1580	T_2	8051	1420	i'	7439	1230				F675	6667	1230
I	7980	1540				z'	8896	1070				F814	7872	1460

FIGURE 3.6: Wavelengths (Å) and widths (Å) of broad-band systems (Bessell, 2005).

where, $\bar{\mathbf{x}}$, the average, N, the Number of the measurements, and x_i is the measurement, and the standard deviation is:

$$\sigma = \sqrt{\frac{\sum_{i=1}^{N}(x_i - \bar{\mathbf{x}})^2}{N-1}} = \sqrt{\frac{(x_1 - \bar{\mathbf{x}}) + (x_2 - \bar{\mathbf{x}}) + ... + (x_N - \bar{\mathbf{x}})}{N-1}} \tag{3.30}$$

where σ, the standard deviation, $\bar{\mathbf{x}}$, the average, x_i is the measurement, and N, the Number of the measurements.

The following formula is used to calculate the errors associated with the different parameter involved z(x,...,y).

$$\triangle z = \sqrt{\left(\frac{\partial z}{\partial x}\cdot\triangle x\right)^2 + ... + \left(\frac{\partial z}{\partial y}\cdot\triangle y\right)^2} \tag{3.31}$$

Sometimes we introduce the weights (w_i) in our calibration to indicate that some of the parameters are more important than others, thus a change in($\bar{\mathbf{x}}$) and the standard deviation (σ):

$$\sigma = \frac{\sum_{i=1}^{N} w_i(x_i - \overline{x})^2}{\sum w_i(N-1)}. \tag{3.32}$$

This expression is used to determine the error in our calibration and calculation to reach the final result.

3.3.4 MATLAB program

MATLAB (**MAT**rix **LAB**oratory) is a software package developed by MATH-WORK to solve mathematical and numerical problems and it is a programming language and interactive system with high capability to verify graphs.

There are 3 mathematics languages. They are MATLAB of The MathWorks used for numerical computation, Mathematica of Wolfram Research, and Maple of MAPLESOFT for mathematics problems and derivations. MATLAB has many advantages: clarity and high

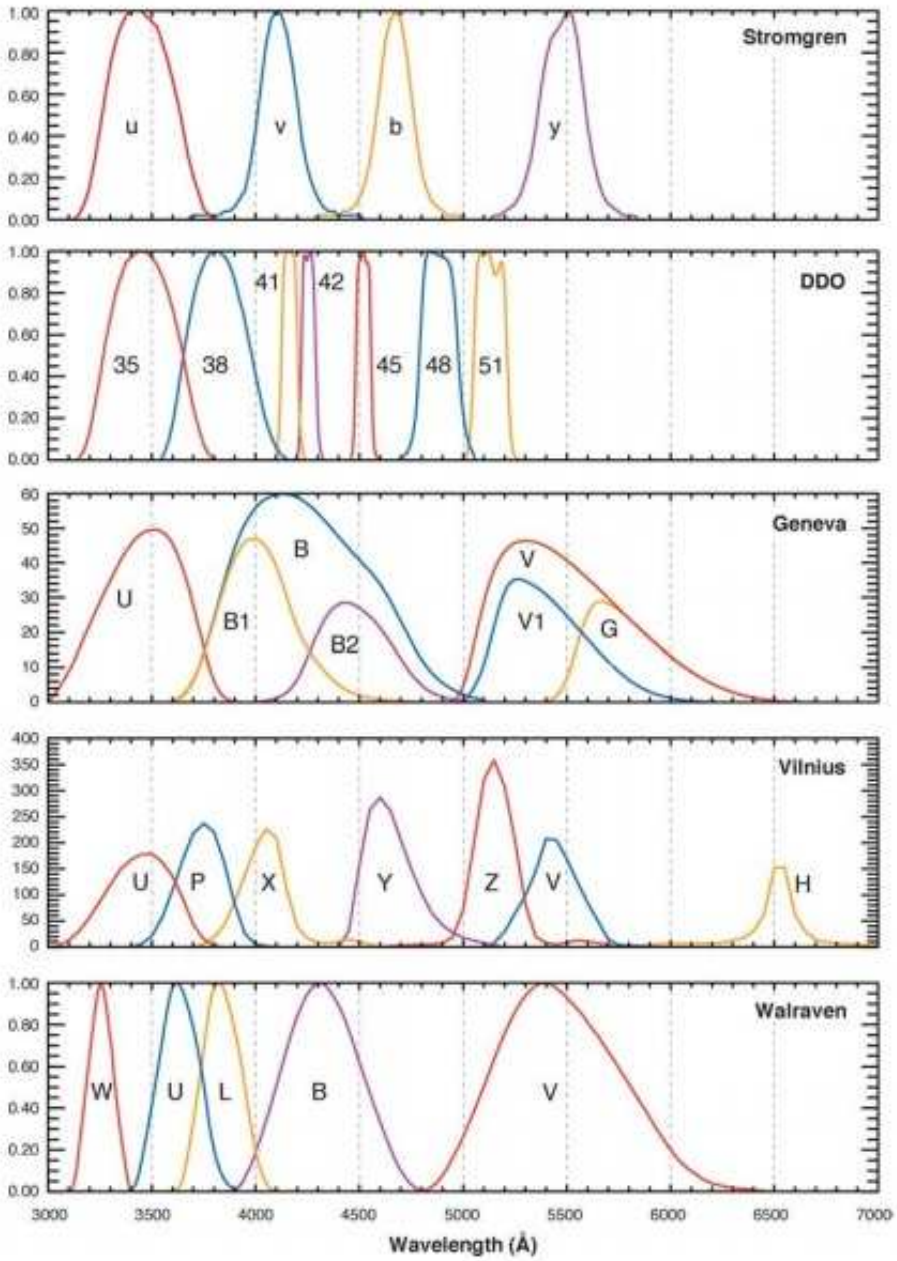

FIGURE 3.7: Schematic passbands of intermediate-band systems (Bessell, 2005)

efficiency, graphics facilities, comprehensive toolboxes and block-sets, and powerful simulation facilities (Xue and Chen, 2008).

In 1970, Cleve Moler, was a professor of Computer Science at the University of New

Strömgren			DDO			Geneva			Vilnius			Walraven		
	λeff	Δλ		λeff	Δλ		λeff	Δλ		λeff	Δλ		λeff	Δλ
u	3520	314	35	3460	383	*U*	3438	170	*U*	3450	400	*W*	3255	143
v	4100	170	38	3815	330	*B*	4248	283	*P*	3740	260	*U*	3633	239
b	4688	185	41	4166	83	*B1*	4022	171	*X*	4050	220	*L*	3838	227
y	5480	226	42	4257	73	*B2*	4480	164	*Y*	4660	260	*B*	4325	449
β_w	4890	150	45	4517	76	*V*	5508	298	*Z*	5160	210	*V*	5467	719
β_n	4860	30	48	4886	186	*V1*	5408	202	*V*	5440	260			
			51	5132	162	*G*	5814	206	*S*	6560	200			

FIGURE 3.8: Wavelengths (Å) and widths (Å) of intermediate-band systems (Bessell, 2005)

Mexico. He wrote in BASIC to solve the linear algebra problems when he had faced difficulty using EISPACK and LINPACK packages which is software written in FORTRAN. In 1984, the MATHWORKS company was established by Cleve Moler and Jack Little four years after starting work on MATLAB, in order to organize and develop it.
In 1980, MATLAB was first written in FORTRAN using LINPACK and EISPACK libraries. In 1983, MATLAB was written using C language and the resulting program was called M-Code. In 1984, MATLAB introduced the first edition: " MATLAB 1.0" and the graphical interface was offered in 1990. Today, the last version is R2016a (Version 9.0), dated March 3, 2016, and it has become the standard language of scientists.
The algorithms of this investigation were mainly programmed in MATLAB 2012a to build the software for calculating the physical and dynamical properties of spectroscopic binaries with the most probable 3-D orbit. M-Cod programs for single-lined and double-lined spectroscopic binaries can be seen in the Appendices.

3.3.5 Application of the methodology to the SB1, HD 471 system

The HD 471 system is a single-lined spectroscopic binary with an orbit for which Table 3.5 shows relevant information: spectral type, global visual magnitude (m), the Hipparcos parallax (Gaia did not determine the HD 471 parallax), the orbital elements (P, T, e, a_1.sin(i), ω_1), and the mass function, ($f(\mathcal{M})$).

From these initial values, we can calculate the global absolute magnitude, M:

$$M = m + 5 + 5\,log(\pi^{''}) = 5.97. \tag{3.33}$$

We suppose that $\Delta m \geq 1.5$ because HD 741 is a SB1. So, the lower limit will be Δm=1.5 and the upper limit, when i = 90°.
For Δm = 1.5, the Edwards process gives S = 0.30. In these conditions, the absolute magnitude of the main component will be M_1 = M - 0.30 = 5.97 - 0.30 = 5.67. By means of our calibrations, the absolute apparent magnitude of 5.67 corresponds to the G8V spectral type

Sp	$B-V$	$V-R$	$b-y$	M_V	BC	T_{eff}	$R/R_\odot$	log g	$\mathfrak{M}/\mathfrak{M}_\odot$	ζ_{RT}	$v \sin i$
O3	–	–	–	–	−4.3?	48000	–	–	50?	–	–
O5	–	–	–	−5?	−4.3?	44000	–	–	30?	–	–
O6	−0.32	−0.15	–	−4.8	−4.25	43000	12?	4.0	25?	–	295
O8	−0.31	−0.15	–	−4.1	−3.93	37000	10	4.0	20?	–	292
B0	−0.29	−0.13	–	−3.3	−3.34	31000	7.2	4.0	17	–	289
B1	−0.26	−0.11	–	−2.9	−2.60	24100	5.3	4.1	10.7	–	287
B2	−0.24	−0.10	−0.09	−2.5	−2.20	21080	4.7	4.1	8.3	–	284
B3	−0.21	−0.08	−0.08	−2.0	−1.69	18000	3.5	4.2	6.3	–	281
B4	−0.18	−0.07	−0.08	−1.5	−1.29	15870	3.0	4.2	5.0	–	278
B5	−0.16	−0.06	−0.07	−1.1	−1.08	14720	2.9	4.2	4.3	–	275
B8	−0.10	−0.02	−0.04	0.0	−0.60	11950	2.3	4.3	3.0	–	264
A0	0.00	0.02	−0.01	0.7	−0.14	9572	1.80	4.3	2.34	–	255
A2	0.06	0.08	0.04	1.3	0.00	8985	1.75	4.3	2.21	–	244
A5	0.14	0.16	0.07	1.9	0.02	8306	1.69	4.2	2.04	–	225
A7	0.19	0.19	0.12	2.3	0.02	7935	1.68	4.2	1.93	–	210
F0	0.31	0.30	0.16	2.7	0.04	7178	1.62	4.3	1.66	–	180
F2	0.36	0.35	0.22	3.0	0.04	6909	1.48	4.3	1.56	–	135
F5	0.44	0.40	0.29	3.5	0.02	6528	1.40	4.3	1.41	6.2	20
F8	0.53	0.47	0.33	4.0	−0.01	6160	1.20	4.4	1.25	5.1	9.0
G0	0.59	0.50	0.36	4.4	−0.05	5943	1.12	4.4	1.16	4.4	6.4
G2	0.63	0.53	0.39	4.7	−0.08	5811	1.08	4.4	1.11	3.7	4.8
G5	0.68	0.54	0.43	5.1	−0.11	5657	0.95	4.5	1.05	2.8	3.4
G8	0.74	0.58	0.48	5.6	−0.16	5486	0.91	4.5	0.97	1.9	2.6
K0	0.82	0.64	0.50	6.0	−0.23	5282	0.83	4.6	0.90	1.5	2.2
K2	0.92	0.74	0.54	6.5	−0.30	5055	0.75	4.6	0.81	1.2	2.0
K3	0.96	0.81	0.57	6.8	−0.33	4973	0.73	4.6	0.79	0.8	2.0
K5	1.15	0.99	0.67	7.5	−0.43	4623	0.64	4.6	0.65	–	1.9
K7	1.30	1.15	0.80	8.0	−0.54	4380	0.54	4.7	0.54	–	1.7
M0	1.41	1.28	–	8.8	−0.72	4212	0.48	4.7	0.46	–	1.5
M2	1.50	1.50	–	9.8	−0.99	4076	0.43	4.7	0.40	–	–
M5	1.60	1.80	–	12.0	−1.52	3923	0.38	4.8	0.34	–	–

FIGURE 3.9: Physical and Geometrical parameters for main sequence star (Gray, 2005).

with a mass of $\mathcal{M}_1 = 0.928 \pm 0.045 \mathcal{M}_\odot$.
Regarding the secondary component, its absolute magnitude will be $M_2 = M_1 + 1.5 = 7.17$. This value corresponds to the K4V spectral type with a mass of $\mathcal{M}_2 = 0.720 \pm 0.024\ \mathcal{M}_\odot$.
According to the expressions (3.14) and (3.15), we obtain the following values of the semi-major axes:

$$a = 1.3855 \pm 0.0076_{A.U},$$

$$a_1 = 0.6064 \pm 0.0294_{A.U}, \text{ and}$$

$$a_2 = 0.7791 \pm 0.0569_{A.U},$$

Sp	$B-V$	$V-R$	$b-y$	M_V	BC	T_{eff}	$R/R_\odot$	$\log g$	ζ_{RT}	$v \sin i$
F0	0.31	–	–	1.0	0.04	7178	7	–	–	135
F2	0.36	–	–	0.9	0.04	6909	–	–	–	128
F5	0.44	–	–	0.8	0.02	6528	–	–	8.5	115
F8	0.54	–	–	0.7	−0.02	6160	8	3.4	7.6	95
G0	0.64	–	–	0.6	−0.09	5943	9	3.2	7.0	75
G2	0.76	–	–	0.5	−0.17	5811	10	3.1	6.7	25
G5	0.90	0.69	–	0.4	−0.29	5657	11	2.8	5.8	5.8
G8	0.96	0.70	0.56	0.3	−0.33	5486	12	2.7	5.2	4.0
K0	1.03	0.77	0.60	0.2	−0.37	5282	14	2.5	4.8	3.0
K2	1.18	0.84	0.68	0.1	−0.45	5055	17	2.1	4.5	2.3
K3	1.29	0.96	0.80	0.1	−0.53	4973	21	–	4.3	2.0
K5	1.44	1.20	0.90	0.0	−0.81	4623	40	–	–	–
K7	1.53	–	0.93	−0.1	−1.15	4380	60	–	–	–
M0	1.57	1.23	0.97	−0.2	−1.36	4212	100	–	–	–
M2	1.60	1.34	1.00	−0.2	−1.52	4076	130	–	–	–
M5	1.58	2.18	–	−0.2	–	3923	–	–	–	–

Masses of class III giants are poorly determined, but are perhaps ≈2–2.5 solar masses.

FIGURE 3.10: Physical and Geometrical parameters for class III giants (Gray, 2005).

Sp type	K0V
V (mag)	7.77± 0.01
π_{Hip} (mas)	19.45± 1.40
π_{Gaia}(mas)	-
P (days)	463.44 ± 0.18
T $_{(MJD)}$	56108.7 ± 0.9
e	0.293 ± 0.003
$a_1 \sin(i)$(Gm)	70.48 ± 0.29
ω_1(degree)	274.7± 0.8
$f(\mathcal{M})(\mathcal{M}_\odot)$	0.0652 ± 0.0008

TABLE 3.5: HD 471. Physical and orbital parameters

and using (1.16), the orbital inclination is,

$$i = 51.1° \pm 2.9° \text{ or } 128.9° \pm 2.9°.$$

The following Table 3.6 shows the corresponding results for different initial values of Δm for HD 471.

When sin(i) = 1, Δm is very close to 3.5. So, the possible scenarios for HD 471 are between Δm = 1.5 and Δm = 3.5.

Now, following the explanations of subsection 3.2.5, we will obtain the maximum and minimum values of ρ'' for different values of Δm (see Table 3.7).

Sp. type	$(J-H)_0$	$(H-K_s)_0$	Sp. type	$(J-H)_0$	$(H-K_s)_0$
O5 V	−0.17	−0.06	K1 V	0.415	0.105
B0 V	−0.15	−0.05	K2 V	0.44	0.11
B2 V	−0.13	−0.04	K3 V	0.49	0.12
B5 V	−0.09	−0.03	K4 V	0.54	0.135
B8 V	−0.06	−0.02	K5 V	0.59	0.145
A0 V	−0.04	0.01	K6 V	0.62	0.15
A2 V	−0.01	0.02	K7 V	0.64	0.16
A5 V	0.03	0.035	M0 V	0.65	0.18
A7 V	0.06	0.04	M1 V	0.64	0.20
F0 V	0.09	0.045	M2 V	0.63	0.23
F2 V	0.12	0.05	M3 V	0.60	0.245
F5 V	0.18	0.055	M4 V	0.56	0.28
F8 V	0.23	0.06	M5 V	0.60	0.34
G0 V	0.26	0.07	M6 V	0.63	0.38
G2 V	0.28	0.075	M7 V	0.65	0.41
G5 V	0.30	0.08	M8 V	0.67	0.44
G8 V	0.34	0.09	M9 V	0.72	0.47
K0 V	0.39	0.10			

FIGURE 3.11: Color indices for main-sequence luminosity class (Straizys and Lazauskaite, 2009).

Sp. type	$(J-H)_0$	$(H-K_s)_0$	Sp. type	$(J-H)_0$	$(H-K_s)_0$
G5 III	0.40	0.09	K5 III	0.76	0.205
G8 III	0.45	0.105	M0 III	0.80	0.22
K0 III	0.50	0.125	M1 III	0.82	0.24
K1 III	0.54	0.14	M2 III	0.84	0.26
K2 III	0.59	0.155	M3 III	0.85	0.285
K3 III	0.65	0.17	M4 III	0.86	0.31
K4 III	0.71	0.185	M5 III	0.87	0.34

FIGURE 3.12: Color indices for Late-type giant luminosity class (Straizys and Lazauskaite, 2009).

Regarding the drawing of the apparent orbit, Figure 3.14 shows only the extreme and the mean cases. Of course, in the case of sin(i), the apparent orbit is always a segment of a straight line.

In conclusion, the most probable values of ρ''_{max} are between 0."0272 $\pm$ 0.0020 and 0."0249$\pm$0.0018. In these conditions, a telescope of 4.30 m (or larger) of diameter will be necessary to try to

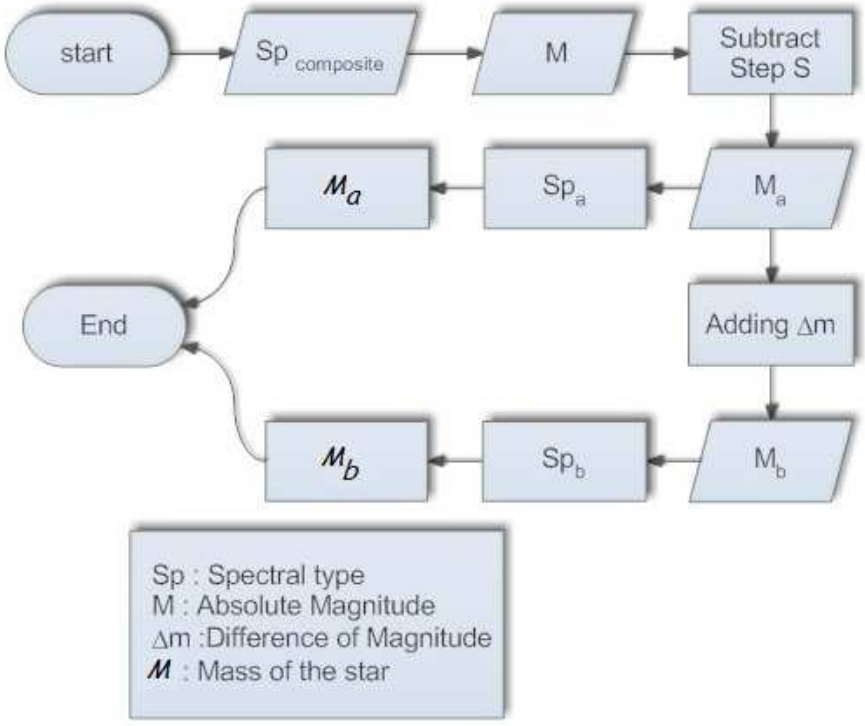

FIGURE 3.13: Algorithm to obtain the mass of the components for SB1

Δm	S	M_1	M_2	Sp_1	Sp_2	$\mathcal{M}_{1(\mathcal{M}_\odot)}$	$\mathcal{M}_{2(\mathcal{M}_\odot)}$	$a_{(A.U)}$	sin(i)	i
1.5	0.30	5.67±0.02	7.17±0.03	G8V	K4V	0.929±0.047	0.723±0.026	1.3855±0.0076	0.777	51.1±2.9
2.0	0.27	5.70±0.02	7.70±0.03	G8V	K5V	0.914±0.045	0.677±0.019	1.3683±0.0070	0.810	54.1±3.0
2.5	0.23	5.74±0.02	8.24±0.02	G8V	K7V	0.910±0.044	0.606±0.016	1.3475±0.0067	0.878	61.4±3.2
3.0	0.18	5.79±0.02	8.79±0.02	G9V	K9V	0.901±0.043	0.559±0.020	1.3294±0.0068	0.927	68.0±3.9
3.5	0.14	5.83±0.02	9.33±0.02	G9V	M1V	0.884±0.042	0.500±0.024	1.3061±0.0078	0.999	$\simeq$ 90.0

TABLE 3.6: Orbital inclination and intermediary parameters as a function of Δm

Δm	a''	ρ''_{max}	ρ''_{min}
1.5	0.0269±0.0019	0.0272±0.0020	0.0093±0.0006
2.0	0.0266±0.0019	0.0267±0.0019	0.0081±0.0006
2.5	0.0262±0.0019	0.0261±0.0019	0.0077±0.0005
3.0	0.0259±0.0019	0.0255±0.0018	0.0046±0.0003
3.5	0.0254±0.0018	0.0249±0.0018	0.0014±0.0003

TABLE 3.7: Semimajor axis and the maximum and minimum values of the angular separation, ρ'', as a function of Δm

optically resolve this system in the epochs when ρ'' is near to the maximum value.

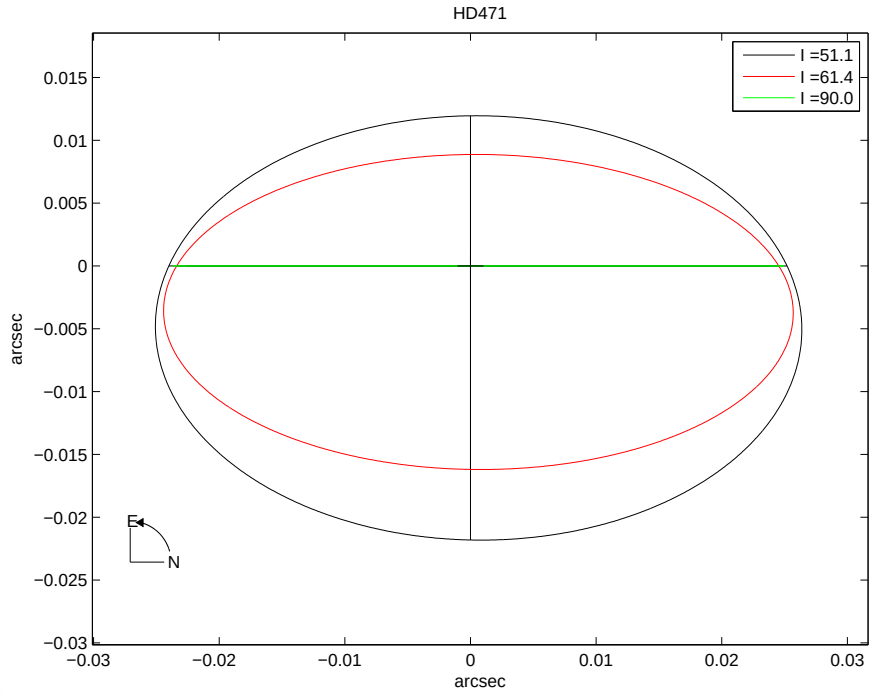

FIGURE 3.14: Apparent orbits of HD 471 with different inclinations

3.4 Double-lined Spectroscopic binaries (SB2)

If the series of the spectral lines of both components are present in the observable spectrum and the orbit and parallax are known, all of that explained in precedent subsections for the SB1 remains valid but, in this case, we have additional information. Indeed, now the orbital parameters are P, T, e, $A_1 = a_1.\sin(i)$, $A_2 = a_2.\sin(i)$, and ω_1 or $\omega = 180^\circ + \omega_1$.
In these conditions, taking into account (4.15), the result is:

$$\frac{A_2}{A_1} = \frac{a_2}{a_1} = \frac{\mathcal{M}_1}{\mathcal{M}_2} = q, \tag{3.34}$$

so, the mass ratio, q, is known.
Hereafter, we will suppose that if the spectroscopic binary is a double-lined SB2, then Δm is less than 1.5 or 2.0 (depending on the observational instrumentation). It is even possible that, in a few cases with $\Delta m = 2.5$ it may also be an SB2. This is not a problem for us because our methodology selects the solution by means of q.
The first example, the binary HD 74089, will be explained in detail. In the following subsections, we will apply our methodology to other 8 cases of SB2 stars.

3.4.1 Application of the methodology to the SB2, HD 74089 system

This is a double-lined binary with a period (1231.9 days). The values of the parallaxes are Hipparcos, 1.85±1.05 mas and Gaia, 3.11 ± 0.24 mas. The color indices are V = 8.53, B-V = 0.88, J-H = 0.482, and H-K = 0.125, which correspond to a late-type giant star. To determine the class of the binary, R.F. Griffin suggested that the spectral types of the components are G8III and G2III-IV (Griffin, 2014b). On the other hand, from Simbad, the spectral type is K0 as reported in the Henry Draper Catalogue. Taking into account the color indices in the Strairzys and Lazauskaite paper, the spectral type is K0III (Straizys and Lazauskaite, 2009). The radial velocity of HD 74089 was first observed with the Cambridge Coravel spectrometer in February 2012. The radial velocity of the second component was established after about 11 months of observation. Griffin determined the orbital elements using 39 observations for the primary and 20 for the secondary component (Griffin, 2014b).

Sp type	K0III
V_T (mag)	8.53 ± 0.01
π_{Hip} (mas)	1.85± 1.06
π_{Gaia}(mas)	3.11 ± 0.24
P (days)	1321.9126 ± 0.0017
T $_{(MJD)}$	56255.501 ± 0.016
e	0.0 ± 0.0
$a_1$sin(i)(Gm)	14.11± 0.07
$a_2$sin(i)(Gm)	15.36± 0.19
ω_1 (degree)	0.0± 0.0
q($\mathcal{M}_1/\mathcal{M}_2$)	1.0880 ± 0.0144

TABLE 3.8: HD 74089. Physical and orbital parameters

We consider the spectral type of HD 74089 to be K0III, with an absolute magnitude of 0.53. Starting with the value of Δm = 0.0 (Edward's step (S = 0)) the resultant spectral type for both components is K0III, with a mass of 1.91 ± 0.42, and an absolute magnitude of 0.53 for each component. The ratio of the masses is 1.00 ± 0.57 which is agreement with that provided by Griffin: 1.088 ± 0.014. For other cases with different values of Δm, see Table 3.9.

The inclination is 59°.0 with maximum and minimum separations of ρ''_{max} =0.00080±0.00007, and ρ''_{min} = 0.00041±0.00040, respectively. It would be necessary to use a large telescope array than 147m to resolve HD 74089 optically.

Δm	S	M_1	M_2	Sp_1	Sp_2	$\mathcal{M}_{1(\mathcal{M}_\odot)}$	$\mathcal{M}_{2(\mathcal{M}_\odot)}$	$a_{(A.U)}$	q $(m_1/\ m_2)$
0.0	0.00	0.53±0.07	0.53±0.07	K0III	K0III	1.91±0.42	1.91±0.42	0.237±0.001	1.000±0.57
0.5	0.19	0.34±0.07	0.84±0.08	K2III	A1IV	1.82±0.40	2.60±0.22	0.252±0.001	0.700±0.31
1.0	0.29	0.25±0.05	1.25±0.06	K3III	A4IV	1.75±0.28	2.31±0.17	0.244±0.007	0.75±0.30

TABLE 3.9: Orbital inclination and intermediary parameters as a function of Δm for HD 74089

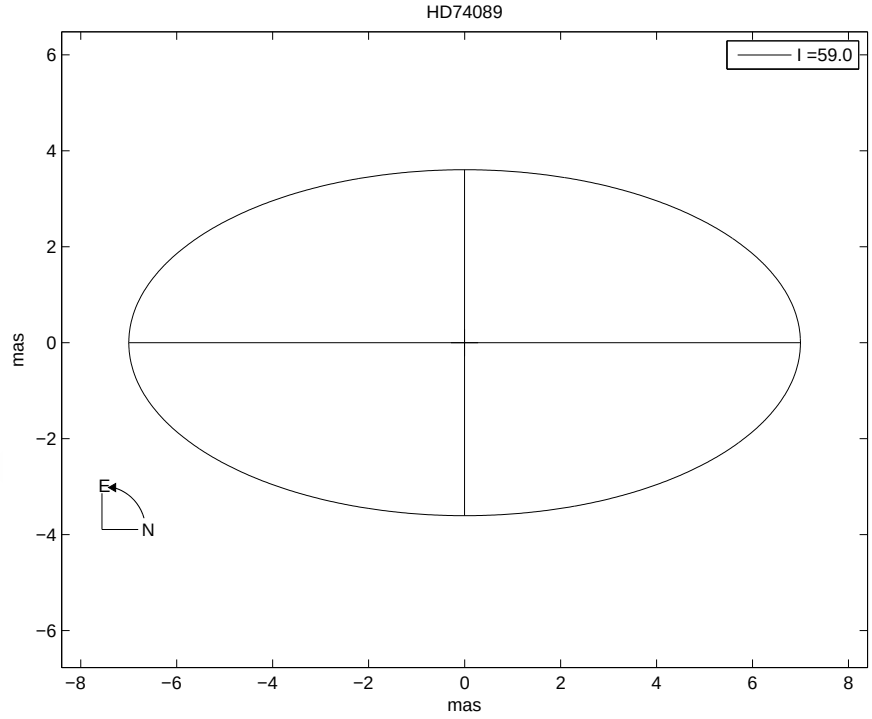

FIGURE 3.15: The most probable apparent orbit of HD 74089

3.5 Testing the Methodology

In this section, in order to prove the utility of the developed methodology, we will apply it to a single-lined spectroscopic binary (HD219834), which have been resolved by speckle interferometry and the which the visual orbits also have been calculated. In this cases we have the complete orbit solution and the physical parameters.

We will use only the spectroscopic parameters of them to apply the methodology described and then we will compare our results with the interferometric elements and to study the agreement between two orbits. to confirm our solution.

Single-lined (HD219834)

The current spectroscopic orbit was published by (Katoh et al., 2013), while the visual orbit was calculated by (Docobo and Tamazian, 2012).

Sp type	G8.5IV
V (mag)	5.19
π_{Hip} (mas)	47.35±1.40
π_{Gaia}(mas)	-
P (days)	2298.15±2.51
T $_{(MJD)}$	53748.271±2.978
e	0.162 ± 0.002
$a_1$sin(i)(Gm)	187.89±0.33
ω_1(degree)	212.13±0.43
$f(\mathcal{M})(\mathcal{M}_\odot)$	0.05023±0.00029

TABLE 3.10: HD219834. Physical and spectroscopic orbital parameters

P $_{(yr)}$	6.314±0.020 (2306.14 $_{days}$)
T $_{(yr)}$	1980.73±0.020 (53728.38 $_{days}$)
e	0.191 ± 0.030
$a^{''}$	0.187±0.003
i (degree)	45.8±0.5
Ω (degree)	342.6±1.5
ω (degree)	28.3±2.5
$\rho^{''}{}_{max}$	0.218±0.004
$\rho^{''}{}_{min}$	0.114±0.004

TABLE 3.11: HD 219834. Visual orbital elements for MCA Aa, Ab (HD 219834)

The allowed values of Δm for HD 219834 are up to 6.0 which yields the maximum value for the absolute magnitude of 9.13 forthe secondary (a main sequence star) with a M0V spectral type. In Table (3.10), we can find the orbital inclination and intermediary parameters.

Δm	S	M_1	M_2	Sp_1	Sp_2	$\mathcal{M}_{1(\mathcal{M}_\odot)}$	$\mathcal{M}_{2(\mathcal{M}_\odot)}$	$a_{(A.U)}$	sin(i)	i
1.5	0.30	2.85±0.05	4.35±0.01	F8IV	F9V	1.35±0.05	1.11±0.04	4.6009±0.0536	0.605	37.3±3.3
3.0	0.18	2.96±0.08	5.96±0.02	G0IV	G9V	1.30±0.02	0.87±0.02	4.4100±0.04841	0.711	45.3±4.1
4.0	0.01	3.05±0.04	7.05±0.03	G3IV	K3V	1.25±0.01	0.73±0.03	4.2797±0.3454	0.796	52.8±4.6
6.0	0.02	3.13±0.05	9.13±0.02	G6IV	M0V	1.20±0.03	0.53±0.02	4.0932±0.3683	0.999	≅ 90.0

TABLE 3.12: Orbital inclination and intermediary parameters as a function of Δm for HD219834

Δm	$a^{''}$	$\rho^{''}{}_{max}$	$\rho^{''}{}_{min}$
1.5	0.2179±0.0171	0.2482±0.0198	0.1532±0.0113
3.0	0.2089±0.0163	0.2376±0.0162	0.1308±0.0104
4.0	0.2026±0.0151	0.2301±0.0133	0.1093±0.0085
6.0	0.1938±0.0135	0.2197±0.0109	0.0732±0.0057

TABLE 3.13: Semimajor axis and the maximum and minimum values of the angular separation, $\rho^{''}$, as a function of Δm

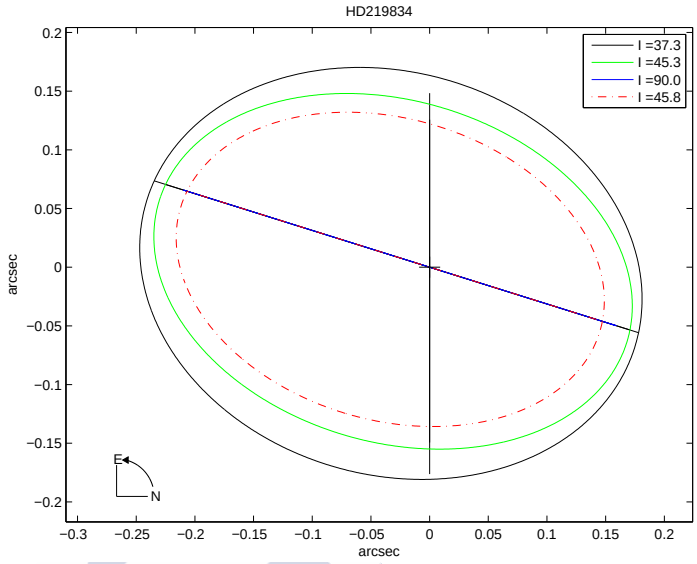

FIGURE 3.16: The apparent orbit of the visual (speckle) orbit (Docobo and Tamazian), in green, compared with other orbits obtained with different inclinations using the present methodology. In black, selected orbit for HD 219834.

We determined the solution for four cases (see Table 3.12) with magnitude differences: 1.5, 3.0, 4.0, and 6.0. The spectral type for the main component ranges from F8IV to G6IV, with a maximum mass of 1.35±0.05 $\mathcal{M}_\odot$ and, for the secondary, the spectral type ranges from F9V to M0V, being 1.11±0.04 $\mathcal{M}_\odot$ the maximum mass.
The values of the extreme separations for the different solutions are shown in Table 3.13. In the case Δm = 3.0 there is strong agreement with visual Docobo and Tamazian orbit, specially taken into account the uncertainties in the orbital elements.

Double-lined binaries (HD 16739, HD 27176, HD 170153, and HD 185734)

In double-lined binaries, the available spectroscopic orbital parameters are P, T, e, A_1 = a_1.sin(i), A_2 = a_2.sin(i), ω, and consequently the mass ratio, q = $\mathcal{M}_1/\mathcal{M}_2$. We will apply the same steps as in the single-lined case, but now the calculated value of q (as a function of Δm), will give us the best solution for the system. In Table 3.14 are represented, for the four testing double-lined binaries, spectroscopic orbital parameters, including the orbits authors. Table 3.15, shows the visual orbital elements for the same binaries.

- **HD 16739**: Applying the methodology with Δm = 0.5, we obtain a''= 0.0493±0.0006 the results suggest that this system probably consists of two main-sequence stars with the spectral types F8V and G2V. The masses would be 1.18±0.03 $\mathcal{M}_\odot$ and 1.04±0.04

Parameters	HD 16739	HD 27176	HD 170153	HD 185734
Sp type	F9V	F0V	F7V	G8III
V_T (mag)	4.928	5.626	3.580	4.673
π_{Hip} (mas)	41.34±0.43	18.50±0.63	124.11±0.87	12.25±0.24
P(days)	330.990±0.004	4145.72±7.67	280.517±0.062	434.208±0.046
T $_{(MJD)}$	49112.400±0.099	43415.7±19.8	46005.6±0.5	51239.58±0.10
e	0.6630±0.0021	0.167±0.004	0.414±0.008	0.5557±0.0009
$a_1$sin(i)(Gm)	71.2±3.5	413±28	608.01±68	131.05±2.70
$a_2$sin(i)(Gm)	80.8±3.6	510.45±8.00	854.74±16	135.1±3.1
ω (degree)	269.927±0.317	158.7±1.9	119.86±0.97	209.41±0.13
q ($\mathcal{M}_1/\mathcal{M}_2$)	1.136±0.104	1.235±0.240	1.406±0.051	1.04 ±0.02
Orbit Authors	(Pourbaix, 2000)	(Pourbaix, 2000)	(Farrington et al., 2010)	(Massarotti et al., 2008)

TABLE 3.14: Physical and spectroscopic orbital parameters for testing double-lined binaries

Orbital information	HD 16739 MCA 8	HD 27176 MCA 14 Aa, Ab	HD 170153 LAB 5 Aa, Ab	HD 185734 MCA 57
P $_{(yr)}$	300.98209 $_{(d)}$	11.350$_{(yr)}$	280.5280± 0.0223$_{(d)}$	434.171±0.015 $_{(d)}$
T $_{(yr)}$	1993.33956 $_{(yr)}$	1977.740±0.056$_{(yr)}$	46004.680±0.949 $_{(d)}$	28230.76±0.62 $_{(d)}$
e	0.6574	0.1670±0.0044	0.428±0.012	0.5420±0.0063
a''	0.05318	0.1329±0000000	0.1244±0.0110	0.0269±0.0008
i (degree)	128.17	125.50±0.73	74.42±0.58	80.80±0.63
Ω(degree)	42.29	350.70±0.61	230.30±0.51	251.00±0.86
ω(degree)	269.29	339.0±1.9	119.3±1.1	34.0±1.3
ρ''_{max}	0.0545	0.1535	0.1423	0.0378
ρ''_{min}	0.0113	0.0705	0.0199	0.0029
Orbit Authors	(Bagnuolo et al., 2006)	(Pourbaix, 2000)	(Farrington et al., 2010)	(Pourbaix, 2000)

TABLE 3.15: Visual orbital elements for testing double-lined binaries

$\mathcal{M}_\odot$, respectively. The ratio of mass is 1.136±0.047 which equals the ratio of the mass provided by the spectroscopic data 1.136±0.104 (see Table 3.14), but the combined spectroscopic - speckle orbit gives a total mass a bit great than ours (0.4 $\mathcal{M}_\odot$ more).

When Δm = 0.5, the separation between the components (0.″0457 - 0.″0092) ranges close to the measured speckle separations (see Table 3.13). There is also a good agreement between the inclinations: 56°.3 or 123°± 3.4 (our solution), and 128.17 (Bagnoulo et al. solution). Figure 3.17 shows the Apparent orbit for spackle one (in green), and that obtains with Δm = 0.5 (dots ellipse)

- **HD 27176**: The composite spectral type of this binary is F6IV, which can be separated into the spectral types, F5IV and F9IV, with a magnitude difference of 0.85. In these conditions, the corresponding masses are 1.74 ± 0.03 $\mathcal{M}_\odot$ and 1.38 ± 0.03 $\mathcal{M}_\odot$, with a ratio of mass of 1.25±0.03 which is very near to that from the spectroscopic orbital solution, 1.24±0.24. The speckle orbit using the Hipparcos parallax gives a total mass of 3.38 $\mathcal{M}_\odot$ (3.12 $\mathcal{M}_\odot$ with our solution). We also obtain the following values for the angular semi-major axis and inclination: 0.″1365 ± 0.0037, and 55.°9 or 124.1 ± 3.2 These values are in concordance with those of the speckle orbit (0.″1329, and 125.5± 0.7, respectively). A very good agrement between the angular distances has been obtained:
(ρ''_{max}) $_{Visual\ orbit}$ - (ρ''_{max}) $_{Calculated}$ = - 0.″0041;

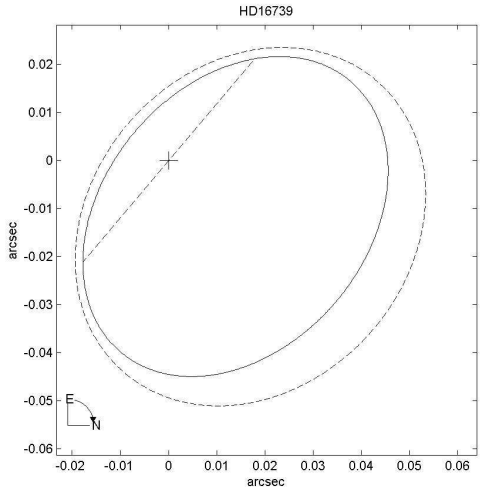

FIGURE 3.17: Apparent orbits for HD 16739. Continuously line represents the speckle orbit of Bagnoulo at al, while dots line is the solution that corresponds to Δm = 0.5.

$(\rho''_{min})_{Visual\ orbit}$ - $(\rho''_{min})_{Calculated}$ = + 0.″0009

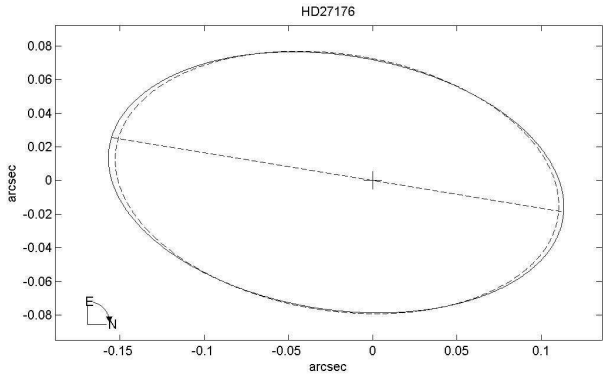

FIGURE 3.18: HD 27176. The very good agreement between the two orbits. In green (continues line), the speckle solution and with dots the solution obtained with this methodology.

- **HD 170153**: The spectral type for this system is F7V. For Δm = 2.0, we obtain a value of q = 1.408±0.058 in perfect agreement with that of the spectroscopic orbit: q = 1.406 ± 0.051. If we work in this scenario, the individuals spectral types are F5V and G2V, with masses: 1.29 ± 0.03 $\mathcal{M}_{\odot}$, and 0.93 ± 0.05 $\mathcal{M}_{\odot}$ respectively. We deduced for

this solution, a'' = 0.1376±0015, and i = 64.°5±3.5. The corresponding values of the maximum and minimum separation are very close: ρ''_{max} = 0.″1423, ρ''_{min} = 0.″0199 (speckle orbit), ρ''_{max} = 0.″1572 ± 0.0280, ρ''_{min} = 0.″0366 ± 0.0050 (our solution).

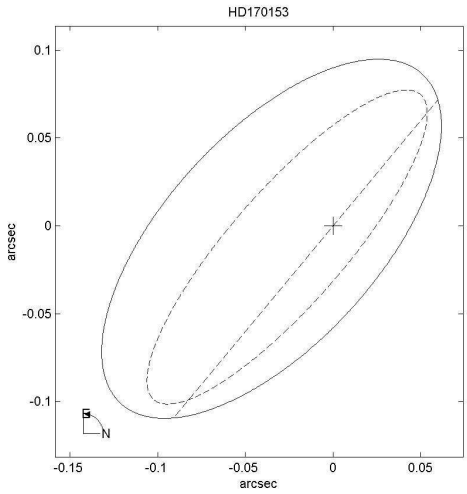

FIGURE 3.19: Apparent orbits of HD170153. In green (continues line), the speckle orbit, and with dots, the solution obtained using our methodology

- **HD 185734**:

  We find for this system of giant components (G8III) that if Δm = 0.3, the results are q = 1.09 ± 0.50 (q = 1.04 ± 0.02 for the spectroscopic orbit), individual spectral types : G2III and G9III (see table B.3, Appendix B), individual masses: = $\mathcal{M}_1$ = 1.89 ± 0.42 $\mathcal{M}_\odot$, $\mathcal{M}_2$ = 1.73 ± 0.28 $\mathcal{M}_\odot$. Semi-major axis:

  a'' = 0.″0211 ± 0.0011 (0.″0269 ± 0.0008 for the speckle orbit).

  The orbital inclination: 86.°2±4.0 (80.°8 for the speckle orbit),

  ρ''_{max} = 0.″0328 ± 0.0026, (0.″0378 for the speckle orbit),

  ρ''_{min} = 0.″0013 ± 0.0007, (0.″0029 for the speckle orbit).

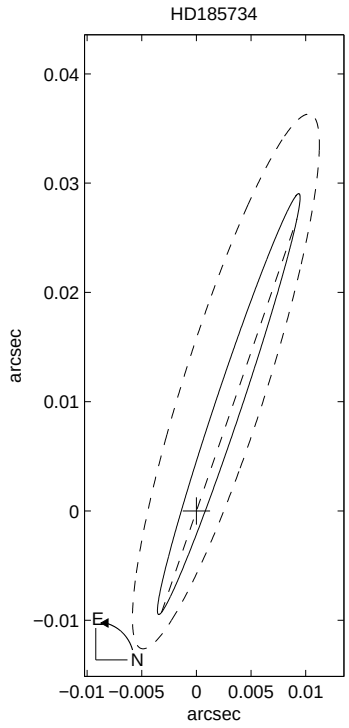

FIGURE 3.20: Very inclined apparent orbits of HD 185734. That calculated by Porbaix (speckle orbit) is represented in green (solid line). Our solution is that with dots.

3.6 The study of different cases of single-lined spectroscopic binaries (SB1)

In this section, we include the detailed study of 15 additional SB1 systems, applying the methodology explained earlier in this chapter. All the binaries have been selected from papers by R. F. Griffin.

3.6.1 HD 4703

This is a single-lined giant SB with 9 magnitude and a probable K2III spectral type (Griffin, 2015c). There is Tycho information about color indices (V=8.93 and B-V=1.14). In the Henry Draper Catalogue, the spectral type is K0 and the Hipparcos parallax is 4.63±1.03 mas. Nevertheless, the Gaia measurement indicates that this binary is twice as far away π_{Gaia} = 2.55 ± 0.35 (mas).

R. Griffin carried out many measurements of radial velocities of this system. The first of them was performed in 1978. In 2015, he added 67 more using the Coravel spectrometer at the Cambridge Observatory in order to calculate the orbital elements (Famaey et al., 2005; Griffin, 2015c).

We will work with the values of 1.5, 4.5, and 9.0 for Δm. In The Table 3.13 gives the corresponding values described in the previous example. In all of the cases, the main component is a giant while the secondary can be a sub-giant or a main-sequence star. The spectral type of the secondary may be from A6IV to M1V. On other hand, and the maximum separation between the components would be from 0.″0120 to 0.″0106 Table 3.14.
Taking into account this last information, a 10 m class telescope would be necessary to resolve this pair. Figure 3.21 shows the apparent orbits corresponding to the three studied case.

Sp type	K2III
V(mag)	8.93 ± 0.02
π_{Hip}(mas)	4.63± 1.03
π_{Gaia}(mas)	2.55± 0.35
P (days)	950.7±0.9
T $_{(MJD)}$	54874.5 ± 2.3
e	0.562 ± 0.010
$a_1$sin(i)(Gm)	42.2± 0.8
ω_1(degree)	30.1± 0.8
$f(\mathcal{M})(\mathcal{M}_\odot)$	0.00333 ± 0.00002

TABLE 3.16: HD 4703. Physical and orbital parameters

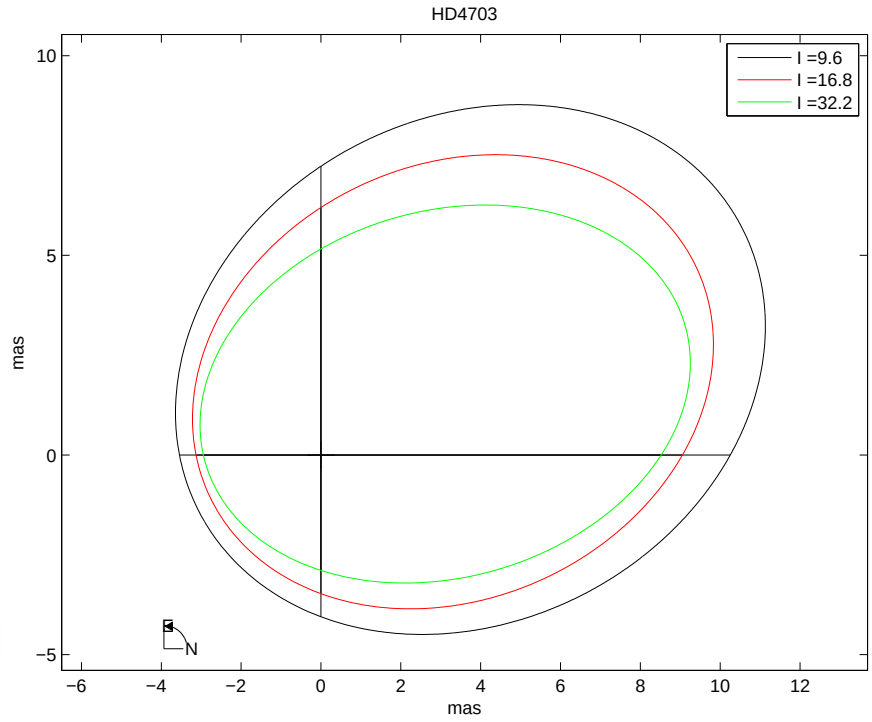

FIGURE 3.21: Apparent orbits of HD 4703 with different inclinations

Δm	S	M_1	M_2	Sp_1	Sp_2	$\mathcal{M}_{1(\mathcal{M}_\odot)}$	$\mathcal{M}_{2(\mathcal{M}_\odot)}$	$a_{(A.U)}$	sin(i)	i
1.5	0.300	0.10±0.02	1.6±0.03	K4III	A6IV	1.73±0.26	2.09±0.13	2.959±0.027	0.123	9.6±0.9
4.5	0.070	0.33±0.02	4.83±0.03	K2III	G3V	1.79±0.57	1.03±0.04	2.675±0.005	0.289	16.8±1.3
9.0	0.002	0.40±0.02	9.40±0.02	K2III	M1V	1.88±0.40	0.50±0.02	2.526±0.046	0.356	32.17±2.0

TABLE 3.17: Orbital inclination and intermediary parameters as a function of Δm for HD 4703

Δm	a''	ρ''_{max}	ρ''_{min}
1.5	0.0077±0.0011	0.0120±0.0020	0.0032±0.0004
4.5	0.0068±0.0009	0.0108±0.0010	0.0028±0.0004
9.0	0.0064±0.0008	0.0106±0.0010	0.0021±0.0003

TABLE 3.18: Semimajor axis and the maximum and minimum values of the angular separation, ρ'', as a function of Δm for HD4703

3.6.2 HD 10171

HD 10171 is a K0III spectral type binary. Its Tycho photometry is V = 9.0, B-V = 1.07. The system was observed in 1971 and 1974 with the old Coravel spectrometer and 58 more observations were performed with the new instrument from 2002 until December 2013 (Griffin, 2015a).
The Hipparcos parallax has an error (-1.39± 1.57 mas) but, fortunately, Gaia provided us with a new parallax, 2.86± 0.26 mas, (Simbad Website, 2016). The orbital elements of this binary were determined for the first time by R.F. Griffin and they are shown in Table 3.15 (ibid.).
In order to apply our methodology, we chose the values of Δm = 1.5, 4.5, 9.0. The possible spectral types for the primary component are from K4III to K0III and from A6IV to M1V for the secondary (Table 3.16). The most probable maximum separation is between $0.''009$ and $0.''008$ (Table 3.17) and, for this concrete situation, we would need a 13m telescope (or larger) to optically resolve the system. In Figure 3.22 are represented the apparent orbits corresponding to the three studied cases.

Sp type	K0III
V_J (mag)	9.00 ± 0.02
V_{Gaia} (mag)	8.562
π_{Hip} (mas)	-1.39± 1.57
π_{Gaia}(mas)	2.86± 0.26
P (days)	640.8 ± 0.5
T $_{(MJD)}$	54206.4 ± 2.5
e	0.38 ± 0.01
$a_1$sin(i)(Gm)	34.90 ± 0.58
ω_1 (degree)	196.3± 1.8
$f(\mathcal{M})(\mathcal{M}_\odot)$	0.00414 ± 0.00017

TABLE 3.19: HD 10171. Physical and orbital parameters

Δm	S	M_1	M_2	Sp_1	Sp_2	$\mathcal{M}_{1(\mathcal{M}_\odot)}$	$\mathcal{M}_{2(\mathcal{M}_\odot)}$	$a_{(A.U)}$	sin(i)	i
1.5	0.300	0.15±0.04	1.65±0.03	K4III	A6V	1.73±0.26	2.07±0.19	2.270±0.035	0.033	10.9±1.0
4.5	0.070	0.46±0.07	4.96±0.01	K0III	G4V	1.89±0.58	1.01±0.04	2.076±0.071	0.317	18.4±1.4
9.0	0.002	0.53±0.07	9.53±0.02	K0III	M1V	1.91±0.04	0.48±0.02	1.944±0.049	0.599	36.8±2.1

TABLE 3.20: Orbital inclination and intermediary parameters as a function of Δm for HD10171

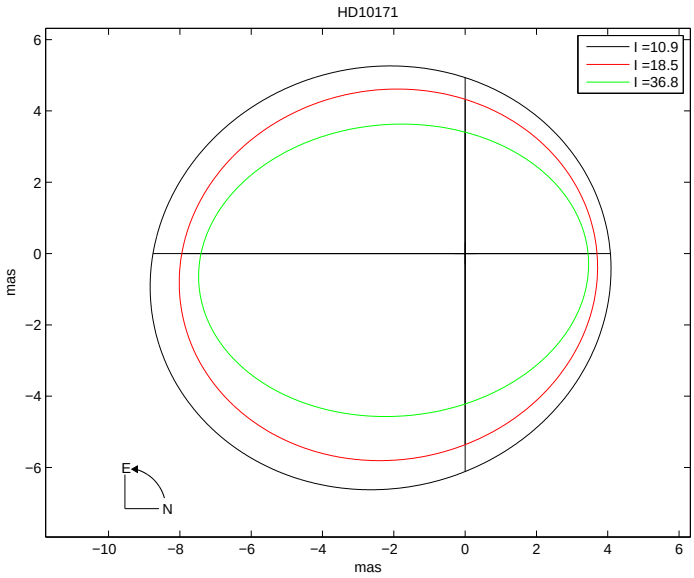

FIGURE 3.22: Apparent orbits of HD 10171 with different inclinations

Δm	a''	ρ''_{max}	ρ'' min
1.5	0.0065 ± 0.0006	0.0090±0.0008	0.0040±0.0004
4.5	0.0059 ± 0.0006	0.0082±0.0008	0.0037±0.0004
9.0	0.0065 ± 0.0005	0.0080±0.0007	0.0034±0.0003

TABLE 3.21: Maximum values of the angular separation, ρ'', as a function of Δm for HD10171

3.6.3 HD 22521

The HD 22521 system is classified as a G0 star in the Henry Draper Catalogue (Cannon and Pickering, 1918), with Tycho 2 photometry V = 6.74, B-V = 0.58 (Høg et al., 2000b). R. Griffin suggested that the spectral type is G0V and, from Simbad, the Hipparcos parallax is 24.78 ± 1.15 mas.

A. Goldin and V. Makarov are the authors of the first publication that provide an astrometric analysis of the orbit with a period of 1119^{+96}_{-63} days and 1091^{+114}_{-74} days. Unfortunately, it was not helpful determine the inclination due to the different periods with different uncertainties in them (Goldin and Makarov, 2006, 2007).

The first four radial-velocities with a mean velocity of -39.2 km/s were performed with the 74 inch reflector at the David Dunlap Observatory (1939-1942), and later three with the OHP Coravel spectrometer with a mean of -40.5 Km/s and 54 radial velocities using Coravel at Cambridge. Griffin suggested that the primary component belongs to main-sequence with 1.1 solar mass, and the upper limit for the secondary is 0.3 solar mass (Griffin, 2014d).

For main sequence stars, we take into account the maximum value for the absolute magnitude of the second component that should be less than 12.54 with an M5V spectral type, (total absolute magnitude $\leq$ 12.54) see Appendix B (Table B.1 - Calibrations).

We obtained the spectral types for the components of HD 22521 as follows: main sequence

(F8-9, G0) for the primary, and (G6, K3, M0, M2) for the secondary.
The HD 22521 system could be optically observed using a telescope with a diameter of at least 1.3 meters, when ρ''_{max} = 0.0891±0.0044 and Δm = 1.5 but, in the last possible scenario studied, preferable case a large telescope would be necessary (see Table 3.20). In Figure 3.23 are drawn the corresponding three apparent orbits.

Sp type	G0V
V_J(mag)	6.738 ± 0.010
π_{Hip} (mas)	24.78± 1.15
π_{Gaia}(mas)	-
P (days)	1009.4± 0.6
T $_{(MJD)}$	55207.7 ± 0.7
e	0.655 ± 0.004
$a_1$sin(i)(Gm)	72.6± 0.6
ω_1 (degree)	326.0± 0.7
$f(\mathcal{M})(\mathcal{M}_\odot)$	0.0150 ± 0.0004

TABLE 3.22: HD 22521. Physical and orbital parameters

Δm	S	M_1	M_2	Sp_1	Sp_2	$\mathcal{M}_{1(\mathcal{M}_\odot)}$	$\mathcal{M}_{2(\mathcal{M}_\odot)}$	$a_{(A.U)}$	sin(i)	i
1.5	0.300	4.02±0.02	5.52±0.01	F8V	G6V	1.18±0.03	0.97±0.04	2.542±0.042	0.423	25.1±1.8
4.5	0.070	4.33±0.01	8.34±0.02	F9V	M0V	1.12±0.05	0.54±0.02	2.425±0.005	0.641	39.9±2.2
9.0	0.002	4.40 ±0.07	12.40 ±0.02	G0V	M4V	1.09±0.04	0.34±0.05	2.222±0.005	0.921	67.3±3.9

TABLE 3.23: Orbital inclination and intermediary parameters as a function of Δm for HD 22521

Δm	a''	ρ''_{max}	ρ''_{min}
1.5	0.0630 ± 0.0031	0.0891±0.0044	0.0183±0.0009
4.5	0.0605 ± 0.0028	0.0638±0.0031	0.0122±0.0006
9.0	0.0576 ± 0.0026	0.0268±0.0013	0.0030±0.0001

TABLE 3.24: Maximum values of the angular separation, ρ'', as a function of Δm for HD22521

3.6.4 HD 26083

This binary is not included in the Ninth Catalogue of Spectroscopic Binary Orbits (Pourbaix et al., 2004). In Simbad, and also in in Henry Draper Catalogue, it is listed as a K0 star with

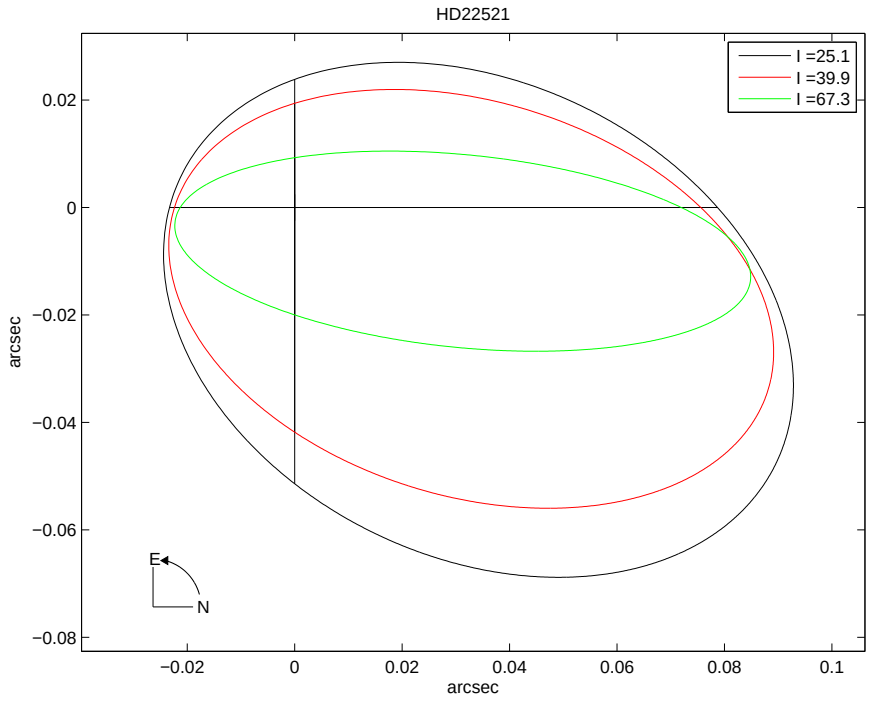

FIGURE 3.23: Apparent orbits of HD 22521 with different inclinations

a B-V color index, 1.096 and V_J= 9.07. The new parallax from Gaia is 2.37±0.28, is quite larger than that measured by Hipparcos, 1.32 ± 1.12 mas. Griffin considers HD 26083 to be a late type giant star with a short orbital period of about 18 days. He observed this binary at the first time in 2013 and he determined that it has a circular orbit using 31 radial-velocity observations at the Cambridge 36 inch Observatory and he mentioned that the spectral type is K0III depending on analysis of $v.sin(i)$ (Griffin, 2015d).

It will be difficult to observe this star visually because the angular separation between the components is very small (0.00050±0.00006 arc seconds).

Sp type	K0III
V_J (mag)	9.09 $\pm$ 0.02
V_{Gaia} (mag)	8.716
π_{Hip} (mas)	1.32$\pm$ 1.12
π_{Gaia}(mas)	2.37$\pm$0.28
P (days)	17.9500 $\pm$ 0.0025
T $_{(MJD)}$	56772.662 $\pm$ 0.025
e	0.0 $\pm$ 0.0
$a_1$sin(i)(Gm)	7.16 $\pm$ 0.07
ω_1 (degree)	0.0 $\pm$0.0
$f(\mathcal{M})(\mathcal{M}_\odot)$	0.0455 $\pm$ 0.0013

TABLE 3.25: HD 26083. Physical and orbital parameters

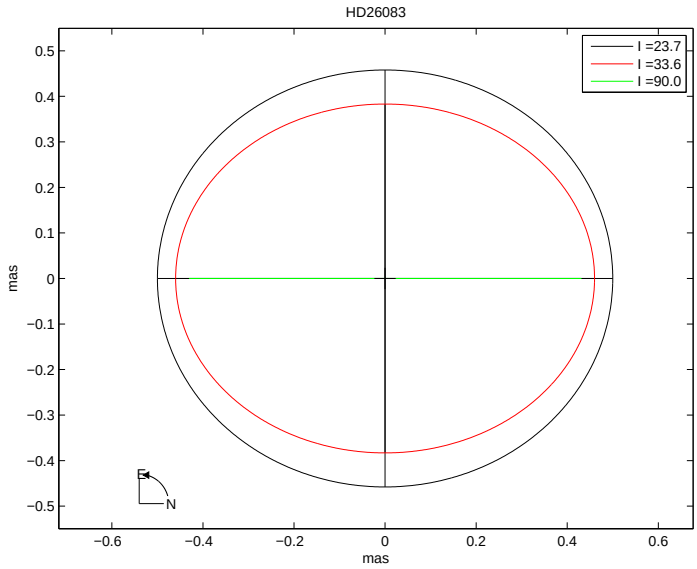

FIGURE 3.24: Apparent orbits of HD 26083 with different inclinations

Δm	S	M_1	M_2	Sp_1	Sp_2	$\mathcal{M}_{1(\mathcal{M}_\odot)}$	$\mathcal{M}_{2(\mathcal{M}_\odot)}$	$a_{(A.U)}$	sin(i)	i
1.5	0.300	0.18$\pm$0.04	1.68$\pm$0.01	K3III	A3V	1.73$\pm$0.26	2.22$\pm$0.06	0.213$\pm$0.011	0.402	23.70$\pm$1.7
3.0	0.180	0.30$\pm$0.05	3.30$\pm$0.02	K3III	F4V	1.76$\pm$0.29	1.38$\pm$0.04	0.197$\pm$0.006	0.553	33.63$\pm$2.0
6.9	0.012	4.47 $\pm$0.06	7.43$\pm$0.03	K0III	K5V	1.89$\pm$0.4	0.67$\pm$0.02	0.185$\pm$0.009	0.999	$\approx$ 90

TABLE 3.26: Orbital inclination and intermediary parameters as a function of Δm for HD 26083

3.6.5 HD 79888

HD 79888 is a G5 spectral type in the Henry Draper Catalogue and a K0V in Simbad. Its orbit has a very short period, about 8 days, and high negative γ-velocity ($V_\circ$), -80 km/s. Simbad also provides Gaia visual magnitude (V_Gaia = 8.829), and the Tycho-2 visual magnitude (V = 9.00 $\pm$ 0.02), with a color index of B-V = 0.8.

Δm	$a^{''}$	$\rho^{''}_{max}$	$\rho^{''}_{min}$
1.5	0.00050±0.00006	0.00055±0.00006	0.00045±0.00005
3.0	0.00046±0.00005	0.00050±0.00005	0.00038±0.00004
6.9	0.00043±0.00005	0.00040±0.00005	0.00030±0.00004

TABLE 3.27: Semimajor axis and the maximum and minimum values of the angular separation, $\rho^{''}$, as a function of Δm for HD26083

The allowed values of Δm for this system are up to 6.5, which yields for the secondary star to the maximum value for the absolute magnitude of a main sequence star, 12.54 with a M5V spectral type. In Table 3.25, we can see the orbital inclination and intermediary parameters for HD 79888.

We determined the solution for three cases of difference magnitude (1.5, 3.0, and 6.5). The spectral type for the first component are (G8-9V), with maximum mass 0.93±0.04 $\mathcal{M}_{\odot}$, and for the second component (with possible spectral types from K4Vto M5V), the maximum value of the mass is 0.72 ±0.02 $\mathcal{M}_{\odot}$.

From the previous analysis, we would need a very large telescope with a diameter of 156 meters to solve this system because, in the most favorable case, the value of the separation is between 0.”00075 and 0.”00057.

Sp type	K0V
V_J(mag)	9.00 ± 0.02
V_{Gaia}(mag)	8.828
π_{Hip} (mas)	6.11± 1.44
π_{Gaia}(mas)	6.78±0.31
P (days)	8.33929 ± 0.00018
T $_{(MJD)}$	56609.73 ± 0.07
e	0.0409 ± 0.0022
$a_1$sin(i)(Gm)	2.680± 0.006
ω_1 (degree)	201.7± 3.2
$f(\mathcal{M})(\mathcal{M}_{\odot})$	0.01104 ± 0.00007

TABLE 3.28: HD 79888. Physical and orbital parameters

Δm	S	M_1	M_2	Sp_1	Sp_2	$\mathcal{M}_{1(\mathcal{M}_{\odot})}$	$\mathcal{M}_{2(\mathcal{M}_{\odot})}$	$a_{(A.U)}$	sin(i)	i
1.5	0.300	5.59±0.02	7.09±0.03	G8V	K4V	0.93±0.04	0.72±0.02	0.095±0.001	0.430	25.50±1.7
3.0	0.180	5.79±0.02	8.79±0.02	G9V	K9V	0.90±0.04	0.54±0.02	0.091±0.001	0.528	31.87±1.9
6.5	0.016	5.95±0.02	12.45±0.03	G9V	M5V	0.87±0.04	0.33±0.05	0.086±0.001	0.761	49.61±2.4

TABLE 3.29: Orbital inclination and intermediary parameters as a function of Δm for 79888

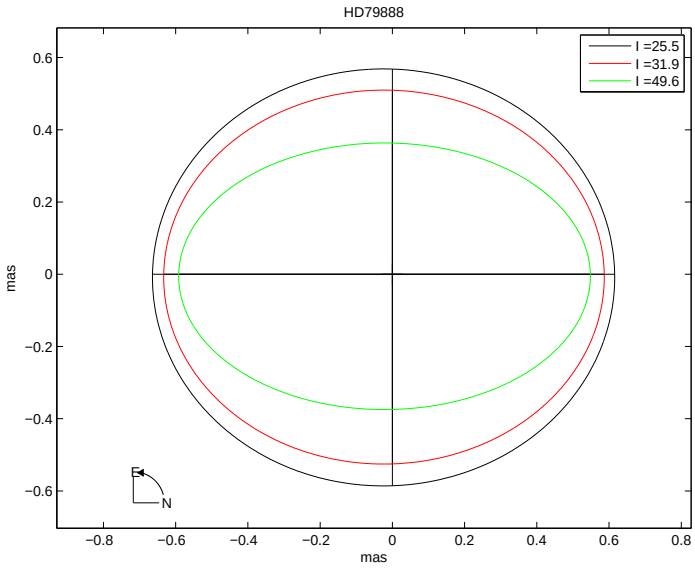

FIGURE 3.25: Apparent orbits of HD79888 with different inclinations

Δm	a''	ρ''_{max}	ρ''_{min}
1.5	0.00064±0.00003	0.00075±0.00003	0.00057±0.00003
3.0	0.00061±0.00003	0.00073±0.00005	0.00051±0.00004
6.5	0.00057±0.00003	0.00060±0.00005	0.00023±0.00004

TABLE 3.30: Maximum values of the angular separation, ρ'', as a function of Δm for 79888

3.6.6 HD 110583

HD 110583 is one of the single-lined stars that Roger Griffin published the orbit in 2014. The photometry was first described as V = 9.40, B-V = 1.07, and U-B = 0.95 (Haggkvist and Oja, 1973), V = 9.43, B-V =1.07 with K1III spectral type (Yoss and Griffin, 1997), and B-V = 1.07 (Soubiran et al., 2008).

Griffin obtained the orbital solution using 35 measurements of radial velocities, one at ESO (Germany), 5 by means of the original spectrometer at the Cambridge Observatory (UK), 13 at OHP (France), and 19 with Coravel at the Cambridge Observatory. Taking into account the small mass function, with a K1III spectral type, Griffin suggested that the masses of the components are 2.0 and 0.2 solar mass (Griffin, 2014a).

As a result of our methodology, the spectral type of the main component must be between K3III and K1III and, for the the companion, from A6IV to M1V. The maximum mass

for the first component is 1.90±0.42 solar mass and, when this happens, the inclination is 27.6° and corresponds to the value of Δm = 9.0. The maximum separation between the components, 0.″0415±0.″0078, would permit us to solve HD 110583 visually if we use a 3.0 m telescope.

Sp type	K1III
V_J (mag)	9.43±0.02
V_{Gaia} (mag)	9.034
π_{Hip} (mas)	-
π_{Gaia}(mas)	2.34± 0.34
P (days)	8161 ± 94
T $_{(MJD)}$	54891± 126
e	0.42 ± 0.06
$a_1$sin(i)(Gm)	146± 12
ω_1 (degree)	244± 8
$f(\mathcal{M})(\mathcal{M}_\odot)$	0.0019 ± 0.0004

TABLE 3.31: HD 110583. Physical and orbital parameters

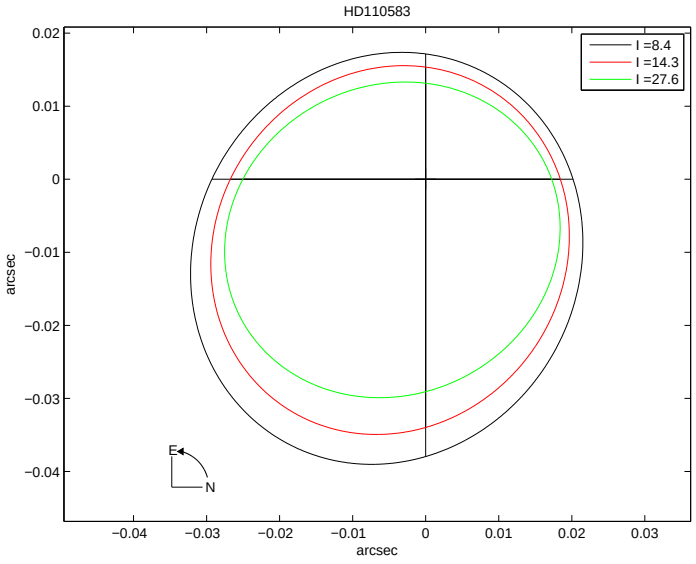

FIGURE 3.26: Apparent orbits of HD 110583 with different inclinations

Δm	S	M_1	M_2	Sp_1	Sp_2	$\mathcal{M}_{1(\mathcal{M}_\odot)}$	$\mathcal{M}_{2(\mathcal{M}_\odot)}$	$a_{(A.U)}$	sin(i)	i
1.5	0.300	0.18±0.05	1.68±0.06	K3III	A6IV	1.74±0.29	2.06±0.13	12.379±0.094	0.146	8.4±0.8
4.5	0.070	0.41±0.06	4.91±0.01	K2III	G3V	1.89±0.41	1.02±0.04	11.313±0.086	0.247	14.3± 1.1
9.0	0.002	0.48±0.07	9.47±0.02	K1III	M1V	1.90±0.42	0.48±0.03	10.584±0.081	0.643	27.6±1.9

TABLE 3.32: Orbital inclination and intermediary parameters as a function of Δm for HD 110583

Δm	a''	ρ''_{max}	ρ''_{min}
1.5	0.0290±0.0042	0.0415±0.0078	0.0169±0.0028
4.5	0.0265±0.0039	0.0386±0.0073	0.0153±0.0025
9.0	0.0248±0.0036	0.0355±0.0069	0.0131±0.0021

TABLE 3.33: Semimajor axis and the maximum and minimum values of the angular separation, ρ'', as a function of Δm for HD110583

3.6.7 HD 111224

HD 111224 belongs to the sub-giant luminosity class, with a K0IV spectral type. The photometry is: V = 9.41, B-V = 0.9, U-B = 0.59 (Haggkvist and Oja, 1973). On the other hand, K. M. Yoss and R. F. Griffin determined the V magnitude to be 9.43 (Yoss and Griffin, 1997). Hipparcos did not measure the parallax but the Gaia mission determined a value of 5.15 $\pm$ 0.35 (mas) and a visual magnitude of 9.075.

G. A. Radford, who was one of Griffin's students, obtained the first radial velocity of this system in 1973. Roger Griffin himself determined the orbital solution using 98 measurements of radial-velocities corresponding to an interval of 31 years since 1982. Of the total, 28 were carried out using the original spectrometer, 37 of them with Coravel in Cambridge, 26 in OHP (France), 5 using 48 inch Coude at DAO (Canada), and 2 in ESO (Germany) (Griffin, 2014a).

The HD 111224 system is an example of a binary with components of different luminosity classes. The principal component is a sub-giant and the secondary belongs to the main sequence. When we applied our methodology, we found that there are a few possibilities for the spectral type of the main component when the value of Δm equals 9.0 because, theoretically, the absolute magnitude is 1.2 which refers to the G8, G9, K0, and K1 spectral types of the sub-giant class (see Appendix C). In any case, K0IV is the most probable solution because this is the combined spectral type of the system.

We would need a telescope larger than 7 m to resolve HD 111224 optically because the value of the maximum separation between the components is $0.''0140 \pm 0.''0009$ when the inclination is 40° and Δm = 9.

Sp type	K0IV
V_J (mag)	9.43±0.02
V_{Gaia} (mag)	9.075
π_{Hip} (mas)	-
π_{Gaia}(mas)	5.15± 0.35
P (days)	861.8 ± 0.4
T $_{(MJD)}$	50968± 4
e	0.322 ± 0.010
$a_1$sin(i)(Gm)	96.2± 1.2
ω_1 (degree)	234.8± 2.1
$f(\mathcal{M})(\mathcal{M}_\odot)$	0.0479 ± 0.0018

TABLE 3.34: HD 111224 Physical and orbital parameters

Δm	S	M_1	M_2	Sp_1	Sp_2	$\mathcal{M}_{1(\mathcal{M}_\odot)}$	$\mathcal{M}_{2(\mathcal{M}_\odot)}$	$a_{(A.U)}$	sin(i)	i
1.5	0.300	2.85±0.01	4.35±0.01	F8IV	F9V	1.36±0.07	1.11±0.04	2.389±0.007	0.146	16.2±1.2
4.5	0.070	3.08±0.01	7.58±0.02	G4IV	K5V	1.23±0.01	0.66±0.02	2.189±0.002	0.247	23.1±1.5
9.0	0.002	3.15±0.12	12.15±0.04	K0IV	M4V	1.20±0.08	0.35±0.05	2.049±0.009	0.643	40.2±2.4

TABLE 3.35: Orbital inclination and intermediary parameters as a function of Δm for HD 111224

Δm	a''	ρ''_{max}	ρ''_{min}
1.5	0.0123±0.0008	0.0168±0.0012	0.0084±0.0006
4.5	0.0113±0.0007	0.0159±0.0011	0.0073±0.0005
9.0	0.0106±0.0007	0.0140±0.0009	0.0052±0.0004

TABLE 3.36: Maximum and minimum values of the angular separation, ρ'', as a function of Δm for HD 111224

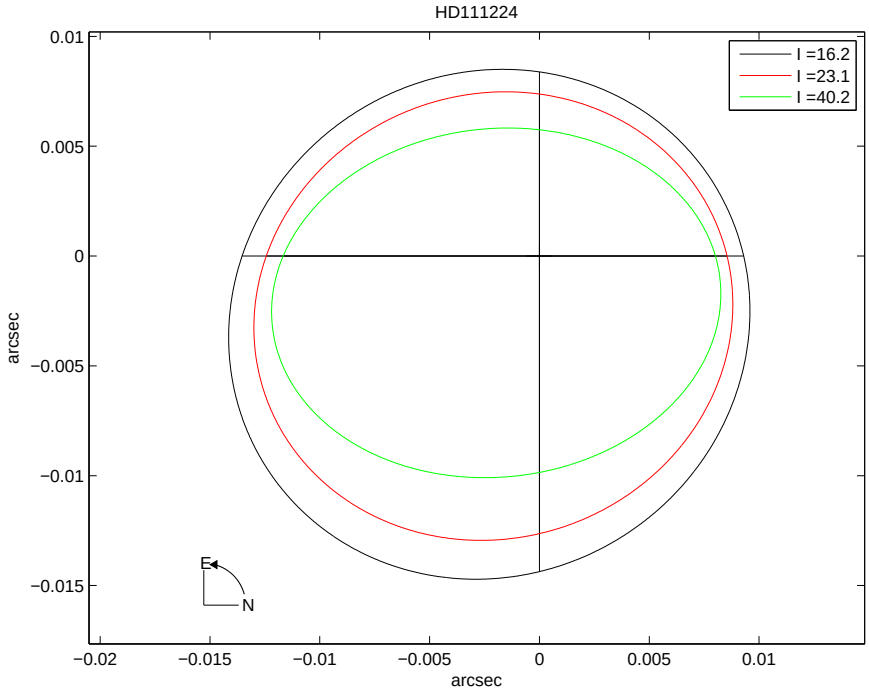

FIGURE 3.27: The most probable apparent orbit of HD 111224

3.6.8 HD 119915

There is little information about this system. Tycho photometry is V=8.56 and B-V=1.38 (the recent Gaia apparent magnitude is 9.253), and, according to Simbad, the spectral type is K4III.

It is important to highlight that the Gaia mission determined the parallax of HD 119915 to be 4.79± 0.24 mas, and the distance of the binary is one-half of the Hipparcos distance, π_{Hip} = 2.21± 0.93 mas.

In order to determine the orbit of this system Roger Griffin used, the radial velocity observations two with the original spectrometer at the Cambridge 36 inch telescope Observatory, one with Haute Provence Coravel, and 72 observations with the new spectrometer in Cambridge until 2014, were used (Griffin, 2014c).

To study the model for this binary, we selected 1.5, 4.5, and 9.0 as values for Δm which led to the spectral types and the masses for the components as we can see in Table 3.34. In any case, the orbital inclination is not higher than 25°.

We conclude that a telescope or an interferometer array with a diameter of more than 38

meters is necessary to resolve HD 119915 optically, especially in the epoch when ρ''_{max} = 0.0031±0.0002 (Table 3.39).

Sp type	K4III
V_J(mag)	8.56 ± 0.20
V_{Gaia}(mag)	9.253 ± 0.200
π_{Hip} (mas)	2.21± 0.93
π_{Gaia}(mas)	4.79±0.24
P (days)	101.137± 0.006
T $_{(MJD)}$	55795.07 ± 0.16
e	0.0 ± 0.0
$a_1$sin(i)(Gm)	7.58± 0.09
ω_1 (degree)	0.0± 0.0
$f(\mathcal{M})(\mathcal{M}_\odot)$	0.0017 ± 0.0001

TABLE 3.37: HD 119915. Physical and orbital parameters

Δm	S	M_1	M_2	Sp_1	Sp_2	$\mathcal{M}_{1(\mathcal{M}_\odot)}$	$\mathcal{M}_{2(\mathcal{M}_\odot)}$	$a_{(A.U)}$	sin(i)	i
1.5	0.300	-0.13±0.03	1.37±0.01	K6III	A5IV	1.2±0.05	2.18±0.01	0.637±0.009	0.123	7.1±0.6
4.5	0.070	0.1±0.03	4.6±0.02	K4III	G1V	1.75±0.26	1.06±0.41	0.599±0.003	0.224	12.9±1.1
9.0	0.002	0.17±0.04	9.17±0.02	K4III	M1V	1.73±0.26	0.52±0.02	0.557±0.002	0.394	23.2±1.5

TABLE 3.38: Orbital inclination and intermediary parameters as a function of Δm for HD119915

Δm	a''	ρ''_{max}	ρ''_{min}
1.5	0.0031±0.0002	0.0031±0.0002	0.0030±0.0002
4.5	0.0029±0.0002	0.0029±0.0002	0.0028±0.0002
9.0	0.0028±0.0002	0.0028±0.0002	0.0025±0.0002

TABLE 3.39: Maximum values of the angular separation, ρ'', as a function of Δm for HD119915

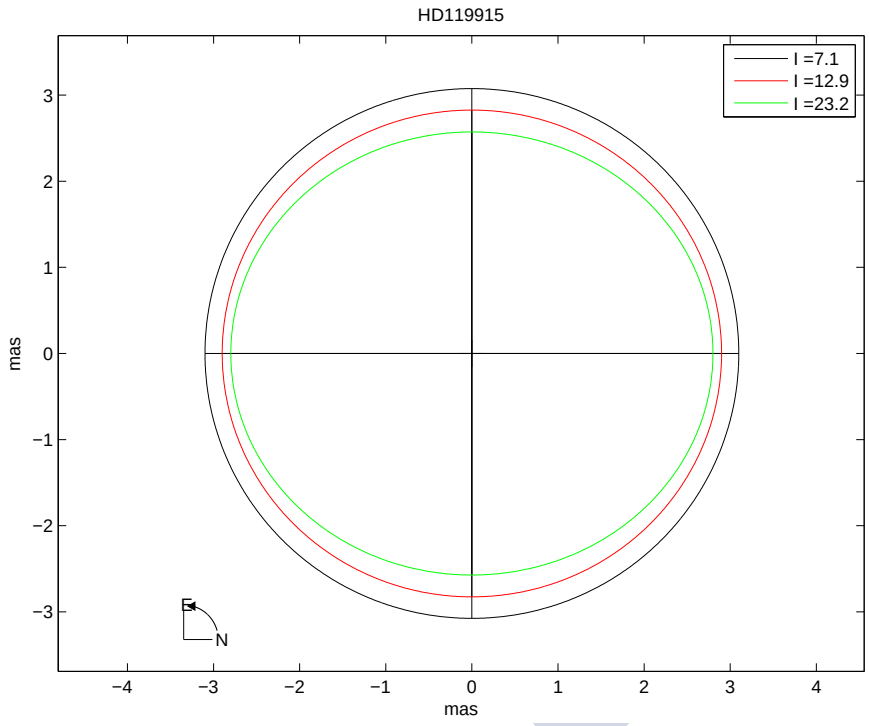

FIGURE 3.28: Apparent orbits of HD119915 with different inclinations

3.6.9 HD 134169

This single-lined spectroscopic binary star has an orbital period of 67.8 days, with a near circular orbit. B.H. Carney determined the photometry of this system three times: V = 7.68, 7.70, 7.69, and B-V = 0.55, 0.52, 0.535 (Carney, 1979, 1980, 1983). The spectral type is G1V from Simbad and the parallax is 17.7±0.81 (mas). Recently, Gaia measured a parallax of 18.95±0.35 (mas) with 7.492 of visual magnitude. Griffin determined the orbit elements of HD 134169 using 47 observations performed with the Coravel program beginning in 2003 until May 2014 (Griffin, 2014e).

We determined the maximum inclination for this system ($i \approx 18°$), when the value of Δm = 8.6 (see Table 3.37). The spectral type is between F4V to F7V for the main component, and between G4V to M4V for the secondary. Regarding the masses, there is not much variation for the primary (between 1.35 and 1.23) but in the case of the secondary, the mass can vary from 1.0 to 0.35 solar masses

To optically solve HD 134169, we would use a telescope with a diameter larger than 13 meters, when the maximum separation between the component is 0.0091±0.0003 arc seconds (Δm = 1.5).

Sp type	F7V
V_J (mag)	7.68 ± 0.01
V_{Gaia} (mag)	7.492
π_{Hip}(mas)	17.27± 0.81
π_{Gaia}(mas)	18.95±0.35
P (days)	68.838 ± 0.013
T $_{(MJD)}$	54275.4 ± 2.0
e	0.096± 0.018
$a_1$sin(i)(Gm)	3.91 ± 0.07
ω_1 (degree)	354± 11
$f(\mathcal{M})(\mathcal{M}_\odot)$	0.00052 ± 0.00003

TABLE 3.40: HD 134169. Physical and orbital parameters

Δm	S	M_1	M_2	Sp_1	Sp_2	$\mathcal{M}_{1(\mathcal{M}_\odot)}$	$\mathcal{M}_{2(\mathcal{M}_\odot)}$	$a_{(A.U)}$	sin(i)	i
1.5	0.300	3.48±0.02	4.98±0.01	F4V	G4V	1.35±0.05	1.01±0.05	0.438±0.004	0.123	8.1±0.8
4.5	0.070	3.79±0.03	8.29±0.02	F6V	K7V	1.25±0.04	0.58±0.02	0.402±0.005	0.224	11.9±1.1
8.6	0.003	3.86±0.02	12.46±0.02	F7V	M4V	1.23±0.03	0.35±0.05	0.383±0.005	0.394	17.9±1.5

TABLE 3.41: Orbital inclination and intermediary parameters as a function of Δm for HD 134169

Δm	a''	ρ''_{max}	ρ''_{min}
1.5	0.0083±0.0001	0.0091±0.0003	0.0075±0.0003
4.5	0.0076±0.0001	0.0084±0.0001	0.0069±0.0007
8.6	0.0073±0.0001	0.0080±0.0001	0.0066±0.0002

TABLE 3.42: Maximum values of the angular separation, ρ'', as a function of Δm for HD 134169

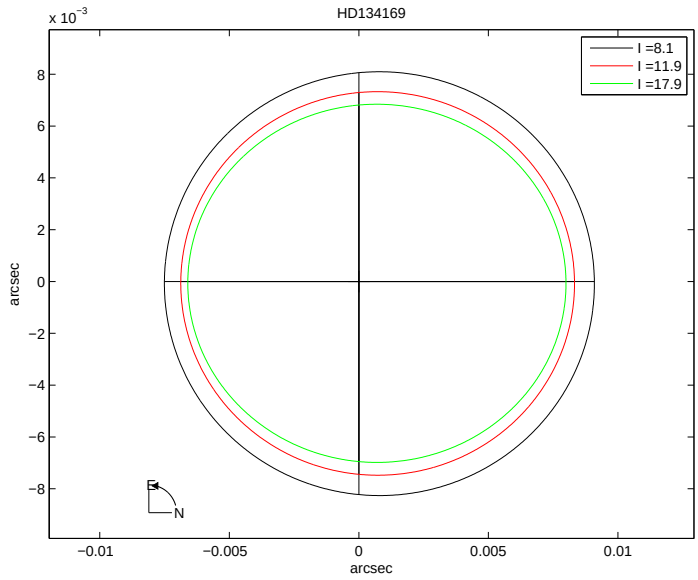

FIGURE 3.29: Apparent orbits of HD134169 with different inclinations

3.6.10 HD 143107

ϵ Aql is a star that was studied in 1900 and the first radial velocity observation of this binary was performed at Lick Observatory. This is bright K type with a long period (about 1270 days). There is no information about it in the Ninth Catalogue of Spectroscopic Binary Orbits (Pourbaix et al., 2004) Simbad recognizes it as a K3III, a double or multiple star with a parallax of 14.73 $\pm$ 0.21(mas). Unfortunately, Gaia did not determine the parallax of this binary. Between 1900 and 1981, 71 radial velocities were performed and, to determine the orbit of this binary, Griffin used 6 observations from Lick (Campbell, 1928), 2 from Palomar Observatory, and 57 observations obtained at the Cambridge Observatory with the 12 inch telescope (Griffin, 1982).
This system could be resolved using a telescope of at least 1.7 meters, taking into account the probable value of angular separation (0.071 $\pm$ 0.003 arc seconds), when Δm equals 1.5 and the orbital inclination is 17.1$\pm$1.3. (See Table 3.44). The spectral types for the components range from K5III to K0III for the main component, with the masses of 1.77$\pm$0.33 to 1.75$\pm$ 0.36 $\mathcal{M}_{\odot}$, and the companion's spectral types are A6IV, G2V, and M2V with masses of 2.13$\pm$ 0.14 to 0.43 $\pm$ 0.03 $\mathcal{M}_{\odot}$.

Sp type	K3III
V_J (mag)	4.130 $\pm$ 0.009
π_{Hip}(mas)	14.73 $\pm$ 0.21
π_{Gaia}(mas)	-
P (days)	1270.0 $\pm$ 1.1
T $_{(MJD)}$	41718$\pm$ 17
e	0.272 $\pm$ 0.026
$a_1$sin(i)(Gm)	86.9 $\pm$ 2.3
ω_1 (degree)	82$\pm$ 5
$f(\mathcal{M})(\mathcal{M}_{\odot})$	0.0162 $\pm$ 0.0013

TABLE 3.43: HD 143107. Physical and orbital parameters

Δm	S	M_1	M_2	Sp_1	Sp_2	$\mathcal{M}_{1(\mathcal{M}_{\odot})}$	$\mathcal{M}_{2(\mathcal{M}_{\odot})}$	$a_{(A.U)}$	sin(i)	i
1.5	0.300	0.01$\pm$0.03	1.51$\pm$0.06	K5III	A6IV	1.77$\pm$0.57	2.13$\pm$0.14	3.613$\pm$0.040	0.294	17.11$\pm$1.1
4.5	0.070	0.24$\pm$0.04	4.73$\pm$0.01	K3III	G2V	1.75$\pm$0.36	1.03$\pm$0.04	3.227$\pm$0.026	0.485	29.04$\pm$1.9
9.0	0.002	0.31$\pm$0.05	9.31$\pm$0.02	K3III	M2V	1.76$\pm$0.29	0.43$\pm$0.03	2.980$\pm$0.002	0.999	$\approx$90

TABLE 3.44: Orbital inclination and intermediary parameters as a function of Δm for HD 143107

Δm	a''	ρ''_{max}	ρ''_{min}
1.5	0.0532$\pm$0.0009	0.0708$\pm$0.0030	0.0371$\pm$0.0011
4.5	0.0475$\pm$0.0008	0.0690$\pm$0.0029	0.0303$\pm$0.0009
9.0	0.0439$\pm$0.0007	0.0455$\pm$0.0010	0.0090$\pm$0.0001

TABLE 3.45: Maximum values of the angular separation, ρ'', as a function of Δm for HD 143107

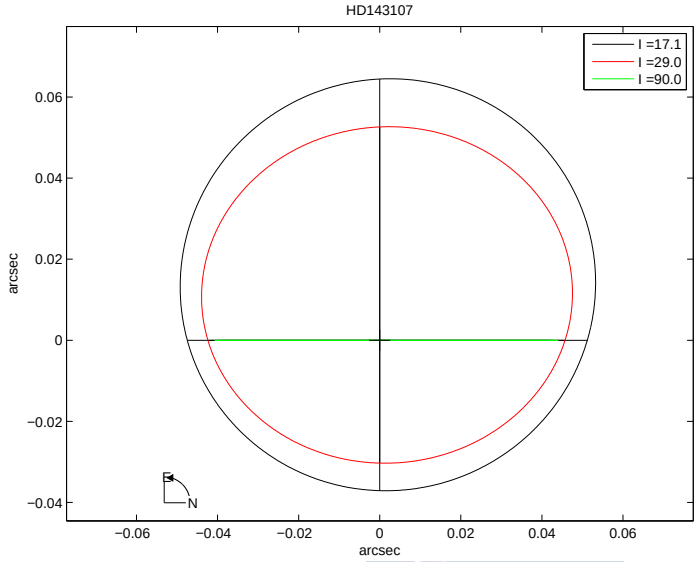

FIGURE 3.30: Apparent orbits of HD141307 with different inclinations

3.6.11 HD 159220

HD 159220 is a single-lined with high rotational velocity, late F-type, and a very short period. It is the companion of HD 159182 in Draco (Griffin, 2011). This system was observed by chance when he tried to observe the HD 159138 and HD 159182 systems.
The trace of the first observation had a wide and weak dip and it seemed to be rapidly rotating F-type. It was not interesting enough to observe again. The second observation (in 2006) was different from the first by about 70 Km/s. This was the reason why Griffin studied this star again, he performed 30 measurements using the spectroscopic binary program, Cambridge radial velocity (Coravel), in the years 2002, 2006, 2007, 2008, 2010. The only publication concerning this system is that by (ibid.), in which he published the orbital elements. Griffin suggested that the spectral type is F8V because it is compatible with Tycho photometry which is V=9.07, B-V= 0.54. Griffin commented that the very short period (2 days) is evidence that HD 159220 is dwarf type and suggested that the spectral type of the secondary component is M2 or M3. Hipparcos has no information about this star but the Gaia mission provided a parallax of 7.18±0.14 mas.

According to the application of our methodology, the spectral type for the primary can vary from F6V to F8V and, for the second component, G5V-M4V. Because the components of this system are very close together (about 0.″00033 to 0.″00026 in the maximum separation), it will be very difficult to solve HD 159220 visually. A telescope of at least 350 meters of diameter would be necessary.

Sp type	F8V
V_T (mag)	9.07 ± 0.02
V_{Gaia} (mag)	8.908
π_{Hip} (mas)	-
π_{Gaia}(mas)	7.18±0.24
P (days)	2.020468 ± 0.000011
T $_{(MJD)}$	54538.0602± 0.0026
e	0.0 ± 0.0
$a_1$sin(i)(Gm)	1.207 ± 0.011
ω_1 (degree)	0.0± 0.0
$f(\mathcal{M})(\mathcal{M}_\odot)$	0.0172 ± 0.0005

TABLE 3.46: HD 159220. Physical and orbital parameters

Δm	S	M_1	M_2	Sp_1	Sp_2	$\mathcal{M}_{1(\mathcal{M}_\odot)}$	$\mathcal{M}_{2(\mathcal{M}_\odot)}$	$a_{(A.U)}$	sin(i)	i
1.5	0.300	3.73±0.02	5.23±0.01	F6V	G5V	1.26±0.03	0.98±0.05	0.0409±0.0004	0.452	26.9±1.8
4.5	0.070	3.96±0.02	8.46±0.02	F7V	K2V	1.20±0.05	0.80±0.03	0.0394±0.0003	0.515	31.0±1.9
8.1	0.004	4.03±0.06	12.13±0.02	F8V	M4V	1.18±0.03	0.34±0.04	0.0360±0.0005	0.999	≈90

TABLE 3.47: Orbital inclination and intermediary parameters as a function of Δm for HD 159220

Δm	a''	ρ''_{max}	ρ''_{min}
1.5	0.00029±0.00001	0.00033±0.00001	0.00020±0.00001
4.5	0.00026±0.00001	0.00032±0.00001	0.00024±0.00001
9.0	0.00024±0.00001	0.00026±0.00001	0.00004±0.00001

TABLE 3.48: Maximum values of the angular separation, ρ'', as a function of Δm for HD 159220

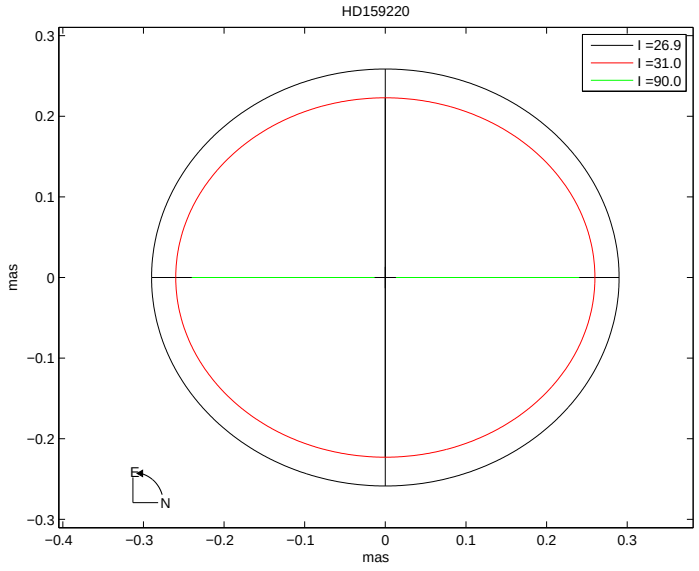

FIGURE 3.31: Apparent orbits of HD159220 with different inclinations

3.6.12 HD 174103

HD 174103 is a single-lined binary recognized in the Henry Draper Catalogue as a K0 spectral type star. The photometry is V = 8.61, B-V = 0.98, H-K = 0.101, and J-H = 0.463 from Simbad (The Tycho-2 Catalogue) which also contains the proper motion and position of one of the brightest stars in the sky (Høg et al., 2000a). The Gaia mission determined the parallax to be 2.43±0.25 mas, previously described by Hipparcos as 2.69±0.63 mas. Griffin suggested that the mass of the primary is 2.0 $\mathcal{M}_{\odot}$ and the second is 0.4 $\mathcal{M}_{\odot}$ which pertains to M2 a main sequence star (Griffin, 2015b). That is very similar to our results, taking into account the accuracy of Griffin's calculations.

Indeed, according to the color index information included in Simbad, the most probable spectral type of the primary is K0III (Straizys and Lazauskaite, 2009) and, in this condition the masses suggested by Griffin are justified.

We consider three cases of Δm = 1.5, 4.5, and 9.0 for this system. And according to our methodology, the spectral types are very close together for the primary component: K2III, K1III, and K0III, with 1.82 to 1.91 solar mass. The spectral types for the secondary would be between A4V to M1V, (2.11 to 0.48 solar mass). Table 3.46 shows the different results obtained. In it, we can see that the case, Δm = 9.0, is in agreement with Griffin's comments and confirms that the primary is probably a giant (K0III).

All previous information guides us to attempt to resolve HD 174103 optically. We would need at least a 30 meters telescope telescope because in general the angular separation is near to 0.″004.

Sp type	K0III
V_J (mag)	8.61 ± 0.01
V_{Gaia} (mag)	8.273
π_{Hip}	2.69± 0.63
π_{Gaia}(mas)	2.43±0.25
P (days)	435.1 ± 0.4
T $_{(MJD)}$	54207± 14
e	0.075 ± 0.015
$a_1$sin(i)(Gm)	17.03 ± 0.29
ω_1 (degree)	37± 12
$f(\mathcal{M})(\mathcal{M}_{\odot})$	0.0455 ± 0.0063

TABLE 3.49: HD 174103. Physical and orbital parameters

Δm	S	M_1	M_2	Sp_1	Sp_2	$\mathcal{M}_{1(\mathcal{M}_{\odot})}$	$\mathcal{M}_{2(\mathcal{M}_{\odot})}$	$a_{(A.U)}$	sin(i)	i
1.5	0.300	0.35±0.05	1.85±0.01	K2III	A4V	1.82±0.33	2.11±0.05	1.773±0.037	0.120	6.9±0.8
4.5	0.070	0.46±0.06	4.96±0.01	K1III	G4V	1.89±0.43	1.02±0.05	1.604±0.052	0.205	11.7±1.0
9.0	0.002	0.53±0.07	9.53±0.02	K0III	M1V	1.91±0.41	0.48±0.03	1.501±0.381	0.380	22.4±1.7

TABLE 3.50: Orbital inclination and intermediary parameters as a function of Δm for HD 174103

Δm	a''	ρ''_{max}	ρ''_{min}
1.5	0.0043±0.0005	0.0050±0.0007	0.0036±0.0004
4.5	0.0039±0.0004	0.0046±0.0006	0.0033±0.0003
9.0	0.0036±0.0004	0.0044±0.0006	0.0030±0.0003

TABLE 3.51: Semimajor axis and the maximum and minimum values of the angular separation, ρ'', as a function of Δm for HD 174103

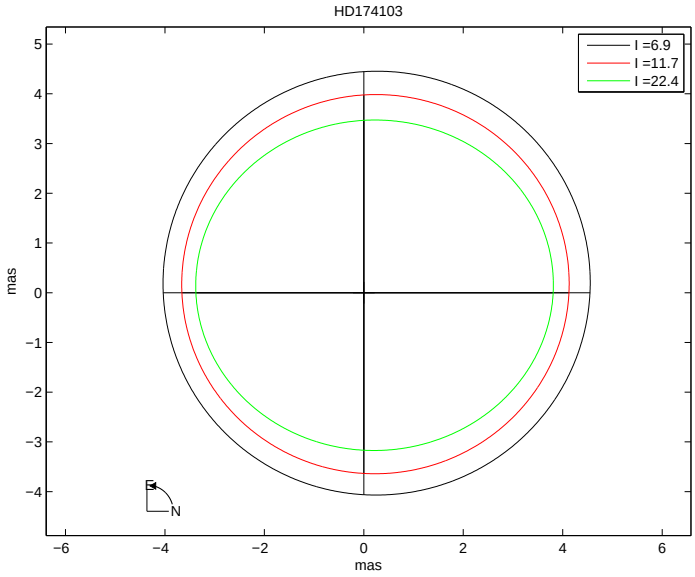

FIGURE 3.32: Orbit with different inclination of HD 174103

3.6.13 HD 176526

Accordingly to the Henry Draper Catalogue, the spectral type is F5 (Cannon and Pickering, 1922) and the photometry is V = 7.69, B-V = 0.47. Under the name, HIP 93137, A. Goldin and V. V. Makarov determined two astrometric periods, 874^{+59}_{-52} and 864 $^{+103}_{-104}$ (Goldin and Makarov, 2006, 2007). The Hipparcos parallax is 17.60±0.84 (mas), and the mission of Gaia determined a parallax with value of a 21.45 ± 0.03 and a visual magnitude 7.527.

Roger Griffin performed 59 observations and he used all of them in order to determine the orbital elements in the framework of the Cambridge Coravel program. The astrometric orbits supported that the inclination was about 90^o. The secondary component is a M0V spectral type (Griffin, 2014e). Depending on our methodology, all of the possibilities for the components are of the main sequence luminosity class. The primary component can be F3V or F4V with masses, 1.41 ± 0.03 to 1.34 ± 0.03 solar mass. The secondary can be between G2V to K9V with masses of 1.04±0.04 to 0.56 ± 0.02, respectively.
We concluded a telescope with a diameter of more than 1.5 meters is enough to optically resolve HD 176526 , especially when the separation between the components is 0.″0951+ 0.″0012.

Sp type	F5V
V_J(mag)	7.69±0.02
V_{Gaia}(mag)	7.527
π_{Hip} (mas)	17.60± 0.84
π_{Gaia}(mas)	21.45±0.03
P (days)	858.100 ± 0.013
T $_{(MJD)}$	55678.3± 1.8
e	0.437 ± 0.006
$a_1$sin(i)(Gm)	96.40 ± 0.09
ω_1 (degree)	92.9± 1.2
$f(\mathcal{M})(\mathcal{M}_\odot)$	0.0486±0.0014

TABLE 3.52: HD 176526. Physical and orbital parameters

Δm	S	M_1	M_2	Sp_1	Sp_2	$\mathcal{M}_{1(\mathcal{M}_\odot)}$	$\mathcal{M}_{2(\mathcal{M}_\odot)}$	$a_{(A.U)}$	sin(i)	i
1.5	0.300	3.23±0.02	4.73±0.01	F3V	G2V	1.41±0.03	1.04±0.04	2.382±0.005	0.638	39.6±2.3
3.0	0.180	3.35±0.02	6.35±0.02	F4V	K1V	1.37±0.03	0.81±0.05	2.293±0.005	0.754	49.0± 2.8
5.1	0.002	0.53±0.07	9.53±0.02	F4V	K9V	1.34±0.03	0.56±0.02	2.189±0.004	0.999	≈ 90

TABLE 3.53: Orbital inclination and intermediary parameters as a function of Δm for HD 176526

Δm	a''	ρ''_{max}	ρ''_{min}
1.5	0.0511±0.0001	0.0951±0.0012	0.0292±0.0002
3.0	0.0492±0.0001	0.0707±0.0010	0.0277±0.0002
5.1	0.0470±0.0001	0.0044±0.0006	0.0264±0.0001

TABLE 3.54: Maximum values of the angular separation, ρ'', as a function of Δm for HD 176526

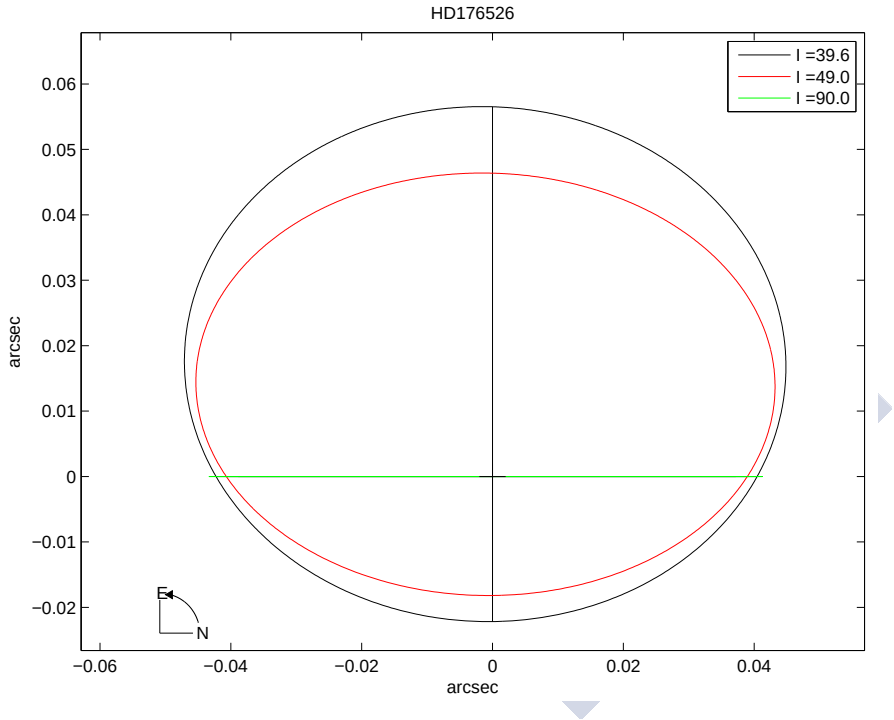

FIGURE 3.33: Apparent orbit of HD 176526 with different inclination

3.6.14 HD 183629

Roger Griffin worked on HD 183629 since 1966 using the original spectrometer at Cambridge observatory, and he obtained 108 photoelectric radial-velocity measurements. In 1930, Redman performed two observations by using 200-inch Hale Telescope at Palomar Observatory in California and Griffin insert it in his list (Radford and Griffin, 1976). This star was classified as K0III spectral type (McCuskey and Seyfert, 1950). In 1970 Griffin determined radial velocities from the Redman observations(Griffin, 1970). The spectral type of the primary was established as a K2-K0III and the companion belongs to the main sequence luminosity. The star appears to be a little brighter than 7.5, which was confirmed recently by the Gaia mission (visual magnitude of 6.958). The Gaia parallax is 3.22 $\pm$ 0.26 mas, and the Hipparcos parallax is 4.79 $\pm$ 0.60 mas . In The 9th Catalogue of Spectroscopic Binary Orbits, the spectral type is K2III-IV (Pourbaix et al., 2004). Simbad recognizes it as a K0III spectroscopic binary (see Table 3.55)

We applied our methodology for the values of Δm = 1.5, 3.0, and 6.2 where the upper limit (6.2) corresponds when the inclination is near 90°. According to our results, the spectral type for the first component ranges from K3III to K0III, with 1.75 to 1.91 solar mass, and between A4V to K2V for the secondary (as Griffin's suggested), with 2.15 to 0.77 solar mass.

The necessary telescope would be larger than 28 meters to resolve HD 183629 by means of high resolution techniques when the angular separation between the components is 0.0042 $\pm$ 0.0004 arc seconds.

Sp type	K0III
V_J (mag)	7.40 $\pm$ 0.01
V_{Gaia} (mag)	6.958
π_{Hip} (mas)	4.79 $\pm$ 0.6
π_{Gaia}(mas)	3.22$\pm$0.26
P (days)	229.83 $\pm$ 0.04
T $_{(MJD)}$	41667.4$\pm$ 0.4
e	0.410 $\pm$ 0.005
$a_1$sin(i)(Gm)	43.9 $\pm$ 0.3
ω_1 (degree)	11.9$\pm$ 0.9
$f(\mathcal{M})(\mathcal{M}_\odot)$	0.064 $\pm$ 0.001

TABLE 3.55: HD 183629. Physical and orbital parameters

Δm	S	M_1	M_2	Sp_1	Sp_2	$\mathcal{M}_{1(\mathcal{M}_\odot)}$	$\mathcal{M}_{2(\mathcal{M}_\odot)}$	$a_{(A.U)}$	sin(i)	i
1.5	0.300	0.23±0.05	1.73±0.01	K3III	A4V	1.75±0.27	2.15±0.06	1.156±0.025	0.461	27.4±1.7
3.0	0.180	0.35±0.06	3.35±0.02	K2III	F4V	1.82±0.49	1.37±0.05	1.081±0.050	0.632	39.2±2.1
6.2	0.021	0.51±0.07	6.71±0.03	K0III	K2V	1.91±0.42	0.77±0.03	1.018±0.054	0.999	≈ 90

TABLE 3.56: Orbital inclination and intermediary parameters as a function of Δm for HD 183629

Δm	a''	ρ''_{max}	ρ''_{min}
1.5	0.0037±0.0003	0.0042±0.0004	0.0033±0.0003
3.0	0.0035±0.0003	0.0037±0.0004	0.0027±0.0003
6.2	0.0033±0.0003	0.0034±0.0006	0.0003±0.0001

TABLE 3.57: Semimajor axis and the maximum and minimum values of the angular separation, ρ'', as a function of Δm for HD 183629

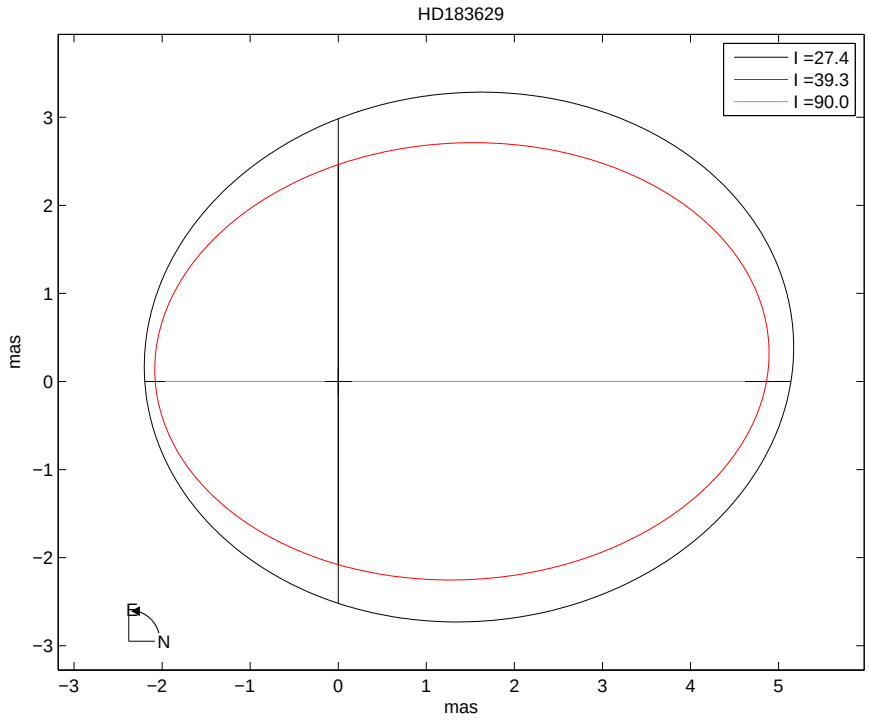

FIGURE 3.34: Apparent orbits of HD 183629 with different inclinations

3.6.15 HD 196758

HR 7897, 1 Aquarii, situated at one-half degree in the northern hemisphere. It is a giant K1III star with 5th magnitude (Roman, 1952). Eggan measurement provided the following photometry data: V = 5.15, B-V=1.06 (Eggen, 1969). The Hipparcos parallax is 13.99 ±0.65 mas, and there is no information from Gaia about the parallax for this system.

HD 196758 has 116 radial velocity observations, 26 obtained with the DAO spectrometer and CCD, 2 at OHP (de Medeiros and Mayor, 1999), 4 at Mount Wilson (Adams et al., 1929), and 4 from Lick observatory (Campbell, 1928), and the rest at the Cambridge Observatory. The rotational velocity as well as the mass function of HD 196758 is small (Griffin, 2014e).

We conclude that the masses for the primary for each case of Δm are very close together: 1.75 to 1.91 solar mass, with K3-0III a spectral type, while the second component spectral types would be A4V to M1V, with masses of 2.15 to 0.48 solar mass. To resolve this system visually we would need a telescope larger than 1.3 meters. Specifically, for Δm = 1.5, we obtain the maximum value of ρ''_{max}, 0.0927±0.0046 (see Table 3.58).

Sp type	K0III
V_J (mag)	5.15±0.02
π_{Hip} (mas)	13.99± 0.65
π_{Gaia}(mas)	-
P (days)	1966.7 ± 2.9
T $_{(MJD)}$	54740± 7
e	0.368 ± 0.009
$a_1$sin(i)(Gm)	81.5± 1.0
ω_1 (degree)	150.7± 1.6
$f(\mathcal{M})(\mathcal{M}_\odot)$	0.0056 ± 0.0002

TABLE 3.58: HD 196758. Physical and orbital parameters

Δm	S	M_1	M_2	Sp_1	Sp_2	$\mathcal{M}_{1(\mathcal{M}_\odot)}$	$\mathcal{M}_{2(\mathcal{M}_\odot)}$	$a_{(A.U)}$	sin(i)	i
1.5	0.300	0.23±0.05	1.73±0.01	K3III	A4V	1.75±0.27	2.15±0.06	4.837±0.013	0.204	11.8±1.1
4.5	0.070	0.46±0.06	4.96±0.01	K1III	G4V	1.89±0.43	1.02±0.05	4.385±0.005	0.357	20.9±1.5
9.0	0.002	0.53±0.07	9.53±0.02	K0III	M1V	1.91±0.41	0.48±0.03	4.107±0.001	0.661	41.4±2.1

TABLE 3.59: Orbital inclination and intermediary parameters as a function of Δm for HD 196758

Δm	a''	ρ''_{max}	ρ''_{min}
1.5	0.0677±0.0031	0.0927±0.0046	0.0428±0.0020
4.5	0.0613±0.0029	0.0844±0.0042	0.0389±0.0019
9.0	0.0575±0.0027	0.0798±0.0040	0.0334±0.0016

TABLE 3.60: Maximum values of the angular separation, ρ'', as a function of Δm for HD 196758

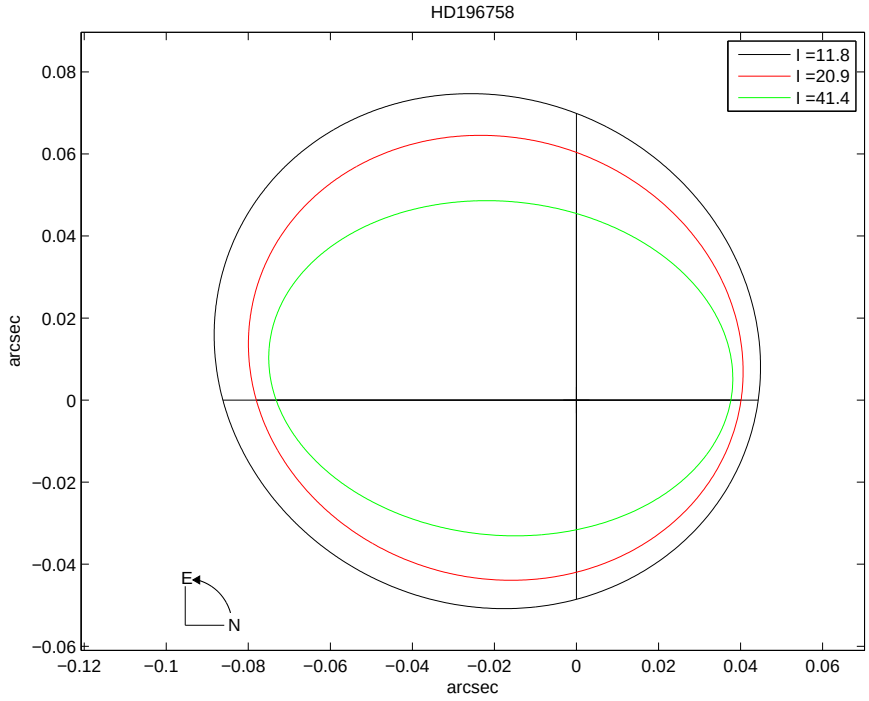

FIGURE 3.35: Apparent orbits of HD196758 with different inclinations

3.7 The study of different cases of double-lined spectroscopic binaries (SB2)

In this section, the detailed study of 8 SB2 systems are included. All the binaries have been selected from papers by R. F. Griffin.

3.7.1 HD 74855

HD 74855 is a spectroscopic binary with a K0 Henry Draper spectral type and high orbital eccentricity. The photometry are, V_{Tycho} = 8.84, B-V = 0.93, and J-H = 0.03. This system has an Hipparcos parallax of 5.46±0.82 mas (Perryman et al., 1997), and a Gaia parallax of 8.13 ± 0.63 mas, with an apparent magnitude of 8.582.

In 1997, R.Griffin used the Coravel spectrometer at Haute-Provence to perform the first observation. Results indicated it to be a single-lined spectroscopic binary. But, in 2007 after

14 observations, it began to appear to as double-lined. In 2016, he calculated the spectroscopic orbit of HD 74855 using 63 radial velocity observations. Suggesting that the brighter component may be either a K0 III-IV or a K0 IV and that the secondary component is a G2 main sequence star (Griffin, 2016).

When we applied our methodology, we found that the best solution is when Δm = 1.75 yields 2.95, 4.70 for the absolute magnitude of the components, with spectral types G0IV and G8V. The masses (in solar mass) are 1.30 $\pm$ 0.02 and 0.90 $\pm$ 0.04, with q = 1.444 $\pm$ 0.045. The orbital inclination of this system is close to 73.°5. The separations between the components would be 0.″032$\pm$0.″004 at the maximum and 0.″0015 $\pm$ 0.″0006 at the minimum. To resolve this system visually, we need a 4 m class telescope, at least.

Sp type	K0IV
V_J (mag)	8.84 $\pm$ 0.01
π_{Hip} (mas)	5.46$\pm$ 1.5
π_{Gaia}(mas)	8.13 $\pm$ 0.63
P (days)	2394$\pm$ 0.28
T $_{(MJD)}$	57072.12$\pm$ 0.24
e	0.8634 $\pm$ 0.0011
$a_1$sin(i)(Gm)	269.3$\pm$ 1.5
$a_2$sin(i)(Gm)	386$\pm$ 7
ω (degree)	285.48$\pm$ 0.38
q ($\mathcal{M}_1$/$\mathcal{M}_2$)	1.4392 $\pm$ 0.0539

TABLE 3.61: HD 74855. Physical and orbital parameters

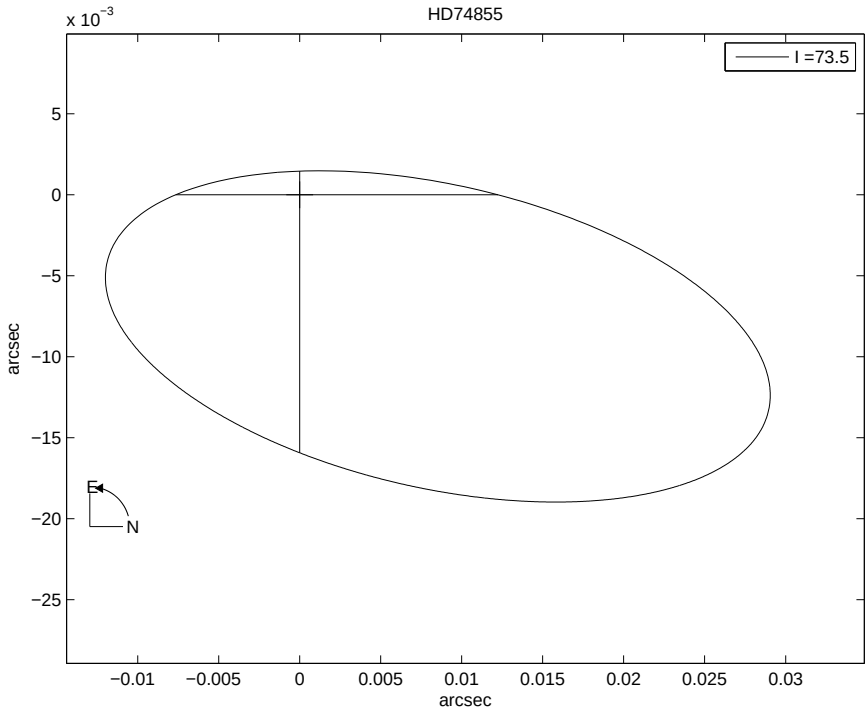

FIGURE 3.36: The most probable apparent orbit of HD74855

3.7.2 HD 85843

This binary was classified as a F8V spectral type by using the spectrogram of dispersion, 75 A/mm (Harlan, 1969). The Hipparcos parallax is 15.50±1.37 mas (van Leeuwen, 2007), with the following photometry provided by Simbad: V = 7.07, B-V = 0.586 from Simbad. Gaia reported a parallax of 14.73 ± 0.87 mas with a visual magnitude of 6.894. Griffin performed the first radial velocity observation for this system in February 2000 (Griffin, 2015d) using the Coravel spectrometer at the Cambridge Observatory. In the first 38 observations, this system appear to behave as a single-lined binary and the observer noticed that a weak dip associated with the secondary star. The orbit was determined from 76 velocities for the primary star and 28 for the secondary star. The elements of HD 85843 are shown in Table 3.62.

Taking the value of q into account, the most probable solution seems to be when the value of Δm = 1.75. For these conditions, the masses of the components are 1.26 ± 0.03 $\mathcal{M}_\odot$ for the main component and 0.93 ± 0.05 $\mathcal{M}_\odot$ for the secondary. The are F6V and G7V spectral types, respectively. From these values, we obtain a mass ratio of 1.349 ± 0.058 which agrees with that obtained from the orbits, The orbital inclination is 57.°0. The maximum angular separation is 0.″053±0.″003 and the minimum is 0.″022±0.″001. A telescope with a diameter larger than 2.25 meters should be used to resolve HD 85843.

Sp type	F8V
V_T (mag)	7.07 $\pm$ 0.01
V_{Gaia} (mag)	6.894
π_{Hip} (mas)	15.50$\pm$ 1.37
π_{Gaia}(mas)	14.73 $\pm$ 0.87
P (days)	1387.5 $\pm$ 1.0
T $_{(MJD)}$	54337$\pm$3
e	0.171 $\pm$ 0.005
$a_1$sin(i)(Gm)	169.2$\pm$ 0.8
$a_2$sin(i)(Gm)	227$\pm$ 6
ω (degree)	40.9$\pm$ 0.4
q ($\mathcal{M}_1/\mathcal{M}_2$)	1.34 $\pm$ 0.03

TABLE 3.62: HD 85843. Physical and orbital parameters

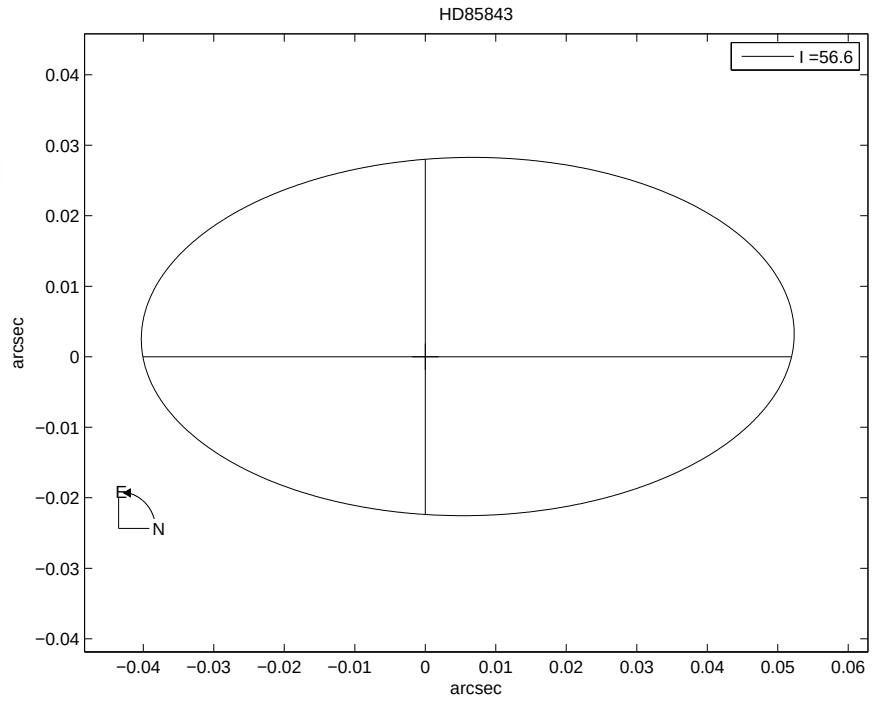

FIGURE 3.37: The most probable apparent orbit of HD85843

3.7.3 HD 112475

HD 112475 was recognized by Simbad as a G3V spectral type. The only publication regarding this system (Yoss and Griffin, 1997) includes the Tycho visual magnitude of 9.63. The

Gaia visual magnitude is 9.27 with a parallax of 8.93± 0.40 mas. Hipparcos did not describe the parallax of this system.

Roger Griffin used 46 radial velocity observations to determine the orbital elements of HD 112475 as seen in Table 3.63. Twenty two of them were performed at the Haute-Provence Observatory (OHP), one at the Dominion Astrophysical Observatory (DAO), one at the European Southern Observatory (ESO), and the rest at the Cambridge Observatory (Griffin, 2012).

When Δm = 1.75 and, after applying Edward's step to the absolute magnitude of the system, the spectral types of the components turn out to be G0V and K1V, with masses of 1.074± 0.04 $\mathcal{M}_\odot$ and 0.83 ± 0.03 $\mathcal{M}_\odot$, and a ratio of 1.30 ± 0.13 $\mathcal{M}_\odot$, which is equal to Griffin's ratio. The maximum and minimum separations between the components are 0.″0155±0.″0011, and 0.″0076±0.″0005, respectively, and the inclination is 18.°3. We need a telescope that is larger than 7.5m in order to optically resolve this binary.

Sp type	G3V
V_T (mag)	9.36 ±0.20
π_{Hip}(mas)	-
π_{Gaia}(mas)	8.93± 0.40
P (days)	691.2 ± 0.4
T $_{(MJD)}$	53280±5
e	0.198 ± 0.007
$a_1$sin(i)(Gm)	112.2± 0.5
$a_2$sin(i)(Gm)	145± 5
ω (degree)	268.7± 2.6
q ($\mathcal{M}_1/\mathcal{M}_2$)	1.30 ± 0.05

TABLE 3.63: HD 112475. Physical and orbital parameters

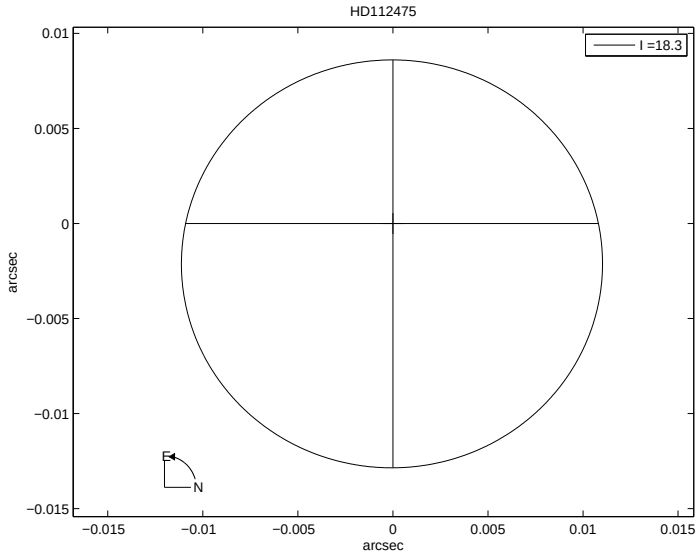

FIGURE 3.38: The most probable apparent orbit of HD198048

3.7.4 HD 129560

HD 129560 is a giant Northern star with a declination of about 85 degrees and a high orbital eccentricity. From Simbad, the Hipparcos parallax is 1.88±0.63 mas, and the spectral type and color indices correspond to K0, and V_T = 8.61, J-H = 0.583, H-K= 0.134, respectively. Griffin suggested that the color indices correspond to the spectral type, K2III, and he determined the orbital solution using 31 radial velocities (Griffin, 2016). The first of them was conducted at Haute-Provence in 1997 and indicated it to be single-lined. The others were obtained during 6 years until 2014 using the 36-inch Cambridge Observatory telescope with two dips that are associated with a double-lined except in the May and July of 2012 observations in which the binary appeared to be single-lined. The radial velocity amplitudes of the components are very similar and Griffin suggested that both components are giants. We used this information in the application of our methodology.

As commented, according to Griffin, the probable spectral type is K2III with an absolute magnitude 0.4 supported by Strizeys' intrinsic color indices (Straizys and Lazauskaite, 2009).

The solution for this system is obtained when Δm = 0.0 (or very close to this value) applying Edward's step = 0.0. In this case, the spectral type for both components is the same (K2III) and the mass is also equal for both, 1.886± 0.40 $\mathcal{M}_\odot$, giving a mass ratio of 1.00 ± 0.57. This solution yields an inclination of 43.°0. The maximum separation between the components is 0.″070±0.″012, therefore, a telescope larger than 1.70m would be sufficient to optically resolve HD 129560.

Sp type	K2III
V_T (mag)	8.61 $\pm$ 0.010
π_{Hip} (mas)	1.88$\pm$ 0.63
π_{Gaia}(mas)	2.46 $\pm$ 0.27
P(days)	26000 $\pm$ 5000
T $_{(MJD)}$	54219$\pm$38
e	0.73 $\pm$ 0.04
$a_1$sin(i)(Gm)	1349$\pm$ 284
$a_2$sin(i)(Gm)	1363$\pm$ 288
ω (degree)	17.00$\pm$ 0.63
q ($\mathcal{M}_1/\mathcal{M}_2$)	1.017 $\pm$ 0.23

TABLE 3.64: HD 129560. Physical and orbital parameters

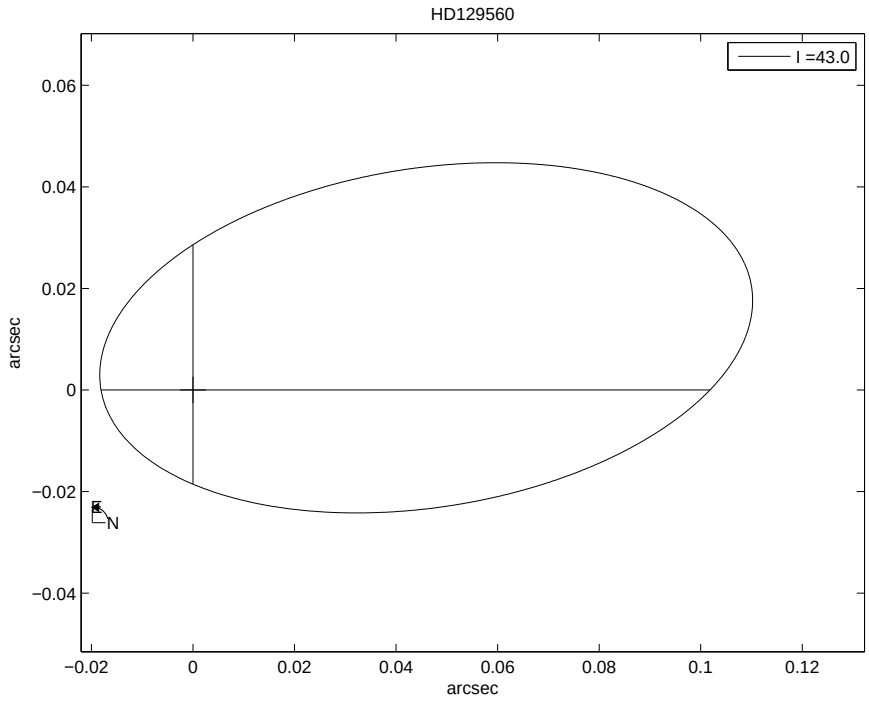

FIGURE 3.39: The most probable apparent orbit of HD129560

3.7.5 HD 171802

HD 171802 was discovered as a double-lined spectroscopic binary by Dr. J. Tomkin from the McDonald Observatory, Texas (USA) in 1987. Its orbit has a very short period and it is

a fifth magnitude with an F spectral type. W.S. Adams had described the spectral type as F2 by direct comparison with spectra of standard stars, according to the Harvard and IAU system. It is a very well detached system with a separation distance of two stellar diameter (Adams et al., 1935). One of the most interesting things about this system is that it has a twin, HD 171834 (HR6987) and they travel in space together with the same parallax (25.96± 0.63 mas), radial velocity, proper motion, magnitude, and spectral type. Both of them moving as one system contain at least four stars. Roger Griffin calculated the orbit of HD 171802 using 42 radial velocity observations, 7 of them obtained by Dr. M. Mayor from the Geneva Observatory, 3 from the European Southern Observatory, and the rest from the Observatoire de Haute-Provence. Griffin separated the components of the system by analysis depending on the ratio of the mass, the photometry, and the area of the depth of the radial velocity, and determined them to be two main sequence stars with a short period.
The photometry (V = 5.38, B-V = 0.38, U-V = -0.4) was obtained from the third list of photometric data for stars in the Equatorial Zone by using a 18-inch reflector (Cousins, 1963). From this information, the spectral type would be F3 or F4 V and, from the ratio of the mass, F3V and F5V. Because the fainter star has a stronger dip than the brighter one, and the ratio of the dip areas on Coravel traces suggests that the difference between the components is about two sub-types. The best choice is F3V and F5V as main sequence components (Griffin, 1996).

We describe the absolute magnitudes for the components using Edward's steps. The absolute magnitude for the first is 3.20 with a F3V spectral type. For the second the absolute magnitude is 3.53 with a F5V spectral type, and the value of Δm = 0.33. The total absolute magnitude is 3.34 and a combined spectral type, F3V.

From our calibrations, the mass of the first component would be 1.424 ± 0.029 $\mathcal{M}_{\odot}$, and for the second, 1.32 ± 0.036 $\mathcal{M}_{\odot}$, so the mass ratio is 1.078 ± 0.046 $\mathcal{M}_{\odot}$. Griffin's ratio of the mass is 1.079 ± 0.004 $\mathcal{M}_{\odot}$. The inclination is 8.°0, with the maximum angular separation of 0.″0010±0.″0002. Unfortunately, we can not observe this binary visually because we need a telescope larger than 117m (which does not exist).

Sp type	F5V
V_J (mag)	5.39 ± 0.01
π_{Hip} (mas)	25.96± 0.63
π_{Gaia}(mas)	-
P (days)	1.4845 ± 0.0001
T $_{(MJD)}$	49413.1661±0.0015
e	0.0 ± 0.0
$a_1$sin(i)(Gm)	0.349± 0.002
$a_2$sin(i)(Gm)	0.384± 0.002
ω (degree)	0.0± 0.0
q ($\mathcal{M}_1/\mathcal{M}_2$)	1.079 ± 0.004

TABLE 3.65: HD 171802. Physical and orbital parameters

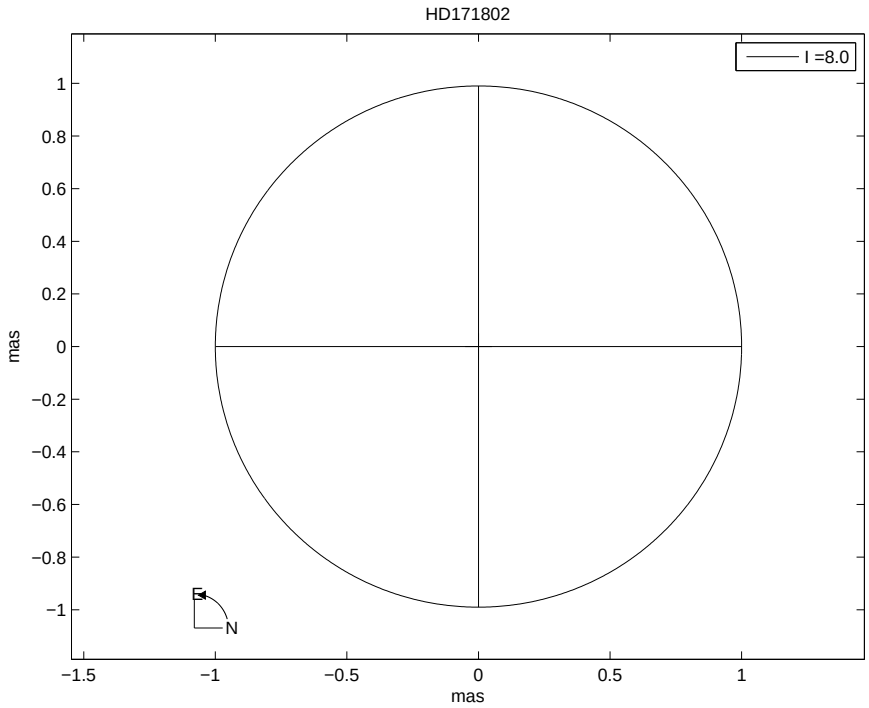

FIGURE 3.40: The most probable apparent orbit of HD171802

3.7.6 HD 194765

This is an equatorial double-lined bright star. The spectral type was first described in the Henry Draper catalogue as a F8 type, Adms (1935), described it as a main sequence class with the same spectral type (Adams et al., 1935). In 1988, H.A. Abt identified it to be a F7V spectral type (Abt, 1988). According to Simbad, the spectral type is F7V with a Hipparcos parallax is 21.84 ±0.57 (mas) and the following photometry: V = 6.7, B-V = 0.52, U-B = 0.02.

Griffin determined the orbital elements for HD 194765 using 68 radial velocities, 6 performed at Mount Wilson Observatory (USA) and 62 using the Coravel program with the 36 inch telescope at Cambridge University (Griffin, 2014b). We presented the solution for this binary at an international conference that took place in the UAE in December 2014 . Because the parallax measured by Hipparcos and Gaia are practically the same, we can assume that the distance to this star is very well known.

Taking into account the value, q = 1.163 ± 0.013, obtained by (ibid.), we found that the best solution is obtained when Δm = 0.75. In this case, the mass for the main component is 1.30 ± 0.04 $\mathcal{M}_\odot$ (with an F5V spectral type), and 1.12 ± 0.04 $\mathcal{M}_\odot$ (with an F9V spectral type) for the companion. The calculated ratio of masses is in perfect agreement with that deduced by Griffin. The orbital inclination is close to 41.°0. We should try to observe HD 194765 visually using a telescope with a diameter of at least 6.5 meters, especially when the components are at maximum separation, 0.″018±0.″001.

Sp type	F7V
V_J (mag)	6.703 ±0.020
V_{Gaia} (mag)	6.549
π_{Hip} (mas)	21.84± 0.57
π_{Gaia}(mas)	21.97 ± 0.34
P (days)	160.833 ± 0.007
$T_{(MJD)}$	54789.51±0.28
e	0.2594 ± 0.0023
$a_1$sin(i)(Gm)	35.27± 0.12
$a_2$sin(i)(Gm)	41.01± 0.20
ω (degree)	104.7± 0.7
q ($\mathcal{M}_1/\mathcal{M}_2$)	1.163 ± 0.007

TABLE 3.66: HD 194765. Physical and orbital parameters

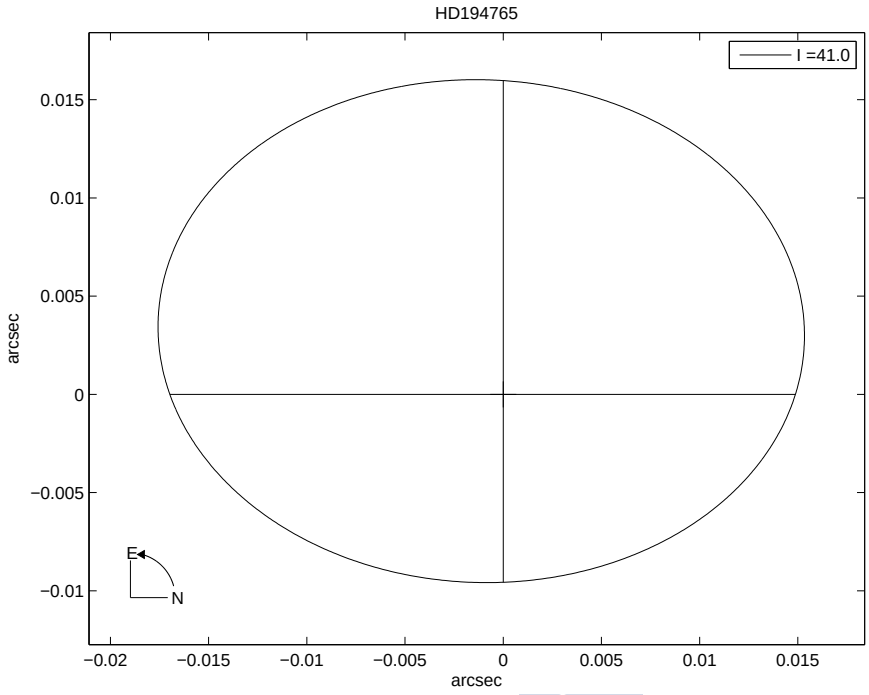

FIGURE 3.41: The most probable apparent orbit of HD194765

3.7.7 HD 197952

NN Delphini is an eclipsing binary of the Algol type (detached), with an apparent magnitude of 8.4 and an F5 spectral type (Henry Draper Catalogue). The first publication for HD 197952 was by V. Makarov as one of 35 new bright medium and high amplitude variables (Makarov et al., 1994). The Tycho photometry color indices are B-V = 0.54, J-H = 0.058, H-K = 0.215 with a visual magnitude of 8.40, which are compatible with F8 main-sequence luminosity class (Straizys and Lazauskaite, 2009). The Hipparcos parallax is 6.28± 0.89 (mas) while Gaia provided no information about HD 197952 . The first orbital calculation of this pair determined it to be eclipsing (Gómez-Forrellad et al., 2003) with a period of 99.27 days after study of the V light curve analysis.

Roger Griffin comments, "*The stellar masses found here, too, are appreciably larger than tables of main-sequence properties allow for stars of types near F7 and F9 such as the mass ratio, in association with the combined colour index, might lead us to expect. The weight of evidence points, therefore, to the stars being somewhat over-mass and over luminous in comparison with main-sequence objects of their colour index, so we could agree with Spanish authors that the star are some what evolved; they could perhaps be classed as one sub-type or so on either side of F8 IV-V.*" R.F Griffin performed 37 observations to determine the orbital solution as a double-lined spectroscopic binary (Griffin, 2014b).

We had some difficulty applying our methodology to HD 197952 because of the variety of information. First, the photometry supports the idea that the composite spectral type belongs to the main sequence class. Second, Griffin suggested that the spectral types for the components are F7-9 IV, with the ratio of the mass 1.095 ± 0.010. Third, Gomez-Forrellad suggested the F8 spectral type with a ratio of mass of 1.00 without errors. Finally, there is a good agreement between the inclination calculated by Gomez (2003), 89.°45 and that by Griffin (2014) 89.°2.

In accordance with R.F.Griffin and taking into account the shape of the dips and the orbital solution, the masses are not equal (ibid.). In order to apply our methodology, we first admitted that the components belong to the main sequence but, in this case, the result (especially the orbital inclination), is very far from the known values. We decided to consider the components as sub-giant but not equal (the Griffin solution supports this). Working with the spectral types, F5IV and F9IV(composite spectral type, F6IV), the magnitude difference will be 0.33 and the corresponding masses, 1.48 ± 0.027 $\mathcal{M}_\odot$ and 1.320 ± 0.035 $\mathcal{M}_\odot$, which are very close to the Griffin masses, 1.454 ± 0.025 $\mathcal{M}_\odot$ and 1.328 ± 0.021 $\mathcal{M}_\odot$, respectively. The value of the inclination is 89.°50. In these conditions, the maximum separation between the components would be 0.″004±0.″001, in the best situation. A 30m class telescope would be necessary to try to optically resolve this interesting system.

Sp type	F8IV-V
V_J(mag)	8.40±0.01
π_{Hip}(mas)	6.28± 0.89
π_{Gaia}(mas)	-
P (days)	99.244± 0.019
T $_{(MJD)}$	56389.39±0.06
e	0.5168 ± 0.0029
$a_1$sin(i)(Gm)	35.30± 0.13
$a_2$sin(i)(Gm)	40.92± 0.23
ω (degree)	350.4± 0.4
q ($\mathcal{M}_1/\mathcal{M}_2$)	1.095 ± 0.010

TABLE 3.67: HD 197952. Physical and orbital parameters

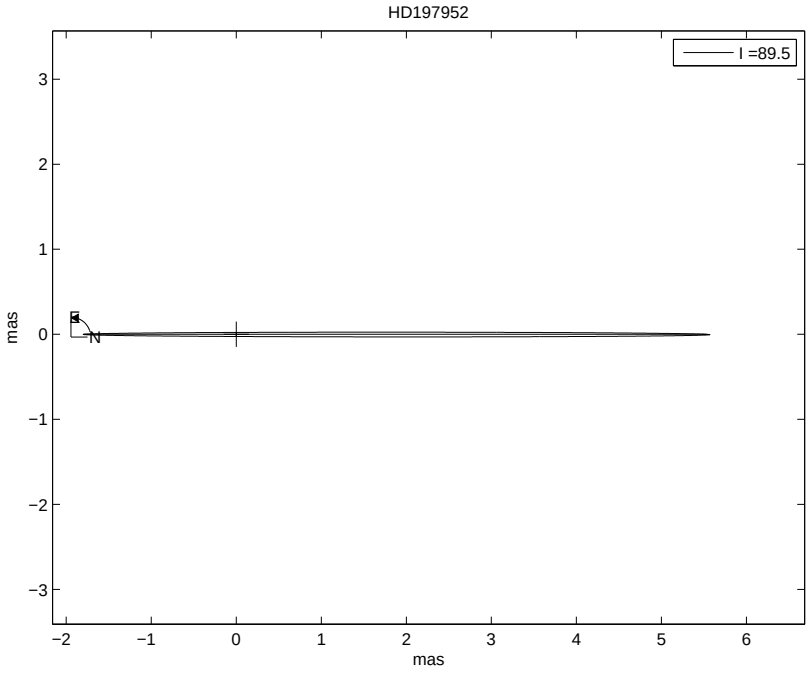

FIGURE 3.42: The most probable apparent orbit of HD197952

3.7.8 HD 198048

In 1972, Anderson and Kraft announced HD 198048 to be a double-lined binary (Anderson and Kraft, 1972). The classification of the spectral type in the Henry Draper Catalogue is G0 (Cannon and Pickering, 1923). Later, W. S. Adms used spectroscopic methods and classified HD 198048 as F8V and F9V spectral types with a visual magnitude of 4.6 (Adams et al., 1921, 1935). The system was listed by Morgan and Bidelman as HR 7955, F8 (Morgan and Bidelman, 1946). N.G. Roman determined the spectral type as F8IV with magnitude of 4.63 (Roman, 1950) and Gyldenkerne fixed the spectral type to be F8V with a visual magnitude of 4.6 (Gyldenkerne, 1955).
HD 198048 is one of 849 stars measured photoelectrically by Bertil Ljunggren and Tarmo Oja using the double refractor of Uppsala Observatory from 1956-1963, with V = 4.49, B-V = 0.54 (Ljunggren and Oja, 1965), the spectral type for the system (F8V), and (V = 4.52, B-V = 0.527) by using the same photoelectric photometer (Häggkvist and Oja, 1966). W.S. Adams and A.H. Joy determined the radial velocities by using the 60 inch and 100 inch telescopes at Mount Wilson (Abt, 1973; Adams and Joy, 1923) from 1993 to 1998. Griffin determined the orbital elements of HD 198048 by means of 38 radial velocity observations at OHP and 15 more with the Cambridge Coravel (Griffin, 1999).

Nevertheless, in the Michigan catalogue of two-dimensional spectral types for HD stars (Houk, 1978), the spectral type for this binary is K5III and this is the spectral type that figures in Simbad. In fact, a new determination of the color indices performed by Tycho and Hipparcos, among others, gives B-V near to 1.5 which is incompatible with the old classification. In this sense, Griffin comments: " we cannot assume that the star is main sequence because its luminosity is great" (Griffin, 1999).

Taking into account all of this information, we consider that the correct spectral type for this binary is K5III and we will use it for applying our methodology. We obtain a value of q = $\mathcal{M}_1$/ $\mathcal{M}_2$ very similar to that presented by Griffin (1.025 $\pm$ 0.015), by simply taking Δm = 0. In this case, both components have the same spectral type (K5III) and the masses: 1.77 $\pm$ 0.50 $\mathcal{M}_\odot$, which gives q = 1.00 $\pm$ 0.5, with 21.°0 being the most probable value of the orbital inclination.

In these conditions, and in the epochs when the angular separation is maximum, its value is close to 0.″022$\pm$0.″002. This supports Griffin's expectation to resolve HD 198048 optically because a 5m class should be sufficient.

Sp type	K5III
V_J (mag)	4.902 $\pm$0.200
π_{Hip}(mas)	7.9$\pm$ 0.32
π_{Gaia}(mas)	-
P (days)	523.36 $\pm$ 0.18
T $_{(MJD)}$	50205.8$\pm$1.0
e	0.547 $\pm$ 0.007
$a_1$sin(i)(Gm)	50.2$\pm$ 0.5
$a_2$sin(i)(Gm)	51.4$\pm$ 0.7
ω (degree)	68.4$\pm$ 0.9
q ($\mathcal{M}_1/\mathcal{M}_2$)	1.025 $\pm$ 0.015

TABLE 3.68: HD 198048. Physical and orbital parameters

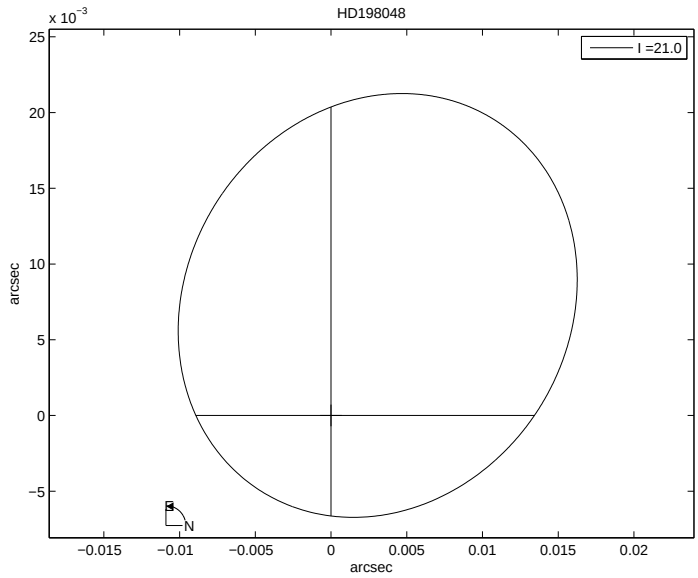

FIGURE 3.43: The most probable apparent orbit of HD198048

3.8 Abstract Tables

In this subsection, we created four tables that show the different results obtained by applying the developed methodology to the all of the spectroscopic binaries studied in this research (including those used as testing): 17 SB1 and 13 SB2. Tables 4.67 (for SB1) and 4.68 (for SB2) show the following information about the physical parameters of the binaries: Column 1, the HD number of the star; Column 2, the Hipparcos parallax; Column 3, the Gaia parallax; Column 4, the total apparent magnitude, Column 5, the composite spectrum; Columns 6 and 7, the individual spectral types for each component; and Columns 8 and 9, the obtained individual masses. Tables 4.69 (for SB1) and 4.70 (for SB2) show relevant dynamical parameters. Column 1, the HD number of the star; Column 2, the relative semimajor axis in astronomical units (AU); Columns 3 and 4, the semimajor axis of the orbits with respect to the center of mass, also in AU; Column 5, the orbital inclination; Column 6, the maximum separation between the components in the most probable apparent orbit expressed in milli-arc seconds (mas); and Column 7, the minimum diameter (in meters) of the telescope necessary to optically resolve the binary.

Two comments must be made regarding these Tables. First, in Table 3.69, we have to consider only the most favorable case in order to resolve the SB1s, that is to say, when delta m is 1.5. Second, it is necessary to remember that regarding the inclination, the two values, i and $180 - i$, are possible.

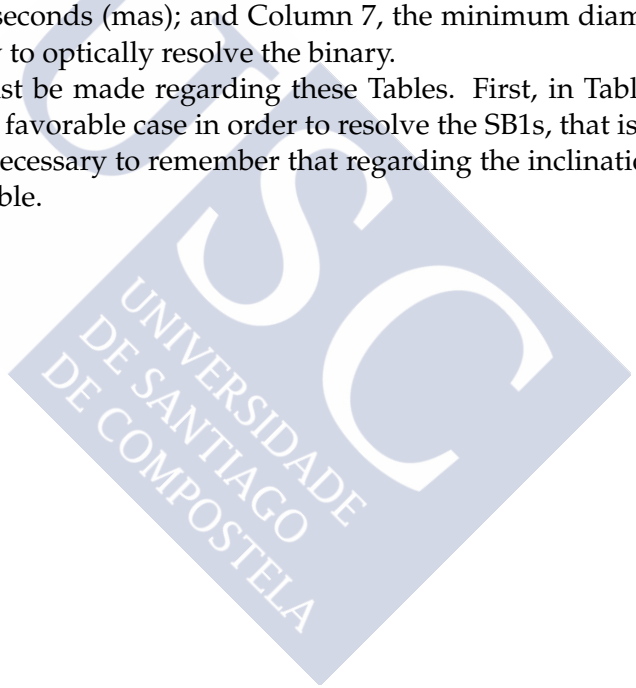

Name (HD)	$\pi_{Hip(mas)}$	$\pi_{Gaia(mas)}$	$m_{(mag)}$	Sp	Sp_1	Sp_2	$\mathcal{M}_1(\mathcal{M}_\odot)$	$\mathcal{M}_2(\mathcal{M}_\odot)$
471	19.45±1.40	-	7.77	K0V	G8V	K4V	0.93±0.05	0.72±0.03
				K0V	G8V	K7V	0.91±0.04	0.61±0.02
				K0V	G9V	M1V	0.88±0.04	0.50±0.02
4703	4.63±1.03	2.55±0.35	8.93	K2III	K4III	A6IV	1.73±0.26	2.09±0.13
				K2III	K2III	G3V	1.79±0.57	1.03±0.04
				K2III	K2III	M1V	1.88±0.40	0.50±0.02
10171	-1.39±1.57	2.86±0.26	9.00	K0III	K4III	A6V	1.73±0.26	2.07±0.02
			8.56	K0III	K0III	G4V	1.89±0.58	1.01±0.04
				K0III	K0III	M1V	1.91±0.04	0.48±0.02
22521	24.78±1.15	-	6.738	G0V	F8V	G6V	1.18±0.03	0.97±0.04
				G0V	F9V	M0V	1.12±0.05	0.53±0.02
				G0V	G0V	M4V	1.09±0.04	0.34±0.05
26083	1.32±1.12	2.37±0.28	9.09	K0III	K3III	A3V	1.73±0.26	2.22±0.06
				K0III	K3III	F4V	1.76±0.29	1.38±0.04
				K0III	K0III	K5V	1.89±0.40	0.67±0.02
79888	6.11± 1.44	6.78±0.31	9.00	K0V	G8V	K4V	0.93±0.04	0.72±0.02
			8.828	K0V	G9V	K9V	0.90±0.04	0.54±0.02
				K0V	G9V	M5V	0.87±0.04	0.33±0.05
110583	-	2.34±0.34	9.43	K1III	K3III	A6IV	1.74±0.29	2.06±0.13
			9.03	K1III	K2III	G3V	1.890±0.41	1.02±0.04
				K1III	K1III	M1V	1.90±0.42	0.48±0.03
111224	-	5.15±0.35	9.43	K0IV	F8IV	F9V	1.36±0.07	1.11±0.04
			9.08	K0IV	G4IV	K5V	1.23±0.01	0.66±0.02
				K0IV	K0IV	M4V	1.20±0.08	0.35±0.05
119915	2.21± 0.93	4.79±0.24	8.56	K4III	K6III	A5IV	1.20±0.05	2.18±0.00
			9.25	K4III	K4III	G1V	1.75±0.26	1.06±0.04
				K4III	K4III	M1V	1.73±0.26	0.52±0.02
134169	17.27±0.81	18.95±0.35	7.68	F7V	F4V	G4V	1.35±0.04	1.01±0.04
			7.49	F7V	F6V	K7V	1.25±0.04	0.58±0.02
				F7V	F7V	M4V	1.23±0.03	0.35±0.05
141307	14.73±0.21	-	4.13	K3III	K5III	A6IV	1.77±0.57	2.13±0.14
				K3III	K3III	G2V	1.75±0.36	1.03±0.04
				K3III	K3III	M2V	1.76±0.29	0.43±0.03
159220	-	7.18±0.24	9.07	G8V	F6V	G5V	1.26±0.03	0.98±0.05
			8.90	G8V	F7V	K2V	1.20±0.05	0.08±0.03
				G8V	F8V	M4V	1.18±0.03	0.44±0.04
174103	2.69±0.63	2.43±0.25	8.61	K0III	K2III	A4V	1.82±0.33	2.11±0.05
			8.27	K0III	K1III	G4V	1.89±0.43	1.02±0.05
				K0III	K0III	M1V	1.91±0.42	0.48±0.03
176526	17.60±0.84	21.45±0.03	7.69	F5V	F3V	G2V	1.41±0.03	1.04±0.04
			7.52	F5V	F4V	K1V	1.37±0.03	0.81±0.04
				F5V	F4V	K9V	1.34±0.03	0.56±0.02
183629	4.79±0.60	3.22±0.26	7.40	K0III	K3III	A4V	1.75±0.27	2.15±0.06
			6.95	K0III	K2III	F4V	1.82±0.49	1.37±0.05
				K0III	K0III	K2V	1.91±0.42	0.77±0.03
196758	13.99±0.65	-	5.15	K0III	K4III	A4V	1.75±0.27	2.15±0.06
				K0III	K4III	G4V	1.89±0.43	1.20±0.05
				K0III	K0III	M1V	1.91±0.41	0.48±0.03
219834	47.34±2.47	-	5.19	F8.5IV	F8IV	F9V	1.35±0.05	1.11±0.04
				F8.5IV	G0IV	G9V	1.30±0.02	0.73±0.03
				F8.5IV	G6IV	M0V	1.20±0.03	0.53±0.02

TABLE 3.69: Physical Parameters SB1

Name (HD)	$\pi_{Hip(mas)}$	$\pi_{Gaia(mas)}$	$m_{(mag)}$	Sp	Sp_1	Sp_2	$\mathcal{M}_1(\mathcal{M}_\odot)$	$\mathcal{M}_2$ $(\mathcal{M}_\odot)$
16739	41.34±0.43	-	4.92	F9V	F8V	G2V	1.18±0.03	1.04±0.04
27176	18.50±0.50	-	5.63	F0V	A8V	F3V	1.74±0.03	1.38±0.03
74089	1.85±1.06	3.11±0.24	8.53	K0III	K0III	K0III	1.91±0.42	1.91±0.42
74855	5.46± 0.82	8.13±0.63	8.84	K0IV	G0IV	G8V	1.30±0.02	0.90±0.04
85843	15.5± 1.37	14.73± 0.87	7.07	F8V	F6V	G7V	1.26±0.03	0.93±0.05
112475	-	8.93±0.40	9.36	G3V	G0V	K1V	1.07±0.04	0.83±0.03
129560	1.88±0.63	2.46±0.27	8.61	K2III	K2III	K2III	1.88±0.04	1.89±0.04
170153	124.11±0.87	-	3.58	F7V	F5V	G2V	1.31±0.03	0.93±0.05
171802	25.96±0.62	-	5.39	F3V	F3V	F5V	1.42±0.03	1.32±0.04
185734	12.25±0.24	-	4.67	G8III	G9III	G2III	1.89±0.42	1.73±0.28
194765	21.84±0.57	21.97±0.34	6.70	F7V	F5V	F9V	1.30±0.04	1.12±0.04
197952	6.28±0.89	-	8.40	F8IV-V	F5IV	F9IV	1.48±0.03	1.32±0.04
198048	7.90±0.32	-	4.90	F5III	K5III	K5III	1.77±0.50	1.77±0.50

TABLE 3.70: Physical Parameters SB2

Name(HD)	$a_{(AU)}$	$a_{1(AU)}$	$a_{2(AU)}$	$i_{(degree)}$	$\rho_{max(mas)}$	D(m)
471	1.386±0.008	0.606±0.029	0.779±0.057	51.1±2.9	0.0272±0.0020	4.3
4703	2.959±0.027	1.618±0.159	1.341±0.226	9.6±0.9	0.0120±0.0020	10.0
10171	2.271±0.0354	1.235±0.155	1.036±0.179	10.9±1.0	0.0090±0.0008	13.0
22521	2.542±0.042	1.147±0.630	1.395±0.320	25.1±1.8	0.0891±0.0044	1.3
26083	0.213±0.012	0.114±0.023	0.096±0.034	23.7±1.7	0.0006±0.0001	213
79888	0.095±0.001	0.042±0.002	0.053±0.004	25.5±1.7	0.0008±0.0001	156
110583	12.379±0.094	6.711±0.071	5.668±0.058	8.4±0.8	0.0415±0.0078	3.0
111224	3.389±0.008	1.071±0.052	1.319±0.077	16.2±1.2	0.0168±0.0012	7.0
119915	0.637±0.009	0.441±0.003	0.226±0.014	7.1±0.6	0.0031±0.0002	38.0
134169	0.438±0.004	0.188±0.010	0.250±0.014	8.1±0.8	0.0091±0.0003	13.0
141307	3.613±0.004	1.973±0.030	1.640±0.051	17.1±1.1	0.0708±0.0030	1.7
159220	0.041±0.001	0.018±0.001	0.023±0.001	26.9±1.8	0.0003±0.0001	355
174103	1.773±0.037	0.950±0.087	0.823±0.165	6.88±0.8	0.0050±0.0007	24.0
176526	2.382±0.005	1.011±0.045	1.371±0.040	39.6±2.3	0.0951±0.0012	1.5
183629	1.156±0.024	0.637±0.051	0.519±0.089	27.5±1.7	0.0042±0.0004	28.0
196758	4.836±0.014	2.666±0.020	2.170±0.037	11.8±1.1	0.0927±0.0046	1.3
219834	4.600±0.110	2.076±0.018	2.524±0.004	37.3±3.3	0.2482±0.0412	1.0

TABLE 3.71: Dynamical Parameters For SB1

Name (HD)	$a_{(AU)}$	$a_{1(AU)}$	$a_{2(AU)}$	$i_{(degree)}$	ρ(mas)	D (m)
16739	1.227±0.116	0.572±0.045	0.649±0.061	56.3±3.4	0.0457±0.0032	2.6
27176	7.380±0.542	3.264±0.246	4.116±0.393	55.9±3.2	0.1576±0.0126	1.0
74089	0.238±0.001	0.118±0.023	0.118±0.023	59.0±3.6	0.0008±0.0001	147
74855	4.556±0.031	1.864±0.092	2.692±0.071	73.5±4.0	0.0320±0.0041	4.0
85843	3.164±0.028	1.347±0.814	1.817±0.067	57.0±3.7	0.5250±0.0031	2.30
112475	2.192±0.005	0.949±0.043	1.243±0.057	18.3±1.6	0.0155±0.0011	7.5
129560	26.737±3.692	13.369±4.009	13.369±4.009	43.0±2.4	0.0704±0.0123	1.7
170153	1.097±0.097	0.456±0.025	0.642±0.041	64.5±3.5	0.1580±0.0119	1.0
171802	0.035±0.001	0.017±0.001	0.019±0.006	8.0±0.7	0.0010±0.0002	117
185734	1.720±0.148	0.817±0.221	0.903±0.242	86.4±4.0	0.0305±0.0027	4.0
194765	1.937±0.129	0.969±0.034	0.969±0.034	41.0±2.3	0.0224±0.0018	5.0
197952	0.777±0.006	0.359±0.015	0.418±0.015	89.5±4.1	0.0184±0.0003	6.5
198048	0.590±0.002	0.277±0.005	0.314±0.007	21.0±1.6	0.0040±0.0005	30.0

TABLE 3.72: Dynamical Parameters For SB2

USC
UNIVERSIDADE
DE SANTIAGO
DE COMPOSTELA

Chapter 4

Detection of Exoplanets

Exoplanets are planets orbiting a star or a binary star outside of our solar system. We also call them "Extra-solar planets". More than one-half of solar type stars belongs to multiple stellar systems and they are considered the best environments to research and understand the formation of exoplanets (Thebault and Haghighipour, 2015).

The study of exoplanets began at the end of the eighties when David W. Lathem suggested the existence of an unseen companion (probably a brown dwarf) in the star, HD114762. Two years later, William D. Cochran predicted that HD 114762 has the first extrasolar planetary system in the case that the orbital inclination is about 90 degrees (Cochran, Hatzes, and Hancock, 1991) but this inclination was not confirmed. Wolszczan and Frail discovered two exoplanets in the PSR1257+12 system, which is a neutron star with three planetary companions (Wolszczan, 1992). A new exoplanet was discovered later in the same system. In 1995, using the radial velocity method, 51 Pegasi b was the first exoplanet found around a main-sequence star by Mayor and Queloz, with about one half of Jupiter mass (Mayor et al., 1995). The first exoplanet detected in a close binary was in the γ Cephei system (Hatzes et al., 2003) and about 40% of all known exoplanets are hot Jupiter or hot, super Jupiter. More than 60 exoplanets belong to multiple star systems (Kitchin, 2011; Roell et al., 2012).

Exoplanets help us increase our knowledge and understand the mechanism and the origin of the universe and also present an explanation of the origin of our planet, "the Earth" and other planets in our solar system. It presents a hope to setup human colonies in the future (Kitchin, 2011). In this chapter we will study the orbital stability of possible exoplanet orbits in the 30 spectroscopic binaries (SB1 and SB2) described in Chapter 3. We will also discuss the habitability for of each of them and will describe the exoplanet detection methods and the space missions to explore and discover amazing planets orbiting other stars.

4.1 Exoplanets in Binary stars

More than one-half of double and multiple stars formed by pre-main sequence and main sequence stars form up to 70% our galaxy's stars (Eggl et al., 2012). At least 57% of G and K dwarf stars and 30% of M dwarfs have a companion (Duquennoy and Mayor, 1991). These multiple star systems provide a suitable environment to understand the formation and evolution of the exoplanets.

Gordon Walker suggested that the spectroscopic binary, γ Cephei, has a planetary companion after he noticed the variation of the radial velocity in the observations (Walker et al.,

1992). In 2003, Artie Hatzes confirmed the existence of the exoplanet around γ Cephei with an orbital semimajor axis of 2.13 AU, as a giant planet with a period of 905.57 days, 0.12 of eccentricity, and $\mathcal{M}$sin i = Jupiter mass, 1.7 $\mathcal{M}_J$, (Hatzes et al., 2003). Here, i represent the inclination of the planetary orbit regarding to the apparent plane, that perpendicular to our sight line. This work was the beginning of a new field that combines theoretical and observational efforts in order to search for the exoplanets around the binary systems.

In September 2011, the Kepler mission discovered the first exoplanet around a binary star based on photometric data, "Kepler-16". The orbit of Kepler-16 has a period of 228 days, 0.7048 AU of semi-major axis, and an eccentricity 0.7048. Its mass is 0.333 the mass of Jupiter, and orbits around a pair of low mass stars, a K type and a red dwarf, and the planetary transit observation presents a direct evidence of a circumbinary planets. (Bromley and Kenyon, 2015; Doyle et al., 2011).The best target to look for that is the habitable zone (HZ) around the M dwarf stars because of the HZ close to the star. The process to detect the exoplanets is easier than around the big stars. This type of low mass star became of inters with the increase of the sensitivity to describe the HZ using the Doppler effect and other detection technologies (Barnes et al., 2007).

In August 2016, A.P. Hatzes at the Thuringian State Observatory (Germany) discovered an Earth-like planet around the closest star to our solar system, Proxima Centauri, which is a member of a multiple star. From its mass, he determined that it is a rocky planet and its surface temperature suggests that it could theoretically have liquid water. His work supported previous propositions about the importance of multiple star systems, especially around the low mass stars in order to understand and search for exoplanets. (Hatzes, 2016).

4.2 Techniques

There are various methods of exoplanet detection, direct detection (imaging techniques), and indirect detection (radial velocity, gravitational microlensing, transits, pulsar timing, and astrometry). Transit and radial velocity methods have the advantage of detecting those planets which are situated close to the host star, and the other techniques are used for the wide orbits (Fischer et al., 2015). Even using these valuable methods, the exoplanets detection is still difficult, because the exoplanets are faint and very close to a bright star, In order to reach a complete image, scientists used two complementary methods, radial velocity and transit method, describe the mass, the radius, and other physical and orbital parameters. We should take into account all of these analysis to resolve the hot star and stellar evolutionary track (Seager et al., 2007). More information about exoplanet detection methods can be seen in the Planetary Habitability Laboratory (PHL) website, (`http://phl.upr.edu/library`). Statistically, 536 planets were discovered by the radial velocity method, 306 using the transit method, 33 with direct image, 18 by gravitational microlensing, and 2 planets by the astrometry method
(`https://exoplanets.nasa.gov/index.html`). Even if a large telescope is available, the reason why it is difficult to observe the exoplanets is due to their faintness, and the large separation distance form the earth.

4.2.1 Radial Velocity

In previous chapters we commented about the mechanism used to determine the radial velocity of spectroscopic binaries. In the case of the exoplanets, the method that is employed is the same but the difficulties are greater because, in an SB, the radial velocity is in km/sec but now we need to detect meter/sec or less. In the radial velocity curve, we will see a little change in a part of the curve like a noise especially when the exoplanets pass along the line of sight, (see Figure (4.1). This method is useful for a bright FGKM main-sequence class, a faint and variable pre-main-sequence, and a brown dwarf (Kalas, 2010). It is not precise enough to detect a planet orbiting around small inclination stars (Placek, 2014).

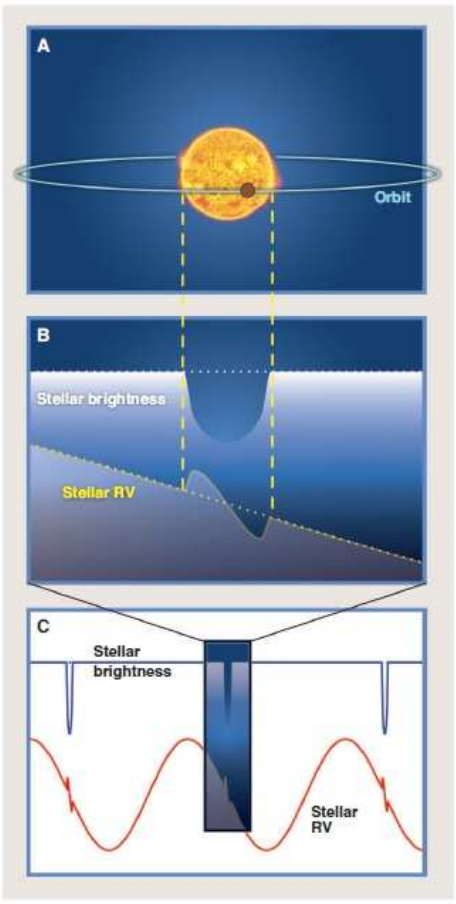

FIGURE 4.1: RV method to detect an exoplanet by changes in the brightness (Howard, 2013)

.

4.2.2 Transit Detections

The transit method is the same used in the case of the eclipsing binaries, that is to say, when the planet passes (see Figure 4.2) between the observer and the host star, causing a very

small change in the intensity of the star. This method of detection is used by the photometer at the Kepler mission which has the necessary sensitivity to detect transits of an Earth-size planets (Carado, 2016). This method also give an opportunity to determine the angle between the host star spin axis and the orbit of the planet which is called obliquity (Albrecht et al., 2012). The transit will be noticeable for exoplanets which have a large radius and a short period, and the transit probability increases depending on the size of the exoplanet (proportionally)and the distance from the host star (inversely).

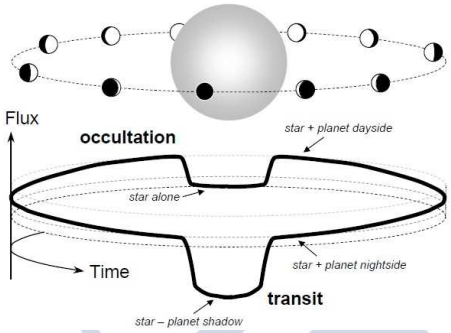

FIGURE 4.2: Transit and eclipse variation (Winn, 2010)

4.2.3 Direct Imaging

The direct imaging method permits the separation of the components of the system (the host star and its companions) directly, by blocking the light from the host star with **coronagraphy** in a ground-based telescope or **star-shade** in a space-based telescope. This method of working with adaptive optics introduces a clear photo for the system with high resolution, and permits using a few observations to determine the orbital elements (eccentricity, period, and longitude of periastron) and the atmospheric characterization of the exoplanets. It is a powerful method to detect planets which are far form the host star, or planets that are larger than Jupiter.

In 2004, the first giant planet was discovered by means of the direct method; it is 4.2 Jupiter mass, and 1.5 Jupiter radius. It was called 2M1207b, and it is near to a brown dwarf, 2MASSWJ 1207334-393254. It was discovered using a very large telescope of the European Southern Observatory (ESO) by Direct VLT/NACO observations (Chauvin et al., 2004). NaCo is short for NAOS-CONICA, NaCo Nasmyth Adaptive Optics System(NAOS), Near-Infrared Imager and Spectrograph (CONICA) which is an infrared camera and spectrometer attached to NAOS (`http://www.eso.org/naco.html`). In 2008, Christian Marois, discovered multiple planets, in the star HR 8799, with 24, 38, and 68, astronomical units using High-contrast observations Keck and Gemini telescopes (Marois et al., 2008).

4.2.4 Gravitational Microlensing

When the light travels close to a massive object, it curves or deflects because of its gravity. This phenomenon introduced by Albert Einstein was a response to the desire and request

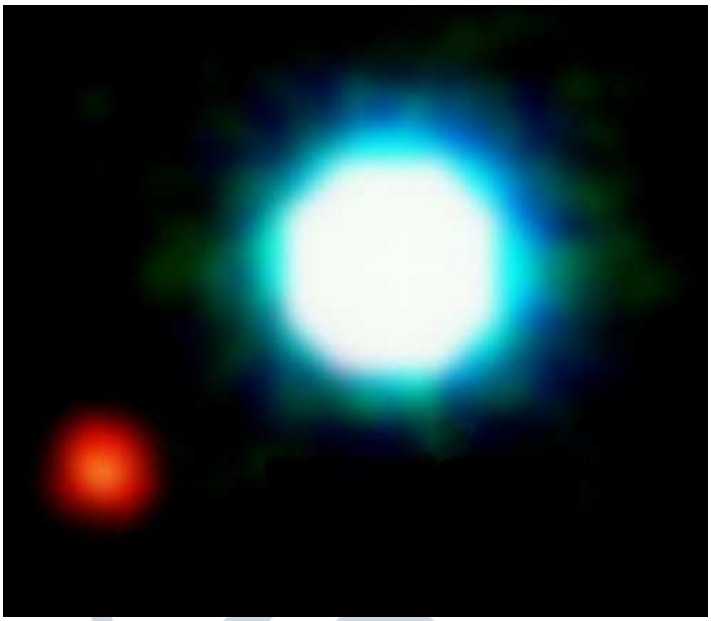

FIGURE 4.3: Composite image of giant planet near a brown dwarf (Chauvin et al., 2004)

of R. W. Mandl in 1935. He published a paper entitled "The lens-like action of a star by the deviation of light in a gravitational field" (Einstein, 1936) but, in reality, he had developed it in about 1911 before he completed the general theory of relativity in 1915 (Renn, Sauer, and Stachel, 1997). In 1991, Shude Mao and Bohdan Paczynski from Princeton University Observatory predicted that research using the microlensing method will be helpful to discover extra-solar planetary systems (Mao and Paczynski, 1991). In 2003, the first exoplanet with 1.5 the mass of Jupiter was detected by this method discovered as a result of a microlensing event, OGLE 2003-BLG-235 (or MOA 2003-BLG-53).

The Microlensing Method focusing determines the brightness of a distant star after a close star pass in front of the observer. The blip in the graph represents a change of the brightness which is evidence that the lens star (the close star) has a planet as a companion (see Figure 4.4 Gravitational Microlensing) for more information see (`https://lco.global/spacebook/gravitational-microlensing/`).

The microlensing method has the ability to detect small exoplanets that are very distant from the host star (Gould et al., 2010), as well as planets that are thousands of light-years away, near to the center of the galaxy (Beaulieu et al., 2008). It is a useful method to determine the properties of the planets but it cannot provide the definitive mass or semimajor axis (Rice, 2014).

4.2.5 Pulsar Timing

This technique detects the frequency of radio waves form a neutron star with a strong magnetic field, and high spin (See Figure 4.5). It looks like a light from a lighthouse. The pulse

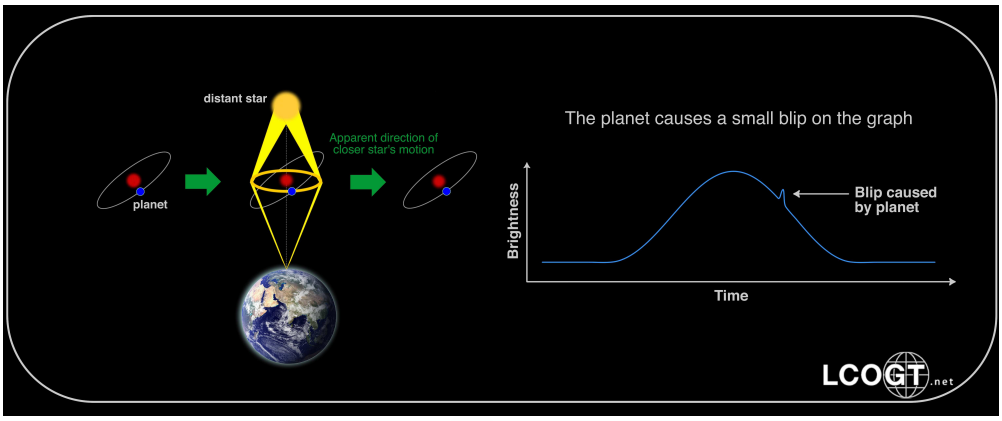

FIGURE 4.4: Gravitational Microlensing (Las Cumbres Observatory website)

of the neutron star is very precise and regular, it also depends on the rotation velocity. These pulses occur from milliseconds to seconds. If there is a variation in the time of pulsing, it means that the star is orbiting around the center of mass with another body or bodies which is evidence of the existence of exoplanets. Recently, Chinese astronomers described the pulsar timing model, pulsar parameters using mathematical model with least squares fitting for pulsar timing observations (Ting-gao et al., 2016). This method has the capability to detect planets with a size 1/10 smaller than the Earth but, unfortunately, it is applicable only for neutron stars.

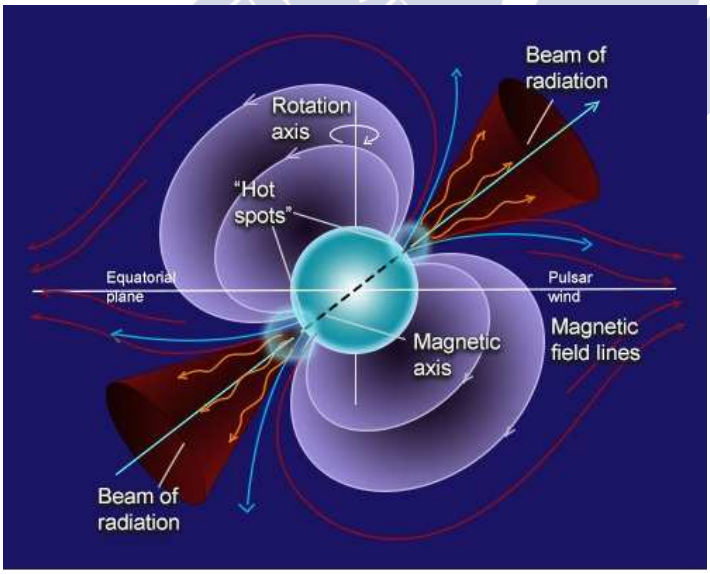

FIGURE 4.5: Neutron-star http://astronomy.nju.edu.cn/AT42202.htm

Aleksander Wolszczan used this procedure to discover the first exoplanets of 6.2 ms pulsar PSR B1257+12. He reperted all of his results concerning the evolution of the solution of this

system in several publication (Wolszczan, 1992; Wolszczan, 2008; Wolszczan et al., 2000a,b; Wolszczan, 2012; Wolszczan et al., 1994)

4.2.6 Astrometry

The Astrometry method depends on measuring the periodic variation in the position of the star on the plane of the sky (Doyle, 2008). It is a favorable method to detect Earth-like planets based on analyzing the wobble of the system (a star and a planet) orbit around the center of mass (Malbet et al., 2009; Shao, 1996). It is a powerful technique for studying the exoplanets around a nearby star (Sahlmann et al., 2013). This method is highly precise and it provides the ratio of the mass for the system. In the case that we know the mass of the star, it yields the mass of the exoplanet. We can observe the signature of the exoplanet using this method better than with others which depend on the inclination of the orbit (Sahlmann, 2012). This method can detect the Earth mass planets in the habitable zone and many of the space missions, like Kepler and K2, depend on this method with a precision of about 1μas (Shao et al., 2009).

In 2007, J.A. Docobo et al. announced at the IAU Commission 26, the possible existence of a very low-mass object as a companion in a triple stellar system, Gliese 22, after they calculated the orbit of the system with a wobble motion (Docobo et al., 2007). This system is an interesting application for the astrometric method. It is a multiple star, a red dwarf system with components Aa and Ab, and a distant component, B, (see the image of the star in K band, Figure 4.6). The expected planet orbits circularly around the second component, Ba, with 16 mass of Jupiter and a period ≈15 yr, and semimajor axis, 0.″35. Figure 4.7 shows the apparent orbit of Gilese 22 (Docobo et al., 2008).

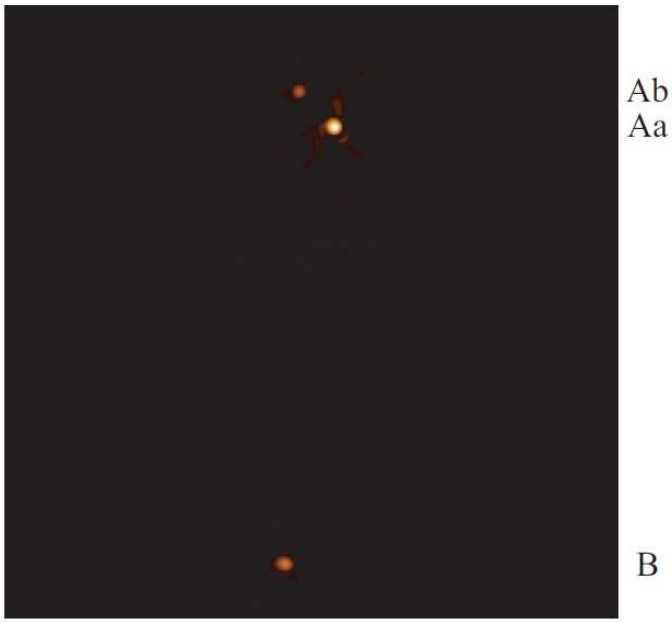

FIGURE 4.6: Gliese 22 system (ibid.)

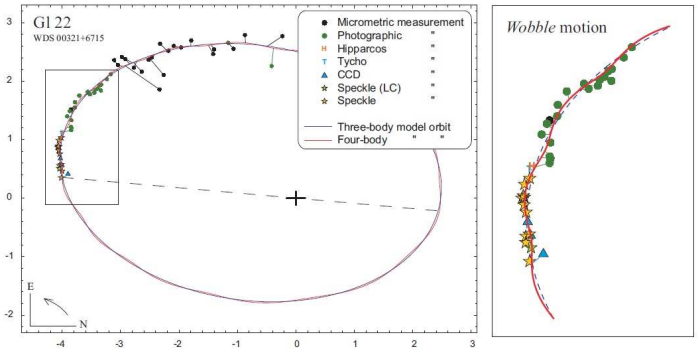

FIGURE 4.7: Apparent orbit of Gliese 22

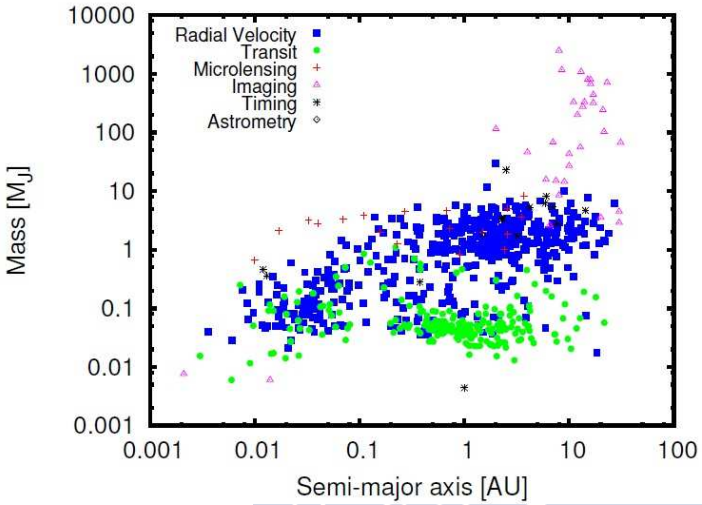

FIGURE 4.8: Extrasolar planets distribution (Schneider, 2011).

Each detection method has advantages regarding the determination of the basic elements, for instance, the transit method yields the diameter and the period of the giant exoplanets. For planets with a short period and larger than the Earth, the radial velocity can determine the mass and the period.

On other hand, the direct imaging method provides an image and the spectra. The spectroscopic characterization, the mass, period, and the orbit can be defined using the combination of the direct images with the astrometric methods (Traub and Oppenheimer, 2010). Figure 4.8 and 4.9 provide information about the characteristics of the exoplanets, each detection method of exoplanets is represented by a different color `http://exoplanet.eu/` (Kitchin, 2011; Schneider, 2011).

4.3 Stability

It is very difficult to find a definition for stability. There are at least 50 concepts related with stability in the field of Astronomy, depending on different initial conditions, physical and

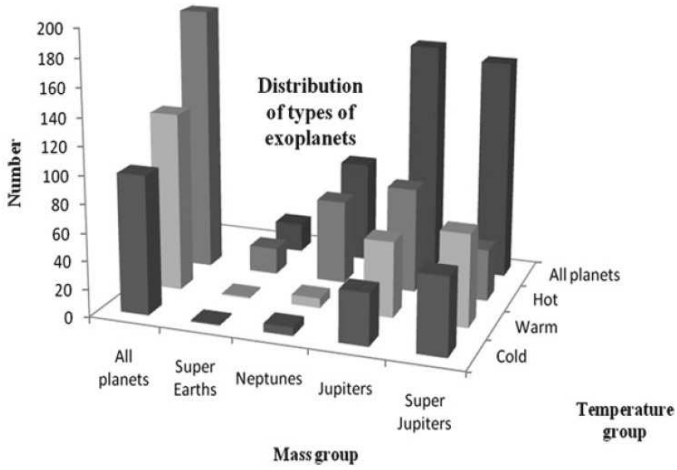

FIGURE 4.9: The distribution of the exoplanets (Kitchin, 2011)

mathematical theorems, and various constants (Szebehely, 1984). Our basic concept for stability is the condition in which the parameters of the orbit (eccentricity, semimajor axis, and the inclination) do not change much during a long period of time.
In this section we will determine the probable stable region for low-mass planets in 17 single-lined and 13 double-lined spectroscopic system. Based on the empirical expression of (Holman and Wiegert, 1999), we can is determine the stability of the planetary orbits around the binary systems by studying the ratio of the mass and the eccentricity of the system for two types of orbits: the inner type (S-type) and the outer type (P-type) . In 1984, R. Dovark classified the stable orbits for planetary system in binary systems into three types:

- The satellite-type orbits (S-type), in which the planet orbits around one of the components of the binary system,
- The planet-type orbits (P-type). In this case, the planet orbits around the both components of the binary star. We will say that it is a circumbinary planet, and
- The librator-type orbits (L- type). The stable orbit is around the Lagrangian points (which is stable only for the mass ratio, $\mu = \mathcal{M}_2/(\mathcal{M}_1+\mathcal{M}_2)$, $\mu \leq 0.04$) (Dvorak, 1984).

Holman - Wiegert empirical expression

R. Dvorak determined the stable zone in three-body problem, by using numerical investigation depending on two values, the ratio of the mass and the eccentricity of the system (especially in the case of the P-type). In 2007, Holman - Wigeret working on the same idea as Dvorak derived an expression as a function of the mass ratio and semimajor axis. They took into account the results of the α Centauri system to develop the expressions below in order to described the critical semimajor axis as a parameter of orbital stability for both types of orbits, (S-type) and (P-type) (Wiegert and Holman, 1997). They used least-squares fit data with the binary conditions as $0.1 \leq \mu \leq 0.9$, and $0.0 \leq e \leq 0.8$ for the S-type, and $0.1 \leq \mu \leq 0.5$, $0.0 \leq e \leq 0.8$ for P-type. The eccentricity (e), the longitude of the ascending node (Ω), the

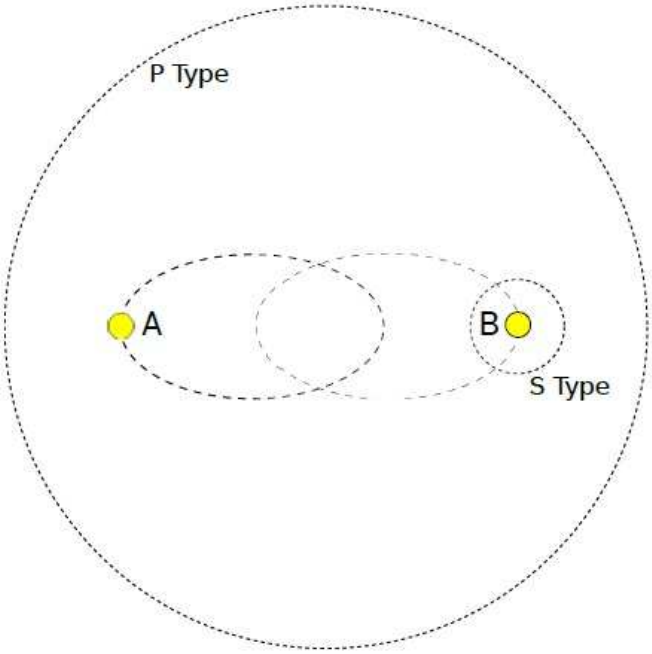

FIGURE 4.10: S-type and P-type planetary orbits (Armstrong, 2015)

.

inclination (i), and the argument of perihelion (ω), were considered equal zero (Holman and Wiegert, 1999). The expression for the S- type (the inner region) is:

$$\frac{a_s}{a} = (0.464 \pm 0.006) + (-0.380 \pm 0.010)\mu + (-0.631 \pm 0.034)e \\ +(0.586 \pm 0.061)\mu e + (0.150 \pm 0.041)e^2 + (-0.198 \pm 0.047)\mu e^2. \tag{4.1}$$

The expression for the P- type (the outer region) is:

$$\frac{a_i}{a} = (1.60 \pm 0.04) + (4.12 \pm 0.09)\mu + (5.10 \pm 0.05)e + (-4.27 \pm 0.17)\mu e \\ +(-2.22 \pm 0.11)e^2 + (-5.09 \pm 0.11)\mu^2 + (4.61 \pm 0.36)\mu^2 e^2. \tag{4.2}$$

Tables 4.1, 4.2, 4.3, and 4.4 include physical parameters of the possible host binaries and the stability conditions for planetary orbits moving around the 30 spectroscopic binaries that we have considered in this study: 17 SB1 (Tables 4.1 and 4.2) and 13 SB2 (Tables 4.3 and 4.4).

As mentioned earlier, it is difficult to determine the stability of the exoplanets orbits, especially those in stellar binary systems. Table 4.1 shows the following data: Column 1, present the name of the binary (HD number); Column 2, the eccentricity (e); Column 3, the semimajor axis of the binary in astronomical units (A.U); Column 4, includes the minimum and the maximum values of Δm for each binary; Column 5 and 6, the masses for each component in solar mass ($\mathcal{M}_\odot$).

Name (HD)	e	$a_{(A.U)}$	Δm	$\mathcal{M}_1(\mathcal{M}_\odot)$	$\mathcal{M}_2(\mathcal{M}_\odot)$
471	0.293±0.003	1.385±0.008	1.5	0.93±0.05	0.72±0.026
		1.306±0.008	3.5	0.88±0.04	0.50±0.024
4703	0.562±0.010	2.959±0.027	1.5	1.73±0.26	2.09±0.13
		2.526±0.046	9.0	1.88±0.40	0.50±0.02
10171	0.380 ± 0.010	2.270±0.035	1.5	1.73±0.26	2.07±0.19
		1.944±0.049	9.0	1.91±0.04	0.48±0.02
22521	0.655 ± 0.004	2.542±0.042	1.5	1.18±0.03	0.97±0.04
		2.222±0.005	9.0	1.09±0.04	0.34±0.05
26083	0.0	0.213±0.011	1.5	1.73±0.26	2.22±0.06
		0.185±0.009	6.9	1.89±0.40	0.67±0.02
79888	0.041 ± 0.002	0.095±0.001	1.5	0.93±0.04	0.72±0.02
		0.086±0.001	6.5	0.87±0.04	0.33±0.05
110583	0.420 ± 0.060	12.379±0.094	1.5	1.74±0.29	2.06±0.13
		10.584±0.081	9.0	1.90±0.40	0.48±0.03
111224	0.322 ± 0.010	2.389±0.007	1.5	1.36±0.07	1.11±0.04
		2.049±0.009	9.0	1.20±0.08	0.35±0.05
119915	0.0	0.637±0.009	1.5	1.20±0.05	2.18±0.01
		0.557±0.002	9.0	1.73±0.26	0.52±0.02
134169	0.096 ± 0.018	0.438±0.004	1.5	1.35±0.05	1.01±0.05
		0.383±0.005	8.6	1.23±0.03	0.35±0.05
143107	0.272 ± 0.026	3.613±0.040	1.5	1.77±0.54	2.13±0.14
		2.980±0.002	9.0	1.76±0.29	0.43±0.03
159220	0.0	0.041±0.001	1.5	1.26±0.03	0.98±0.05
		0.006±0.001	9.0	1.18±0.03	0.34±0.04
174103	0.075±0.015	1.773±0.037	1.5	1.82±0.33	2.11±0.05
		1.501±0.381	9.0	1.91±0.41	0.48±0.03
176526	0.437± 0.006	2.382±0.005	1.5	1.41±0.03	1.04±0.04
		2.189±0.004	5.1	1.34±0.03	0.56±0.02
183629	0.410±0.005	1.156±0.025	1.5	1.75±0.27	2.15±0.06
		1.018±0.054	6.2	1.91±0.42	0.77±0.03
196758	0.368 ± 0.009	4.837±0.013	1.5	1.75±0.27	2.15±0.06
		4.107±0.001	9.0	1.91±0.41	0.48±0.03
219834	0.162 ± 0.002	4.601±0.054	1.5	1.35±0.05	1.11±0.04
		4.093±0.368	6.0	1.20±0.03	0.53±0.02

TABLE 4.1: Physical parameters for the 17 single-lined spectroscopic binaries

Name (HD)	$a_{1S_{max}(A.U)}$	$a_{1S_{min}(A.U)}$	$a_{1Pmin(A.U)}$	$a_{2S_{max}(A.U)}$	$a_{2S_{min}(A.U)}$
471	0.272	0.230	4.306	0.220	0.175
	0.280	0.242	**4.519**	0.198	0.149
4703	0.319	0.090	**9.904**	0.350	0.138
	0.369	0.224	9.6350	0.202	0.029
10171	0.342	0.236	**6.941**	0.379	0.282
	0.417	0.353	6.664	0.200	0.090
22521	0.244	0.018	**9.372**	0.224	0.020
	0.252	0.087	8.764	0.157	0.089
26083	0.053	0.052	**0.465**	0.063	0.062
	0.068	0.067	0.418	0.034	0.032
79888	0.023	0.022	**0.217**	0.027	0.026
	0.029	0.029	0.209	0.016	0.186
110583	1.747	1.097	33.819	1.923	1.319
	2.156	1.748	**38.267**	1.063	0.370
111224	0.443	0.360	**7.530**	0.392	0.299
	0.447	0.412	6.739	0.239	0.144
119915	0.140	0.135	1.272	0.209	0.207
	0.240	0.238	**1.410**	0.109	0.105
134169	0.116	0.112	**1.148**	0.096	0.090
	0.128	0.125	0.984	0.058	0.052
143107	0.643	0.529	**10.280**	0.722	0.617
	0.776	0.713	9.310	0.350	0.232
159220	0.012	0.012	**0.095**	0.010	0.010
	0.014	0.013	0.079	0.006	0.069
174103	0.420	0.400	**4.288**	0.464	0.446
	0.525	0.516	3.692	0.227	0.200
176526	0.372	0.253	**8.142**	0.314	0.178
	0.388	0.291	7.785	0.242	0.105
183629	0.164	0.105	**3.576**	0.162	0.115
	0.191	0.150	3.567	0.116	0.057
196758	0.737	0.519	**14.599**	0.831	0.633
	0.901	0.772	13.954	0.431	0.206
219834	1.085	1.006	**12.767**	0.955	0.866
	1.137	1.080	12.485	0.677	0.586

TABLE 4.2: The stability limits for exoplanet orbits around each component and both components, in the 17 single-lined spectroscopic binaries

Name (HD)	e	$\mathcal{M}_1(\mathcal{M}_\odot)$	$\mathcal{M}_2(\mathcal{M}_\odot)$	$a_{(A.U)}$
16739	0.663±0.002	1.18±0.03	1.04±0.04	1.221±0.116
27176	0.167±0.004	1.74±0.03	1.38±0.03	0.738±0.542
74089	0.0	1.91±0.42	1.91±0.42	0.237±0.001
74855	0.863±0.001	1.30±0.02	0.90±0.04	4.556±0.031
85843	0.171±0.005	1.26±0.03	0.93±0.05	3.164±0.028
112475	0.198±0.007	1.07±0.04	0.83±0.03	2.192±0.005
129560	0.730±0.040	1.89±0.40	1.89±0.40	26.737±3.691
170153	0.414±0.008	1.31±0.03	0.93±0.05	1.097±0.096
171862	0.0	1.42±0.03	1.32±0.04	0.036±0.002
185734	0.556±0.001	1.89±0.42	1.73±0.28	1.720±0.148
194765	0.259±0.002	1.30±0.04	1.12±0.04	0.777±0.005
197952	0.517±0.003	1.48±0.02	1.32±0.04	0.590±0.002
198048	0.547±0.007	1.77±0.50	1.77±0.50	1.937±0.129

TABLE 4.3: Physical parameters for the 13 double-lined spectroscopic binaries

Name (HD)	$a_{1S_{max}(A.U)}$	$a_{1S_{min}(A.U)}$	$a_{1Pmin(A.U)}$	$a_{2S_{max}(A.U)}$	$a_{2S_{min}(A.U)}$
16739	0.1134	0.0011	**4.473**	0.1073	- 0.0104
27176	0.150	0.136	**2.140**	0.175	0.162
74089	0.065	0.064	**0.539**	0.065	0.064
74855	0.240	-0.354	**17.875**	0.223	-0.453
85843	0.760	0.704	**8.946**	0.535	0.462
112475	0.499	0.455	**6.324**	0.430	0.372
129560	2.040	-0.856	**98.003**	2.040	-0.856
170153	0.180	0.130	**3.73**	0.149	0.090
171862	0.010	0.010	**0.081**	0.001	0.009
185734	0.202	0.077	**6.030**	0.193	0.064
194765	0.015	0.013	**0.227**	0.014	0.011
197952	0.073	0.034	**2.007**	0.069	0.027
198048	0.226	0.087	**6.671**	0.226	0.087

TABLE 4.4: The stability limits for exoplanet orbits around each component and both components (circumbinary planets), in the 13 double-lined spectroscopic binaries

The description of Table 4.3 is similar to Table 4.1 except that, in this last case, the Column corresponding Δm has been deleted because Δm is fixed now.

Tables 4.2, and 4.4 list, the name of the binary (HD number) in Column 1. Columns 2 and 3 indicate the stability limits of the exoplanets orbits in the case of an S-type orbit around the main component (as a minimum value ($a_{S\,min}$) and maximum value ($a_{S\,max}$)) in astronomical units (A.U), Column 4 shows the stability limits for the exoplanet in the case of a P-type orbits where bold values indicate a minimum value ($a_{P\,min}$) (especially for the SB1 because different Δm are possible) also in astronomical units (A.U); and Columns 5 and 6 contain the same information as Columns 2 and 3 but, in this case, for orbits around the secondary component. It is necessary to take into account that in Table 4.2 (SB1), the two values given for each binary correspond to the two values of Δm mentioned in Table 4.1.

On the other hand, in order to understand the orbit stability around each star, we have to mention here that the stability is given between two values of the distance: the first one is $a_{S\,max\,(A.U)}$, which represents the largest distance around the star at which the orbit of the exoplanet is stable even with the existence of the second component. The second value $a_{S\,min}\ (A.U)$, represents the closest separation to the star where the existence of the stable orbits of exoplanets is possible in this situation the stability is not guaranteed, we have to take into account the spectral type and the size of the star because, in some cases, the radius of the star is very close to the minimum value for the stability which means that the stability analysis by Holman and Wiegert cannot be used as the restricted three-body problem is not a valid model. Moreover, in some cases, the maximum stability limit might be in side the star. For example, in the case of the systems, HD 26083, HD 159220, HD 74089, HD 171862, the minimum distances of stability are 0.0533, 0.0120, 0.0600, and 0.0096 AU, the star radius being close to these values.

The minus sign in the value of the stability, $a_{S\,min\,(A.U)}$ for HD 16739, HD 74855, and HD 129560 is due to the uncertainty in the semimajor axis using the Holman-Wiegert expression which means that stability in the S-type system is not guaranteed.

4.4 Habitability

C.S. Cockell from the UK Centre for Astro-biology, University of Edinburgh, introduced an interesting definition for habitability, which is the ability of the environment to support metabolic activities for at least one known organism, and that these activities support its survival, growth, maintenance, or reproduction processes (Cockell et al., 2016).

The atmosphere of a habitable exoplanet can contain different components: carbon dioxide (CO_2), carbon monoxide (CO), methane (CH_4), and the most important ingredient, water (H_2O), which is the source of life (Swain et al., 2009; Tinetti et al., 2012).

The best state for the water to support the basic processes of life, the liquid state, requires suitable temperature on the exoplanet; not cold or hot, and its temperature depends on various parameters, internal parameters such as radio activity and the components of the atmosphere. The external parameter depends on the source of the radiation, which is proportional with the distance from the nearest star. When searching exoplanets, the first step is to determine the habitable zone where the possibility to find liquid water exists. The HZ is looks like a spherical shell around a single star or around a binary star.

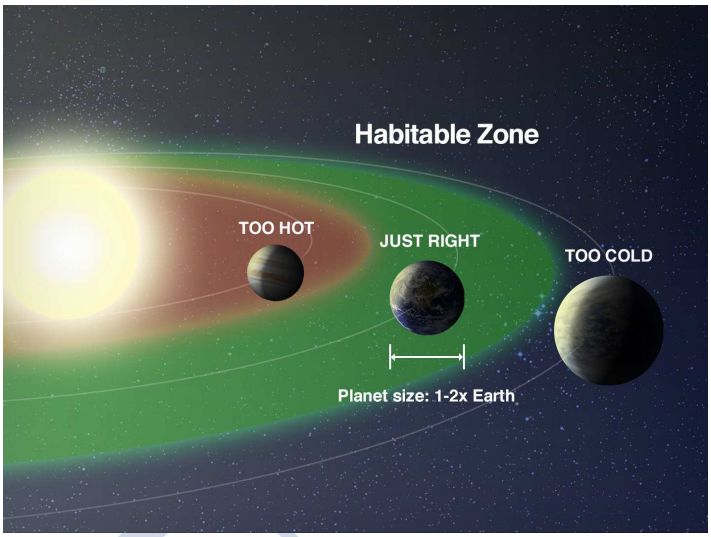

FIGURE 4.11: The habitable zone for our solar system (https://exoplanets.nasa.gov).

There are five parameters that we should take into account when we want to study the habitability in the binary system: the masses of both components ($\mathcal{M}_1$, $\mathcal{M}_2$), the period (P), the eccentricity (e), and the semimajor axis of the exoplanet orbit (a) (Mason et al., 2013). We should mention here that the semimajor axis and the eccentricity of the exoplanets can change because the gravity of the host star creates the tidal force which directly causes the migration of the exoplanet out of the habitable zone. For this reason, the number of habitable exoplanets is reduced, in general (Barnes et al., 2007; Barnes et al., 2008), and the habitability changes over time.

In a binary star with a separation of less than 50 AU, especially in the S-type systems, the HZ and the stability around a component is influenced by the gravity of the other component, causing perturbation in the orbit of the exoplanet and its ability to contain liquid water (Eggl et al., 2012).

The Habitable Exoplanets Catalog (HEC), established in 2011, is a website that is updated periodically and presents valuable information, and statistical and physical analysis about all known exoplanets up-to-date. HEC is an part of The Planetary Habitability Laboratory (PHL), University of Puerto Rico, and it is a virtual laboratory that investigates the habitability of the exoplanets in the universe http://phl.upr.edu/projects/habitable-exoplanets-catalog. Next the HEC artistic rendition depicts the exoplanets that have a possibility to contain liquid water.

In order to study the habitable zone for spectroscopic binaries, we fix the following parameters: the temperature based on the table related with spectral types that was developed by (Gray, 2005), the mass as a result of our methodology from previous chapters, and the luminosity using the luminosity-absolute magnitude relation,

$$\frac{L}{L_\odot} = -\frac{M_v - M_{v\odot} - (BC - BC_\odot)}{2.5}, \tag{4.3}$$

HD	$a_{(A.U)}$	Sp_1	Sp_2	$T_1(K)$	T_2(K)	$L_1(L\odot)$	$L_2(L\odot)$	$\mathcal{M}_1(\mathcal{M}_\odot)$	$\mathcal{M}_2(\mathcal{M}_\odot)$
471	1.386±0.008	G8V	K4V	5486	4798	0.47	0.090	0.93±0.05	0.72±0.03
		G9V	M1V	5384	4144	0.37	0.005	0.88±0.04	0.50±0.02
4703	2.959±0.027	K4III	A6IV	4798	8121	42.07	20.890	1.73±0.26	2.09±0.13
		K2III	M1V	5055	4144	41.69	0.005	1.88±0.40	0.50±0.02
10171	2.270±0.035	K4III	A6V	4798	8121	42.07	13.550	1.73±0.26	2.07±0.19
		K0III	M1V	5282	4144	39.81	0.005	1.91±0.04	0.48±0.02
22521	2.542±0.042	F8V	G6V	6160	5600	2.21	0.640	1.18±0.03	0.97±0.04
		G0V	M4V	5943	3974	1.51	0.001	1.09±0.04	0.34±0.05
26083	0.213±0.011	K3III	A3V	4973	8758	48.75	21.090	1.73±0.26	2.22±0.06
		K0III	K5V	5282	4623	39.81	0.001	1.89±0.40	0.67±0.02
79888	0.095±0.001	G8V	K4V	5486	4798	0.45	0.090	0.93±0.04	0.72±0.02
		G9V	M5V	5384	3923	0.37	0.001	0.87±0.04	0.33±0.05
110583	12.379±0.094	K3III	A6IV	4973	8121	44.05	20.320	1.74±0.29	2.06±0.13
		K1III	M1V	5168	4144	40.18	0.005	1.90±0.42	0.48±0.03
111224	2.389±0.007	F8IV	F9V	6160	6051	6.49	1.820	1.36±0.07	1.11±0.04
		K0IV	M4V	5282	3974	3.80	0.001	1.20±0.08	0.35±0.05
119915	0.637±0.009	K6III	A5IV	4502	8306	39.45	24.880	1.20±0.05	2.18±0.01
		K4III	M1V	4798	4144	42.70	0.005	1.73±0.26	0.52±0.02
134169	0.438±0.004	F4V	G4V	6655	5537	4.01	0.860	1.35±0.05	1.01±0.05
		F7V	M4V	6216	3974	2.61	0.001	1.22±0.03	0.35±0.04
143107	3.613±0.040	K5III	A6IV	4625	8121	42.07	10.560	1.77±0.54	2.13±0.14
		K3III	M2V	4973	4076	44.05	0.004	1.76±0.29	0.43±0.03
159220	0.041±0.000	F6V	G5V	6405	5657	2.62	0.750	1.26±0.03	0.98±0.05
		F8V	M4V	6160	3974	2.21	0.001	1.18±0.03	0.44±0.04
174103	1.773±0.037	K2III	A4V	5055	8532	44.05	16.900	1.82±0.33	2.11±0.05
		K0III	M1V	5282	4144	39.81	0.005	1.90±0.42	0.48±0.03
176526	2.382±0.005	F3V	G2V	6782	5811	4.76	1.110	1.41±0.03	1.04±0.04
		F4V	K9V	6385	4296	5.25	0.019	1.34±0.03	0.56±0.02
183629	1.156±0.025	K3III	A4V	4973	8532	44.05	16.900	1.75±0.27	2.15±0.06
		K0III	K2V	5282	5055	39.81	0.180	1.91±0.42	0.77±0.03
196758	4.837±0.013	K4III	A4V	4798	8532	38.72	16.900	1.75±0.27	2.15±0.06
		K0III	M1V	5282	4144	39.81	0.005	1.90±0.41	0.48±0.03
219834	4.601±0.013	K8IV	F9V	6160	6051	6.52	1.610	1.35±0.05	1.11±0.04
		K6IV	M0V	4501	4212	2.94	0.009	1.20±0.03	0.53±0.02

TABLE 4.5: Stellar parameters used to study the habitable zone for the 17 single-lined spectroscopic binaries

HD	$a_{(A.U)}$	Sp_1	Sp_2	T_1(K)	T_2(K)	$L_1(L\odot)$	$L_2(L\odot)$	$\mathcal{M}_1(\mathcal{M}_\odot)$	$\mathcal{M}_2(\mathcal{M}_\odot)$
16739	1.222±0.116	F8V	G2V	6160	5811	2.21	1.30	1.18±0.03	1.04±0.04
27176	7.380±0.542	A8V	F3V	7682	6782	9.70	4.47	1.74±0.03	1.38±0.03
74089	0.230±0.001	K0III	K0III	5282	5282	39.81	39.81	1.91±0.42	1.91±0.42
74855	4.556±0.031	G0IV	G8V	5486	5486	5.75	0.38	1.30±0.02	0.90±0.04
85843	3.164±0.028	F6V	G7V	5543	8121	2.69	0.59	1.26±0.03	0.93±0.05
112475	2.192±0.005	G0V	K1V	5168	5600	1.51	0.23	1.07±0.04	0.83±0.03
129560	26.737±3.692	K2III	K2III	5055	5055	41.69	41.69	1.89±0.40	1.89±0.40
170153	1.097±0.097	F5V	G2V	6528	5811	3.44	0.54	1.31±0.03	0.93±0.05
171802	0.036±0.000	F3V	F5V	6782	6528	4.94	3.59	1.42±0.03	1.32±0.04
185734	1.720±0.015	G9III	G2III	5384	5811	41.69	37.33	1.42±0.03	1.32±0.04
194765	0.777±0.005	F5V	F9V	6528	6051	3.59	1.81	1.30±0.04	1.12±0.04
197952	0.590±0.002	F5IV	F9IV	6528	6051	8.55	5.97	1.48±0.02	1.32±0.04
198048	1.937±0.129	K5III	K5III	4625	4625	42.07	42.07	1.77±0.50	1.77±0.50

TABLE 4.6: Stellar parameters used to study the habitable zone for the 13 double-lined spectroscopic binaries

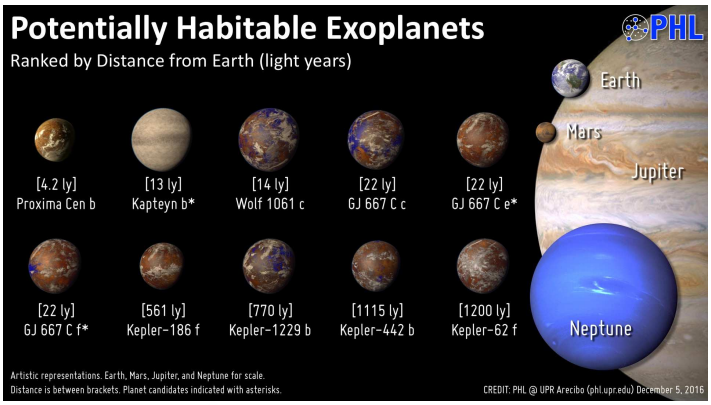

FIGURE 4.12: List of a rocky exoplanets that they can maintain surface liquid water (PHL), compression with our solar system.

where, L is the luminosity of the star, M_v is the absolute magnitude ($M_{v\odot}$ = 4.82), and BC is the bolometric correction ($BC_\odot$ = -0.08).

In 2013, Tobias Muller and Nader Haghighipour developed an interactive website (`http://astro.twam.info/hz/`) to determine the habitable zone for single star, double star, and multiple star systems (Müller and Haghighipour, 2014). This amazing website has a habitable zone calculator, and the gallery contains tables, plots, and videos as simulations of a known exoplanet's motion around the star. There are four models in this website: Kopparapu et al., 2014, Kopparapu et al., 2013, Selsis et al., 2007, and Kasting, Whitmire, and Reynolds, 1993. It the HZ calculator on this website describe the stability using the Holman and Wiegert, 1999 model. This the same method that we used previously to describe the radii of the stability around single-lined and double-lined spectroscopic binaries.

As we mentioned before, the habitable zone provides the area around each component or around both components in which the existence of liquid water is possible. We have calculated all parameters (see Tables 4.5, 4.6), which allow us to use a methodology of (Müller and Haghighipour, 2014) to describe the habitable zone around the stars of our sample of 30 spectroscopic binaries. Tables 4.5 and 4.6 list in Column 1, the name of the star; Column 2, the semimajor axis of the binary in astronomical units (A.U); Columns 3 and 4; the spectral type for the primary component and the secondary; Columns 5 and 6, the temperature of each component in Kelvin degrees (K); Columns 7 and 8, the luminosity of each component in the solar luminosity ($L_\odot$), and Columns 9 and 10, the mass of the each component in solar mass ($\mathcal{M}_\odot$).

We take into account that liquid water exists in an environment with an atmospheric pressure of 1 atm within a temperature range of 273 K to 373 K which is dependent on the distance from the center-mass of the system and the luminosity of the stars. The habitable zone was calculated using the (ibid.) method and we classified these results into three subtypes depending on the width of the habitable zone (WHZ) in AU compared with the width of our solar system which is about 0.7 AU (Kopparapu, 2013). Taking into account the difference in the class of each system, 50% of our results show habitable zones within the following ranges: $0.5 \leq$ WHZ ≤ 2.5 , 23%, $2.5 <$ WHZ ≤ 5, and 27 %, $5 <$ WHZ. This WHZ yields an

increased possibility of the existence of liquid water, especially around giants stars. Unfortunately, it also expands the area to search for habitable exoplanets requiring more observing time.

4.5 The Graphics of the Stability and Habitable Zones around the 17 single-lined and 13 double-lined spectroscopic binaries studied in this work

In previous two sections, we have identified stability and habitable zones and now we combine these two parameters in order to find stable orbits in the habitable zone. When there is a match between the habitable and the stable areas, it presents an interesting situation, and the possibility to contain an exoplanet with a stable orbit where it is possible to find liquid water. Fortunately, 17% of our systems have these stability and habitability properties but, only in planetary P-type orbits, because the distance between the stellar components is very short for all of the binaries in our sample. The systems HD 4703, HD 10171, HD 13107, HD 171862, and HD 194765 present a possibility to find habitable exoplanets around the binary star (circumbinary planets).

The following 30 graphics for each spectroscopic binary studied (graphics from 4.13 to 4.29 for 17 SB1 and graphics from 4.30 to 4.42 for SB2) were obtained using the interactive website created by Müller and Haghighipour, 2014. In all of them, the habitable zone is green in colour and the average stability zone (the Muller and Haghighipour software considers not the maximum and minimum conditions such as the Wiegert and Holman criterion but an average of them) is represented by the dotted curves.

The Stability and Habitable Zone around 17 single-lined spectroscopic binaries

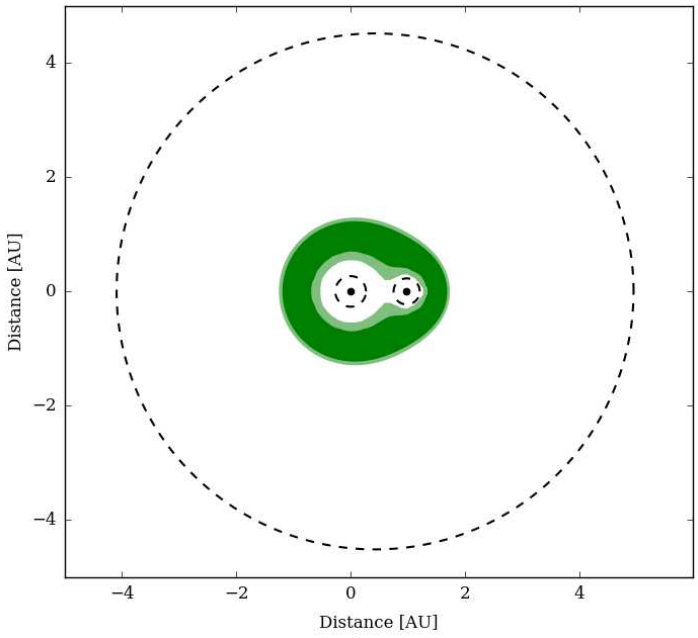

FIGURE 4.13: Stability and Habitable Zones for SB1 HD 471

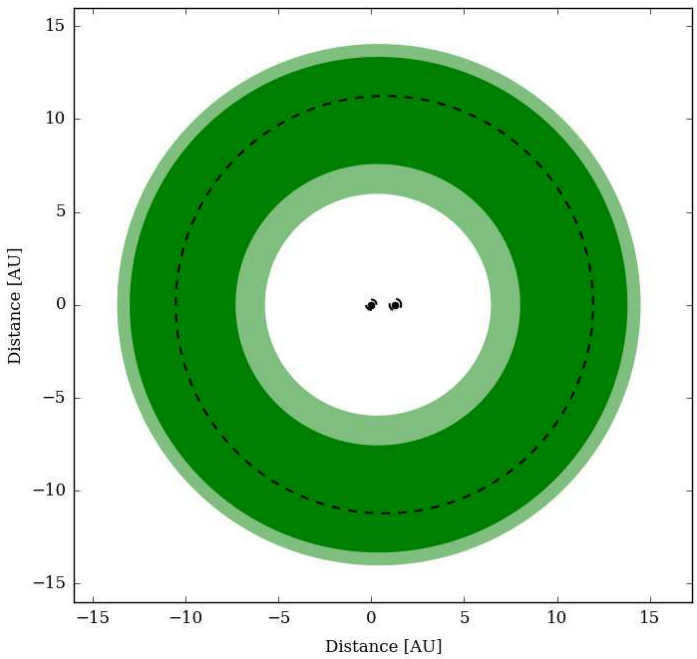

FIGURE 4.14: Stability and Habitable Zones for SB1 HD 4703

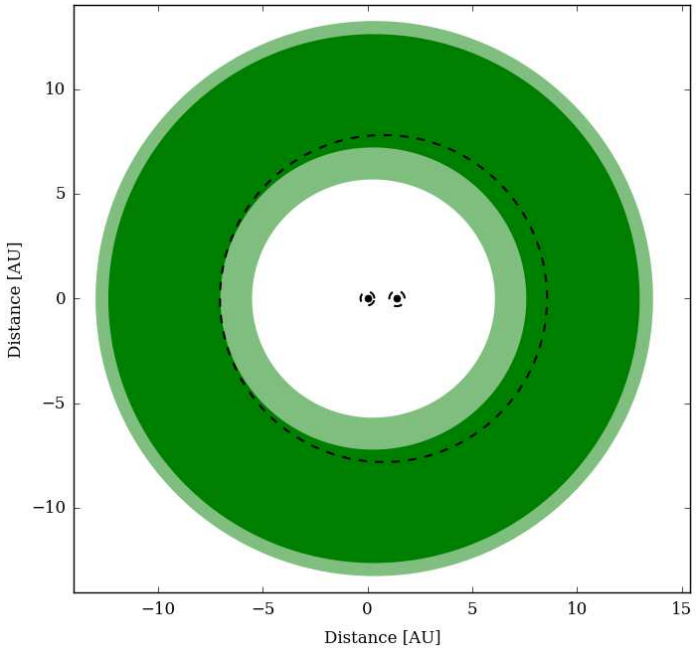

FIGURE 4.15: Stability and Habitable Zones for SB1 HD 10171

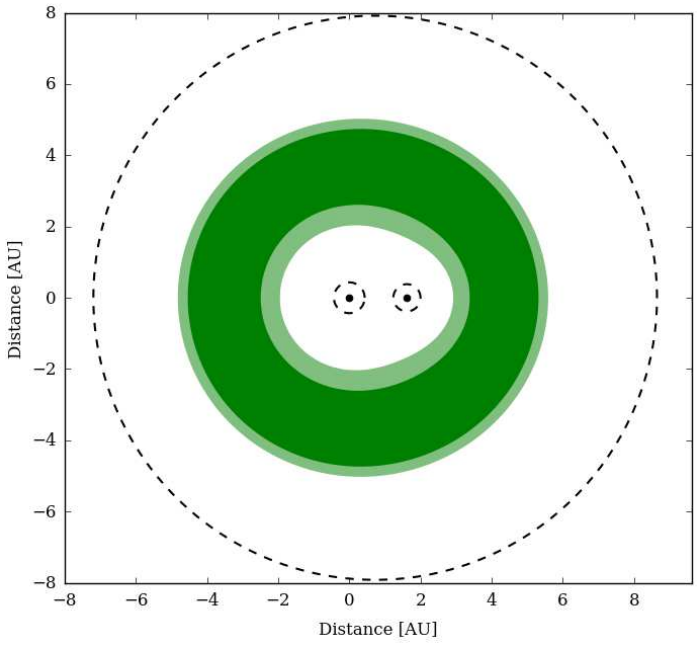

FIGURE 4.16: Stability and Habitable Zones for SB1 HD 11224

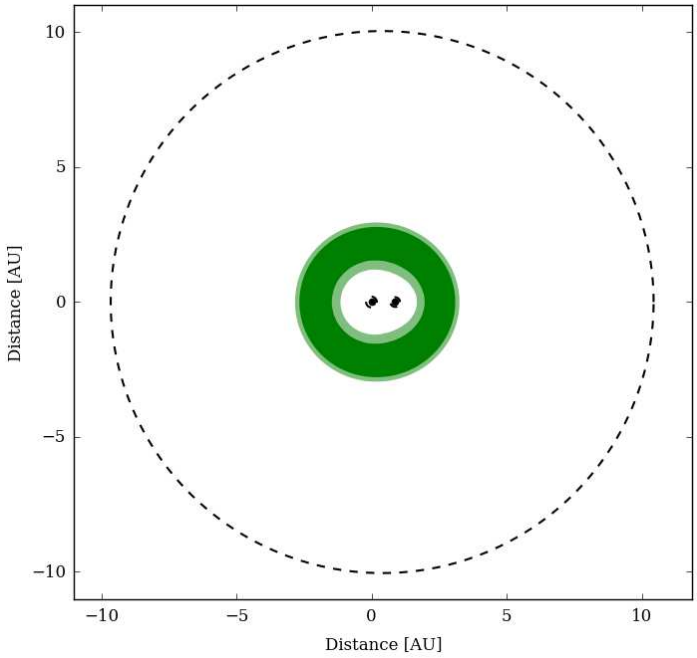

FIGURE 4.17: Stability and Habitable Zones for SB1 HD 22521

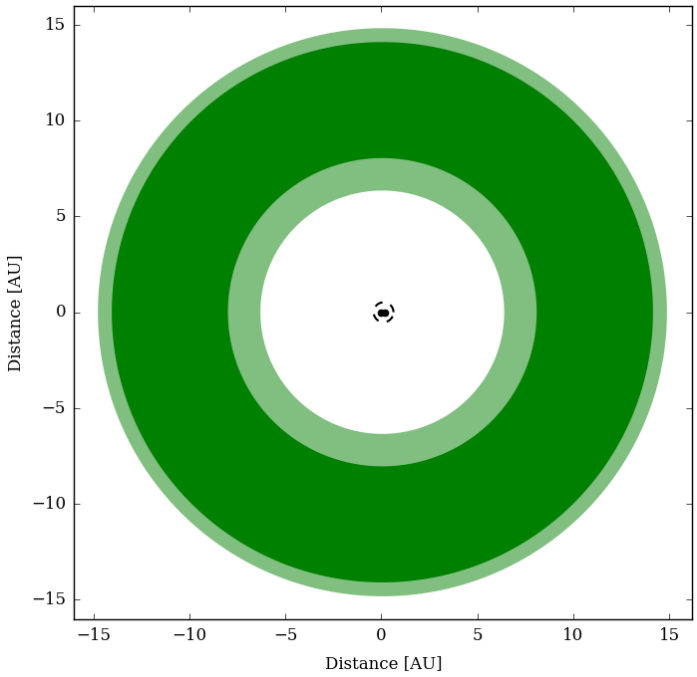

FIGURE 4.18: Stability and Habitable Zones for SB1 HD 26083

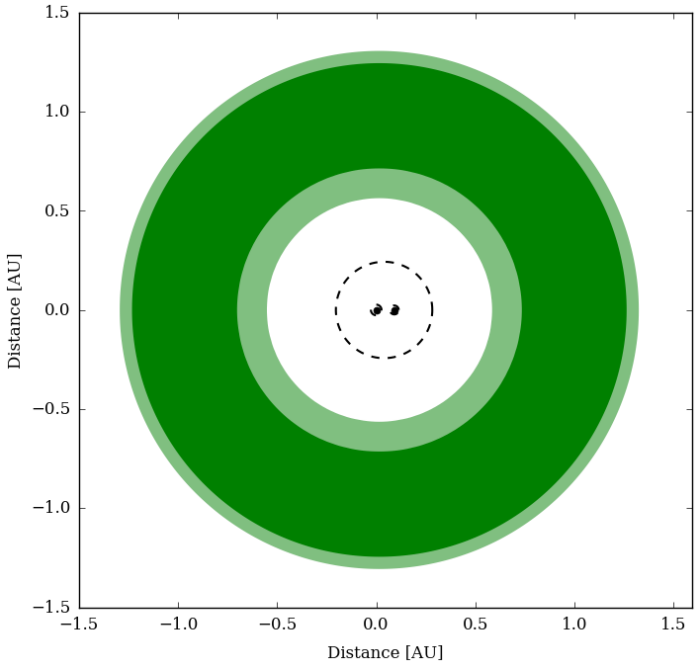

FIGURE 4.19: Stability and Habitable Zones for SB1 HD 79888

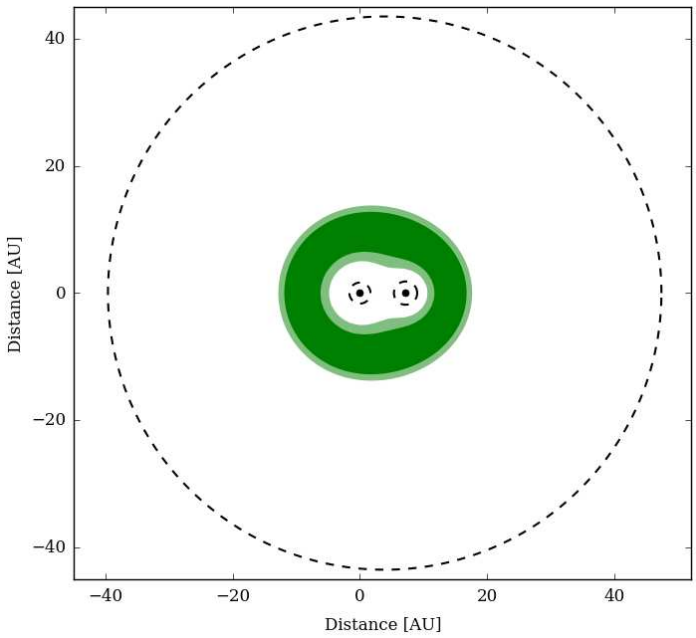

FIGURE 4.20: Stability and Habitable Zones for SB1 HD 110583

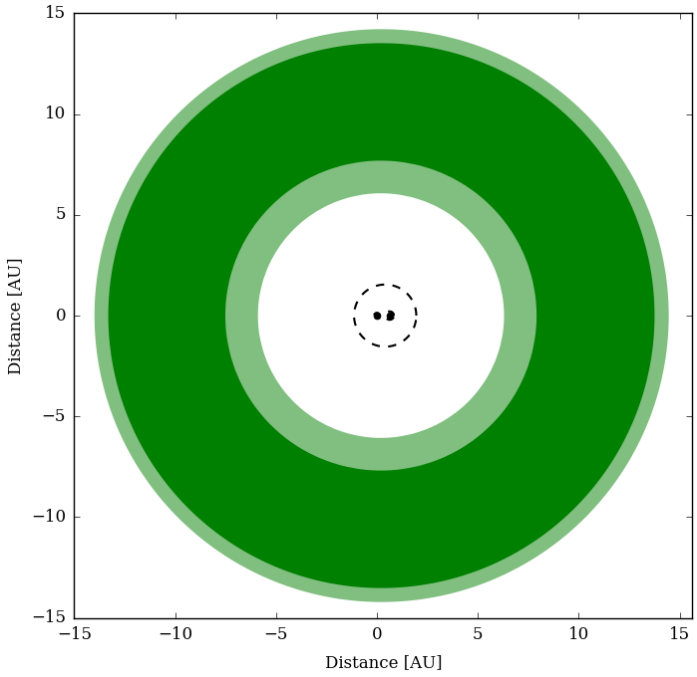

FIGURE 4.21: Stability and Habitable Zones for SB1 HD 119915

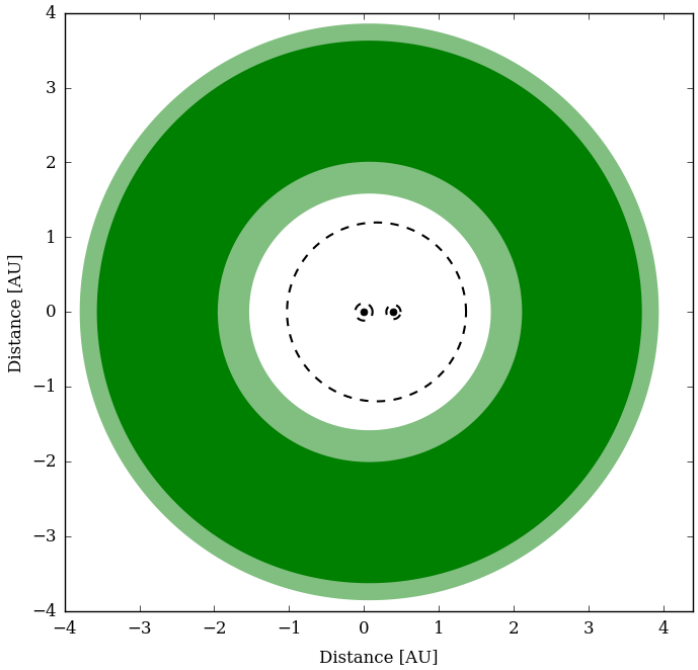

FIGURE 4.22: Stability and Habitable Zones for SB1 HD 134169

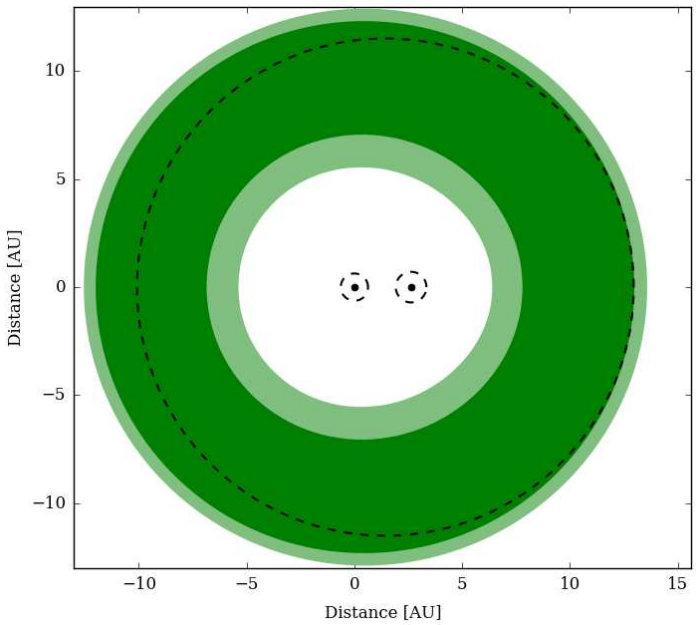

FIGURE 4.23: Stability and Habitable Zones for SB1 HD 143107

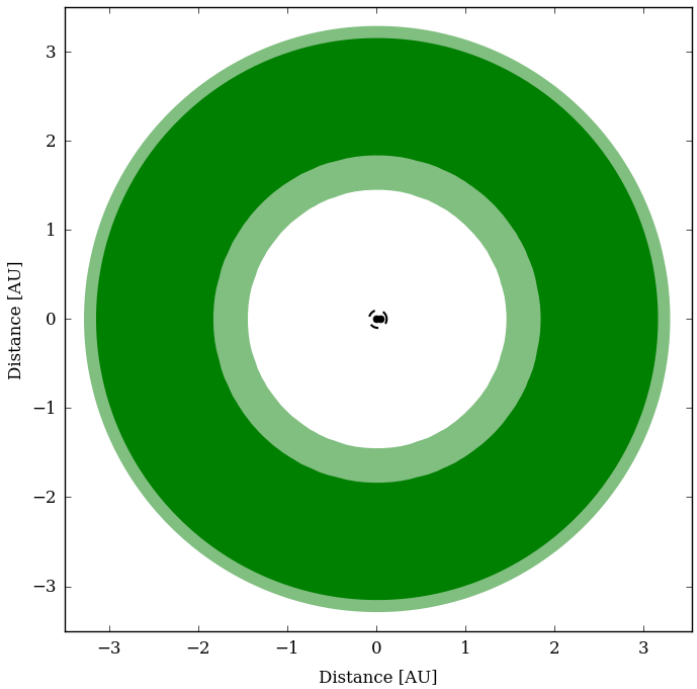

FIGURE 4.24: Stability and Habitable Zones for SB1 HD 159220

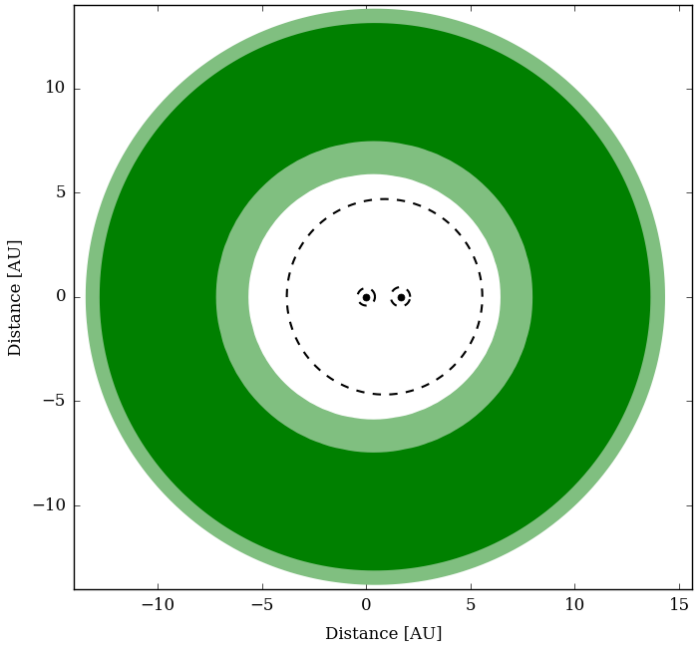

FIGURE 4.25: Stability and Habitable Zones for SB1 HD 174103

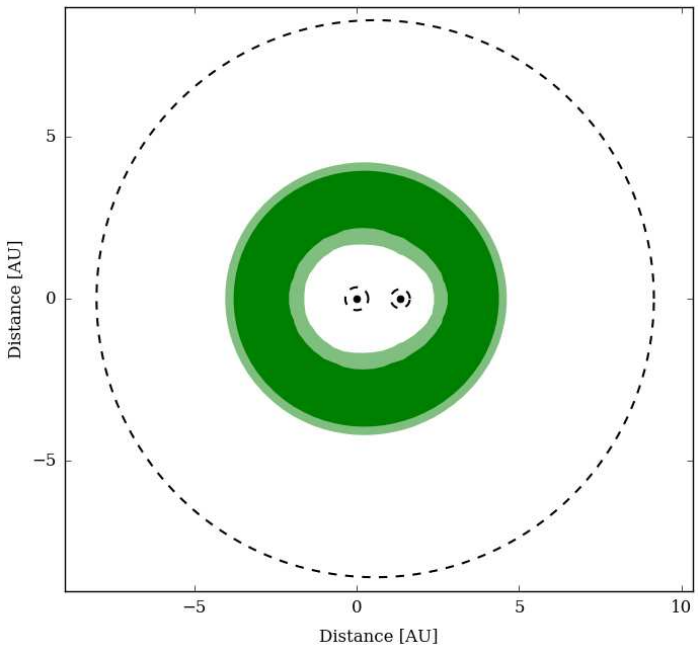

FIGURE 4.26: Stability and Habitable Zones for SB1 HD 176526

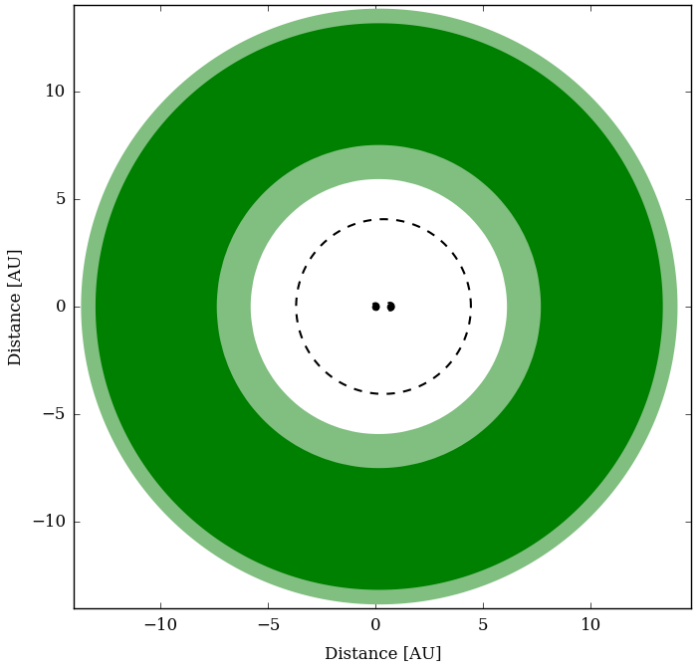

FIGURE 4.27: Stability and Habitable Zones for SB1 HD 183629

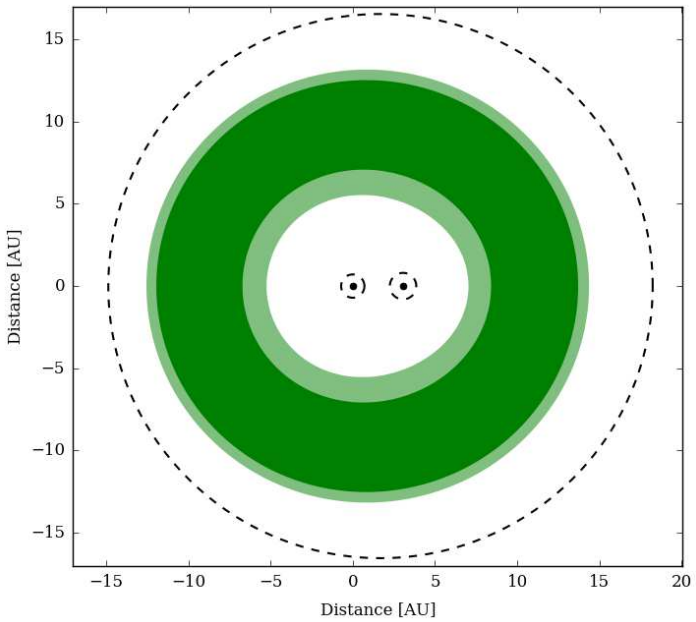

FIGURE 4.28: Stability and Habitable Zones for SB1 HD 196758

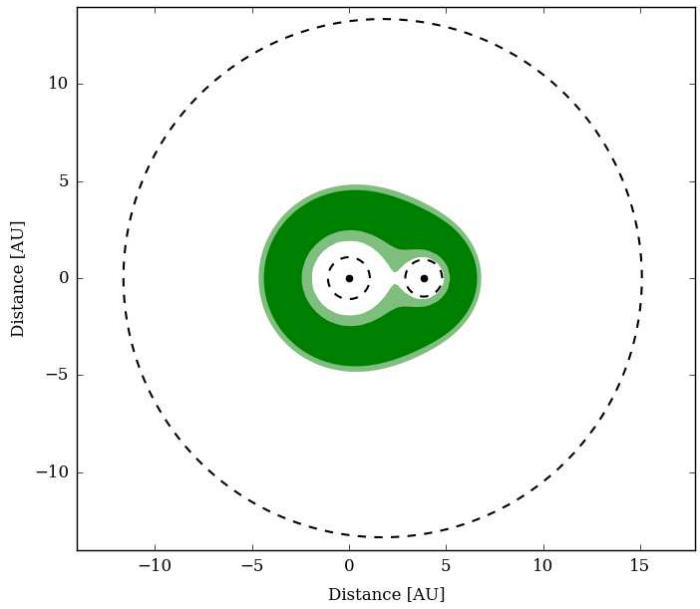

FIGURE 4.29: Stability and Habitable Zones for SB1 HD 219834

The Stability and Habitable Zone around 13 double-lined spectroscopic binaries

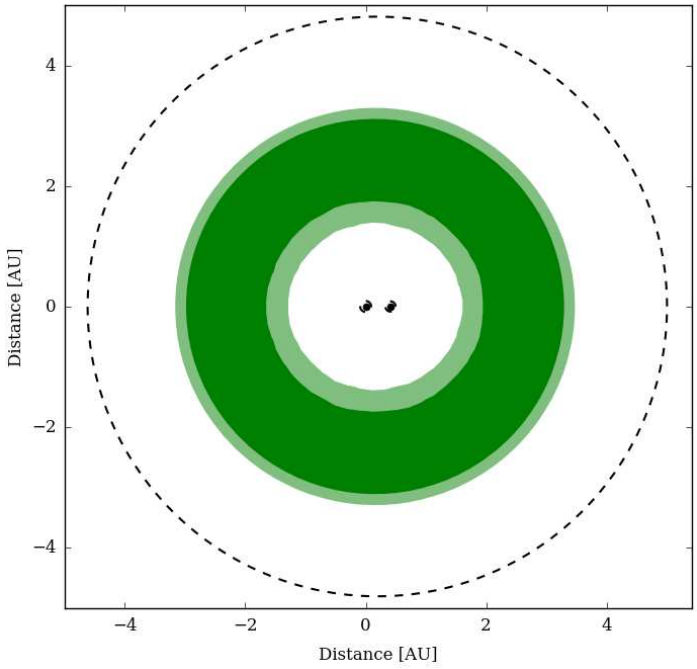

FIGURE 4.30: Stability and Habitable Zones for SB2 HD 16739

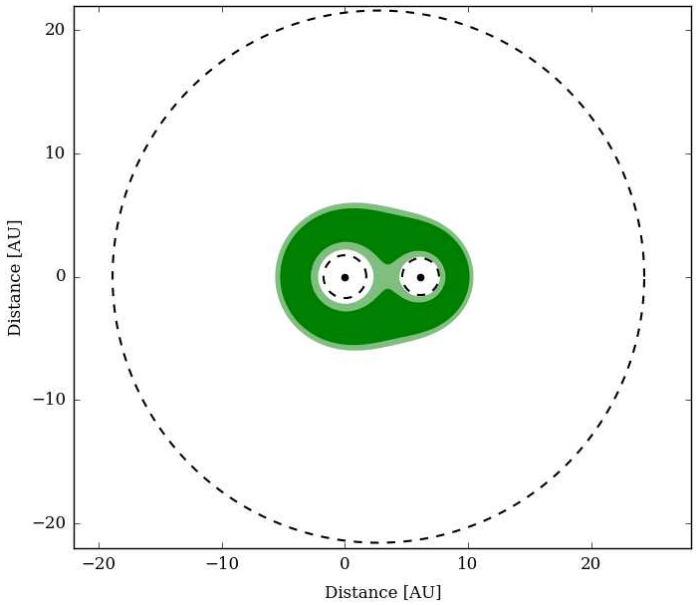

FIGURE 4.31: Stability and Habitable Zones for SB2 HD 27176

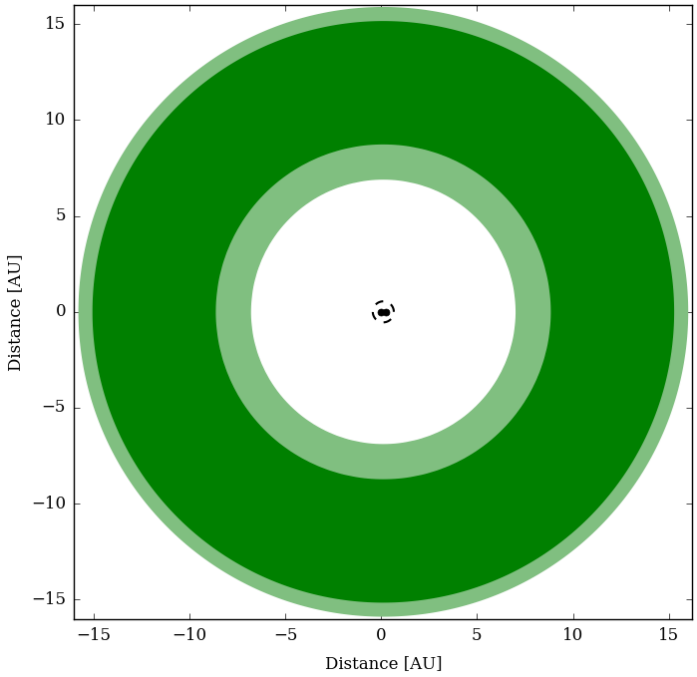

FIGURE 4.32: Stability and Habitable Zones for SB2 HD 47089

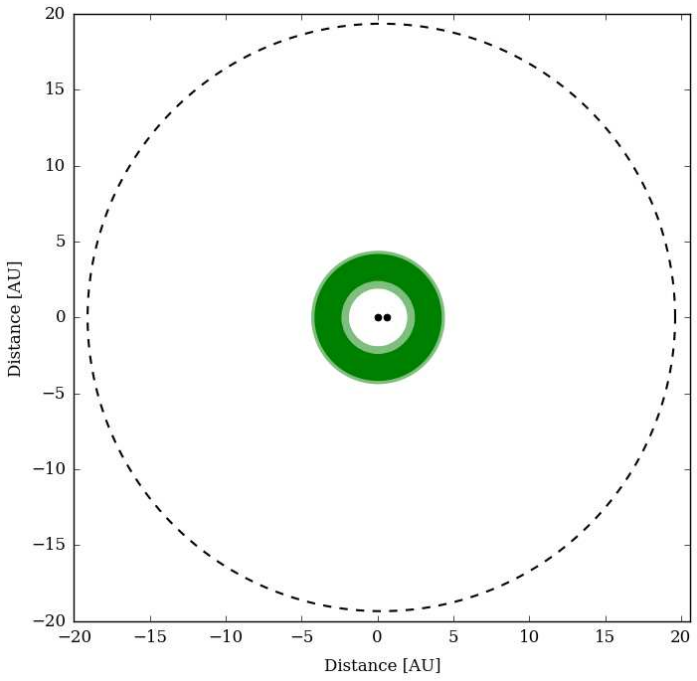

FIGURE 4.33: Stability and Habitable Zones for SB2 HD 47855

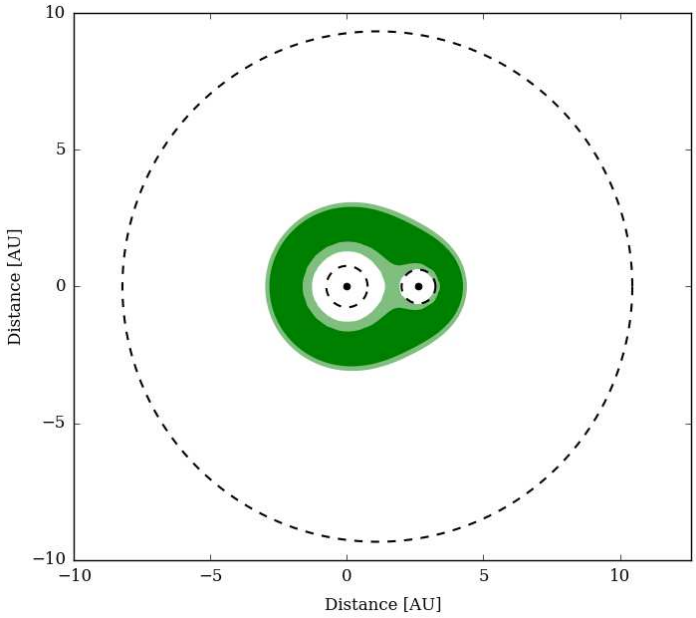

FIGURE 4.34: Stability and Habitable Zones for SB2 HD 85843

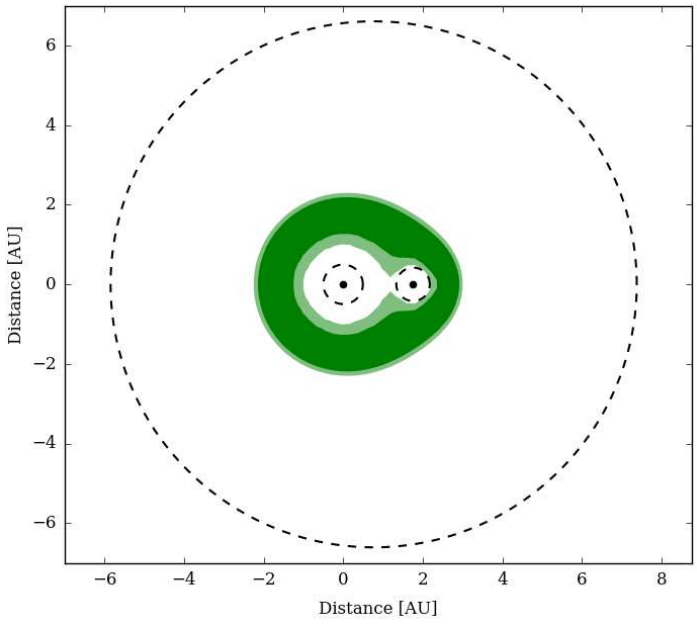

FIGURE 4.35: Stability and Habitable Zones for SB2 HD 112475

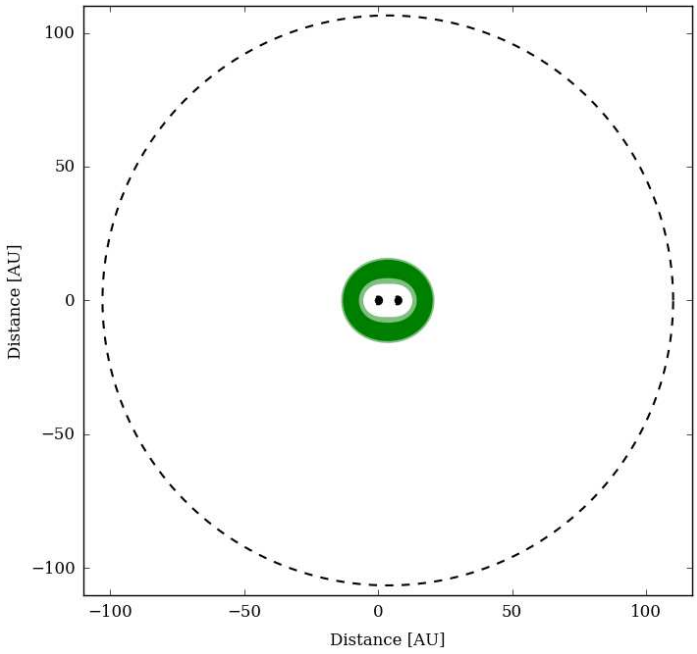

FIGURE 4.36: Stability and Habitable Zones for SB2 HD 129560

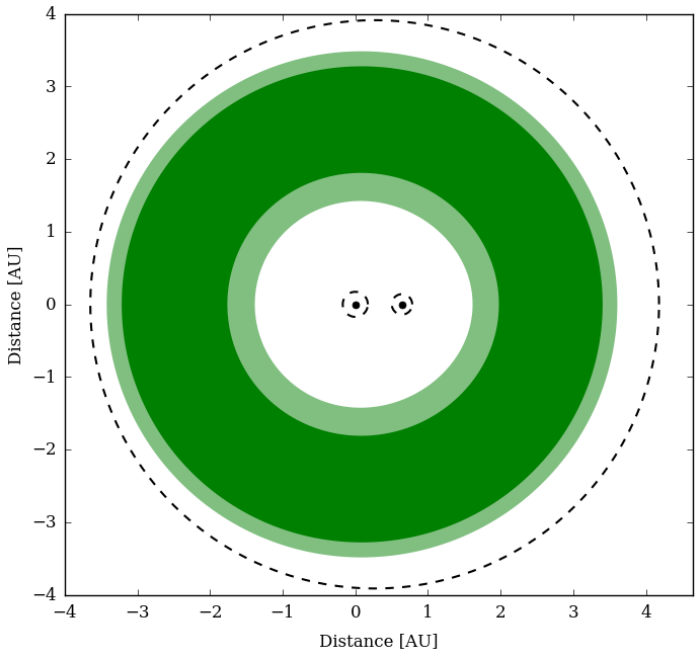

FIGURE 4.37: Stability and Habitable Zones for SB2 HD 170153

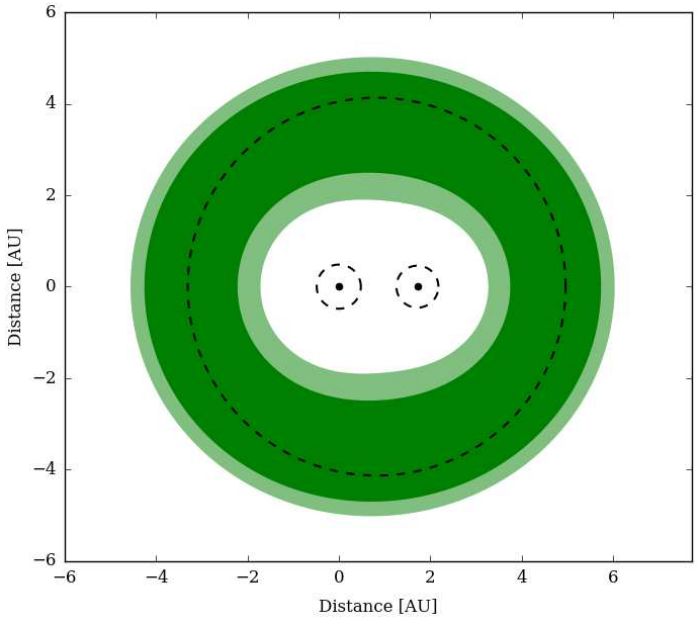

FIGURE 4.38: Stability and Habitable Zones for SB2 HD 171862

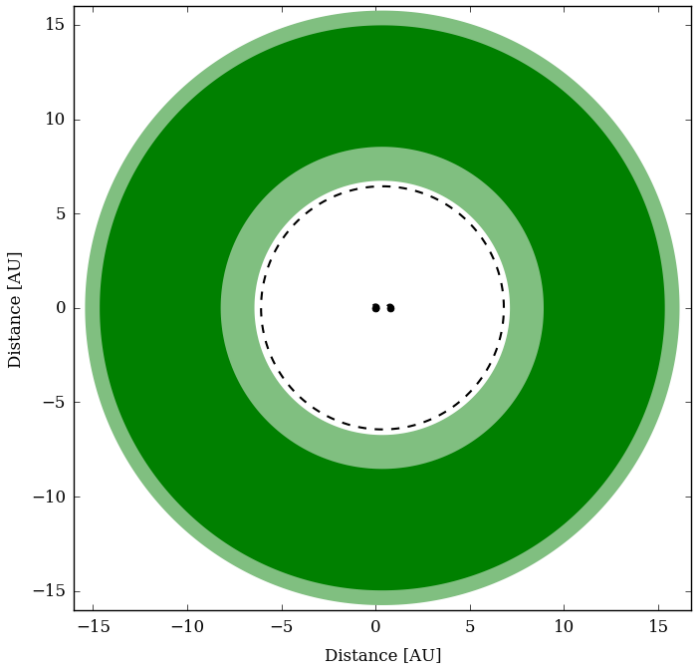

FIGURE 4.39: Stability and Habitable Zones for SB2 HD 185734

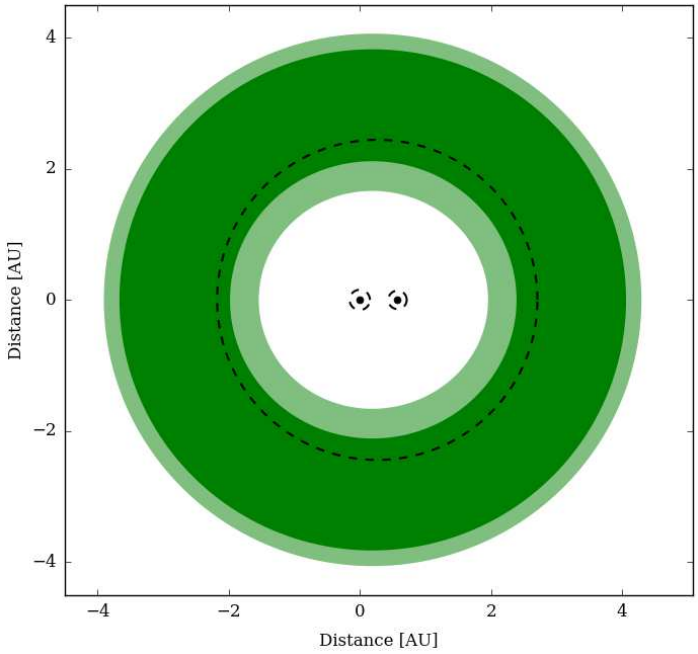

FIGURE 4.40: Stability and Habitable Zones for SB2 HD 194765

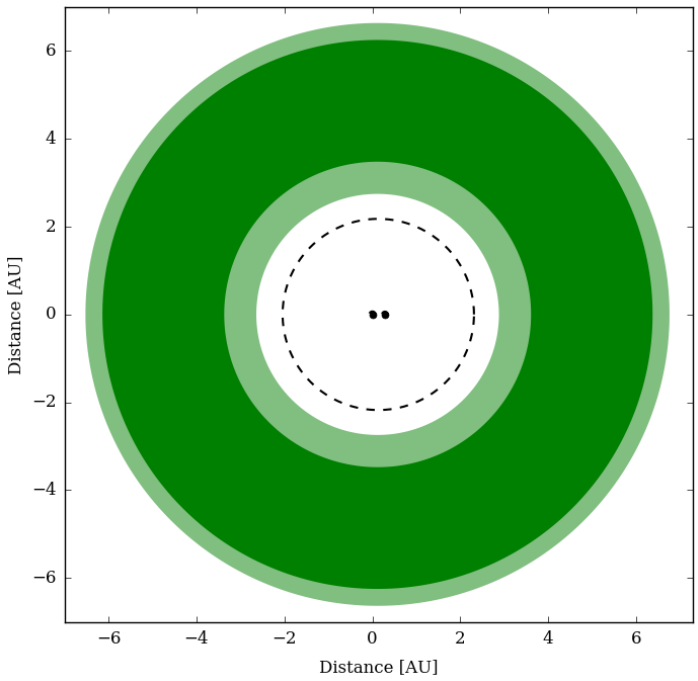

FIGURE 4.41: Stability and Habitable Zones for SB2 HD 197952

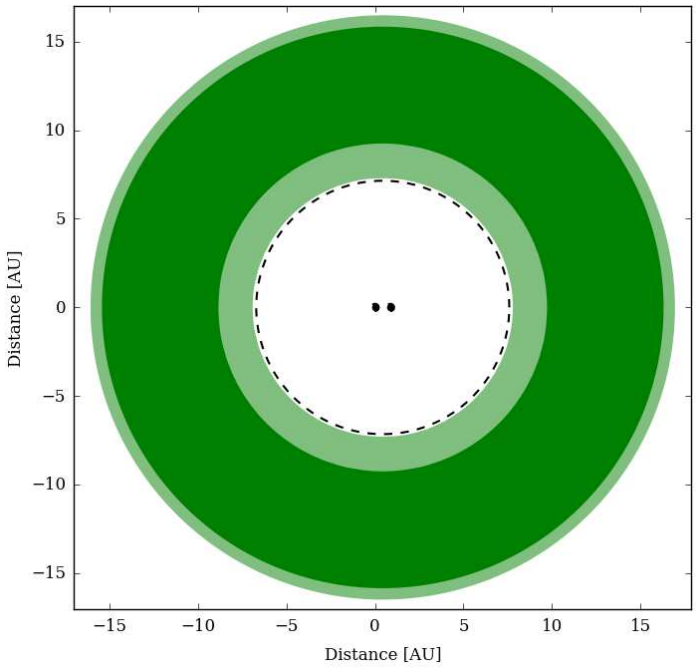

FIGURE 4.42: Stability and Habitable Zones for SB2 HD 198048

4.6 Cataloged Exoplanets in Binary Systems

one of the most important sources concerning exoplanets, The Exoplanet Orbit Database (EOD) website, provides amazing information: methods of detection, planets discovered by the Kepler Mission, stellar parameters, orbit parameters, and references. It is available at the internet website `http://exoplanets.org`. EOD contains data for 2950 confirmed planets of 5454 exoplanets until March, 2017 (Han et al., 2014). We depend on the data from EOD in order to search the exoplanets in binary systems and we found that there are just 92 exoplanets, 84 in visual binaries, 7 in eclipsing binaries, and one in a spectroscopic binary system (γ Cep).

Table 4.7 shows relevant information about exoplanets in binary stellar systems: Column 1 gives the number of the exoplanet in the table; Column 2, the name; Column 3, the right ascension of the binary, Column 4, the orbital period in days; Column 5, the periastron time; Column 6, the orbital eccentricity; Column 7, the semimajor axis in astronomical units (A.U); Column 7, the argument of periastron, ω; Column 9, the mass of the exoplanet in Jupiter mass multiplied by the sinus of its orbital inclination regarding the apparent plane ($\mathcal{M}_{Jupiter}$); Column 10, the orbital reference; Column 11, the type of the binary star (TBS) V (Visual), S (Spectroscopic), E (Eclipsing); and Column 12, the type of the exoplanet orbit (TPO), S or P.

Planet Stability in the Spectroscopic System, γ Cep

To date, only one planet has been discovered in a spectroscopic binary system (not eclipsing). It belongs to SB1 γ Cep, HD 222404, HIP 116727, and HR 8974. The mass of the main component is 1.40$\pm$ 0.12 $\mathcal{M}_{\odot}$ with a K1 III-IV spectral type and the second component has a mass, 0.409$\pm$0.018 $\mathcal{M}\odot$ with a spectral type of M4V (Neuhäuser et al., 2007).
In 2002, R. Griffin determined the orbit for this system using the 36 inch telescope at the Cambridge University. The orbital period is 24135 $\pm$ 349 days, eccentricity of 0.389 $\pm$ 0.017, and the mass function of 0.0166 $\pm$ 0.0025 solar mass (Griffin, Carquillat, and Ginestet, 2002). γ Cep b is an exoplanet that is orbiting around the primary component of γ Cep (S-type orbit) to a distance of 2.044 $\pm$ 0.057 AU and with Mp sin i = 1.60 $\pm$ 0.13 M_{Jup} (see Figure 4.43, γ Cep A and B picture using the Adaptive Optics camera on the Japanese 8 m Subaru telescope at Mauna Kea Observatory, Hawaii (Neuhäuser et al., 2007; Torres, 2007)).

γ Cep b is within the stability zone (See Figures 4.44 and 4.45) but it is a gaseous planet with a mass of 19 Jupiter masses (Torres, 2007). This planet is out of the habitable zone but is possible that other planets with a semimajor axis of more than 3.50 AU and moving around the main component could be habitable.

4.7 Exoplanet Program Missions

The main space scientific missions to research the exoplanets, are / were Thw well known scientific space missions, CoRoT, Kepler & K2, NN-Explore, and GAIA, were designed to investigate exoplanets.

	NAME	α (h:m:s)	Period(day)	T (J.D)	e	a (A.U)	ω(deg)	$\mathcal{M}$sin(i) ($\mathcal{M}$Jupiter)	Orb. Ref	TBS	TPO
1	HD 142 b	00:06:19	350.3	2451963	0.26	1.04292	303	1.3057	Butler 2006	V	S
2	HD 1237 b	00:16:11	133.71001	2451545.86	0.511	0.494668	290.7	3.3748	Naef 2001	V	S
3	GJ 15 A b	00:18:21	11.4433	-	0	0.0716678	90	0.0168	Howard 2014	V	S
4	HD 3651 b	00:39:22	62.218	2453932.6	0.596	0.29472	245.5	0.228975	Wittenmyer 2009	V	S
5	HD 4113 b	00:43:13	526.62	2453778	0.903	1.27266	317.7	1.64829	Tamuz 2008	V	S
6	HD 7449 b	01:14:29	1275	2455298	0.82	2.33982	339	1.3131	Dumusque 2011	V	S
7	upsilon And b	01:36:48	4.6171363	2454425.017	0.013	0.0593858	50.9829	0.669277	Wright 2009	V	S
8	upsilon And c	01:36:48	241.33335	2454265.567	0.223848	0.830445	250.76	1.91855	Wright 2009	V	S
9	upsilon And d	01:36:48	1278.1218	2453937.728	0.267395	2.52452	269.685	4.11582	Wright 2009	V	S
10	HD 11964 c	01:57:10	37.910254	2454366.648	0.301733	0.226601	101.941	0.0770689	Wright 2009	V	S
11	HD 11964 b	01:57:10	1944.5898	2454170.722	0.041	3.1288	154.961	0.608106	Wright 2009	V	S
12	HAT-P-32 b	02:04:10	2.150008	2454415.982	0	0.0342627	0	0.861357	Hartman 2011	V	p
13	GJ 86 b	02:10:24	15.76491	2451903.36	0.0416	0.114217	269	4.00104	Butler 2006	V	S
14	WASP-77 A b	02:28:37	1.3600309	2455870.45	0	0.0240531	90	1.75912	Maxted 2013	V	S
15	HD 16141 b	02:35:20	75.523	2450338	0.252	0.355656	42	0.249652	Butler 2006	V	S
16	30 Ari B b	02:36:58	335.1	2454538	0.289	0.99475	307	9.87792	Guenther 2009	V	S
17	HD 19994 b	03:12:46	466.2	2453757	0.266	1.30567	346	1.32681	Wittenmyer 2009	V	S
18	HD 20782 b	03:20:03	591.9	2451083.8	0.97	1.36607	147.7	1.9	O'Toole 2009	V	S
19	epsilon Ret b	04:16:29	428.1	2450836	0.06	1.19471	216	1.37669	Butler 2006	V	S
20	HD 28254 b	04:24:51	1116	2454049	0.81	2.14768	301	1.1614	Naef 2010	V	S
21	HD 38529 b	05:46:35	14.310195	2454384.815	0.243663	0.1272	95.3538	0.803263	Wright 2009	V	S
22	HD 38529 c	05:46:35	2146.0503	2452255.921	0.355094	3.6002	17.9023	12.2603	Wright 2009	V	S
23	HD 40979 b	06:04:30	264.15	2453919	0.252	0.846038	323.4	4.02224	Wittenmyer 2009	V	S
24	KELT-2 A b	06:10:40	4.1137912	2455974.603	0	0.0549707	90	1.52019	Beatty 2012	V	S
25	HD 46375 b	06:33:13	3.023573	2451071.53	0.063	0.0399038	114	0.227201	Butler 2006	V	S
26	XO-2 b	07:48:06	2.615857	2454147.749	0	0.0368369	90	0.566437	Burke 2007	V	S
27	XO-2S b	07:48:07	18.157	2456413.11	0.18	0.134393	331.9	0.259	Desidera 2014	V	S
28	XO-2S c	07:48:07	120.8	2456408.1	0.1528	0.47557	264.5	1.371	Desidera 2014	V	S
29	HD 65216 b	07:53:42	613.09998	2450762	0.41	1.37427	198	1.21636	Mayor 2004	V	S
30	HD 75289 b	08:47:40	3.509267	2450830.34	0.034	0.047858	141	0.46004	Butler 2006	V	S
31	55 Cnc b	08:52:36	14.651	2453035	0.004	0.113377	110	0.801471	Endl 2012	V	S
32	55 Cnc c	08:52:36	44.38	2453083	0.07	0.237305	356	0.164558	Endl 2012	V	S
33	55 Cnc d	08:52:36	4909	2453490	0.02	5.47467	254	3.54451	Endl 2012	V	S
34	55 Cnc e	08:52:36	0.736546	2455568.011	0	0.0154393	90	0.0261924	Endl 2012	V	S
35	55 Cnc f	8:52:36	261.2	2450080.911	0.32	0.773567	139	0.172877	Endl 2012	V	S
36	HD 79498 b	09:15:05	1966.1	2453210.9	0.59	3.13296	221	1.34632	Robertson 2012	V	S
37	HD 80606 b	09:22:38	111.4367	2454424.857	0.934	0.447343	300.6	3.89024	Moutou 2009	V	S
38	gamma Leo A b	10:19:58	428.5	2451236	0.144	1.29554	206.7	10.3722	Han 2010	V	S
39	HD 89744 b	10:22:11	256.78	2451505.5	0.673	0.902604	195.1	8.18778	Wittenmyer 2009	V	S
40	WASP-31 b	11:17:45	3.405909	2455189.283	0	0.0466223	90	0.477154	Anderson 2011	V	S
41	K2-22 b	11:17:56	0.381078	-	-	0.00867627	-	-	Sanchis-Ojeda 2015	E	S
42	HD 99492 b	11:26:47	17.0431	2450468.7	0.254	0.121908	219	0.106179	Butler 2006	V	S
43	HD 101930 b	11:43:30	70.459999	2453145	0.11	0.302019	251	0.299187	Lovis 2005	V	S
44	11 Com b	12:20:43	326.03	2452899.6	0.231	1.17872	94.8	16.1284	Liu 2008	V	S
45	HD 109749 b	12:37:16	5.24	2453013.55	0	0.0629198	0	0.27467	Fischer 2006	V	S
46	HD 114762 b	13:12:20	83.9151	2449889.106	0.3354	0.362932	201.28	11.6351	Kane 2011	V	S
47	HD 114729 b	13:12:44	1114	2450520	0.167	2.10235	93	0.944758	Butler 2006	V	S
48	tau Boo b	13:47:16	3.312433	2455652.108	0.023	0.0480039	90	4.13	Brogi 2012	V	S
49	HD 125612 b	14:20:54	559.40487	2454894.848	0.45899	1.3728	41.4902	3.06805	Lo Curto 2010	V	S
50	HD 125612 c	14:20:54	4.15474	2454420.173	0.27499	0.0522124	103.511	0.0580667	Lo Curto 2010	V	S
51	HD 126614 A b	14:26:48	1244	2453808	0.41	2.36847	243	0.385706	Howard 2010	V	S
52	alpha Cen B b	14:39:39	3.2357	2455280.17	0	0.0418506	0	0.00354639	Dumusque 2012	V	S
53	HD 132563 B b	14:58:22	1544	2452593	0.22	2.62431	158	1.49247	Desidera 2011	V	S
54	HD 137388 b	15:35:40	330	2455209	0.36	0.88883	86	0.227816	Dumusque 2011	V	S
55	HD 142022 b	16:10:17	1928	2450941	0.53	2.93163	170	4.46762	Eggenberger 2006	V	S
56	HD 147513 b	16:24:01	528.40002	2451123	0.26	1.30958	282	1.17965	Mayor 2004	V	S
57	HD 156846 b	17:20:34	359.51001	2453998.09	0.8472	1.11751	52.23	11.0076	Tamuz 2008	V	S
58	GJ 676 A b	17:30:11	1056.8	2455411.9	0.326	1.81539	85.7	4.89701	Forveille 2011	V	S
59	HAT-P-57 b	18:18:58	2.465295	-	0	0.0406092	90	-	Hartman 2015	V	S
60	HD 177830 b	19:05:21	410.1	2450254	0.096	1.13872	189	1.31967	Butler 2006	V	S
61	KOI-13 b	19:07:53	1.76358799	2455138.744	0	0.0342279	-	-	Shporer 2011	V	S
62	HD 178911 B b	19:09:03	71.484	2453808.1	0.114	0.344904	168.2	7.29127	Wittenmyer 2009	V	P
63	Kepler-16 b	19:16:18	228.776	2455346.5	0.0069	0.646795	318	-	Doyle 2011	E	P
64	Kepler-444 b	19:19:00	3.6001053	2454966.26	0.16	0.0419153		-	Campante 2015	V	S
65	Kepler-444 c	19:19:00	4.5458841	2454964.522	0.31	0.0489676	-	-	Campante 2015	V	S
66	Kepler-444 d	19:19:00	6.189392	2454967.787	0.18	0.0601536	-	-	Campante 2015	V	S
67	Kepler-444 e	19:19:00	7.743493	2454968.093	0.1	0.0698427	-	-	Campante 2015	V	S
68	Kepler-444 f	19:19:00	9.740486	2454967.879	0.29	0.0813861	-	-	Campante 2015	V	S
69	Kepler-420 b	19:24:54	86.647661	2458000	0.772	0.381935	141.3	-	Santerne 2014	V	S
70	HD 185269 b	19:37:12	6.8378503	2453154.089	0.295952	0.0765701	171.817	0.954212	Johnson 2006	V	S
71	Kepler-35 b	19:37:59	131.458	2454920.3	0.042	0.48628	11.6336	-	Welsh 2012	E	P
72	Kepler-47 b	19:41:11	49.514	-	0	0.267621	-	-	Orosz 2012	E	S
73	Kepler-47 c	19:41:11	303.158	-	0	0.895669	-	-	Orosz 2012	E	P
74	16 Cyg B b	19:41:52	798.5	2446549.1	0.681	1.66027	85.8	1.63997	Butler 2006	V	S
75	Kepler-34 b	19:45:45	288.822	2454890.1	0.182	0.86856	7.90716	-	Welsh 2012	E	P
76	HD 188015 b	19:52:05	461.2	2451787	0.137	1.19018	222	1.46957	Butler 2006	V	S
77	PH-1 b	19:52:52	138.506	2454970	0.0539	0.629412	348	-	Schwamb 2013	E	p
78	HD 189733 b	20:00:44	2.21857567	2454279.437	0	0.0309953	90	1.14039	Bouchy 2005	V	S
79	HD 190360 b	20:03:37	2915.0369	2453541.662	0.313105	3.97285	12.9274	1.53512	Wright 2009	V	S
80	HD 190360 c	20:03:37	17.111027	2454389.63	0.23747	0.129216	5.18038	0.0589738	Wright 2009	V	S
81	HD 195019 b	20:28:18	18.20132	2451015.5	0.0138	0.136688	231	3.57989	Butler 2006	V	S
82	HD 196050 b	20:37:52	1378	2450843	0.228	2.51056	187	2.8434	Butler 2006	V	S
83	HD 196885 b	20:39:52	1333	2452554	0.48	2.54171	78	2.9439	Fischer 2009	V	S
84	WASP-94 A b	20:55:08	3.9501907	2456416.401	0	0.0532427	90	0.418542	Neveu-VanMalle 2014	V	S
85	WASP-94 B b	20:55:08	2.00839	2456574.359	0	0.0334746	-	0.619839	Neveu-VanMalle 2014	V	S
86	HD 204941 b	21:32:24	1733	2456015	0.37	2.55427	228	0.26689	Dumusque 2011	V	S
87	HD 212301 b	22:27:31	2.245715	2453549.195	0	0.034116	0	0.39615	Lo Curto 2006	V	S
88	HD 213240 b	22:31:00	882.7	2451499	0.421	1.88529	201	4.53249	Butler 2006	V	S
89	HAT-P-1 b	22:57:47	4.4652934	2454363.947	0	0.0553326	90	0.531143	Bakos 2007	V	S
90	gamma Cep b	23:39:21	905.574	2453121.925	0.12	1.9793	49.6	1.51728	Hatzes 2003	S	S
91	HD 222582 b	23:41:52	572.38	2450706.7	0.725	1.33658	319.01	7.63003	Butler 2006	V	S
92	WASP-8 b	23:59:36	8.158715	2454675.429	0.31	0.080153	274.27	2.13728	Queloz 2010	V	S

TABLE 4.7: Information regarding planetary orbits in binaries

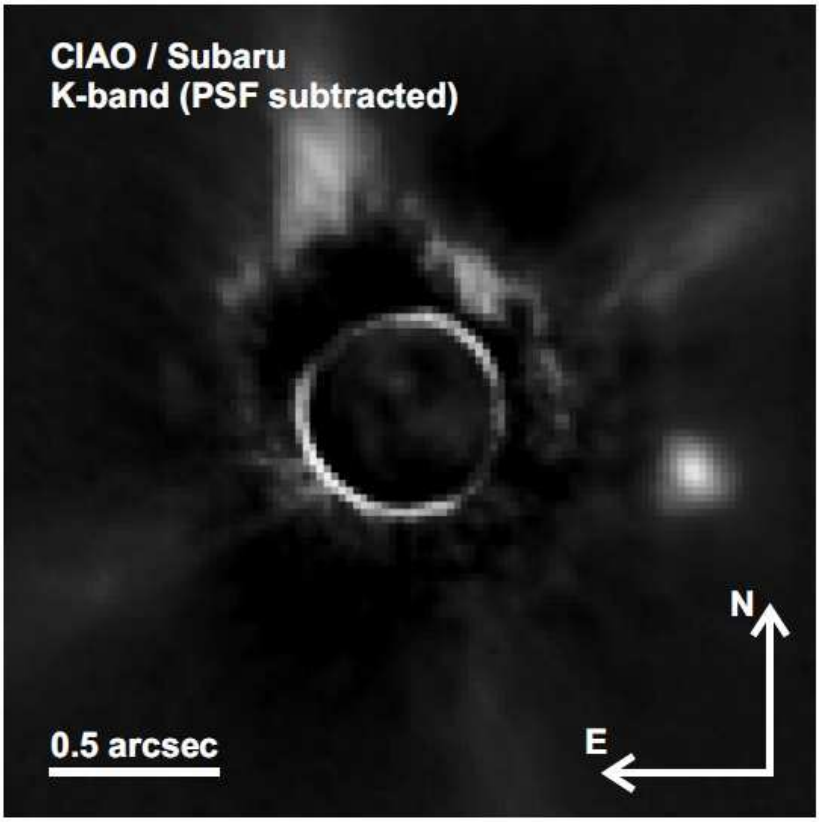

FIGURE 4.43: γ Cep A and B (Neuhäuser et al., 2007).

4.7.1 CoRoT mission

CoRoT (**CO**nvection, **RO**tation and planetary **T**ransit) launched in October 2006, was the first space mission to search for extrasolar planets based on the transit technique. More than 163.000 stars, were observed by the CoRoT mission using high quality photometry (Maceroni et al., 2010; Moutou and Deleuil, 2015).

In the next year, the first planet was detected. It was a hot gas giant with 1.03 Jupiter mass and a period of 1.5 days around a yellow dwarf star. It received the denomination of COROT-Exo-1b.

The CoRoT mission was led by the French agency, CNES, in collaboration with the ESA. Spain, Brazil, Belgium, Germany, and Austria aslo participated in the mission. The CoRoT, equipments included a 27 cm telescope and two CCD cameras. It is able to observe stars with 14-15th magnitude and detect small, warm, and hot giant or super terrestrial planets, several times larger than the Earth with long periods (Baglin et al., 2007; Garrido and Deeg, 2006). CoRoT detected the change in the brightness of the stars due to star-quakes inside the stars which is helpful to determine the mass, chemical composition, and the age of the stars. This successful mission (see Figure 4.46) ended in June 2013 after to discovering 28 exoplanets.

It has ground stations located in Kiruna (Sweden), Aussaguel (France), Hartebeesthoek

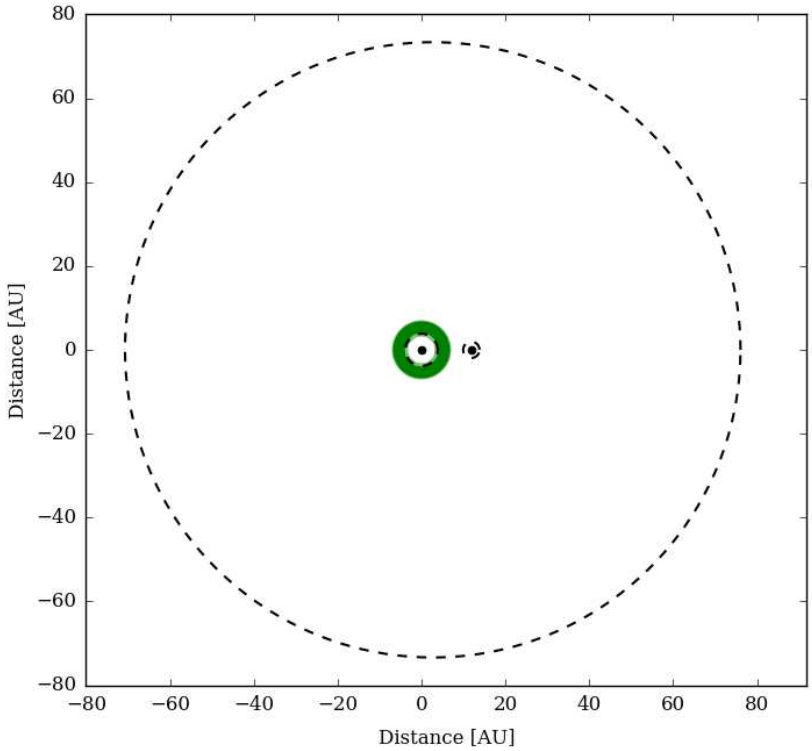

FIGURE 4.44: Stability and Habitable Zones for γ Cep spectroscopic system

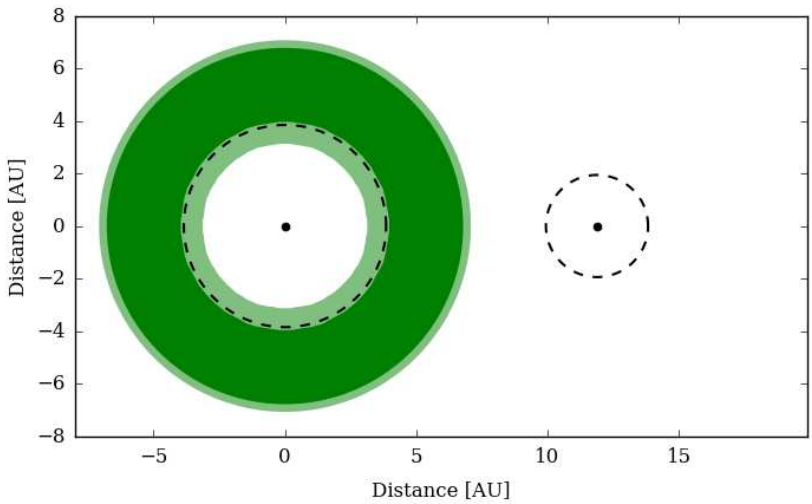

FIGURE 4.45: Stability and Habitable Zones for γ Cep spectroscopic system inner view

(South Africa), Kourou (French Guyana), Alcantara (Brazil) and Vienna (Austria). More information is valuable at the website,
http://www.esa.int/Our_Activities/Space_Science/COROT_overview.

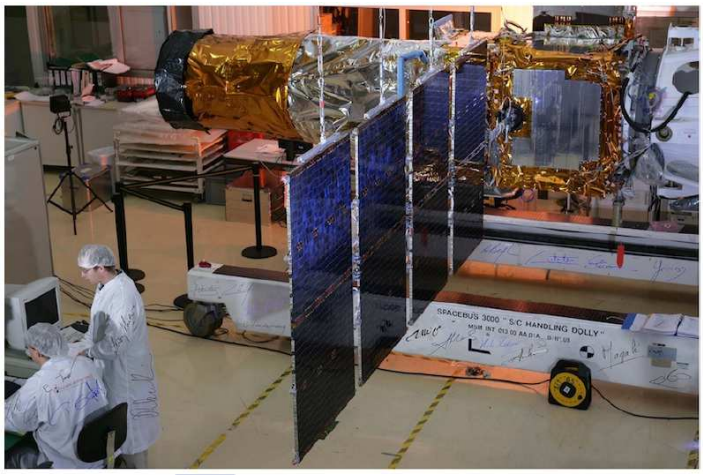

FIGURE 4.46: The CoRoT satellite, in 2005 (Moutou and Deleuil, 2015).

4.7.2 Kepler & K2 missions

In 2001, NASA created Kepler (see Figure 4.47) as a mission to discover Earth-like planets. Kepler has a photometer, attached to a 0.95 m Schmidth telescope, prepared to apply also the transit method. This method has the advantage of being able to detect small mass exoplanets. It is difficult to observe them by other methods such as, radial velocity, astrometry, and ground-based interferometry. The Kepler mission was able to determine the frequency of Mars-sized planets and planets in multiple systems as well as to determine their mass and the density.

Kepler had the ability to detect the transit of an exoplanets in G2 dwarf of the 12th magnitude. This mission began on March 7, 2009 and observed about 156,000 stars in the first 6 weeks (Basri, Borucki, and Koch, 2005; Borucki et al., 2010; Koch et al., 2010) and confirmed 2330 planets in February 1, 2017.
K2 is the mission that will extend the work plane for Kepler for a maximum of 2-3 years until 2018, and it will monitor the southern and northern hemisphere of the celestial sphere 10 times more than the original mission, as well as provide photometric data and observation data of approximately 40,000 targets on the ecliptic plane. The Director of this memory, Prof. J. A. Docobo suggested this idea to observe on the ecliptic plane in the European project entitled "We Should Look For Them In The Area Where They Can Probably Find Us". For more details about the missions, the discoveries, the awards, and about team, see the website: https://keplerscience.arc.nasa.gov/objectives.html.

4.7.3 Large Binocular Telescope Interferometer (LBTI)

The LBTI is an optical telescope, that consists of two 8 m telescopes, and is located in Arizona (USA), (see Figure 4.48) from the website
http://nexsci.caltech.edu/missions/LBTI/. Beginning in 2004, was built in different stages, and it was fully operated in 2008. LBTI funded by NASA, was developed

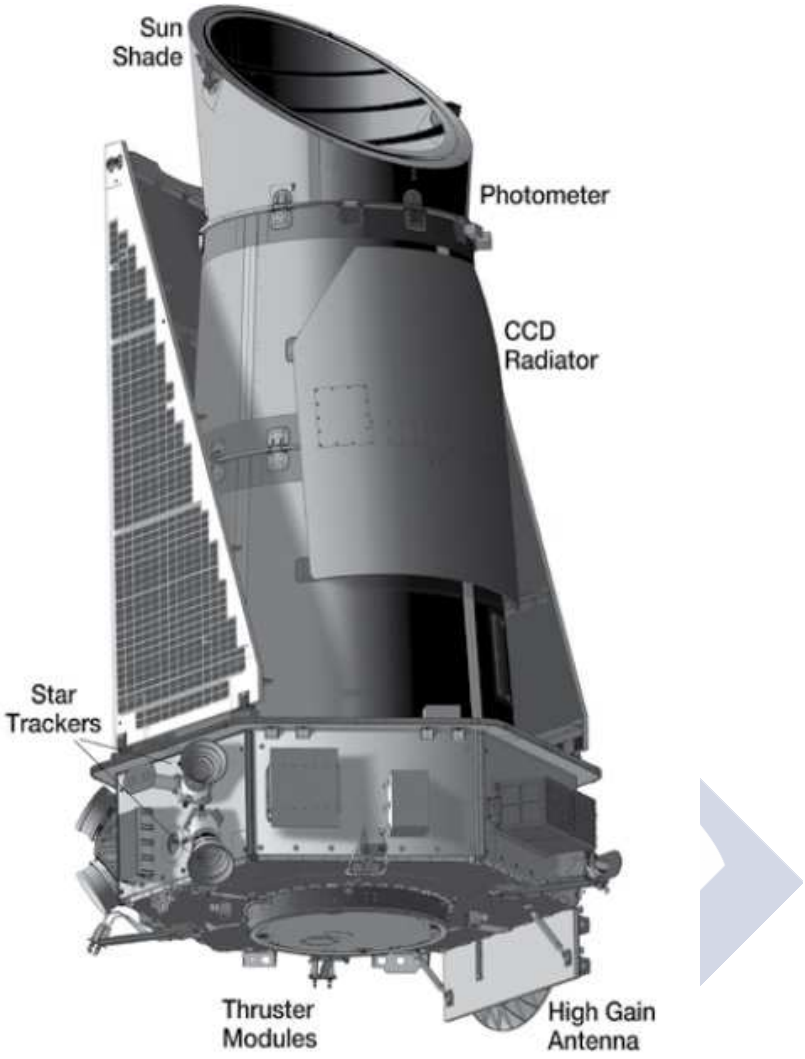

FIGURE 4.47: the Kepler Space Telescope photometer instrument (NASA).

to explore and discover exoplanetary systems. It also supports the detection of the habitable zone around the exoplanets directly, by detecting the thermal emission (Kennedy et al., 2015).

4.7.4 NASA-NSF Exoplanet Observational Research (NN-Explore)

NN-Explore is a partnership between the National Aeronautics and Space Administration (NASA) and the National Science Foundation (NSF). It will begin the operations in September 2018 when an extremely precise Doppler spectrometer (EPDS) will be installed on the 3.5 m telescope at the WIYN Observatory, the second largest telescope at Kitt Peak National Observatory in Arizona. This mission will help to detect and determine the characterization

FIGURE 4.48: Large Binocular Telescope Interferometer (LBTI)

of the exoplanets providing radial velocities for nearby stars,
https://exoplanets.nasa.gov/exep/NNExplore/.

NASA supports and manages all of these missions and will establish three more missions between 2018-2020, the Wide Field Infrared Survey Telescope (WFIRST), the Transiting Exoplanet Survey Satellite (TESS) , and the James Webb Space Telescope (JWST) which will without a doubt provide high-value data which will help the researcher to discover like-Earth exoplanets and to try to find the Earth-twin, if it exists.

4.8 Exoplanets and GAIA

Gaia (**G**lobal **A**strometric non-**I**nterferometric for **A**strophysics), is a mission of the European Space Agency. It was launched in December 2013, the main purpose for this mission was to describe 3D space catalogue, using spectroscopic, astrometric, and photometric observations for more than one billion astronomical objects, especially for stars that brighter than V=16 mag.

Gaia consist of, one billion pixels camera, and three instruments: the astrometric field, the spectro-photometry, and the radial velocity spectrometer. This mission search for the exoplanets, which is one of Gaia scientific goals, by looking for giant planets, and habitable terrestrial exoplanets.
It is expected by using photometric measurements (detecting the dip) that few thousand of hot Jupiter and massive planets will discover using transiting method, (Gaia Collaboration et al., 2016). Gaia can detect the exoplanet by finding the wobble using astrometric observations, which helpful to determine the mass of the planets, better than the radial velocity method which present the lower limit.

Due to the extreme precision of its astrometric measurements, GAIA can detect giant planets orbiting around other stars by measuring the displacement with respect to the center of mass that they induce in the star. The expected outcome is to find every giant planet with an orbital period between 1.5 and 9 years within a 150 light-year radius. According to the estimations it would mean between 10000 and 50000 detections.For more information see the websites https://gaia.esac.esa.int/, http://sci.esa.int/gaia/.

FIGURE 4.49: Gaia space mission

List of Figures

List of Tables

USC
UNIVERSIDADE
DE SANTIAGO
DE COMPOSTELA

Bibliography

Abt, H. A. (Dec. 1973). "Catalog of Individual Radial Velocities, 12ˆ{h}-24ˆ{h}, Measured by Astronomers of the Mount Wilson Observatory". In: ApJS 26, p. 365.

— (Aug. 1988). "Maximum separations among cataloged binaries". In: ApJ 331, pp. 922–931.

Abt, H. A. and S. G. Levy (Mar. 1976). "Multiplicity among solar-type stars". In: ApJS 30, pp. 273–306.

Adams, W. S. and A. H. Joy (Apr. 1923). "The radial velocities of 1013 stars." In: ApJ 57.

Adams, W. S., A. H. Joy, G. Stromberg, and C. G. Burwell (Jan. 1921). "The parallaxes of 1646 stars derived by the spectroscopic method." In: ApJ 53.

Adams, W. S., A. H. Joy, R. F. Sanford, and G. Stromberg (Nov. 1929). "The radial velocities of 741 stars." In: ApJ 70.

Adams, W. S., A. H. Joy, M. L. Humason, and A. M. Brayton (Apr. 1935). "The Spectroscopic Absolute Magnitudes and Parallaxes of 4179 Stars". In: ApJ 81, p. 187.

Aitken, R. G. (1935). *The binary stars*.

Albrecht, Simon, Joshua N Winn, John A Johnson, Andrew W Howard, Geoffrey W Marcy, R Paul Butler, Pamela Arriagada, Jeffrey D Crane, Stephen A Shectman, Ian B Thompson, et al. (2012). "OBLIQUITIES OF HOT JUPITER HOST STARS: EVIDENCE FOR TIDAL INTERACTIONS AND PRIMORDIAL MISALIGNMENTSThe data presented herein were collected with the Magellan (Clay) Telescope located at Las Campanas Observatory, Chile, and the Keck I telescope at the WM Keck Observatory, which is operated as a scientific partnership among the California Institute of Technology, the University of California, and the National Aeronautics and Space Administration." In: *The Astrophysical Journal* 757.1, p. 18.

Aller, L. H., I. Appenzeller, B. Baschek, H. W. Duerbeck, T. Herczeg, E. Lamla, E. Meyer-Hofmeister, T. Schmidt-Kaler, M. Scholz, W. Seggewiss, W. C. Seitter, and V. Weidemann, eds. (1982). *Landolt-Börnstein: Numerical Data and Functional Relationships in Science and Technology - New Series " Gruppe/Group 6 Astronomy and Astrophysics " Volume 2 Schaifers/Voigt: Astronomy and Astrophysics / Astronomie und Astrophysik " Stars and Star Clusters / Sterne und Sternhaufen*, p. 54.

Aller, R. M. (Mar. 1930). "Doppelsternbeobachtungen". In: *Astronomische Nachrichten* 238, p. 71.

— (1932). "Doppelsternbeobachtungen". In: *Astronomische Nachrichten* 245.13, pp. 213–224.

— (Mar. 1934). "Doppelsternbeobachtungen". In: *Astronomische Nachrichten* 251, p. 273.

— (Sept. 1935). "Orbita de la estrella doble OΣ 77". In: *Astronomische Nachrichten* 256, p. 245.

— (July 1936). "Doppelsternbeobachtungen". In: *Astronomische Nachrichten* 259, p. 133.

— (Feb. 1939). "Orbita de la estrella doble Σ 1932 (ADS 9578 β 7214)". In: *Astronomische Nachrichten* 268, p. 23.

Aller, R. M. (1941). "Observacions De estrellas Dobles". In: *Las Ciencias, Ano VI* 2, p. 259.
— (1947). "Medidas De Estrellas Dobles ". In: *Las Ciencias, Ano VI* 24, p. 603.
Anderson, K. S. and R. P. Kraft (Mar. 1972). "A Search for Small-Amplitude Spectroscopic Binaries among Main-Sequence F-Type Stars." In: ApJ 172, p. 631.
Armstrong, David John (2015). "On the abundance of circumbinary exoplanets". PhD thesis. University of Warwick.
Baglin, A, M Auvergne, P Barge, E Michel, C Catala, M Deleuil, W Weiss, Cristiana Dumitrache, Nedelia A Popescu, Marian Doru Suran, et al. (2007). "The CoRoT mission and its scientific objectives". In: *AIP Conference Proceedings*. Vol. 895. 1. AIP, pp. 201–209.
Bagnuolo Jr., W. G., S. F. Taylor, H. A. McAlister, T. ten Brummelaar, D. R. Gies, S. T. Ridgway, J. Sturmann, L. Sturmann, N. H. Turner, D. H. Berger, and D. Gudehus (May 2006). "First Results from the CHARA Array. V. Binary Star Astrometry: The Case of 12 Persei". In: AJ 131, pp. 2695–2699.
Balega, Y. Y. and V. P. Ryadchenko (Feb. 1984). "Digital Speckle Interferometry of Binary Stars". In: *Soviet Astronomy Letters* 10, pp. 95–98.
Balega, Y. Y. and N. A. Tikhonov (June 1977). "Speckle interferometry of some bright stars with the 6 meter telescope." In: *Soviet Astronomy Letters* 3, pp. 272–273.
Balega, Y. Y., A. A. Tokovinin, E. A. Pluzhnik, and G. Weigelt (Nov. 2002). "The Spectroscopic and Interferometric Orbit of Gliese 150.2". In: *Astronomy Letters* 28, pp. 773–777.
Baranne, A., M. Mayor, and J. L. Poncet (1979). "CORAVEL - A new tool for radial velocity measurements". In: *Vistas in Astronomy* 23, pp. 279–316.
Barnes, R., S. N. Raymond, B. Jackson, and R. Greenberg (Oct. 2007). "Tides and the Evolution of Planetary Habitability". In: *AAS/Division for Planetary Sciences Meeting Abstracts #39*. Vol. 39. Bulletin of the American Astronomical Society, p. 468.
Barnes, Rory, Sean N Raymond, Brian Jackson, and Richard Greenberg (2008). "Tides and the evolution of planetary habitability". In: *Astrobiology* 8.3, pp. 557–568.
Basri, Gibor, William J Borucki, and David Koch (2005). "The Kepler Mission: A wide-field transit search for terrestrial planets". In: *New Astronomy Reviews* 49.7, pp. 478–485.
Batten, A. H. (1973). *Binary and multiple systems of stars*.
— (June 1989). "Two Centuries of Study of Algol Systems". In: Space Sci. Rev. 50, pp. 1–8.
Batten, A. H., J. M. Fletcher, and P. J. Mann (1978). "Seventh catalogue of the orbital elements of spectroscopic binary systems." In: *Publications of the Dominion Astrophysical Observatory Victoria* 15, pp. 121–295.
Beaulieu, JP, E Kerins, S Mao, D Bennett, A Cassan, S Dieters, BS Gaudi, A Gould, V Batista, R Bender, et al. (2008). "Towards A Census of Earth-mass Exo-planets with Gravitational Microlensing". In: *arXiv preprint arXiv:0808.0005*.
Belikov, A. N. (July 1995). "Stellar Mass Catalogue (SMAC). Preliminary version". In: *Bulletin d'Information du Centre de Donnees Stellaires* 47, p. 9.
Bell, Stephanie (2001). "Measurement Good Practice Guide No. 11 (Issue 2)". In: *A Beginner's Guide to Uncertainty of Measurement. National Physical Laboratory Teddington, Middlesex, United Kingdom*.
Bessell, Michael S (2005). "Standard photometric systems". In: *Annu. Rev. Astron. Astrophys.* 43, pp. 293–336.
Binnendijk, L. (1960). *Properties of double stars; a survey of parallaxes and orbits.*

Blaauw, A (1963). "Basic astronomical data". In: *ed. K. Aa. Strand, University of Chicago*, p. 383.

Bonneau, D., O. Chesneau, D. Mourard, and P. Stee (Dec. 2010). "Spectro-Interferometric Observations of Interacting Massive Stars with VEGA/CHARA". In: *Binaries - Key to Comprehension of the Universe*. Ed. by A. Prša and M. Zejda. Vol. 435. Astronomical Society of the Pacific Conference Series, p. 241.

Borucki, William J, David Koch, Gibor Basri, Natalie Batalha, Timothy Brown, Douglas Caldwell, John Caldwell, Jørgen Christensen-Dalsgaard, William D Cochran, Edna DeVore, et al. (2010). "Kepler planet-detection mission: introduction and first results". In: *Science* 327.5968, pp. 977–980.

Bromley, Benjamin C and Scott J Kenyon (2015). "Planet formation around binary stars: Tatooine made easy". In: *The Astrophysical Journal* 806.1, p. 98.

Campbell, W. W. (1928). "Catalogue of observed velocities." In: *Publications of Lick Observatory* 16, pp. 1–346.

Cannon, A. J. and E. C. Pickering (1918). "The Henry Draper catalogue 0h, 1h, 2h, and 3h". In: *Annals of Harvard College Observatory* 91, pp. 1–290.

— (1922). "The Henry Draper catalogue : 17h and 18h". In: *Annals of Harvard College Observatory* 97.

— (1923). "The Henry Draper catalogue : 19h and 20h". In: *Annals of Harvard College Observatory* 98.

Carado, Bertrand (2016). "Characterizing Kepler Objects of Interest Using the Algorithm EXONEST". PhD thesis. State University Of New York.

Carney, B. W. (Oct. 1979). "Subdwarf ultraviolet excesses and metal abundances". In: ApJ 233, pp. 211–225.

— (Jan. 1980). "Southern metal-poor stars - UBVRI photometry". In: AJ 85, pp. 38–43.

— (May 1983). "A Photometric Search for Halo Binaries - Part Two - Results". In: AJ 88, p. 623.

Chauvin, Gael, A-M Lagrange, C Dumas, B Zuckerman, D Mouillet, I Song, J-L Beuzit, and P Lowrance (2004). "A giant planet candidate near a young brown dwarf-Direct VLT/NACO observations using IR wavefront sensing". In: *Astronomy & Astrophysics* 425.2, pp. L29–L32.

Cid Palacios, R. (Oct. 1958). "On the necessary and sufficient observations for determination of elliptic orbits in double stars". In: AJ 63, p. 395.

— (1960). "Método de cálculo de órbitas elípticas en estrellas dobles visuales y aplicación al par ADS13169." In: *Pub.Real Academic de Ciencias de Zaragoza serie 3º* XV.1.

Cochran, W. D., A. P. Hatzes, and T. J. Hancock (Oct. 1991). "Constraints on the companion object to HD 114762". In: ApJ 380, pp. L35–L38.

Cockell, C. S., T. Bush, C. Bryce, S. Direito, M. Fox-Powell, J. P. Harrison, H. Lammer, H. Landenmark, J. Martin-Torres, N. Nicholson, L. Noack, J. O'Malley-James, S. J. Payler, A. Rushby, T. Samuels, P. Schwendner, J. Wadsworth, and M. P. Zorzano (Jan. 2016). "Habitability: A Review". In: *Astrobiology* 16, pp. 89–117.

Cousins, A. W. J. (1963). "Photometric Data for Stars in the Equatorial Zone (Third List)". In: *Monthly Notes of the Astronomical Society of South Africa* 22, p. 12.

Couteau, P. (1978). *L'observation des etoiles doubles visuelles, suivie d'un catalogue de 744 etoiles doubles pour tous instruments*.

de Jager, C. and H. Nieuwenhuijzen (May 1987). "A new determination of the statistical relations between stellar spectral and luminosity classes and stellar effective temperature and luminosity". In: A&A 177, pp. 217–227.

de Medeiros, J. R. and M. Mayor (Nov. 1999). "A catalog of rotational and radial velocities for evolved stars". In: A&AS 139, pp. 433–460.

Docobo, J. A. (June 1985). "On the analytic calculation of visual double star orbits". In: *Celestial Mechanics* 36, pp. 143–153.

— (May 2012). "The use of Docobo's analytic method for calculating visual double star orbits". In: *Orbital Couples: Pas de Deux in the Solar System and the Milky Way*. Ed. by F. Arenou and D. Hestroffer, pp. 119–123.

Docobo, J. A. and M. Andrade (Nov. 2006). "A Methodology for the Description of Multiple Stellar Systems with Spectroscopic Subcomponents". In: ApJ 652, pp. 681–695.

Docobo, J. A. and V. S. Tamazian (Feb. 2012). "New orbit for WDS23191-1328". In: *Information Circular. IAU Commission 26* 176, pp. 2–2.

Docobo, J. A., J. F. Ling, C. Prieto, J. M. Costa, M. T. Costado, and P. Magdalena (Dec. 2001). "Catalog of Orbits and Ephemerides of Visual Double Stars". In: Acta Astron. 51, pp. 353–356.

Docobo, J. A., P. P. Campo, M. Andrade, and E. P. Horch (Oct. 2014a). "An analytic algorithm to calculate the inclination, ascending node, and semimajor axis of spectroscopic binary orbits using a single speckle measurement and the parallax". In: *Astrophysical Bulletin* 69, pp. 461–471.

Docobo, J. A., R. F. Griffin, V. S. Tamazian, E. P. Horch, and P. P. Campo (Nov. 2014b). "The three-dimensional orbit and physical properties of the binary COU 2031 (WDS 04464+4221, HIP 22196, HD 30090)". In: MNRAS 444, pp. 3641–3646.

Docobo, J. A., R. F. Griffin, P. P. Campo, and A. A. Abushattal (Apr. 2017). "Precise orbital elements, masses and parallax of the spectroscopic-interferometric binary HD 26441". In: *ArXiv e-prints (accepted in MNRAS)*. arXiv: 1704.03245 [astro-ph.SR].

Docobo, JA et al. (2007). "On the possible existence of a very low-mass object in the triple stellar system Gliese 22 (HIP 2552)". In: *IAU Commun* 26.162, pp. 3–4.

Docobo, JA, VS Tamazian, YY Balega, M Andrade, D Schertl, G Weigelt, P Campo, and M Palacios (2008). "A methodology for studying physical and dynamical properties of multiple stars. Application to the system of red dwarfs Gl 22". In: *Astronomy & Astrophysics* 478.1, pp. 187–191.

Dommanget, J. (Jan. 1981). "The nature of the orbit of a visual binary calculated from three fundamental positions and the area constant". In: A&A 94, pp. 45–51.

Doyle, Laurance R (2008). "Overview of extrasolar planet detection methods". In: *Extrasolar Planets*, p. 1.

Doyle, Laurance R, Joshua A Carter, Daniel C Fabrycky, Robert W Slawson, Steve B Howell, Joshua N Winn, Jerome A Orosz, Andrej Prsa, William F Welsh, Samuel N Quinn, et al. (2011). "Kepler-16: a transiting circumbinary planet". In: *Science* 333.6049, pp. 1602–1606.

Duquennoy, A. and M. Mayor (Aug. 1991). "Multiplicity among solar-type stars in the solar neighbourhood. II - Distribution of the orbital elements in an unbiased sample". In: A&A 248, pp. 485–524.

Duquennoy, Antoine and Michel Mayor (1991). "Multiplicity among solar-type stars in the solar neighbourhood. II-Distribution of the orbital elements in an unbiased sample". In: *Astronomy and Astrophysics* 248, pp. 485–524.

Dvorak, R. (Dec. 1984). "Numerical experiments on planetary orbits in double stars". In: *Celestial Mechanics* 34, pp. 369–378.

Edwards, T. W. (Apr. 1976). "MK classification for visual binary components". In: AJ 81, pp. 245–249.

Eggen, O. J. (1969). "Three-colours photometry of 4000 northern stars." In: *Royal Greenwich Observatory Bulletins* 137, p. 165.

Eggl, Siegfried, Elke Pilat-Lohinger, Nikolaos Georgakarakos, Markus Gyergyovits, and Barbara Funk (2012). "An analytic method to determine habitable zones for S-type planetary orbits in binary star systems". In: *The Astrophysical Journal* 752.1, p. 74.

Einstein, A. (Dec. 1936). "Lens-Like Action of a Star by the Deviation of Light in the Gravitational Field". In: *Science* 84, pp. 506–507.

Elipe, A. and V. Lanchares (Dec. 1988). "The use of spline functions for solving spectroscopic binary orbits". In: *Astrophysical Letters and Communications* 27, pp. 265–274.

Famaey, B., A. Jorissen, X. Luri, M. Mayor, S. Udry, H. Dejonghe, and C. Turon (Jan. 2005). "Local kinematics of K and M giants from CORAVEL/Hipparcos/Tycho-2 data. Revisiting the concept of superclusters". In: A&A 430, pp. 165–186.

Farrington, C. D., T. A. ten Brummelaar, B. D. Mason, W. I. Hartkopf, H. A. McAlister, D. Raghavan, N. H. Turner, L. Sturmann, J. Sturmann, and S. T. Ridgway (June 2010). "Separated Fringe Packet Observations with the CHARA Array. I. Methods and New Orbits for χ Draconis, HD 184467, and HD 198084". In: AJ 139, pp. 2308–2318.

Fischer, Debra A, Andrew W Howard, Greg P Laughlin, Bruce Macintosh, Suvrath Mahadevan, Johannes Sahlmann, and Jennifer C Yee (2015). "Exoplanet detection techniques". In: *arXiv preprint arXiv:1505.06869*.

Gaia Collaboration, T. Prusti, J. H. J. de Bruijne, A. G. A. Brown, A. Vallenari, C. Babusiaux, C. A. L. Bailer-Jones, U. Bastian, M. Biermann, D. W. Evans, and et al. (Nov. 2016). "The Gaia mission". In: A&A 595, A1, A1. arXiv: 1609.04153 [astro-ph.IM].

Garrido, R. and H. J. Deeg (Dec. 2006). "Exoplanet Detection and the CoRoT Mission". In: *Lecture Notes and Essays in Astrophysics* 2, pp. 27–48.

Goldin, A. and V. V. Makarov (Sept. 2006). "Unconstrained Astrometric Orbits for Hipparcos Stars with Stochastic Solutions". In: ApJS 166, pp. 341–350. eprint: astro-ph/0606293.

— (Nov. 2007). "Astrometric Orbits for Hipparcos Stochastic Binaries". In: ApJS 173, pp. 137–142. arXiv: 0706.0361.

Gómez-Forrellad, J. M., F. Sánchez-Bajo, M. Corbera-Subirana, E. Garc´a-Melendo, and J. Vidal-Sainz (2003). "Photometric study of the binary system NN Del". In: Ap&SS 283, pp. 297–304.

Gould, A, Subo Dong, BS Gaudi, A Udalski, IA Bond, J Greenhill, RA Street, M Dominik, T Sumi, MK Szymański, et al. (2010). "Frequency of solar-like systems and of ice and gas giants beyond the snow line from high-magnification microlensing events in 2005-2008". In: *The Astrophysical Journal* 720.2, p. 1073.

Gray, D. F. (Sept. 2005). *The Observation and Analysis of Stellar Photospheres*.

Gray, David F (2005). *The observation and analysis of stellar photospheres*. Cambridge University Press.

Griffin, R. and R. Griffin (Sept. 1986). "Composite spectra. I - HR 6902". In: *Journal of Astrophysics and Astronomy* 7, pp. 195–223.

Griffin, R. E. M., K. P. Schroder, A. Misch, and R. F. Griffin (Feb. 1992). "Optical Spectra of Zeta-Aurigae Binary Systems - Part Three - the 1989 Eclipse of Tau-Persei". In: A&A 254, p. 289.

Griffin, R. F. (1961). "Photoelectric measurements of the λ5250A Fe I triplet and the D lines in G and K stars". In: MNRAS 122, p. 181.

— (May 1967). "A Photoelectric Radial-Velocity Spectrometer". In: ApJ 148, p. 465.

— (1969). "Photoelectric radial velocities of four K stars". In: MNRAS 145, p. 163.

— (1970). "Photoelectric radial velocities of 87 seventh-magnitude K stars previously observed by Redman." In: MNRAS 148, pp. 211–225.

— (Dec. 1980). "Spectroscopic binary orbits from photoelectric radial velocities. Paper 35: HD 170737". In: *The Observatory* 100, pp. 193–197.

— (June 1982). "Spectroscopic binary orbits from photoelectric radial velocities. Paper 44: epsilon Aquilae". In: *The Observatory* 102, pp. 82–85.

— (Dec. 1983). "Spectroscopic binary orbits from photoelectric radial velocities. A synopsis of papers 1-50". In: *The Observatory* 103, pp. 273–275.

— (Aug. 1985). "Spectroscopic binary orbits from photoelectric radial velocities. Paper 63: HD 14346". In: *The Observatory* 105, pp. 126–128.

— (Oct. 1990). "Spectroscopic binary orbits from photoelectric radial velocities. Paper 94: HD 139444 (with a bulletin on HD 5373)". In: *The Observatory* 110, pp. 150–152.

— (Dec. 1991). "Spectroscopic binary orbits from photoelectric radial velocities. A synopsis of papers 1-100". In: *The Observatory* 111, pp. 291–298.

— (Apr. 1995). "Spectroscopic binary orbits from photoelectric radial velocities. Paper 121: 61 Ceti". In: *The Observatory* 115, pp. 84–90.

— (Aug. 1996). "Spectroscopic binary orbits from photoelectric radial velocities. Paper 129: HR 6985". In: *The Observatory* 116, pp. 233–241.

— (Oct. 1999). "Spectroscopic binary orbits from photoelectric radial velocities. Paper 148: HR 7955". In: *The Observatory* 119, pp. 272–283.

— (June 2000a). "Spectroscopic binary orbits from photoelectric radial velocities. A synopsis of papers 101-150". In: *The Observatory* 120, pp. 195–201.

— (Feb. 2000b). "Spectroscopic binary orbits from photoelectric radial velocities. Paper 150: zeta Cancri C". In: *The Observatory* 120, pp. 1–47.

— (Oct. 2005). "Spectroscopic binary orbits from photoelectric radial velocities - Paper 184: HD 196383, HD 109070, HD 118157, and HD 121213". In: *The Observatory* 125, pp. 300–315.

— (Dec. 2008). "Spectroscopic binary orbits from photoelectric radial velocities: A synopsis of papers 151 - 200". In: *The Observatory* 128, pp. 448–462.

— (Apr. 2010). "Spectroscopic binary orbits from photoelectric radial velocities - Paper 211: HD 128642, HD 144601, HD 150172, and HD 155641". In: *The Observatory* 130, pp. 75–88.

— (Apr. 2011). "Spectroscopic binary orbits from photoelectric radial velocities - Paper 217: HD 159220, HD 211922, HD 212859, and HD 219726". In: *The Observatory* 131, pp. 70–82.

— (Dec. 2012). "Spectroscopic binary orbits from photoelectric radial velocities - Paper 227: HD 108815, HD 112475, HD 115463, and HD 117319". In: *The Observatory* 132, pp. 356–372.
— (Dec. 2013). "Spectroscopic binary orbits from photoelectric radial velocities - Paper 233: HD 17922, HD 78899, HD 103613, and HD 160934, with a Note on HD 113449". In: *The Observatory* 133, pp. 322–350.
— (Feb. 2014a). "Spectroscopic binary orbits from photoelectric radial velocities. Paper 234: HD 110583, HD111224, HD 114864, and HD 118264". In: *The Observatory* 134, pp. 14–33.
— (June 2014b). "Spectroscopic binary orbits from photoelectric radial velocities. Paper 236: HD 45762, HD 74089, HD 194765, HD 197952 (NN Del), HDE 353012, and HD 215622". In: *The Observatory* 134, pp. 109–138.
— (Aug. 2014c). "Spectroscopic binary orbits from photoelectric radial velocities. Paper 237: UU Cnc, HD 67788, HD 79888, HD 119915, and HD 120649". In: *The Observatory* 134, pp. 172–195.
— (Oct. 2014d). "Spectroscopic binary orbits from photoelectric radial velocities. Paper 238: HD 22521, BD +15 1538, HR 4285, and HR 5835". In: *The Observatory* 134, pp. 245–267.
— (Dec. 2014e). "Spectroscopic binary orbits from photoelectric radial velocities. Paper 239: HD 134169, HD 176526, 1 Aquarii, and HD 219420". In: *The Observatory* 134, pp. 316–339.
— (Feb. 2015a). "Spectroscopic binary orbits from photoelectric radial velocities. Paper 240: BD+59 224, HD 9592, HD 10171, HD 11738, and nu Ceti". In: *The Observatory* 135, pp. 15–41.
— (Apr. 2015b). "Spectroscopic binary orbits from photoelectric radial velocities. Paper 241: HR 1884, HD 174103, HD 182563, and HR 8442, with a note on zeta Cephei". In: *The Observatory* 135, pp. 71–95.
— (June 2015c). "Spectroscopic binary orbits from photoelectric radial velocities. Paper 242: HD 471, HD 3791, HD 4703, and HD 8739". In: *The Observatory* 135, pp. 122–141.
— (Dec. 2015d). "Spectroscopic binary orbits from photoelectric radial velocities. Paper 245: HD 26083, HD 26441, HD 51001, and HD 85843". In: *The Observatory* 135, pp. 321–342.
Griffin, R. F., J.-M. Carquillat, and N. Ginestet (Apr. 2002). "Spectroscopic binary orbits from photoelectric radial velocities. Paper 163: HD 213503/4 and HD 220636/7 with a conjecture concerning gamma Cephei". In: *The Observatory* 122, p. 90.
Griffin, R. F. and J. J. Eitter (Aug. 2000). "Spectroscopic binary orbits from photoelectric radial velocities. Paper 153: HR 7798". In: *The Observatory* 120, pp. 260–268.
Griffin, R. F. and B. Emerson (Feb. 1975). "Spectroscopic binary orbits from photoelectric radial velocities. I - HD 45088". In: *The Observatory* 95, pp. 23–27.
Griffin, R. F. and R. O. Redman (1960). "Photoelectric measurements of the λ4200 A CN band and the G band in G8-K5 spectra". In: MNRAS 120, p. 287.
Griffin, R. F. and A. D. Thackeray (Dec. 1958). "Coronal lines in the post-maximum spectra of RS OPH 1958". In: *The Observatory* 78, pp. 245–247.
Griffin, RF (2016). "SPECTROSCOPIC BINARY ORBITS FROM PHOTOELECTRIC RADIAL VELOCITIES". In: *OBSERVATORY* 136.1252, pp. 125–138.
Gyldenkerne, K. (1955). "Preliminary list of photoelectric classification indices for 234 bright northern G and K stars". In: *Publikationer og mindre Meddeler fra Kobenhavns Observatorium* 165, pp. 1–5.

Häggkvist, L. and T. Oja (1966). "Photoelectric photometry of bright stars". In: *Arkiv for Astronomi* 4, pp. 137–163.

Haggkvist, L and T Oja (1973). "Photoelectric photometry of stars near the north galactic pole". In: *Astronomy and Astrophysics Supplement Series* 12, p. 381.

Han, E., S. X. Wang, J. T. Wright, Y. K. Feng, M. Zhao, O. Fakhouri, J. I. Brown, and C. Hancock (Sept. 2014). "Exoplanet Orbit Database. II. Updates to Exoplanets.org". In: PASP 126, p. 827. arXiv: 1409.7709 [astro-ph.EP].

Harlan, E. A. (Sept. 1969). "MK classifications for F- and G-type stars. I." In: AJ 74, pp. 916–919.

Hartkopf, W. I., P. Harmanec, and E. F. Guinan, eds. (Aug. 2007). *Binary Stars as Critical Tools and Tests in Contemporary Astrophysics (IAU S240)*. Vol. 240. IAU Symposium, Harmanec.

Hartkopf, W. I., B. D. Mason, H. A. McAlister, N. H. Turner, D. J. Barry, O. G. Franz, and C. M. Prieto (Feb. 1996). "ICCD Speckle Observations of Binary Stars. XIII. Measurements During 1989- 1994 From the Cerro Tololo 4 M Telescope". In: AJ 111, p. 936.

Hatzes, A. P. (Aug. 2016). "Astronomy: Earth-like planet around Sun's neighbour". In: Nature 536, pp. 408–409.

Hatzes, Artie P, William D Cochran, Michael Endl, Barbara McArthur, Diane B Paulson, Gordon AH Walker, Bruce Campbell, and Stephenson Yang (2003). "A planetary companion to γ Cephei A". In: *The Astrophysical Journal* 599.2, p. 1383.

Heintz, W. D. (1978). "Double stars /Revised edition/". In: *Geophysics and Astrophysics Monographs* 15.

Heintz, WD (1978). "Double Stars (Reidel, Dordrecht)". In: *Worley, CE (1962). Astron. J* 67.407, p. 61.

Høg, E., C. Fabricius, V. V. Makarov, S. Urban, T. Corbin, G. Wycoff, U. Bastian, P. Schwekendiek, and A. Wicenec (Nov. 2000a). "(Erratum) Letter to the Editor - The Tycho-2 catalogue of the 2.5 million brightest stars". In: A&A 363, p. 385.

— (Mar. 2000b). "The Tycho-2 catalogue of the 2.5 million brightest stars". In: A&A 355, pp. L27–L30.

Holman, Matthew J and Paul A Wiegert (1999). "Long-term stability of planets in binary systems". In: *The Astronomical Journal* 117.1, p. 621.

Horch, E. P., L. A. P. Bahi, J. R. Gaulin, S. B. Howell, W. H. Sherry, R. Baena Gallé, and W. F. van Altena (Jan. 2012). "Speckle Observations of Binary Stars with the WIYN Telescope. VII. Measures during 2008-2009". In: AJ 143, 10, p. 10.

Houk, N. (1978). *Michigan catalogue of two-dimensional spectral types for the HD stars*.

Howard, Andrew W (2013). "Observed properties of extrasolar planets". In: *Science* 340.6132, pp. 572–576.

Kalas, Paul (2010). "Direct imaging of massive extrasolar planets". In: *Proceedings of the International Astronomical Union* 6.S276, pp. 279–286.

Kasting, James F, Daniel P Whitmire, and Ray T Reynolds (1993). "Habitable zones around main sequence stars". In: *Icarus* 101.1, pp. 108–128.

Katoh, N., Y. Itoh, E. Toyota, and B. Sato (Feb. 2013). "Determination of Orbital Elements of Spectroscopic Binaries Using High-dispersion Spectroscopy". In: AJ 145, 41, p. 41.

Kennedy, Grant M, Mark C Wyatt, Vanessa Bailey, Geoffrey Bryden, William C Danchi, Denis Defrère, Chris Haniff, Philip M Hinz, Jérémy Lebreton, Bertrand Mennesson, et al.

(2015). "EXO-zodi modeling for the large binocular telescope interferometer". In: *The Astrophysical Journal Supplement Series* 216.2, p. 23.

Kitchin, Christopher R (2011). *Exoplanets: Finding, exploring, and understanding alien worlds*. Springer Science & Business Media.

Koch, David G, William J Borucki, Gibor Basri, Natalie M Batalha, Timothy M Brown, Douglas Caldwell, Jørgen Christensen-Dalsgaard, William D Cochran, Edna DeVore, Edward W Dunham, et al. (2010). "Kepler mission design, realized photometric performance, and early science". In: *The Astrophysical Journal Letters* 713.2, p. L79.

Kopal, Z. (1959). *Close binary systems*.

— (1990). *Mathematical theory of stellar eclipses*.

Kopal, Zdenek (1959). "Close binary systems". In: *The International Astrophysics Series, London: Chapman & Hall, 1959*.

Kopparapu, Ravi Kumar (2013). "A revised estimate of the occurrence rate of terrestrial planets in the habitable zones around Kepler M-dwarfs". In: *The Astrophysical Journal Letters* 767.1, p. L8.

Kopparapu, Ravi Kumar, Ramses Ramirez, James F Kasting, Vincent Eymet, Tyler D Robinson, Suvrath Mahadevan, Ryan C Terrien, Shawn Domagal-Goldman, Victoria Meadows, and Rohit Deshpande (2013). "ERRATUM:"HABITABLE ZONES AROUND MAIN-SEQUENCE STARS: NEW ESTIMATES"(2013, ApJ, 765, 131)". In: *The Astrophysical Journal* 770.1, p. 82.

Kopparapu, Ravi Kumar, Ramses M Ramirez, James SchottelKotte, James F Kasting, Shawn Domagal-Goldman, and Vincent Eymet (2014). "Habitable zones around main-sequence stars: dependence on planetary mass". In: *The Astrophysical Journal Letters* 787.2, p. L29.

Labeyrie, A., D. Bonneau, R. V. Stachnik, and D. Y. Gezari (Dec. 1974). "Speckle Interferometry. III. High-Resolution Measurements of Twelve Close Binary Systems". In: ApJ 194, p. L147.

Lanchares, V. (1992). "Method for the Calculation of Orbits of Spectroscopic - Interferometric Binaries with Mixed Data". In: *IAU Colloq. 135: Complementary Approaches to Double and Multiple Star Research*. Ed. by H. A. McAlister and W. I. Hartkopf. Vol. 32. Astronomical Society of the Pacific Conference Series, p. 238.

Lehmann-Filhés, R. (July 1894). "Über die Bestimmung einer Doppelsternbahn aus spectroskopichen Messungen der im Visionsradius liegenden Geschwindigkeitscomponente". In: *Astronomische Nachrichten* 136, p. 17.

Ljunggren, B. and T. Oja (1965). "Photoelectric measurements of magnitudes and colours for 849 stars". In: *Arkiv for Astronomi* 3, pp. 439–465.

Maceroni, C, D Cardini, C Damiani, D Gandolfi, J Debosscher, A Hatzes, EW Guenther, and C Aerts (2010). "Eclipsing binaries with pulsating components: CoRoT 102918586". In: *arXiv preprint arXiv:1004.1525*.

Makarov, V., U. Bastian, E. Hoeg, V. Grossmann, and A. Wicenec (Nov. 1994). "35 new bright medium- and high-amplitude variables discovered by the TYCHO instrument of the HIPPARCOS satellite". In: *Information Bulletin on Variable Stars* 4118.

Malbet, F, A Sozzetti, P Lazorenko, R Launhardt, D Ségransan, F Delplancke, N Elias, M Muterspaugh, A Quirrenbach, S Reffert, et al. (2009). "Detecting and characterizing extrasolar planetary systems with astrometry: review from the Blue Dots astrometry working group". In: *arXiv preprint arXiv:0912.0400*.

Malkov, O. Y. (Dec. 2007). "Mass-luminosity relation of intermediate-mass stars". In: MNRAS 382, pp. 1073–1086.

Mao, S. and B. Paczynski (June 1991). "Gravitational microlensing by double stars and planetary systems". In: ApJ 374, pp. L37–L40.

Marois, Christian, Bruce Macintosh, Travis Barman, B Zuckerman, Inseok Song, Jennifer Patience, David Lafrenière, and René Doyon (2008). "Direct imaging of multiple planets orbiting the star HR 8799". In: *Science* 322.5906, pp. 1348–1352.

Mason, B. D., G. L. Wycoff, W. I. Hartkopf, G. G. Douglass, and C. E. Worley (Dec. 2001). "The 2001 US Naval Observatory Double Star CD-ROM. I. The Washington Double Star Catalog". In: AJ 122, pp. 3466–3471.

Mason, Paul A, Jorge I Zuluaga, Joni M Clark, and Pablo A Cuartas-Restrepo (2013). "Rotational Synchronization May Enhance Habitability for Circumbinary Planets: Kepler Binary Case Studies". In: *The Astrophysical Journal Letters* 774.2, p. L26.

Massarotti, A., D. W. Latham, R. P. Stefanik, and J. Fogel (Jan. 2008). "Rotational and Radial Velocities for a Sample of 761 HIPPARCOS Giants and the Role of Binarity". In: AJ 135, pp. 209–231.

Mayor, M., D. Queloz, G. Marcy, P. Butler, R. Noyes, S. Korzennik, M. Krockenberger, P. Nisenson, T. Brown, T. Kennelly, C. Rowland, S. Horner, G. Burki, M. Burnet, and M. Kunzli (Oct. 1995). "51 Pegasi". In: IAU Circ. 6251.

McAlister, H. A. (Dec. 1976a). "Speckle interferometry of eta Orionis." In: PASP 88, pp. 957–959.

— (June 1976b). "Spectroscopic binaries as a source for astrometric and speckle interferometric studies." In: PASP 88, pp. 317–322.

McCuskey, S. W. and C. K. Seyfert (July 1950). "Stellar Spectra in Milky way Regions. II. a Region in Cygnus." In: ApJ 112, p. 90.

Morgan, W. W. and W. P. Bidelman (Sept. 1946). "On the Interstellar Reddening in the Region of the North Polar Sequence and the Normal Color Indices of A-Type Stars." In: ApJ 104, p. 245.

Moutou, C. and M. Deleuil (Oct. 2015). "CoRoT pictures transiting exoplanets". In: *ArXiv e-prints*. arXiv: 1510.01372 [astro-ph.EP].

Mullaney, James (2005). *Double & Multiple Stars, and How to Observe Them*. Springer Science & Business Media.

Müller, Tobias WA and Nader Haghighipour (2014). "Calculating the habitable zones of multiple star systems with a new interactive Web site". In: *The Astrophysical Journal* 782.1, p. 26.

Neuhäuser, R., M. Mugrauer, M. Fukagawa, G. Torres, and T. Schmidt (Feb. 2007). "Direct detection of exoplanet host star companion γ Cep B and revised masses for both stars and the sub-stellar object". In: A&A 462, pp. 777–780. eprint: astro-ph/0611427.

Ochsenbein, François, Patricia Bauer, and James Marcout (2000). "The VizieR database of astronomical catalogues". In: *Astronomy and Astrophysics Supplement Series* 143.1, pp. 23–32.

Perryman, M. A. C., L. Lindegren, J. Kovalevsky, E. Hoeg, U. Bastian, P. L. Bernacca, M. Crézé, F. Donati, M. Grenon, M. Grewing, F. van Leeuwen, H. van der Marel, F. Mignard, C. A. Murray, R. S. Le Poole, H. Schrijver, C. Turon, F. Arenou, M. Froeschlé, and C. S. Petersen (July 1997). "The HIPPARCOS Catalogue". In: A&A 323.

Placek, Ben (2014). *Bayesian detection and characterization of extra-solar planets via photometric variations*.

Popper, D. M. (1980). "Stellar masses". In: ARA&A 18, pp. 115–164.

Pourbaix, D. (Aug. 2000). "Resolved double-lined spectroscopic binaries: A neglected source of hypothesis-free parallaxes and stellar masses". In: A&AS 145, pp. 215–222.

Pourbaix, Dimitri, Andrei A Tokovinin, Alen H Batten, Francis C Fekel, William I Hartkopf, Hugo Levato, Nidia I Morrell, Guillermo Torres, and S Udry (2004). "SB9: The ninth catalogue of spectroscopic binary orbits". In: *Astronomy & Astrophysics* 424.2, pp. 727–732.

Radford, G. A. and R. F. Griffin (Feb. 1976). "Spectroscopic binary orbits from photoelectric radial velocities. Paper 6: HD 183629". In: *The Observatory* 96, pp. 18–21.

Renn, Jürgen, Tilman Sauer, and John Stachel (1997). "The origin of gravitational lensing: A postscript to Einstein's 1936 Science paper". In: *Science* 275.5297, pp. 184–186.

Rice, Ken (2014). "The detection and characterization of extrasolar planets". In: *Challenges* 5.2, pp. 296–323.

Roell, T, R Neuhäuser, A Seifahrt, and M Mugrauer (2012). "Extrasolar planets in stellar multiple systems". In: *Astronomy & Astrophysics* 542, A92.

Roman, N. G. (Nov. 1950). "A Correlation Between the Spectroscopic and Dynamical Characteristics of the Late F - and Early G - Type Stars." In: ApJ 112, p. 554.

— (July 1952). "The Spectra of the Bright Stars of Types F5-K5." In: ApJ 116, p. 122.

Romanishin, W (2002). "An Introduction to Astronomical Photometry Using CCDs". In: *University of Oklahoma* 31.

Roy, A.E. and D. Clarke (2003). *Astronomy: Principles and Practice, Fourth Edition (PBK)*. Taylor & Francis. ISBN: 9780750309172.

Russell, H. N. (May 1902). "An Improved Method of Calculating the Orbit of a Spectroscopic Binary". In: ApJ 15, p. 252.

Sahade, J. and F. B. Wood (1978). *Interacting binary stars*.

Sahlmann, J, PF Lazorenko, A Mérand, D Queloz, D Ségransan, and J Woillez (2013). "Astrometric detection of exoplanets from the ground". In: *SPIE Optical Engineering+ Applications*. International Society for Optics and Photonics, 88641B–88641B.

Sahlmann, Johannes (2012). "Observing exoplanet populations with high-precision astrometry". PhD thesis. University of Geneva.

Schmidt-Kaler, Th (1965). "Landolt-Bornstein, KH Hellwege, Ed". In: *Springer-Verlag, Berlin and New York), New Ser., Group* 6, p. 301.

Schneider, J (2011). "Extrasolar Planets Encyclopaedia, 2006". In: *URL http://exoplanet. eu*.

Seager, S, M Kuchner, CA Hier-Majumder, and B Militzer (2007). "Mass-radius relationships for solid exoplanets". In: *The Astrophysical Journal* 669.2, p. 1279.

Selsis, Franck, JF Kasting, Benjamin Levrard, J Paillet, I Ribas, and X Delfosse (2007). "Habitable planets around the star Gliese 581?" In: *Astronomy & Astrophysics* 476.3, pp. 1373–1387.

Shao, Michael (1996). "Astrometric detection of Earth-like planets with OSI". In: *The Search for Extra-Solar Terrestrial Planets: Techniques and Technology*. Springer, pp. 85–88.

Shao, Michael, Geoff Marcy, Joseph H Catanzarite, Stephen J Edberg, Alain Leger, Fabien Malbet, Didier Queloz, Matthew W Muterspaugh, Charles Beichman, Debra A Fischer, et al. (2009). "Astrometric Detection of Earthlike Planets". In: *arXiv preprint arXiv:0904.0965*.

Soubiran, C, O Bienaymé, TV Mishenina, and VV Kovtyukh (2008). "Vertical distribution of Galactic disk stars-IV. AMR and AVR from clump giants". In: *Astronomy & Astrophysics* 480.1, pp. 91–101.

Straizys, V. and G. Kuriliene (Dec. 1981). "Fundamental stellar parameters derived from the evolutionary tracks". In: Ap&SS 80, pp. 353–368.

Straizys, V and Romualda Lazauskaite (2009). "Intrinsic color indices and luminosity sequences of stars in the 2MASS two-color diagram". In: *arXiv preprint arXiv:0907.2398*.

Swain, MR, G Tinetti, G Vasisht, P Deroo, C Griffith, J Bouwman, Pin Chen, Y Yung, A Burrows, LR Brown, et al. (2009). "Water, methane, and carbon dioxide present in the dayside spectrum of the exoplanet HD 209458b". In: *The Astrophysical Journal* 704.2, p. 1616.

Szebehely, V. (Dec. 1984). "Review of concepts of stability". In: *Celestial Mechanics* 34, pp. 49–64.

Taylor, John R and ER Cohen (1998). "An introduction to error analysis: the study of uncertainties in physical measurements". In: *Measurement Science and Technology* 9.6, p. 1015.

Thebault, Ph and N Haghighipour (2015). "Planet formation in Binaries". In: *Planetary Exploration and Science: Recent Results and Advances*. Springer, pp. 309–340.

Tinetti, Giovanna, Jonathan Tennyson, Caitlin A Griffith, and Ingo Waldmann (2012). "Water in exoplanets". In: *Philosophical Transactions of the Royal Society of London A: Mathematical, Physical and Engineering Sciences* 370.1968, pp. 2749–2764.

Ting-gao, Yang, Gao Yu-ping, Tong Ming-lei, Zhao Cheng-shi, and Gao Feng (2016). "Mathematical Model for Measuring Pulsar Parameters by Pulsar Timing Observations and Precision Estimation". In: *Chinese Astronomy and Astrophysics* 40.2, pp. 256–265.

Tokovinin, A., D. A. Fischer, M. Bonati, M. J. Giguere, P. Moore, C. Schwab, J. F. P. Spronck, and A. Szymkowiak (Nov. 2013). "CHIRON-A Fiber Fed Spectrometer for Precise Radial Velocities". In: PASP 125, p. 1336. arXiv: 1309.3971 [astro-ph.IM].

Torres, G. (Jan. 2007). "The Planet Host Star γ Cephei: Physical Properties, the Binary Orbit, and the Mass of the Substellar Companion". In: ApJ 654, pp. 1095–1109. eprint: astro-ph/0609638.

Traub, Wesley A and Ben R Oppenheimer (2010). "Direct imaging of exoplanets". In: *Exoplanets* 1, pp. 111–156.

van Citters, G. W. (Sept. 1974). "Photoelectric radial velocities - I. Technique." In: MNRAS 168, pp. 469–478.

van Leeuwen, F., ed. (2007). *Hipparcos, the New Reduction of the Raw Data*. Vol. 350. Astrophysics and Space Science Library.

Vidal, E. (Dec. 1948). "On parabolic orbits of double stars with application to 7,1639 (ADS 8539)". In: AJ 54, p. 77.

Walker, G. A. H., D. A. Bohlender, A. R. Walker, A. W. Irwin, S. L. S. Yang, and A. Larson (Sept. 1992). "Gamma Cephei - Rotation or planetary companion?" In: ApJ 396, pp. L91–L94.

Wenger, M., F. Ochsenbein, D. Egret, P. Dubois, F. Bonnarel, S. Borde, F. Genova, G. Jasniewicz, S. Laloë, S. Lesteven, and R. Monier (Apr. 2000). "The SIMBAD astronomical database. The CDS reference database for astronomical objects". In: A&AS 143, pp. 9–22. eprint: astro-ph/0002110.

Wiegert, P. A. and M. J. Holman (Apr. 1997). "The Stability of Planets in the Alpha Centauri System". In: AJ 113, pp. 1445–1450. eprint: astro-ph/9609106.

Wilsing, J. (Nov. 1893). "Über die Bestimmung von Bahnelementen enger Doppelsterne aus spectroskopischen Messungen der Geschwindigkeits Componenten." In: *Astronomische Nachrichten* 134, p. 89.

Wilson, R. E. (1953). "General catalogue of stellar radial velocities." In: *Carnegie Institute Washington D.C. Publication*.

Winn, Joshua N (2010). "Exoplanet Transits and Occultations". In: *Exoplanets* 1, pp. 55–77.

Wolszczan, A. (June 1992). "PSR1257+12: A Neutron Star with Planetary Companions". In: *AAS/Division for Planetary Sciences Meeting Abstracts #24*. Vol. 24. Bulletin of the American Astronomical Society, p. 969.

Wolszczan, A (2008). "Fifteen years of the neutron star planet research". In: *Physica Scripta* 2008.T130, p. 014005.

Wolszczan, A, IM Hoffman, M Konacki, SB Anderson, and KM Xilouris (2000a). "A 25.3 day periodicity in the timing of the pulsar PSR B1257+ 12: a planet or a heliospheric propagation effect?" In: *The Astrophysical Journal Letters* 540.1, p. L41.

Wolszczan, A, O Doroshenko, M Konacki, M Kramer, A Jessner, R Wielebinski, F Camilo, DJ Nice, and JH Taylor (2000b). "Timing observations of four millisecond pulsars with the Arecibo and Effelsberg radio telescopes". In: *The Astrophysical Journal* 528.2, p. 907.

Wolszczan, Alex (2012). "Discovery of pulsar planets". In: *New Astronomy Reviews* 56.1, pp. 2–8.

Wolszczan, Alexander et al. (1994). "Confirmation of Earth-mass planets orbiting the millisecond pulsar PSR B1257+ 12". In: *Science-AAAS-Weekly Paper Edition-including Guide to Scientific Information* 264.5158, pp. 538–542.

Xue, Dingyu and YangQuan Chen (2008). *Solving applied mathematical problems with MATLAB*. CRC Press.

Yoss, KM and RF Griffin (1997). "Radial velocities andDDO, BV photometry of Henry Draper G5-M stars near the North Galactic Pole". In: *Journal of Astrophysics and Astronomy* 18.2-3, pp. 161–227.

Mr. Ahmad Abushattal and Professor José Ángel Docobo, 2017, April 21.